# Rock thermal energy storage (RTES) for renewable heating and cooling

Leyla Amiri

Department of Mining and Materials Engineering

McGill University

Quebec, Canada

August 2019

A Thesis Submitted to McGill University in partial fulfilment of the requirement for the degree of Doctor of Philosophy

**THIS THESIS IS DEDICATED TO**

**MY BEAUTIFUL FAMILY.**

# Abstract

Thermal energy storage (TES) systems have been extensively employed as an elegant approach to partially fulfill the enormous energy demand in industrial applications, such as mining, geothermal, oil and gas, and construction industries by deploying the available renewable energies or using alternative energy solutions. TES allows for energy to be stored in the form of heat during times of low/no demand and used later when demand rises. Energy storage efficiency depends on many design and operational factors, which are not easy to empirically quantify. Among these factors, the permeability of porous media is not well-understood and plays a fundamental role on storage efficiency. Computational modelling is a feasible approach to predict the primary parameters to design and evaluate and optimize the performance of TES systems. Hence, this study begins with a comprehensive review of fluid flow and heat transfer mechanisms in porous media. Then, numerical investigation was performed to estimate the pressure drop through the packed bed of large spherical particles with two sets of models: pore-scale and volume-averaged. The numerical models were developed, analyzed, and validated with experimental data. Further, a new Ergun/Forchheimer correlation was proposed and employed to study the impact of various design and operating parameters, such as porosity, particle size, mass flowrate, aspect ratio, properties of storage material, and inlet air temperature on the overall performance of large-scale TES systems. Two energy sources were used based on their availability in the field: seasonal ambient air and exhaust streams from a diesel generator. The fluid flow behavior inside a packed rock bed thermal energy storage system was investigated by developing a transient, 3D computational fluid dynamics and a heat transfer model that accounts for interphase energy balance for energy conservation, using a local thermal non-equilibrium approach. The heat transfer phenomenon in the rock-pile was empirically validated. The model also provides useful information for evaluating the performance of packed beds of large rocks and in caved zones. The proposed TES system has great potential to be a green solution to meet heating/cooling and ventilation demands of deep underground mines, as well as the heating demand of the remote communities in the cold climates by reducing the burning of fossil fuels and carbon emissions.

# Résumé

Les systèmes de stockage d'énergie thermique (TES) ont été largement utilisés en tant qu'approche élégante pour répondre en partie à l'énorme demande en énergie des applications industrielles telles que les industries minière, géothermique, pétrolière et gazière et de la construction en déployant les énergies renouvelables disponibles ou en utilisant des solutions énergétiques alternatives. Le TES permet de stocker l'énergie sous forme de chaleur en période de faible demande ou sans demande, puis de l'utiliser ultérieurement lorsque la demande augmente. L'efficacité du stockage de l'énergie dépend de nombreux facteurs de conception et d'exploitation, qu'il est difficile de quantifier empiriquement. Parmi ces facteurs, la perméabilité des milieux poreux n'est pas bien comprise et joue un rôle fondamental dans l'efficacité du stockage. La modélisation informatique est une approche réalisable pour prédire les principaux paramètres permettant de concevoir, d'évaluer et d'optimiser les performances des systèmes TES. Par conséquent, cette étude commence par un examen complet des mécanismes d'écoulement des fluides et de transfert de chaleur dans les milieux poreux. Ensuite, une étude numérique a été réalisée pour estimer la chute de pression dans le lit de garnissage de grosses particules sphériques avec deux ensembles de modèles: l'échelle des pores et la moyenne volumique. Les modèles numériques ont été développés, analysés et validés avec des données expérimentales. En outre, une nouvelle corrélation Ergun / Forchheimer a été proposée et utilisée pour étudier l'incidence de divers paramètres de conception et de fonctionnement, tels que la porosité, la taille des particules, le débit massique, le rapport de longueur, les propriétés du matériau de stockage et la température de l'air aspiré sur la performance globale de systèmes TES à grande échelle. Deux sources d'énergie ont été utilisées en fonction de leur disponibilité sur le terrain: l'air ambiant saisonnier et le flux d'échappement d'un générateur diesel. Le comportement de l'écoulement des fluides dans un système de stockage d'énergie thermique à lit de roche tassée a été étudié en utilisant une approche de non équilibre thermique local et en développant une dynamique des fluides 3D transitoire avec un modèle de transfert de chaleur prenant en compte le bilan énergétique interphasique pour la conservation de l'énergie. Le phénomène de transfert de chaleur dans le tas de roches a été validé empiriquement. Le modèle fournit également des informations utiles pour évaluer la performance des lits compactés de grosses roches et dans des zones creusées. Le système TES proposé pourrait constituer une solution verte pour répondre aux besoins de chauffage / refroidissement et de ventilation des mines souterraines profondes, ainsi qu'au besoin de chauffage des communautés isolées des régions froides en réduisant la combustion de combustibles fossiles et les émissions de carbone.

# Acknowledgments

I would like to express my special gratitude to my supervisor, Professor Ferri Hassani, for his continuous support and inspiration. His friendly guidance and expert advice have been invaluable throughout all stages of my Ph.D. studies.

I sincerely appreciate the immense technical knowledge and support from my co-supervisor, Professor Agus Sasmito. His wealth of knowledge in the field of Mining Engineering and fluid flow and heat transfer in porous media in particular is inspiring. He has been a tremendous mentor for me.

I am particularly thankful for the advice of Professor Seyed Ali Ghoreishi Madiseh within the years of my doctoral studies. I am grateful for his extended discussions and valuable suggestions which have contributed greatly to the improvement of the thesis.

I would like to express my gratitude to my fellow friends Edris Madadian, Jeff Templeton, Marco Antonio Rodrigues de Brito and Mahmoud Alzoubi for providing me assistance, criticisms and useful insights.

I am also grateful to all the members of the EMERG lab and Mine Multiphysics research group at Mining and Materials Department for sharing their knowledge and friendship.

I gratefully acknowledge Ultra Deep Mining Network (UDMN) and McGill Engineering Doctoral Awards (MEDA), for providing me funds that made my Ph.D. work easier.

Finally my deep and sincere gratitude to my beautiful parents, Emad and Mina, and my lovely sister Mehrnoosh for their continuous and unparalleled love, help and support. I am forever indebted to them for giving me the opportunities and experiences that have made me who I am.

And most of all, I owe my deepest gratitude to my husband and love of my life, Nima, for his affection, encouragement, understanding and patience and for always showing how proud he is of me.

# Contribution of Authors

In accordance with the guidelines of the Faculty of Graduate Studies and Research of McGill University "Guidelines for a Manuscript Based Thesis Preparation", the prepared manuscripts and contribution of authors are presented below.

Leyla Amiri is the principal author of this work, supervised by Professor Ferri Hassani and Professor Agus Sasmito from the Department of Mining and Materials Engineering, McGill University, Quebec, Canada.

Professor Ferri Hassani and Professor Agus Sasmito, the supervisors and directors of the thesis, co-authored all manuscripts, and provided scientific guidance in the planning and execution of the work.

Professor Seyed Ali Ghoreishi Madiseh, the advisor of this thesis, co-authored all manuscripts and provided scientific guidance in the planning and execution of the work as well as co-editing and reviewing manuscripts.

Mr. Marco Antonio Rodrigues de Brito, Mr. Durjoy Baidya and Mr. Ali Fahrettin Kuyuk co-authored the manuscript extracted from $6^{th}$ and $7^{th}$ chapters and contributed to the final version of the manuscripts.

Details of the papers published, accepted and submitted are provided below:

A. Journal Papers

- **L. Amiri,** S.A. Ghoreishi-Madiseh, F.P. Hassani, and A.P. Sasmito, Estimating pressure drop and Ergun/Forchheimer parameters of flow through packed bed of spheres with large particle diameters, *Powder Technology* (2019).
- **L. Amiri**, M.A. Rodrigues de Brito, D. Baidya, A.F. Kuyuk, S.A. Ghoreishi-Madiseh, AP. Sasmito, and Ferri P. Hassani, Numerical investigation of rock-pile based waste heat storage for remote communities in cold climates, *Applied Energy* (2019).
- **L. Amiri**, M.A Rodrigues de Brito, S.A. Ghoreishi-Madiseh, A.P. Sasmito, and Ferri P. Hassani, Numerical study of volume averaged porous media heat transfer and fluid flow model for thermal energy storage in packed rock beds, *Under review*
- S.A. Ghoreishi-Madiseh, A. Safari, **L. Amiri**, D. Baidya, M.A Rodriguesde Brito, A.F. Kuyuka (2019). Investigation of viability of seasonal waste heat storage in rock piles for remote communities in cold climates. Energy Procedia 159, 66-71.
- A.F. Kuyuka, **S**.A. Ghoreishi-Madiseh, F.P. Hassani, A.P. Sasmito, **L. Amiri,** J.D. Templeton (2019) Performance and economic assessment of large-scale deep-lake cooling systems: A Canadian example. Energy Procedia 158, 43-48.
- **L. Amiri,** E. Madadian and F.P. Hassani, Energo- and exergo-technical assessment of ground-source heat pump systems for geothermal energy production from underground mines, *Environmental Technology* (2018)
- **L. Amiri**, S.A. Ghoreishi-Madiseh, A.P. Sasmito, F.P. Hassani, Effect of buoyancy-driven natural convection in a rock-pit mine air preconditioning system acting as a large-scale thermal energy storage mass, *Applied Energy* (2018).
- **L. Amiri,** S.A. Ghoreishi-Madiseh, A.P. Sasmito, F.P. Hassani, Evaluation of Heat Transfer Performance between Rock and Air in Seasonal Thermal Energy Storage Unit, *Energy Procedia* (2017) 142, 576-581.
- N Gharib, B. Bharathan, **L. Amiri**, M. McGuinness, F.P. Hassani, A.P. Sasmito, Flow characteristic and wear prediction of Herschel-Bulkley non-Newtonian paste backfill in pipe elbows, *The Canadian Journal of Chemical Engineering* (2017) in press (doi:10.1002/cjce.22749).
- S.A. Ghoreishi-Madiseh, **L. Amiri**, A.P. Sasmito, F.P. Hassani, A Conjugate Natural Convection Model for Large Scale Seasonal Thermal Energy Storage Units: Application in Mine Ventilation, *Energy Procedia* (2017) 105, 4167-4172.
- S.A. Ghoreishi-Madiseh, A.P. Sasmito, F.P. Hassani, **L. Amiri,** "Performance evaluation of large scale rock-pit seasonal thermal energy storage for application in underground mine ventilation." *Applied Energy* (2017).
- S.A. Ghoreishi-Madiseh, A.P. Sasmito, F.P. Hassani, **L. Amiri** "Heat Transfer Analysis of Large Scale Seasonal Thermal Energy Storage for Underground Mine Ventilation", *Energy Procedia*, Volume 75, August 2015, Pages 2093–2098 (doi:10.1016/j.egypro.2015.07.324).

B. Papers presented at conferences

- **L. Amiri**, A.P. Sasmito, F.P. Hassani, **S**.A. Ghoreishi-Madiseh (2019). Friction factor correlation for airflow through broken rocks and its applications in mine ventilation. 17th North American Mine Ventilation Symposium (NAMVS), Montreal, Canada.
- **S**.A. Ghoreishi-Madiseh, A. Safari, **L. Amiri**, D. Baidya, M.A Rodriguesde Brito, A.F. Kuyuka (2019). Investigation of viability of seasonal waste heat storage in rock piles for remote communities in cold climates. 10th International Conference on Applied Energy (ICAE), Hong Kong, China
- A.F. Kuyuka, **S**.A. Ghoreishi-Madiseh, F.P. Hassani, A.P. Sasmito, **L. Amiri,** J.D. Templeton (2019) Performance and economic assessment of large-scale deep-lake cooling systems: A Canadian example. 10th International Conference on Applied Energy (ICAE), Hong Kong, China
- J.D. Templeton, **L. Amiri**, A.F. Kuyuka, S.A. Madiseh, F.P. Hassani, A.P. Sasmito (2019). Evaluation of the Hydraulic Recovery Potential in a Lake-Sourced Underground Mine Refrigeration System. Proceedings of the 11th International Mine Ventilation Congress, 705-712
- **L. Amiri**, S.A. Ghoreishi-Madiseh, A.P. Sasmito, F.P. Hassani. (2017). Evaluation of Heat Transfer Performance between Rock and Air in Seasonal Thermal Energy Storage Unit. 9th International Conference on Applied Energy, ICAE2017, 21-24 August 2017, Cardiff, UK
- J.D. Templeton, **L. Amiri**, M. Dabbas, F.P. Hassani, A.P. Sasmito, S.A. Madiseh, (2017) Feasibility of refrigerating deep underground mines with cold lake water. CIM 2017, At Montreal, Canada
- **L. Amiri**, S.A. Ghoreishi-Madiseh, F.P. Hassani, A.P. Sasmito. (2016). Heat transfer analysis of using large scale thermal energy storage systems for mine ventilation purposes. 15th World Renewable Energy Congress
- S. A. Ghoreishi-Madiseh, **L. Amiri**, A.P. Sasmito, F.P. Hassani. (2016). A Conjugate natural convection model for large scale seasonal thermal energy storage units: application in mine ventilation. The 8th International Conference on Applied Energy – ICAE2016, At Beijing, China. Published in Energy Procedia, Elsevier 2016.
- **L. Amiri**, S.A. Ghoreishi-Madiseh, A.P. Sasmito, F.P. Hassani. (2016). An investigation into application of large scale seasonal thermal energy storage systems in mine ventilation. The 15th World Renewable Energy Congress 2016 (15th WREC), At Jakarta Convention Center Indonesia.
- **L. Amiri**, F.P. Hassani, A.P. Sasmito, S.A. Ghoreishi-Madiseh. (2016). Harvesting geothermal energy from active mines of Canada; a field study, CIM 2016, At Vancouver, Canada.

# Table of Contents

# List of Tables

# List of Figures

# CHAPTER 1

## 1. Introduction

Energy costs, risk reduction, and environmental concerns are among the top priorities for most industrial operations, driving engineering innovation to reduce energy (especially fossil fuel) consumption and greenhouse gas emissions while remaining competitive (Ghomshei and Meech 2005, Bharathan, Sasmito et al. 2017). As a result, industries are looking at renewable energy options to shift away from dependence on fossil fuels. They are implementing cleaner production technologies and focusing on enhancing its energy efficiency (Hilson 2003, Hall, Scott et al. 2011, Ghoreishi-Madiseh, Sasmito et al. 2017). Among these technologies, thermal energy storage (TES) systems have been receiving increasing attention at the industrial scale.

### 1.1. Background

Among energy-intensive industries, underground mining operations are generally associated with very high energy demands, especially for ventilation (Kurnia, Sasmito et al. 2014) and heating and cooling systems, which provide a comfortable and safe working environment underground: they provide fresh air from the surface, remove noxious and flammable gases (Chatterjee, Zhang et al. 2015), and control ambient temperatures. Depending on the depth and size of a mine, ventilation costs can account for up to 40% of the total electricity used and 60% of operating costs (Karacan 2007). In ultra-deep (> 2.5 km) underground mines, a huge amount of air (e.g., 1.3 million cfm for LaRonde Mine, Quebec, Canada) must be cooled before sending it down the intake shaft because the temperature increases by up to 12°C/km depth (Templeton, Ghoreishi-Madiseh et al. 2014) and diesel equipment underground generates heat. A 30 MW cooling station operates at the LaRonde Mine at an annual cost of approximately C$20 million per year (Sbarba 2012, Kurnia,

Sasmito et al. 2014). In extremely cold regions like Canada, heating costs are high in winter, when air must be heated to > 0°C on the surface and sent to the lower mining levels, where it must be cooled again.

Preconditioning, heating, and cooling needs in ultra-deep mines are usually met by burning fossil fuels (mostly natural gas, propane, or diesel) and using electricity (taken from the grid or generated with diesel generators), respectively. These conventional technologies need to be replaced with new technologies that are more energy efficient and use renewable energy sources. This shift might be encouraged by energy price variations in the last 5 decades and pending carbon taxes (e.g., in Canada and Australia). Research on new technologies has focused on using seasonal thermal energy as well as recovering and storing waste heat in remote communities in cold climates and mining environments (Brown 2000, Madiseh, Ghomshei et al. 2012, Wu, Wang et al. 2014, Ghoreishi-Madiseh, Safari et al. 2019) and has highlighted several techno-economic advantages of using large-scale energy storage units (Persson and Westermark 2013, Colclough and McGrath 2015, Sommer, Valstar et al. 2015, Ghoreishi-Madiseh, Fahrettin Kuyuk et al. 2019).

Storage of large quantities of thermal energy (hot or cold) can increase energy efficiency in mine ventilation systems (Sylvestre 1999). This novel concept takes advantage of the huge rock mass volume available on the surface of the mine to store heat. Seasonal variations in ambient temperature provide the opportunity to store thermal energy in broken/porous rock in the form of sensible heat (Ghoreishi-Madiseh, Sasmito et al. 2017, Amiri, Ghoreishi-Madiseh et al. 2018). Some mining operations (e.g., Creighton and Kidd Creek mines in Canada) could make use of the huge mass of waste rock as a massive seasonal thermal energy storage (STES) unit to create a unique “natural heat exchanger”, where fresh air is moved through the waste rock in an open pit (Sylvestre 1999). STES technologies can also be used to store waste heat in remote small

communities and large commercial operations in cold regions by coupling a large-scale STES system with a diesel exhaust heat recovery system (Ghoreishi-Madiseh, Safari et al. 2018, Ghoreishi-Madiseh, Fahrettin Kuyuk et al. 2019). Although many researchers have focused on design and optimization of ground-coupled heat exchangers (Li, Zhao et al. 2005, Florides and Kalogirou 2007, Sharqawy, Said et al. 2009), using waste rock as a TES system requires more investigation.

Whereas several studies have modelled heat transfer and fluid flow in a packed rock bed (PRB), most are limited due to reduction of one or more dimension, simplification from interphase energy balance local thermal nonequilibrium to a less realistic local thermal equilibrium, or neglect of friction losses. Therefore, three-dimensional (3D) computational modelling is ideal to obtain more in-depth information into phenomena occurring within the PRB of broken rocks that can be used to enhance the heating and cooling capacity of STES systems.

## 1.2. Objectives

The general objective of this thesis is to assess the performance of the TES systems using waste rock as a heat storage material and air as a heat transfer fluid. The specific objectives of this project focus on three main topics:

1- Understand the fundamentals of fluid flow through the packed bed of broken rocks, predict the pressure loss through such a porous media by developing a numerical pore-scale model of a packed bed of large spherical particles, and compare with a volume-averaged model and analytical solutions.
2- Evaluate the performance of large-scale STES systems by developing, for the first time, a 3D large-scale transient numerical model of fluid flow and heat transfer and applying it to a case study—Creighton Mine, Ontario, Canada.

3- Evaluate the novel concept of coupling a large-scale STES system with a diesel exhaust heat recovery system in remote communities, and apply it to a case study—Kwadacha, northern British Columbia, Canada.

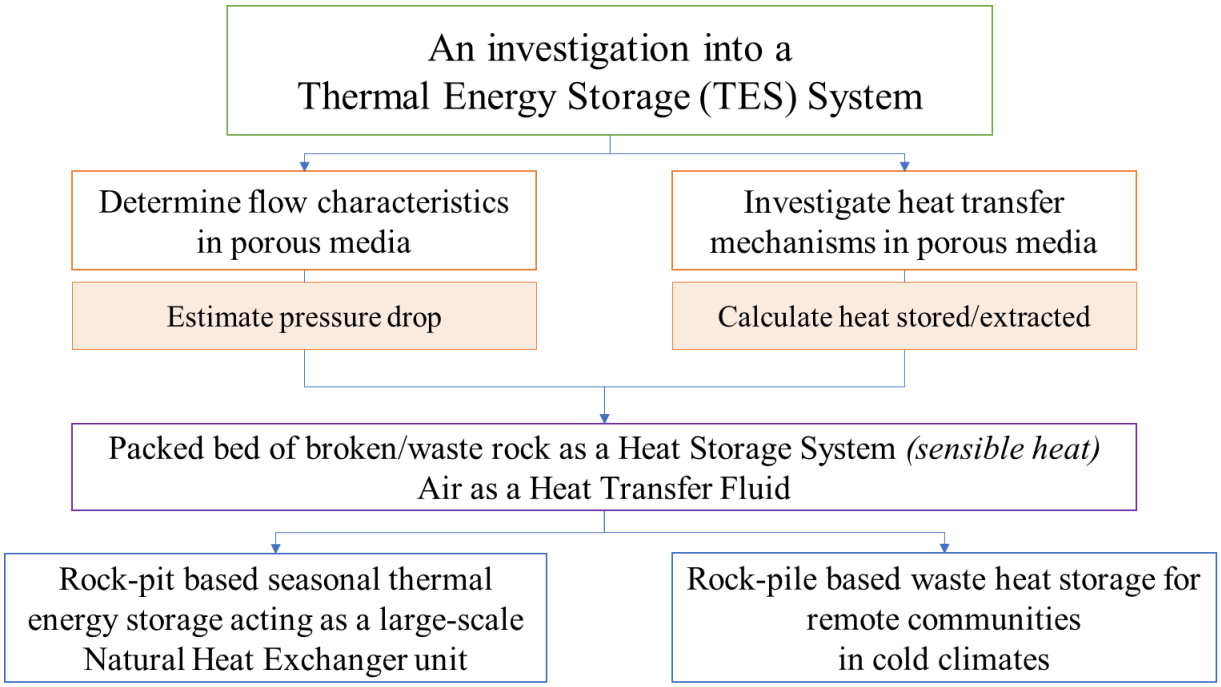


Figure 1.1.The overall workflow of this thesis

### 1.3. Outline of thesis

The thesis is organized into the following chapters:

Chapter 1 briefly summarizes the background and the necessity for this research.

Chapter 2 is a literature review on fluid flow and heat transfer in porous media, as well as the energy demand in underground mining, available renewable energies in mine sites, and thermal energy storage systems and their application, different methods, standpoint from underground mine ventilation energy network.

Chapter 3 deals with estimating pressure loss and Ergun/Forchheimer parameters in a packed bed of large spherical particles (such as rocks).

Chapter 4 presents the friction factor correlation for airflow through broken rocks and its applications in mine ventilation.

Chapter 5 presents the effect of buoyancy-driven natural convection in a rock-pit mine air preconditioning system acting as a large-scale thermal energy storage mass.

Chapter 6 presents a detailed numerical investigation of the novel concept of coupling a conical shape, rock-pile based large-scale STES system with a diesel exhaust heat recovery system in remote communities in cold regions.

Chapter 7 develops a numerical study of volume-averaged porous media heat transfer and fluid flow model for TES in PRBs.

Chapter 8 presents conclusions based on the results and offers suggestions for potential future work.

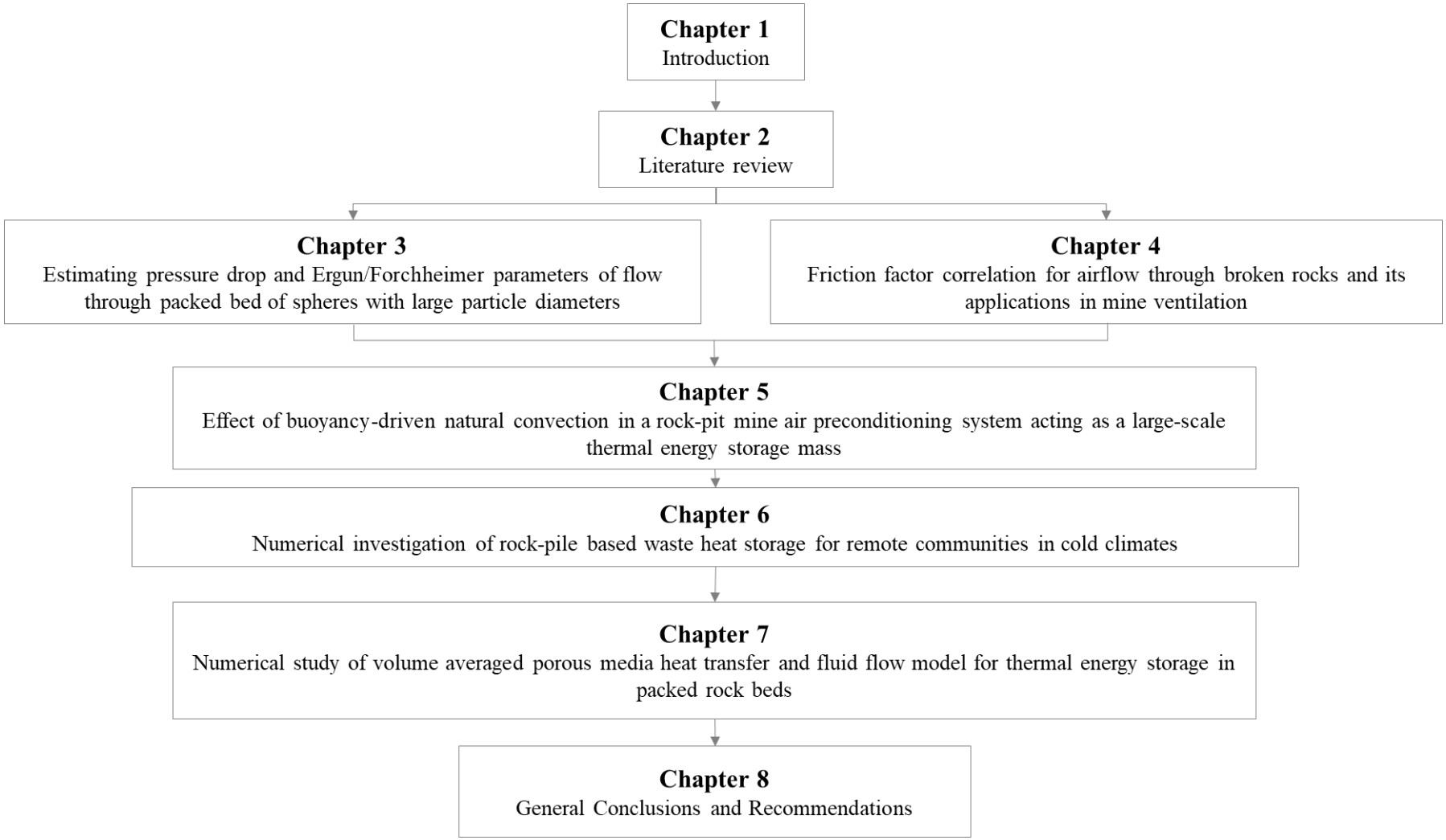


Figure 1.2.The overall outline of this thesis

# CHAPTER 2

## 2. Literature Review

Several technical and mechanical issues must be addressed before a packed bed thermal energy storage (TES) system is designed and operated. Accurate prediction of various parameters like pressure losses and heat transfer mechanisms—and understanding the effect of operational parameters associated with these parameters—is necessary for TES system design, efficiency analysis, and optimal performance of TES systems. In addition, detailed analysis of fluid flow and heat transfer in porous media (e.g., packed rock beds or PRBs) helps engineers develop ideas for designing and optimizing TES systems. Therefore, this chapter provides an overview of fluid flow and heat transfer in porous media. Then, the heat sources in underground mining, as well as the energy demands and available renewable energy in mine sites and remote communities are described. Meanwhile, the motivations for performing this study are elaborated. The main fluid flow and heat transfer approaches are reviewed and the application of a PRB TES in mining industry is described. Finally, a case study of successful application of a natural heat exchanger in Creighton mine is presented.

### 2.1. Fluid flow in porous media

Porous media can be categorized as natural (e.g., broken and fractured rock, gravel, sand) or artificial (e.g., packed bed of particles) (Dullien 1975, Sahimi 2011). Studies dealing with fluid flow and heat transfer in several kinds of porous media have been performed by mining engineers, civil engineers, and hydrologists (Fand, Kim et al. 1987, Kececioglu and Jiang 1994, Seguin, Montillet et al. 1998). This phenomenon occurs in many industrial settings, such as TES systems, underground mine ventilation systems, and broken rock associated with mining operations. Understanding the fluid flow behavior within pores and the associated viscous and inertia terms for predicting the pressure gradient is crucial for evaluating these widely used applications, where the pressure loss determines fan power requirements.

Although variations in—and prediction of—pressure drop in different porous media and effects of bed geometry have been studied (Coulaud, Morel et al. 1988), several aspects remain to be investigated, both numerically and experimentally. For example, fluid flow behavior through pores of packed beds of large particles is not completely understood. Further, for underground mining ventilation system design, there is no universal equation to calculate the pressure drop through a PRB made of large-sized broken rock. Unlike channel flow, fluid flow through porous media is complex due to the random structure of porous media, with high spatial variability in internal geometric features like porosity, permeability, and tortuosity (Burdine 1953). Hence, understanding the pressure gradient requires that the fluid flow through the pores is investigated, followed by the energy exchange rate between the air and solid phases—and all heat transfer mechanisms involved. Finally, broadly applicable relationships for many kinds of porous media have not yet been developed: findings are mainly based on experimental data for specific conditions and solutions are valid only for specific porous media under those conditions.

There are two widely employed methods to predict the pressure drop through the porous media: the Ergun equation and the Forchheimer equation. According to the literature, neither has specific advantages over the other (Dukhan, Bağcı et al. 2014) and both have been used. Both equations have viscous term and inertia terms, but they differ by correction factors (Table 2.1).

Table 2.1. Original and modified constants used in Ergun/Forchheimer correlations for media with different porosities and particle sizes

| | Model | Constant A | Constant B | Porosity ε | Particle size (mm) |
|---|---|---|---|---|---|
| Ergun-based studies | (Ergun and Orning 1949) | 150 | 1.75 | 0.35–0.55 | – |
| | (Happel 1958) | 165 | – | 0.2–0.78 | – |
| | (Dudgeon 1966) | 326–287 | 1.24–1.58 | 0.37–0.38 | 15.97–21.33 |
| | (England and Gunn 1970) | 180 | 2.0 | 0.35 | – |
| | (Kyan, Wasan et al. 1970) | 236–184 | 14.1–12.1 | 0.68–0.83 | 0.42–0.03 |
| | (Rumpf and Gupte 1971) | 162–124 | 1.49–1.09 | 0.36–0.64 | 0.67 |
| | (Reichelt 1972) | 200 | 2.0 | 0.36 | 9.71–24.5 |
| | (Macdonald, El-Sayed et al. 1979) | 124–162 | 1.09–1.49 | 0.37–0.64 | 0.68 |
| | (du Plessis and Woudberg 2008) | 170–200 | 1.35–2.00 | 0.2–0.8 | – |
| | **Model** | **Carman-Kozeny coefficient** | | **Porosity ε** | **Particle size (mm)** |
| Forchheimer-based studies | (Beavers and Sparrow 1969) | 5 | | 0.35–0.55 | - |
| | (England and Gunn 1970) | 5 | | 0.35 | - |
| | (Fand, Kim et al. 1987) | 5.12–5.33 | | 0.35 | 2–3.7 |
| | (Comiti and Renaud 1989) | 3.89 | | 0.31–0.46 | 1.12–4.99 |
| | (Rode, Midoux et al. 1994) | 5.11–5.28 | | 0.4 | 2.5–3.2 |
| | (Bağcı, Dukhan et al. 2014) | 2.82–3.69 | | 0.35 | 1-3 |

### 2.1.1. Ergun correlation and Ergun-based studies

The pioneering semi-empirical study by Ergun (1952) presented a correlation to describe the pressure drop within a packed bed of spherical particles as a function of porosity and particle diameter:

$$\frac{\Delta p}{\mathrm{L}} = \nabla p = -\left(\frac{\boldsymbol{A} \times (1-\varepsilon)^2 \mu \mathbf{U}}{d^2 \times \varepsilon^3} + \frac{\boldsymbol{B} \times (1-\varepsilon) \rho \mathbf{U}^2}{d \times \varepsilon^3}\right) \tag{2.1}$$

where $\nabla p$ is the pressure loss per unit length ($\Delta p$/L) in units; A, B are Ergun coefficients; ε is porosity; $d$ is particle diameter; $\rho$ is fluid density; **U** is physical velocity; and $\mu$ is dynamic viscosity.

The generality of constants A and B is widely debated (Lacroix, Nguyen et al. 2007, Montillet, Akkari et al. 2007, du Plessis and Woudberg 2008, du Plessis, Liebenberg et al. 2013). Many researchers (Fand, Kim et al. 1987, Comiti and Renaud 1989, Kececioglu and Jiang 1994) claimed

that these values are not constants for all porous media and should be empirically obtained for each case. (Macdonald, El-Sayed et al. 1979) recommended using different values for A and B, depending on factors like porosity, particle size, and particle roughness. The square root of the permeability is recommended as a suitable characteristic length for defining the Reynolds number ($Re_k$) in porous media, which is a measure of laminar or turbulent flow:

$$\mathrm{Re_k} = \frac{\text{inertial forces}}{\text{viscous forces}} = \frac{\boldsymbol{\rho}\mathbf{U}}{\mu}\sqrt{K} \tag{2.2}$$

where $\rho$ is fluid density, $\mathbf{U}$ is physical velocity, $\mu$ is dynamic viscosity, and $K$ is permeability.

(Ward 1964) developed and validated an equation applicable to both laminar and turbulent flow in porous media. The pressure gradient can be calculated as a function of the fluid viscosity, fluid density, and macroscopic velocity. Like many other researchers, Ward utilized the square root of the permeability as a characteristic length scale. Glass beads, sand, gravel, and granular activated carbon were used to represent the porous media. Among them, the glass beads media were assumed to be uniform in particle size.

(Hicks 1970) proposed experimental determinations of Ergun constant values that differed from original Ergun values, even for a packed bed of smooth spheres. He claimed that the Ergun equation is inappropriate for packed beds of spheres where channeling occurs, and deviations from the "all pressure drop correlations" should be expected for different kinds of beds of spheres, especially at higher flow velocities. Consequently, the values in the Ergun correlation differ in terms of Reynolds number and are commonly recognized to not be constants. These coefficients can be used to predict transfer rates in beds with flow regimes as a function of the Reynolds number. Hicks asserts that the pressure drop equation, as well as the friction factor correlation, are not intended to be a general correlation for packed bed and that the Ergun equation may just be valid for a range of Reynolds number. Therefore, this well-known correlation should be restricted to a certain fluid flow range in porous media.

(Tallmadge 1970) also stated that the Ergun equation does not sufficiently describe bed behavior at high Reynolds number (Equation 2.3). He studied packed beds of spheres over a wide range of porosity (0.35–0.88) at high Reynolds number and proposed an improved friction factor equation for wide ranges of both porosity and Reynolds number, which considers the noticeable effect of Reynolds number on the turbulent flow regime (Equation 2.4).

(Ergun 1952)

$$f = \frac{150}{Re} + 1.75 \tag{2.3}$$

(Tallmadge 1970)

$$f = \frac{150}{Re} + \frac{4.2}{Re^{1/6}} \tag{2.4}$$

(Macdonald, El-Sayed et al. 1979) stated that the most serious problem in predicting the pressure drop in porous media is the lack of parameters characterizing such a medium. Thus, the geometric characteristic parameters must be functions of the medium rather than universal constants and must be empirically obtained for specific porous media. They proposed the following equation:

$$f\frac{\varepsilon^3}{1-\varepsilon} = \frac{180(1-\varepsilon)}{Re} + B \tag{2.5}$$

where B is a function of particle roughness and varies from 1.8 (smooth particles) to 4 (rough particles). The authors claimed that their proposed equation is accurate for a broad range of unconsolidated porous media (porosity range 0.36–0.92), which is one advantage of this study relative to others in the literature. Their results suggest that substituting the $\varepsilon^3$ from the Ergun equation with $\varepsilon^{3.6}$ may give a more accurate porosity function. The other important outcomes of their study are two proposed correlations for calculating $A$ from particle size $d$ as well as ε:

$$A = 3.27 + 118.2d \tag{2.6}$$

$$A = 214.25 - 151.72\varepsilon \tag{2.7}$$

where $d$ varies from 0.46 to 316 mm and porosity varies from 0.35 to 0.65.

(Dybbs and Edwards 1984) reviewed the results of laser anemometry and flow visualization methods to analyze fluid flow behavior of several liquid flows like water, silicone oils, and mineral seal oil in a packed bed of spheres, including glass and Plexiglas particles (diameter 12.7 mm, porosity 0.394). Various flow regimes were used from the Darcy to turbulent flow regime with a range of Reynolds number from 0.16 to 700. An analytical equation was proposed based on their

experimental results, which yielded similar pressure drop behavior for all flow regimes. Also, the applicability of their results to other transport phenomena was discussed.

(Fand, Kim et al. 1987) obtained experimental fluid flow data within randomly packed bed of uniform (2, 3, and 4 mm diameter) and non-uniform (2.8, 3.3, and 3.7 mm average diameter) spherical particles. They used water as a fluid passing through porous media. The validity of Darcy and Darcy-Forchheimer flow regime for packed beds of uniform and non-uniform particles were found to be consistent. They also proposed the Kozeny-Carman constant equal to 5.34. They claimed that the modified Ergun constants (A=182 and B =1.92) yield more accurate pressure drop estimations in the Forchheimer regime for all examined packed bed of spheres in their study. However, their proposed Ergun constants for the turbulent regime were A=225 and B=1.61.

(Rode, Midoux et al. 1994) performed a literature survey on electrochemical shear rate sensors to study fluid flow behavior in packed beds of spherical particles of 5 mm diameter with a porosity of 0.4. They found extremely non-homogenous local flow within the pores. They considered characteristic length scales to determine the velocity changes in the pores, especially at high Reynolds number ranges. They also claimed that circular electrochemical probes can be practically utilized to measure the local velocity gradients, even in extremely fluctuating flow conditions.

(Comiti and Renaud 1989) tested packed beds of spherical particles (1.12 and 4.99 mm diameter) and proposed a constant value 141 for A and 1.63 for B. They also showed that the fluid flow behavior within packed beds of parallelepipedal particles, for example wood chips used in the paper pulp industry, is not the same as the fluid flow within packed beds of particles. In order to analyze the structural characteristics of packed beds, they used two parameters, the tortuosity and the specific surface area, as main restrictions to determine pressure drop in porous media.

(Kececioglu and Jiang 1994) determined the water flow resistance in packed beds of 3 and 6 mm diameter uniform spherical particles. Their experimental results distinguished the flow regime segregation criteria during water flow through a randomly packed bed of spherical beads. Flow rates varied between $5.07 \times 10^{-6}$ and $4.92 \times 10^{-3}$ m/s. They stated that the data in the literature is insufficient to understand the flow regimes through packed beds. They considered a different characteristic length scale from those of (Fand, Kim et al. 1987). They also believed that the square root of the permeability may be the most appropriate characteristic length scale in such porous

media, not the particle diameter. They used a modified form of the Ergun correlation to estimate the pressure drop in Forchheimer and turbulent regimes.

(Seguin, Montillet et al. 1998) focused on local measurements of fluid movements in porous media accompanied by signal oscillation analysis, which helped predict the start of the transition regime. They used packed bed of spherical particles of 5 and 8 mm diameter. They also investigated the influence of fluid flow direction on pressure drop in porous media. They used a capillary model to investigate fluid flow behavior within the porous media, which took into consideration the porosity, tortuosity, and specific surface area of the porous media. They also studied the fluid flow behavior at higher velocities to investigate the flow regime transition from laminar to turbulent. They found that transition regimes in porous media, unlike open pipe flow, was gradual and did not emerge at the same Reynolds number in all sections in the porous media.

(Venkataraman and Rao 1998) analyzed resistance equations for fluid flow within porous media. They organized published data related to the pressure drop in porous media, focusing on friction factor and Reynolds number definitions. Similar to many other researchers, they determined the frictions factor and Reynolds number by considering the square root of the permeability as the proper characteristic length scale in porous media.

(Jamialahmadi, Müller-Steinhagen et al. 2005) experimentally measured the pressure drop and heat transfer coefficients in packed beds of 32 mm diameter spheres over a wide range of superficial gas velocities. They presented a theoretical model to calculate the pressure drop and heat transfer coefficients to compare the experimental data.

(Zeng and Grigg 2006) used the Forchheimer number—the ratio of pressure drop attributed to interactions between fluid and solid to that consumed by viscous resistance—for nitrogen flow in sandstone and limestone. They reconciled the Forchheimer number and stated that it provides a wide applicability and a strong physical sense. They presented the Forchheimer number as a critical value for the predicting the starting point of the Darcy-Forchheimer flow regime.

(Moutsopoulos 2007) developed a new analytical equation to compute the water stored/extracted from an aquifer, including modified viscous coefficients. They also investigated the unsteady flow in a semi-infinite aquifer. They stated that the influence of inertial forces is dominant for short

terms; however, the viscous effects can be seen for longer times. They used the Forchheimer equation in their study.

(Montillet, Akkari et al. 2007) examined the validity and applicability of available correlations to predict pressure drop in packed beds of spheres. They obtained a new set of data by using dense and loosely packed beds with a wide range of bed geometric aspect ratios (3.8–14.5). They proposed a new correlation for predicting pressure drops through these packed beds of spheres for broad ranges of Reynolds numbers up to 2500. They modified the equation proposed by (Rose 1945) and (Rose and Rizk 1949), and adapted it by introducing a new correlating factor as a function of the porosity and bed geometric aspect ratio (Equation 2.8):

$$f = a\left(\frac{1-\varepsilon}{\varepsilon^3}\right)\left[\frac{D}{d_p}\right]^{0.20}\left[1000Re^{-1} + 60Re^{-0.5} + 12\right] \qquad \begin{matrix}\text{for dense packings} & a = 0.061 \\ \text{for loose packings} & a = 0.050\end{matrix} \qquad (2.8)$$

(Ozahi, Gundogdu et al. 2008) predicted the pressure drop through a packed bed of spherical and non-spherical (cylindrical) particles to examine the applicability of the Ergun correlation to packed beds of non-spherical particles (i.e., effects of sphericity). They used particles ranging from 6 to 18 mm and porosities of 0.36–0.56. They concluded that the Ergun equation can be used in all packed beds of particles with sphericity ranging from 0.55 to 1.00, with a maximum deviation of ±20%. They also stated that the constant Ergun values are not only affected by particle geometry, but also they may change in packed beds with the same particle size due to different arrangements of particles in the bed.

(Huang, Wan et al. 2013) experimentally investigated one-dimensional uniform flow in porous media using four packed beds of 3, 5, 8, and 10 mm diameter spheres. They showed that Darcy's Law approximates fluid flow by ignoring the inertial term at low velocity. Thus, nonlinearity is related to the inertial term in porous media, even before the turbulent flow appears. They also stated that the Forchheimer correlation with constant coefficients can interpret fluid flow behavior in porous media. They indicated that the Ergun coefficients have certain relations with porosity and would change for different porous media.

(Kundu, Kumar et al. 2016) experimentally investigated the single-phase fluid flow behavior within different kinds of porous media using three particle diameters (2.5, 3.5, and 5 mm) to generate packed beds of uniform and non-uniform particle sizes. They presented the pressure

gradient correlation as a function of velocity. Two characteristic length scales, particle diameter, and permeability of porous media, were considered to determine the friction factor and Reynolds number. They described all different flow regimes in porous media and categorized them according to the interactions between solid and fluid, and the pressure drop and the viscous forces in a wide range of Reynolds numbers. They concluded that the flow regime varies from the Darcy to the Forchheimer flow regime in the critical Reynolds number range (5–10) in a packed bed of 2.5 mm spherical particles.

(Feng, Zhang et al. 2019) claimed that the experimental correlations of pressure drop and friction factor differ for packed beds of spherical particles. They experimentally investigated the pressure drop behavior of air flow in packed bed with sinter particles and introduced the concept of the modified pressure drop (also called the reduced pressure drop) as a function of air superficial velocity and particle diameter in porous media. The particle size and porosity varied from 6 to 35 mm and 0.42 to 0.53, respectively, in their experimental set-up. The modified pressure drop slowly increased with decreasing particle diameter for a given air flow rate and increased as a first power relationship with the air velocity, which is consistent with previous published literature. They also stated that randomly packed beds may directly result in the presence of inertial resistance loss, which dominates in the resistance loss of air flow at high Reynolds number.

### 2.1.2. Forchheimer correlation and Forchheimer-based studies

To calculate the pressure drop in porous media, the Forchheimer equation is also used. This empirical correlation was developed by using analogy with pipe flow, with coefficients as correction factors to account for viscosity and inertial terms (Dukhan, Bağcı et al. 2014):

$$\frac{\Delta p}{\mathrm{L}} = \nabla p = -\left(\frac{\mu \mathbf{U}}{K} + F\frac{\rho \mathbf{U}^2}{\sqrt{K}}\right) \tag{2.9}$$

where F is the Forchheimer coefficient that accounts for inertia drag. Forchheimer equation uses the following equation for the permeability as a function of particle size and porosity:

$$K = \frac{d^2 \times \varepsilon^3}{36k(1-\varepsilon)^2} \tag{2.10}$$

where $k$ is the Carman-Kozeny constant. The viscous resistance coefficient ($\alpha$=1/K) and inertial resistance coefficient ($\beta = \frac{F}{\sqrt{K}}$) determine the porous structure and must be determined to calculate the pressure gradient through porous media analytically.

(Beavers and Sparrow 1969) measured water flow behavior in five metallic fibrous porous media. The square root of the permeability was used as a characteristic dimension. They developed their study based on Forchheimer equation and proposed the friction factor as a function of Reynolds number:

$$f = \frac{1}{Re_k} + 0.074 \tag{2.11}$$

They claimed that their proposed equation is valid for metallic fibrous porous media without free ends in the medium.

(Vafai and Tien 1981) determined the importance of inertial forces on fluid flow (air, water, light oil, and engine oil) and heat transfer in porous media (particle diameters 0.1–1 mm) based on the Forchheimer equation. They stated that fluid flow analysis within the complex structure of a porous medium can be conducted by the Forchheimer equation, but the correlations should be redefined for each specific medium. Thus, due to the complexity of porous media, it is very difficult to propose a general solution for predicting the pressure drop.

(Antohe, Lage et al. 1997) developed their study based on the Forchheimer model to predict the permeability and inertia coefficient of compressed aluminum porous media using air as a heat transfer fluid (HTF). Nine porous media were tested (porosity 0.3–0.7) and Forchheimer coefficients were calculated (0.3–0.9). They also discussed the limitations of measuring hydraulic characteristics in an experimental set-up.

(Teruel and Rizwan 2009) stated that no general equation can be found in the literature to predict the Forchheimer coefficient as a function of different parameters of the porous structure. Hence, the Forchheimer equation is not able to predict pressure drop and friction factor in all kinds of porous media. They found that the Forchheimer coefficients strongly depend on the porosity and are less dependent on flow regime.

(Weise, Meinicke et al. 2019) derived a pressure drop model of two-phase flow based on the Forchheimer correlation using sponges (porosity 0.83–0.95) as porous media. They also assessed the validity of their model across a wide range of Reynolds number.

(Zhou, Hu et al. 2016) formulated the friction factor equation comprising both viscous and inertia terms based on the Forchheimer correlation. They analyzed the friction factor to predict the pressure drop in rock fractures, the effect of flow regimes, and the rock roughness on the pressure drop investigated by (Zhou, Hu et al. 2016). They also stated that their proposed equation has a better physical significance as well as more accurate predictive performance.

The literature review highlights numerous achievements in experimental and numerical study on fluid (primarily water) flow through packed beds of small spheres. However, no quantitative studies examine the airflow behavior in packed bed of large spheres. In this thesis, I attempt to develop a numerical pore-scale model with large rock size typical of the mining industry (i.e., 0.04–1.2 m rock fragments). Differences among pressure drop correlations reported in the literature render them difficult to use without performing computational analysis of the complex porous media structure. Therefore, one goal of this thesis is to numerically investigate the effects of particle size, porosity, and air velocity on pressure drop in such porous media using published data. The literature survey on fluid flow in porous media shows some disagreement regarding how to define the appropriate criteria for flow regimes transition, pressure drop prediction, and characteristic length scale that should be used in determining the Reynolds number and friction factor.

In summary, published experimental, analytical, and numerical data primarily encompass packed beds of small particles in pre-Darcy, Darcy, Forchheimer, and turbulent flow regimes and primarily consider water as a HTF. The study presented here uses packed beds of large particles and considers air as the HTF. Understanding fluid flow in these packed beds can directly facilitate predicting the pressure drop through these packed beds in many industrial applications, for example in the design of mine ventilation systems and heat storage systems, and thus assist in interpreting and predicting the fan power demand for circulating air in such media.

## 2.2. Heat transfer in porous media

Heat transfer is a very common phenomenon that occurs in many engineering applications involving porous media, including TES systems, geothermal energy extraction, and solar energy storage systems. The high specific surface area per volume unit of porous media (usually in the order of $10^9$/m) optimizes heat transfer and makes it a promising structure for storing/extracting energy (Weller, Slater et al. 2010). As a result, numerous experimental, analytical, and numerical studies have investigated fluid flow and heat transfer in porous media for a variety of applications.

### 2.2.1. Thermal conductivity in porous media

The effective thermal conductivities of different types of porous media have been investigated using a variety of methods and conditions. Determining the thermal properties of porous structures like TES systems is crucial to their design and operation. Also, heat transfer mechanisms should be quantified to evaluate porous media. Published thermal data on packed particle beds relate to a two-phase porous structure: solid phase (subscript *s*) and fluid phase (subscript *f*). The effective thermal conductivity ($k$) of such a structure depends on the thermal conductivity of both phases ($k_s$ and $k_f$), and the volume of the solid (1–ε) and fluid phases (ε), where ε is the porosity of the bed (Table 2.2).

Table 2.2. Fundamental effective thermal conductivity models for two-phase porous media

| Model | Equation | References |
|---|---|---|
| Parallel model | $k_{Max} = (1-\varepsilon)k_s + \varepsilon k_f$ | (Nield and Bejan 2006) |
| Maxwell–Eucken model (1) | $k = k_s \frac{2k_s + k_f - 2(k_s - k_f)\varepsilon}{2k_s + k_f + (k_s - k_f)\varepsilon}$ | (Wang, Carson et al. 2006, Gong, Wang et al. 2014) |
| Maxwell–Eucken model (2) | $k = k_f \frac{2k_f + k_s - 2(k_f - k_s)(1-\varepsilon)}{2k_f + k_s + (k_f - k_s)(1-\varepsilon)}$ | (Wang, Carson et al. 2006, Gong, Wang et al. 2014) |
| EMT models | $(1-\varepsilon)\frac{k_s - k}{k_s - 2k} + \varepsilon\frac{k_f - k}{k_f + 2k} = 0$ | (Wang, Carson et al. 2006, Gong, Wang et al. 2014) |
| Series model | $\frac{1}{k_{Min}} = \frac{1-\varepsilon}{k_s} + \frac{\varepsilon}{k_f}$ | (Nield and Bejan 2006) |

In general, the actual effective thermal conductivity is between $k_{Max}$ and $k_{Min}$. More complicated correlations to determine the overall thermal conductivity of packed beds have been proposed and their applicability can be categorised into three main groups: $k_s \ll k_f$ , $k_s \gg k_f$ and $k_s \cong k_f$. In the case of PRBs with air as a HTF, we have: $k_{Rock} \cong 2.68\ (W/(m.K) \gg k_{air} \cong 0.024\ (W/(m.K)$. It should be noted that the distribution of both phases in the bed can have a meaningful effect on the $k$ of the system. In addition, $k$ may also depend on the particle size and pore size distribution, especially at high temperatures when pore sizes are large enough that convective heat transfer is possible.

### 2.2.2. Heat transfer coefficient and Nusselt number

The best-fit correlations are based on experimental and computational data (Wakao, Kaguei et al. 1979, Gunn 1987, Khan, Beasley et al. 1991, Mehrabian, Shiehnejadhesar et al. 2014). An extensive array of approaches to model convective heat transfer for porous media have been published (Table 2.3). Although these correlations can predict the heat transfer characteristics of porous media consisting of small particles, their applicability to packed beds of large particles has not been confirmed. The main factors that have a meaningful effect on the prediction of forced convection are the Nusselt number (Nu), Reynolds number ($\mathrm{Re_d}$), Prandtl number (Pr), and porosity of the packed bed (Achenbach 1995).

Table 2.3. Published equations for determining convective heat transfer for two-phase porous media

| Equation | Application range | References |
|---|---|---|
| $Nu = 1.77(\pm 1.39) + 0.29\varepsilon^{-0.81} Re_d^{0.73} Pr^{0.5}$ | $\varepsilon = 0.41 - 0.54$ | (Singhal, Cloete et al. 2017) |
| $Nu = 2 + 1.1 Re_d^{0.6} Pr^{0.33}$ | $Re_d = 15 - 10^4$ | (Wakao and Kagei 1982) |
| $Nu = \left(2 + \frac{12(1-\varepsilon)}{\varepsilon}\right) + \frac{1}{2}(1-\varepsilon)^{1/2} Re_d^{0.6} Pr^{0.33}$ | $Re_d = 3 \times 10^{-3} - 5 \times 10^3$<br>$\varepsilon = 0.36 - 0.96$ | (Kuwahara, Shirota et al. 2001, Nakayama 2014) |
| $Nu = \left(2 + \frac{8(1-\varepsilon)}{\varepsilon}\right) + \frac{1}{2}(1-\varepsilon)^{1/2} Re_d^{0.6} Pr^{0.33}$ | $\varepsilon = 0.2 - 0.9$ | (Pallares and Grau 2010) |
| $Nu = \left(\frac{1-\varepsilon}{\varepsilon}\right)(0.5 Re_d^{0.5} + 0.2 Re_d^{0.67}) Pr^{0.33}$ | $Re_d = 20 - 10^4$<br>$\varepsilon = 0.34 - 0.78$ | (Kreith, Manglik et al. 2012) |

| | | |
|---|---|---|
| $Nu = (0.255/\varepsilon)Re_d^{0.6}Pr^{0.33}$ | $Re_d > 10^2$ | (Nield and Bejan 2006) |
| $Nu = 0.269Re_d^{0.88}Pr^{0.33}$ | $Re_d = 9 - 96$<br>$Pr = 2.2 - 3.3$ | (Guardo, Coussirat et al. 2006) |
| $Nu = (7 - 10\varepsilon + 5\varepsilon^2)(1 + 0.7Re_d^{0.2}Pr^{0.33}) + (1.33 - 2.4\varepsilon + 1.2\varepsilon^2)Re_d^{0.7}Pr^{0.33}$ | $Re_d < 10^5$<br>$\varepsilon = 0.35 - 0.99$ | (Gunn 1987) |

With new advanced experimental technologies, it is now possible to characterize physical and thermophysical properties of porous media. Moreover, advanced computational tools make it possible to analyze heat transfer phenomena in a variety of porous media, especially when the media are complex or inaccessible (e.g., the caved-zone in a longwall mining operation).

When fluid flows through a packed bed, several heat transfer mechanisms will be present (primarily conduction and convection), which must be taken into account to fully understand the operation of a TES system (Ghoreishi-Madiseh, Sasmito et al. 2015, Amiri, Ghoreishi-Madiseh et al. 2017, Ghoreishi-Madiseh, Sasmito et al. 2017). One of the main advantages of TES technology is the fact that a high heat transfer rate can be achieved during operation due to the large total interphase heat transfer area. During non-operating periods, with the absence of flow the heat conduction and consequently dispersion and heat losses can be maintained at low levels.

Heat transfer mechanisms in porous media are usually numerically analyzed via:

1. the pore-scale method (see section 2.2.3)
2. the volume averaging method (i.e., representative elementary volume (REV) model; see section 2.2.4)

The physical and theoretical understanding of the fluid flow behavior within porous media is fundamentally linked with the definition of length scales. Length scales can be categories as pore-scale (i.e., microscopic scale), local-scale (i.e., macroscopic scale) and field-scale (Sposito, Jury et al. 1986). In recent years, the process of scaling up from microscopic to macroscopic to field-scale has received significant attention (Hlushkou, Hormann et al. 2013, Mathey 2013, Nordlund, Lopez Penha et al. 2013, Gavriil, Vakouftsi et al. 2014, Pan, Chen et al. 2016).

Macroscopic properties (e.g., porosity, permeability) are generally defined by the REV model. Thus, they can be determined by the volume averaging technique of microscopic properties over the REV. Volume averaging makes the boundary value problem simpler by considering only the large-scale flow behavior. This can be developed by averaging the governing equations over the REV (Whitaker 1986). If the REV model is correctly chosen, adding extra volume, around it will not have a meaningful effect on the results (Nield and Bejan 2006). The smallest macroscopic length scales, $d_{\mathrm{Fluid}}$ and $d_{\mathrm{Solid}}$ , are an average pore and particle diameter, respectively, while the largest macroscopic length scale, $L$, is the characteristic length of flow domain. Also, the macroscopic length scales, $l$, is the characteristic length of REV. In most cases, the volume averaged method is valid when $l \geq 5d_{\mathrm{Fluid}}$, $l \geq 5d_{\mathrm{Solid}}$ and $l \ll L$ are satisfactory (Whitaker 1986).

The pore-scale (Manz, Gladden et al. 1999, Blunt 2001, Wang, Yang et al. 2018) and other advanced numerical methods (Manz, Gladden et al. 1999, Jiang, Khadilkar et al. 2002) have made it possible to study transport phenomena in porous media at the pore scale. The challenge is to accurately define the pore space geometry to obtain detailed predictions of macroscopic properties of the porous media (Blunt 2001). In recent years, several numerical models have been developed to study the behavior of fluid flow and heat transfer in porous structures. The most relevant to this study is from Thompson and Fogler (1997), who developed a packed bed of spherical particles (porosity of 0.38–0.45 and particle size 1–8 cm) to study the fluid flow behavior within such a porous media. They used the network strategy to incorporate microscopic heterogeneity into the media and quantitatively compare the experimental macroscopic parameters and the pore-scale fluid mechanics. Then, from the microscale geometry in discrete pores, fluid conductivities were numerically solved by the Navier-Stokes equations for flow through the pores. Finally, the permeabilities of packed beds comprising various uniform spherical particles were calculated and compared with the experimental results. Another study (Balhoff, Thompson et al. 2007) coupled the packed bed of spheres and adjacent continuum-scale models, the heterogeneity of the packed bed, as well as the resistance of the adjacent medium to show that the pore-scale model and macroscopic behavior completely differ when they are directly coupled rather than using decoupled boundary conditions.

### 2.2.3. Pore-scale method

For the pore-scale model, the mass, momentum and energy equations are directly solved; no other terms need to be introduced. The major difficulties of this method are associated with geometry development in addition to mesh generation. Furthermore, utilizing a pore-scale model needs more time and has higher computational cost. The heat transfer characteristics between the fluid and the surface of ceramic foams with pore-scale modelling was studied by (Wu, Caliot et al. 2011). Their porous structure was generated by periodic regular structures formed with packed tetrakaidecahedra. They also proposed a local volumetric heat transfer coefficient correlation as a function of porosity and fluid velocity. They stated that the local heat transfer coefficient growths with the Reynolds number and it is independent on the porosity.

(Du, Li et al. 2017) worked on a fully coupled heat transfer model of porous structure. They analyzed the thermal performance of a solar receiver using a pore-scale model. They considered three heat transfer phenomena simultaneously: the heat conduction of porous structure, the heat convection between the solid and air phase, and the radiation heat transfer in porous media. They also proposed the Nusselt number correlation as a function of Reynolds number which could be employed in volume-averaged models.

In another study by (Zafari, Panjepour et al. 2015), the real geometries of foam with dimensions 10×10×10 mm was used to investigate the heat and mass transfer phenomena through pores. They found that the non-equilibrium thermal condition occurs within the foam with porosities of 0.85–0.90 and that the local and average convection coefficient and Nusselt number strongly positively and negatively depend on the porosity. On the other hand, the local and average convection coefficient increase when introducing the higher air velocity through the porous media. Furthermore, the air density reduction due to temperature gradient increases the air velocity through the porous media by up to 70% (Zafari, Panjepour et al. 2015). Also, direct numerical simulation techniques were applied to study the geochemical processes with subsurface flow through the pores at the pore scale level by (Molins, Trebotich et al. 2012).

### 2.2.4. Volume averaging method

The first step of developing the volume-averaged model is to introduce accurate empirical (or semi-empirical) terms to the momentum and energy equation. Then, the effects of different

parameters of porous media on the fluid flow behavior and heat transfer phenomena can be studied. Two conditions are assumed: local thermal equilibrium (LTE) or local thermal nonequilibrium (LTNE) (Kim and Jang 2002). The LTE condition between the solid and fluid phase in porous media cannot always be achieved, thus, the LTNE assumption is widely used to study fluid flow as well as conjugate heat transfer phenomena (Amiri, Ghoreishi-Madiseh et al. 2017, Amiri, Ghoreishi-Madiseh et al. 2018).

The effects of LTE and LTNE assumptions on the fluid and solid phase temperature has been intensively investigated. Whereas some studies (e.g., (Quintard and Whitaker 2000, Al-Sumaily, Hussen et al. 2014)) have shown that the temperature difference between rock and fluid in the LTNE condition is insignificant, which makes the LTE assumption appropriate, others (e.g., (Ghoreishi-Madiseh, Sasmito et al. 2017, Amiri, Ghoreishi-Madiseh et al. 2018) showed that LTNE can be more accurate for studying the heat exchange rate between rock and air; thus, even a very small difference in rock and fluid temperatures should be taken into account. For instance, in their studied of heat transfer phenomena in geothermal systems, Shaik et al. (2006) found that the LTE assumption would will lead a difference of 20°C in recycling fluid temperature within 25 years of operation. Further, (Al-Sumaily, Hussen et al. 2014) asserted that the LTE condition cannot adequately describe the fluid temperature in a porous media in a higher range of temperature. (Gelet, Loret et al. 2013) showed that LTNE models are the only accurate model to study heat transfer through a porous reservoir. In the other study, (Xu, Song et al. 2011) used the steady heat and mass transfer models of the porous media. They numerically solved the energy and momentum equation to study the effect of the porosity with a range of 0.15 to 0.35, particle size with a range of 0.025 to 0.125 mm, and air velocity with a range of 0.75 to 1.75 m/s on the performance of the system. They also used the LTNE equations in their study. However, in the other study (Cheng, He et al. 2013), volume-averaging technique were used for the porous absorber domain by assuming the homogeneous solid and fluid phase properties as well as the LTE equation.

(Kim and Jang 2002) proposed a general criterion for LTE in terms of some important engineering parameters, including the Prandtl number (Pr), Reynolds number (Re), Darcy number (Da), and Nusselt number (Nu) by the following equation:

$$\mathrm{Pr}\ Re\, Da^{0.5}\, \varepsilon\, Nu \ll 1 \tag{2.12}$$

The effect of LTE in a porous medium will be stronger if Pr, Re, or Da decrease or Nu increases; furthermore, when the effective thermal conductivity ratio goes up, the LTE condition can be assumed because Pr is inversely proportional to it (Kim and Jang 2002).

## 2.3. Underground mine environmental condition

### 2.3.1. Heat source in underground mines

Several heat sources contribute to heating air underground, including rock walls, equipment, and auto-compression—the conversion of potential energy into thermal energy (Hartman, Mutmansky et al. 2012, Sbarba 2012). The temperature of broken rock depends on the depth and site-specific geothermal gradient, which influence the potential to harvest geothermal energy (Hartman, Mutmansky et al. 2012, Sbarba 2012). Machinery and mining equipment produce large amounts of waste heat because their efficiency is only approximately 33% (Sbarba 2012). Heat in an underground mine means more ventilated cold air is required.

### 2.3.2. Energy demand in underground mine

The industrial sector (mining, chemical, petroleum, and base metals) consumes approximately 37% of the world's total delivered energy and among them, mining industry contributes about 9% (Abdelaziz, Saidur et al. 2011) (Masnadi, Grace et al. 2015, Yu, Gao et al. 2016). Energy intensity is a major hurdle to future development of the global mining industry. It derives from two major issues:

1) the insatiable demand of the mining industry for energy for electricity, heating, and cooling
2) unpredictable fossil fuel prices caused by numerous political and economic factors

This enormous energy need is accompanied by a long-term rising trend in fossil fuel prices. Therefore, energy costs constitute a growing portion of the total operating costs of mining operations, which will be exacerbated by the introduction of carbon taxes by some industrial countries (Ploeg and Withagen 2014). The unreliable nature of the energy market is a fundamental risk source, making operating costs difficult to predict. These major issues have motivated the mining industry to seek new energy sources and technologies (e.g., absorption chillers and heat

pumps; (Wu, Wang et al. 2014) to help improve the energy efficiency, reduce energy demand, and shrink the carbon footprint of operations (Bharathan, Sasmito et al. 2017).

Among the energy-intensive activities at an underground mine, ventilation (fresh air, air heating and cooling) is a top contributor. Ventilation energy demands are in form of electricity (to run main/booster/auxiliary fans for air delivery or mechanical refrigeration for cooling) or thermal heat (Chatterjee, Zhang et al. 2015). The heating demand is usually met by burning fossil fuels (mostly natural gas, propane or diesel), whereas cooling uses electricity (taken from the grid or generated with diesel generators).

Mine ventilation is essential to run a comfortable and safe working environment underground; it also clear out noxious and flammable gases (Chatterjee, Zhang et al. 2015). In Canada and other countries such as the USA and Australia, the quality and quantity of ventilation air is regulated. For example, the fresh air flow required in hard rock mines in the Canadian province of Ontario is regulated at 0.06 $m^3/s$ per kW of diesel engine power at a wet bulb globe air temperature below 27°C (Mayala, Veiga et al. 2016). To ensure good air quality, especially in the deepest galleries and work faces, enormous amount of fresh air (100–1000 $m^3/s$) are required. In extremely cold climates, like winter in Canada and many areas in the USA, intake air must be preheated to above 0°C before sending it down the main ventilation shaft(s) because blowing very cold air to the down-cast ventilation shaft(s) can have serious consequences:

i. extreme cooling of workspaces, affecting worker their health and productivity
ii. accumulation of ice within the shaft
iii. freezing of subsurface facilities

Preheating and cooling practices account for 50–80% of annual ventilation operating costs ($4–20 million), depending on the mine depth, production, temperature, and air flow rate (Karacan 2007, Bharathan, Sasmito et al. 2017). Over the past few years, several studies have focused on cost-effective ventilation solutions for underground mines (Kurnia, Xu et al. 2016).

### 2.3.3. Renewable energies and alternative energy solutions as an energy source

In recent years, there has been a interest in the application of renewable energy and waste heat recovery (Brown 2000, Madiseh, Ghomshei et al. 2012). However, limited research has focused

on the techno-economic advantages of using large-scale energy storage units in large-scale heating/cooling systems (Persson and Westermark 2013, Colclough and McGrath 2015, Sommer, Valstar et al. 2015). Some part of the energy demand in different industrial sectors can be fulfilled by storing the available renewable energies or using alternative energy solutions. The following section presents the renewable energy sources available at mine site and remote communities.

- ***Geothermal energy***

Geothermal energy has proven to be stable, accessible, and safe to use for power production with minimal and controllable environmental impacts (Kömürcü and Akpınar 2009). From 1975 to 2010, the worldwide installed geothermal capacity grew more than 8-fold, from 1,300 MWe to 10,715 MWe (Gallup 2009, Bu, Ma et al. 2012). The ground temperature at 10–20 m depth remains constant and independent of climatic variations (Sanner 1993). Deeper in the ground, temperatures increase at an average rate of 10–30°C/km (Ednie and Hassani 2007). Despite the advantages of this renewable energy, a barrier to geothermal development is the high capital cost associated with drilling wells to access high-temperature rock, which can account for as much as 50% of the total cost of a geothermal project (Bu, Ma et al. 2012). Solutions to decrease the cost of drilling include using existing shafts, tunnels and openings in underground mines and more recently, using abandoned wells has been evaluated (Kujawa, Nowak et al. 2006, Davis and Michaelides 2009, Templeton, Ghoreishi-Madiseh et al. 2014).

- ***Seasonal thermal energy***

Storage of large quantities of thermal energy can increase energy efficiency in mine ventilation systems (Sylvestre 1999). This unique concept takes advantage of the huge volumes of waste/broken rock mass available on the surface of the mine for the purpose of seasonal thermal heat storage (STES). Seasonal variations in ambient temperature provide permit storing thermal energy (hot and cold) in the broken rock mass in form of sensible heat. Seasonal heat storage for heating and cooling applications seems to be an effective solution to compensate for seasonal energy demands (Novo, Bayon et al. 2010, Ghoreishi-Madiseh, Hassani et al. 2015, Ghoreishi-Madiseh, Sasmito et al. 2017).

To create a STES system, huge volumes of waste rock are dumped into a decommissioned pit to create a large seasonal heat storage mass. This massive STES unit provides the mining operation

with a natural heat exchanger. The amount of sensible thermal energy stored in the STES system depends on the temperature difference between the air and rock mass. By passing ventilation air through the PRB, seasonal temperature oscillations can be moderated, reducing ventilation costs up to 80% (Sylvestre 1999, Ghoreishi-Madiseh, Sasmito et al. 2017, He, Luo et al. 2017). As a natural and renewable energy storage technique, STES can help deep underground mines meet refrigeration and air preheating requirements and reduce associated greenhouse gas emissions.

- ***The exhaust streams of a diesel generator***

A diesel generator is a combination of an internal combustion diesel engine and an electric generator. Even with the best available technology, diesel engines have an efficiency of only about 35%. That means that typically, up to 65% of the total energy input is discarded in the form of heat through exhaust gases (Bari and Hossain 2013). In these generators, from every 3 kW of fuel energy consumed, 1kW becomes electricity and the other 2 kW are wasted (Ghoreishi-Madiseh, Kuyuk et al. 2019), from which half (1 kW) is present on the exhaust gas (Bari and Hossain 2013).

Waste heat recovery of the exhaust streams of a diesel generator can be an indirect way of saving a considerable amount of primary fuel and decreasing the system's impact on global climate change (Pandiyarajan, Pandian et al. 2011). Rather than using the heat directly, the usual focus is to use the heat for power generation through organic Rankine cycles or thermoelectric generators because electrical power is more versatile (Ghoreishi-Madiseh, Kuyuk et al. 2019). However, conversion of heat to other energy forms has significant associated losses, and in a scenario where demand exists, direct heating can be a potential asset. For instance, for a remote, cold village with huge shipping costs, even recovering a fraction of the discarded heat can lead to significant savings in heating fuel (Mokkapati and Lin 2014).

One major challenge that often arises in implementing an alternative energy solution is the mismatch between demand and supply. In case of combined heating and power generation, lower heating demand in the summer enhances the challenge (Erlund and Zevenhoven 2018). Any waste heat recovery system faces problems because of this difference between the periods of availability and demand of the heating energy (Hasnain 1998). To confront this issue, a common approach is to employ STES techniques that store the surplus of the recovered waste heat during low heat

demand periods in a suitable storage medium (e.g., TES system) for several months to use when the heating demand rises (Ghoreishi-Madiseh, Kuyuk et al. 2019).

## 2.4. Thermal energy storage techniques

In recent years, TES systems have become attractive (Ghoreishi-Madiseh, Sasmito et al. 2017). TES systems fall within three main categories: sensible heat, latent heat, and thermochemical storage systems. Sensible heat storage is the cheapest and easiest to implement, thus it is the only competitive TES system type. The selection of TES system mostly depends on the storage period (i.e. short-term vs. long-term), availability of the medium, operating conditions, and purpose of project.

### 2.4.1. Sensible heat storage

Sensible heat storage involves increasing the temperature of the storage material without changing the phases. Consequently, a storage material with high specific heat capacity is preferred. Another important factor is long-term stability under many charging/discharging cycles (Hasnain 1998). Sensible heat storage has several applications like space heating on an industrial scale. In addition, the heat storage medium can be liquid (e.g., water, oil, molten salts) or solid (e.g., rocks, sand) (Hasnain 1998).

- ***Sensible heat storage in rocks***

For low- and high-temperature TES systems, rock are ideal as the solid storage medium because rock has a high specific heat capacity and is inexpensive. Liquids are less suitable because they have high vapor pressure. A rock mass consists of a huge amount of broken rock through which the heat transporting fluid can flow. The thermal energy is stored in the fragmented rock by forcing heated air into the rock and extracted by recirculating ambient air into the heated bed. Apart from the thermophysical properties of the material, the energy stored in this porous medium depends on rock size, shape, density, and HTF.

Storage of thermal energy in rocks is used very often for temperatures up to 100°C in conjunction with solar air heaters (King and Burns 1981, Hasnain 1998). For example, rocks can store

approximately 45 kJ/kg or 1.25kJ/$m^3$ for a temperature change of 50°C. Rock storage can also be used for a high temperature range—up to 1000°C depending on the rock melting point. Another type of bed is called a fluidized bed, which like PRBs, can be employed for low- to high-temperature TES system applications (Hasnain 1998). The interphase heat exchange rate between the HTF and the storage component is much faster in fluidized beds than in PRBs, which can be considered an important factor in numerous applications (Ergun and Orning 1949, Dwivedi and Upadhyay 1977). The fluidized bed TES systems can also be employed for waste heat recovery applications (Zhang, Wang et al. 2013).

### 2.4.2. Latent heat storage

Latent heat storage is also a promising technique because of the high energy storage density of the storage material. The energy storage capacity for a latent heat storage system is defined by the phase transition at a constant temperature (Kurnia and Sasmito 2018). For example, 80 times more energy is required to melt 1 kg of ice than to raise the temperature of 1 kg of water by 1°C. This means that a much smaller weight and volume of material is needed to store a given amount of energy (Da Cunha and Eames 2016). Another advantages of latent heat storage systems, like phase change material storage media, is their isothermal behavior during both charging and discharging phases (Velraj, Seeniraj et al. 1999). Many studies have been performed on the utilization of phase change materials as storage material to improve the heat exchange rate in TES systems (Zalba, Marın et al. 2003, Sharma, Tyagi et al. 2009). There are many phase change materials and many new developments within the technique are ongoing (Fan and Khodadadi 2011).

## 2.5. Application of the packed bed thermal energy storage system

TES systems are necessary to compensate for differences between energy supply and demand. Two primary applications for TES systems are waste heat recovery and seasonal thermal energy systems. In general, a packed bed receives energy during its charging cycle. For STES systems, the energy source is ambient air and it will change continuously during the charge/discharge phase. In the charging phase, hot ambient air is passed through the bed to increase the bed temperature

until the outlet temperature reaches the inlet fluid temperature (maximum possible). The stored energy is extracted from the bed by reversing the direction of fluid flow and injecting cold ambient air (during the winter time). Packed bed performance depends on the time-dependent temperature of the inlet and outlet fluid, as well as the pressure loss through the packed bed during both charging and discharging phases.

Even though the problem of heat storage within packed beds of particles has been widely and thoroughly studied in the recent years, very little practical information is available for application of PRBs of large broken rocks, which represents an ideal energy storage system is some settings. Air is considered a perfect HTF for this type of system. To design these systems, a method is required to quantify the two most important and critical parameters: the pressure drop through the PRB and the rate of heat transfer between the HTF and rocks. As discussed in previous sections, many models have been developed (Table 2.5). Published studies suggest that a combined numerical and experimental approach is ideal. The design considerations mainly include the effect of pressure loss on the fan power demand and the energy exchange rate between fluid and solid phases.

Table 2.4. Recent (since 2015) studies on rock-bed thermal energy storage (TES) systems that use air as heat transfer fluid (HTF)

| Reference | Comments |
|---|---|
| (Nahhas, Py et al. 2019) | Concentrated solar power plants and the long-term use of different storage material at temperatures up to 400°C. The thermal stability of rocks at high temperature is satisfactory. Rock physical properties remain constant at high temperature. |
| (Cárdenas, Davenne et al. 2019) | Optimized a packed bed for utility-scale applications. Effects of particle size, aspect ratio, and storage mass evaluated in terms of exergy efficiency of the system. |
| (Singh, Sørensen et al. 2019) | Numerical investigation of a high-temperature truncated conical packed bed TES. |
| (Esence, Bruch et al. 2019) | One-dimensional numerical model proposed to evaluate the thermal behavior of several packed bed configurations at temperatures up to 200°C. |

| | |
|---|---|
| (Davenne, Garvey et al. 2018) | Thermal stores with a perfect gas as the HTF. Theoretical model of a simplified packed bed proposed. Concluded that during discharge phase, cooled areas will result in a lower pressure drop causing higher flowrate. |
| (Nahhas, Py et al. 2018) | Environmental impacts of waste rock packed bed storage system assessed. |
| (Jemmal, Zari et al. 2017) | Potential of two types of siliceous rocks to be used as storage material in a packed bed system. Temperature dependence of thermal properties of siliceous rocks and their mechanical and physical characteristics addressed. |
| (Tiskatine, Oaddi et al. 2017) | Behavior and suitability of rock in a range of high temperatures for TES applications. Concluded that according to several criteria, dolerite, granodiorite, hornfels, gabbro, and quartzitic sandstone suitable as storage materials for air-based TES systems. |
| (Bruch, Molina et al. 2017) | Experimental study to establish repeatable behaviors over multiple charge/discharge cycles in the case of rock/oil thermoclines. Influences of operating parameters (fluid velocity, temperatures), operating control and partial loads assessed. |
| (Allen, von Backström et al. 2015) | Simple design equations to predict the pressure drop and heat transfer in packed bed of crushed rocks (particle size 2.6–7.3 cm) proposed. |
| (Agalit, Zari et al. 2015) | Numerical method to solve the TES system described and required physical equations reviewed. |
| (Singh, Deshpandey et al. 2015) | Packed bed heat storage system numerically investigated over time showing the importance of variable thermophysical properties in real applications. Effect of several operating parameters on system efficiency evaluated. |
| (Zanganeh, Pedretti et al. 2015) | TES unit designed for round-the-clock operation of a concentrated solar power plant. Impact of several design and operational parameters on thermal losses, pumping power, discharge outflow temperature, and overall storage efficiency presented using numerical models. |

The pioneering experimental study of heat transfer phenomena through packed bed of particles (Furnas 1930) showed that the heat transfer coefficient changes with fluid velocity through the porous media, but fluid temperature does not have a meaningful effect on the heat transfer coefficient. Furthermore, the packing arrangement can significantly affect fluid flow resistance within the pores. Furnas also demonstrated that the heat transfer coefficient decreases with increasing particle diameter in the bed.

Subsequent work by (Meier, Winkler et al. 1991) experimentally and mathematically examined a packed bed of 15 cm rocks with a height of 120 cm. Air (up to 700°C) was injected from the top. Then, the stored heat was discharged by injecting cold air from the bottom. Their model and experimental data agreed well in terms of temperature stratification within the bed and the pressure and heat loss. (Bayón and Rojas 2013) developed a single-phase, one-dimensional model to evaluate the effect of the size of the bed on charging and discharging duration time. They assumed the temperature-independent thermophysical properties for both solid (e.g., rock) and fluid phases (e.g., molten salt). They proposed guideline plots that can be useful in the design process of thermocline prototypes but cautioned that the small prototype tanks do not necessarily perform similarly as do scaled-up tanks.

(Modi and Perez-Segarra 2014) developed a one-dimensional model to evaluate TES system performance using molten salt and thermal oils as HTFs and a wide range of storage temperatures. They also considered constant thermophysical properties for storage materials (e.g., rocks and sand) and temperature-dependent properties for the fluid phase. (Yang and Garimella 2013) evaluated the effect of particle size and mass flow rate of HTF on TES performance during charging and discharging. Similar studies (Li, Van Lew et al. 2011, Van Lew, Li et al. 2011) used the same assumptions with regards to solid and fluid properties and primarily focused on effect of particle size and bed porosity on TES system performance. (Zanganeh, Pedretti et al. 2015) designed a 7.2 $GWh_{th}$ TES system and assessed PRB performance in terms of thermal and pressure losses and overall efficiency of the system. They also evaluated the effect of the TES cone angle (0–30 degrees) and rock diameter (1–4 cm). The required storage volume could be slightly reduced with increasing cone angle, but total thermal losses slightly decreased. They also showed that the pressure loss increased dramatically with decreasing particle size and concluded that rock diameter should be optimized to maximize efficiency and minimize pressure loss through the bed.

(Bader, Pedretti et al. 2015) numerically evaluated a tubular cavity-receiver that uses air as the HTF because air has no limitations regarding temperature constraints and can directly couple the solar collector with the packed bed. However, the lower volumetric heat capacity and convective heat transfer of air compared to conventional HTFs, such as thermo-oil and molten salt, need to be taken into consideration. A dynamic numerical heat transfer model was developed by (Zanganeh, Pedretti et al. 2012) to study the fluid dynamics through a TES system where the packed bed is

buried in the ground. They used temperature-based thermophysical properties in the range of 20–650°C and validated numerical results against experimental data. They recorded an overall 95% thermal efficiency in their proposed TES.

(Dreißigacker, Zunft et al. 2013) addressed the mechanical failures caused by the punctiform contacts in the packed bed. They developed a simulation tool to study the thermo-mechanical behavior during charging and discharging phases by coupling a mechanical model of a packed bed (based on the discrete element method) with thermal model of a regenerator storage. They also implemented time-step control to reduce the computation time and cost. (Anderson, Shiri et al. 2014) worked on a packed bed filled with 6 mm alumina particles and air as the HTF. According to their study, a critical aspect for designing and evaluating such a TES system is related to the appropriate selection of heat transfer coefficient between two phases. A summary of heat transfer equations for several packed bed systems is provided in (Singh, Saini et al. 2010). Nusselt numbers and friction factors have also been proposed for packed bed of spherical and non-spherical particles in a range of sphericity and porosities. (Singh, Saini et al. 2006) evaluated the effect of bed characteristic (e.g., particle sphericity and bed porosity) and operating parameters (e.g., Reynolds number) on heat transfer and pressure loss through a packed bed solar energy storage system comprising large sized elements (up to 186 mm). They proposed new correlations for Nusselt number and friction factor as a function of Reynolds number, particle sphericity from 0.55 to 1.00, and bed porosity from 0.3 to 0.6. Later, (Singh, Saini et al. 2013) extended their study to lower porosities and performed an experimental study to validate their developed correlations. They also stated that the maximum thermo-hydraulic parameter is associated with a spherical particle.

The main advantages of using rock as a storage material and air as the HTF in TES systems can are economic and environmental. Rocks are abundant and reasonably cheap. They are durable and can work in wide range of temperatures. Heat transfer between air and rock can occur directly. In addition, there are no safety, no gas emission, or environmental concerns related to rocks used in TES systems.

Although these TES systems have many merits, they have rarely been investigated. Most published studies have a very limited scope and are restricted to small-scale systems, which are not applicable to industrial-scale mining operations. For example, (Hänchen, Brückner et al. 2011) implemented an unsteady, one-dimensional model to study the convection and conduction heat transfer between

air and rock; the air and rock properties were assumed to be constant. They validated the numerical data against a pilot-scale experimental model at 800 K. They also performed a parametric study that showed that particle diameter, air velocity, dimension of the bed, and rock properties affected the overall performance of the PRB. They found that the overall efficiency of the system increased with decreasing the particle diameter. (Andreozzi, Buonomo et al. 2012) performed a numerical investigation of sensible TES systems with porous media. They used commercial Computational Fluid Dynamics (CFD) Fluent code with the LTNE condition and air as the HTF to determine the effect of mass flow rate (0.1–0.3 kg/m$^2$s) and porosity for a packed bed of spheres (0.2–0.6) and for a packed bed of foam (0.86) on the total performance of the TES system. Their geometry was a cylinder 0.6 m diameter ×1.0 m high). They used two materials to generate porous media: cordierite spheres and alumina ceramic foams. They found that increasing the volumetric flow rate cause the reduction in the charging and discharging times. Also, the bed porosity has a significant effect on the amount of stored energy. The capacity of storing thermal energy decrease as the porosity increase.

The current thesis aims to accurately predict the pressure loss and heat transfer through porous media from a large-scale numerical model that includes geometrical characteristics of the packed bed, the heat exchange rate between broken rock and air.

### 2.5.1. Natural heat exchanger unit (case study: Creighton Mine, Sudbury, Ontario)

Key research on heat transfer in large-scale TES systems for mine ventilation has been published by(Sylvestre 1999, Schafrik 2015, Amiri, Ghoreishi-Madiseh et al. 2017, Ghoreishi-Madiseh, Sasmito et al. 2017, Amiri, Ghoreishi-Madiseh et al. 2018). The empirical approach suggested by Sylvester (Sylvestre 1999) is capable of estimating the heat storage capacity at the Creighton Mine rock-pit. Although this approach is based on an empirical thermodynamic approach, it does not provide applicable engineering tools for designing such systems. Schafrik (Schafrik 2015) developed a numerical simulation model for Creighton Mine and validated results at the bench scale. However, the validity of the results has yet to be scrutinized at the full scale. Use of CFD modelling to investigate air flow through porous media of broken rock mass does not elucidate heat transfer mechanisms involved in heat storage phenomena—an essential need if we are to

understand and improve the performance of these large-scale TES systems (Bracke and Bussmann). Many authors have based their work on designing and understanding ground-coupled heat exchangers (Li, Zhao et al. 2005, Florides and Kalogirou 2007, Sharqawy, Said et al. 2009), and accepted methods for large fragmented rock bodies, such as those at Creighton and Kidd Creek mines, are fundamentally empirical in nature (Envers 1986, Stachulak 1991).

Creighton and Kidd Creek mines have the opportunity to repurpose a huge mass of their waste rock as a massive seasonal thermal energy storage (STES) unit. In this type of heat exchanger, fresh air is passed through the huge mass of porous rocks dumped into an open pit. Employing STES at Creighton Mine reduced seasonal variations in the temperature of the intake fresh air passing through the natural heat exchanger unit (Ghoreishi-Madiseh, Amiri et al. 2017). As mining extends to depths beyond current norms at Creighton Mine, implementation of STES has improved energy management and has led to considerable savings in capital/operating costs. Whereas published field data and empirical models provide details and insight into the overall system behavior, they cannot do so on the local level. For example, spatial variation in temperature and air velocity inside the rock-pit over time is very difficult to measure directly and cannot be predicted using an empirical model. A three-dimensional (3D) model, on the other hand, can resolve not only global behavior but also local transport phenomena at any given position and time.

To the best of my knowledge, no validated 3D model of rock-pit STES is available in literature. The numerical model is the initial step to gain more in-depth information into phenomena occurring inside the rock-pit, which later can be used to improve heating and cooling capacity. There is a fundamental need to develop a multi-dimensional model for a rock-pit STES, which is able to capture all transient transport phenomena involved. A numerical model can also be a promising tool for design, optimization, and even innovation in large-scale TES systems. Thus, the main goal of the present study is to develop a numerical simulation model to assist scientists and engineers with acquiring an in-depth understanding of fluid flow and heat transfer in large-scale seasonal TES systems and improve heating and cooling capacity.

## References


Abdelaziz, E., R. Saidur and S. Mekhilef (2011). "A review on energy saving strategies in industrial sector." Renewable and sustainable energy reviews 15(1): 150-168.

Achenbach, E. (1995). "Heat and flow characteristics of packed beds." Experimental Thermal and Fluid Science 10(1): 17-27.

Agalit, H., N. Zari, M. Maalmi and M. Maaroufi (2015). "Numerical investigations of high temperature packed bed TES systems used in hybrid solar tower power plants." Solar Energy 122: 603-616.

Al-Sumaily, G. F., H. M. Hussen and M. C. Thompson (2014). "Validation of thermal equilibrium assumption in free convection flow over a cylinder embedded in a packed bed." International Communications in Heat and Mass Transfer 58: 184-192.

Allen, K. G., T. W. von Backström and D. G. Kröger (2015). "Rock bed pressure drop and heat transfer: Simple design correlations." Solar Energy 115: 525-536.

Amiri, L., S. A. Ghoreishi-Madiseh, A. P. Sasmito and F. P. Hassani (2017). "Evaluation of Heat Transfer Performance between Rock and Air in Seasonal Thermal Energy Storage Unit." Energy Procedia 142: 576-581.

Amiri, L., S. A. Ghoreishi-Madiseh, A. P. Sasmito and F. P. Hassani (2018). "Effect of buoyancy-driven natural convection in a rock-pit mine air preconditioning system acting as a large-scale thermal energy storage mass." Applied Energy 221: 268-279.

Anderson, R., S. Shiri, H. Bindra and J. F. Morris (2014). "Experimental results and modeling of energy storage and recovery in a packed bed of alumina particles." Applied Energy 119: 521-529.

Andreozzi, A., B. Buonomo, O. Manca, P. Mesolella and S. Tamburrino (2012). Numerical investigation on sensible thermal energy storage with porous media for high temperature solar systems. Journal of Physics: Conference Series, IOP Publishing.

Antohe, B., J. Lage, D. Price and R. Weber (1997). "Experimental determination of permeability and inertia coefficients of mechanically compressed aluminum porous matrices." Journal of fluids engineering 119(2): 404-412.

Bader, R., A. Pedretti, M. Barbato and A. Steinfeld (2015). "An air-based corrugated cavity-receiver for solar parabolic trough concentrators." Applied energy 138: 337-345.

Bağcı, Ö., N. Dukhan and M. Özdemir (2014). "Flow regimes in packed beds of spheres from pre-Darcy to turbulent." Transport in porous media 104(3): 501-520.

Balhoff, M. T., K. E. Thompson and M. Hjortsø (2007). "Coupling pore-scale networks to continuum-scale models of porous media." Computers & Geosciences 33(3): 393-410.

Bari, S. and S. N. Hossain (2013). "Waste heat recovery from a diesel engine using shell and tube heat exchanger." Applied Thermal Engineering 61(2): 355-363.

Barker, J. J. (1965). "HEAT TRANSFER IN PACKED BEDS." Industrial & Engineering Chemistry 57(4): 43-51.

Bayón, R. and E. Rojas (2013). "Simulation of thermocline storage for solar thermal power plants: From dimensionless results to prototypes and real-size tanks." International Journal of Heat and Mass Transfer 60: 713-721.

Bear, J. (2013). Dynamics of fluids in porous media, Courier Corporation.

Beavers, G. S. and E. M. Sparrow (1969). "Non-Darcy flow through fibrous porous media." Journal of Applied Mechanics 36(4): 711-714.

Bharathan, B., A. P. Sasmito and S. A. Ghoreishi-Madiseh (2017). "Analysis of energy consumption and carbon footprint from underground haulage with different power sources in typical Canadian mines." Journal of Cleaner Production 166(Supplement C): 21-31.

Blunt, M. J. (2001). "Flow in porous media—pore-network models and multiphase flow." Current opinion in colloid & interface science 6(3): 197-207.

Bracke, R. and G. Bussmann "Heat-Storage in Deep Hard Coal Mining Infrastructures."

Brown, D. W. (2000). A hot dry rock geothermal energy concept utilizing supercritical CO2 instead of water. Proceedings of the twenty-fifth workshop on geothermal reservoir engineering, Stanford University.

Bruch, A., S. Molina, T. Esence, J. F. Fourmigué and R. Couturier (2017). "Experimental investigation of cycling behavior of pilot-scale thermal oil packed-bed thermal storage system." Renewable Energy 103: 277-285.

Bu, X., W. Ma and H. Li (2012). "Geothermal energy production utilizing abandoned oil and gas wells." Renewable Energy 41(0): 80-85.

Burdine, N. (1953). "Relative permeability calculations from pore size distribution data." Journal of Petroleum Technology 5(3): 71-78.

Cárdenas, B., T. R. Davenne, J. Wang, Y. Ding, Y. Jin, H. Chen, Y. Wu and S. D. Garvey (2019). "Techno-economic optimization of a packed-bed for utility-scale energy storage." Applied Thermal Engineering 153: 206-220.

Chatterjee, A., L. Zhang and X. Xia (2015). "Optimization of mine ventilation fan speeds according to ventilation on demand and time of use tariff." Applied Energy 146: 65-73.

Cheng, Z. D., Y. L. He and F. Q. Cui (2013). "Numerical investigations on coupled heat transfer and synthetical performance of a pressurized volumetric receiver with MCRT–FVM method." Applied Thermal Engineering 50(1): 1044-1054.

Colclough, S. and T. McGrath (2015). "Net energy analysis of a solar combi system with Seasonal Thermal Energy Store." Applied Energy 147: 611-616.

Comiti, J. and M. Renaud (1989). "A new model for determining mean structure parameters of fixed beds from pressure drop measurements: application to beds packed with parallelepipedal particles." Chemical Engineering Science 44(7): 1539-1545.

Coulaud, O., P. Morel and J. Caltagirone (1988). "Numerical modelling of nonlinear effects in laminar flow through a porous medium." Journal of Fluid Mechanics 190: 393-407.

Da Cunha, J. P. and P. Eames (2016). "Thermal energy storage for low and medium temperature applications using phase change materials–a review." Applied Energy 177: 227-238.

Davenne, T. R. G., S. D. Garvey, B. Cardenas and J. P. Rouse (2018). "Stability of packed bed thermoclines." Journal of Energy Storage 19: 192-200.

Davis, A. P. and E. E. Michaelides (2009). "Geothermal power production from abandoned oil wells." Energy 34(7): 866-872.

Dreißigacker, V., S. Zunft and H. Müller-Steinhagen (2013). "A thermo-mechanical model of packed-bed storage and experimental validation." Applied energy 111: 1120-1125.

du Plessis, G. E., L. Liebenberg and E. H. Mathews (2013). "Case study: The effects of a variable flow energy saving strategy on a deep-mine cooling system." Applied Energy 102(0): 700-709.

du Plessis, J. P. and S. Woudberg (2008). "Pore-scale derivation of the Ergun equation to enhance its adaptability and generalization." Chemical Engineering Science 63(9): 2576-2586.

Du, S., M.-J. Li, Q. Ren, Q. Liang and Y.-L. He (2017). "Pore-scale numerical simulation of fully coupled heat transfer process in porous volumetric solar receiver." Energy 140: 1267-1275.

Dudgeon, C. (1966). "An experimental study of the flow of water through coarse granular media." La Houille Blanche(7): 785-801.

Dukhan, N., Ö. Bağcı and M. Özdemir (2014). "Experimental flow in various porous media and reconciliation of Forchheimer and Ergun relations." Experimental Thermal and Fluid Science 57: 425-433.

Dullien, F. (1975). "Single phase flow through porous media and pore structure." The Chemical Engineering Journal 10(1): 1-34.

Dwivedi, P. N. and S. Upadhyay (1977). "Particle-fluid mass transfer in fixed and fluidized beds." Industrial & Engineering Chemistry Process Design and Development 16(2): 157-165.

Dybbs, A. and R. V. Edwards (1984). A New Look at Porous Media Fluid Mechanics — Darcy to Turbulent. Fundamentals of Transport Phenomena in Porous Media. J. Bear and M. Y. Corapcioglu. Dordrecht, Springer Netherlands: 199-256.

Ednie, H. and F. Hassani (2007). "Extracting geothermal heat from mines." CIM MAGAZINE 2(2): 18.

England, R. and D. Gunn (1970). "Dispersion, pressure drop, and chemical reaction in packed beds of cylindrical particles." Transactions of the institution of chemical engineers and the chemical engineer 48(7-10): T265-&.

Envers, P. (1986). "Controlled air through efficient system at inco." Canadian Mining Journal 107(7): 12-14.

Ergun, S. (1952). "Fluid flow through packed columns." Chem. Eng. Prog. 48: 89-94.

Ergun, S. and A. A. Orning (1949). "Fluid flow through randomly packed columns and fluidized beds." Industrial & Engineering Chemistry 41(6): 1179-1184.

Erlund, R. and R. Zevenhoven (2018). Hydration of Magnesium Carbonate in a Thermal Energy Storage Process and Its Heating Application Design. 11.

Esence, T., A. Bruch, J.-F. Fourmigué and B. Stutz (2019). "A versatile one-dimensional numerical model for packed-bed heat storage systems." Renewable Energy 133: 190-204.

Fan, L. and J. M. Khodadadi (2011). "Thermal conductivity enhancement of phase change materials for thermal energy storage: a review." Renewable and sustainable energy reviews 15(1): 24-46.

Fand, R., B. Kim, A. Lam and R. Phan (1987). "Resistance to the flow of fluids through simple and complex porous media whose matrices are composed of randomly packed spheres." Journal of Fluids engineering 109(3): 268-273.

Feng, J., S. Zhang, H. Dong and G. Pei (2019). "Frictional pressure drop characteristics of air flow through sinter bed layer in vertical tank." Powder Technology 344: 177-182.

Florides, G. and S. Kalogirou (2007). "Ground heat exchangers—A review of systems, models and applications." Renewable Energy 32(15): 2461-2478.

Furnas, C. (1930). "Heat transfer from a gas stream to bed of broken solids." Industrial & Engineering Chemistry 22(1): 26-31.

# Connecting Text

*Chapter 2 was the starting point of this study of Thermal Energy Storage (TES) systems. It focused on fluid flow and heat transfer in porous media and published correlations to predict the pressure drop and heat storage capacity in TES systems. It was concluded that published correlations were developed based on porous media comprising small particles, which is not the case in most mining and civil applications. The necessity for TES systems was also elaborated upon: they use renewable energy that could help meet the high energy demands of mining industry. Finally, the application of a TES system for underground mine ventilation and the motivations for performing this study were presented.*

*According to the literature, available correlations fail to predict flow behavior in packed beds with larger (in the scale of metres) particle sizes. Thus, the main objective of Chapter 3 was to develop a three-dimensional (3D) pore-scale mathematical model of a packed bed of spheres with large particle diameters and validate the model against experimental data. Ergun and Forchheimer theories, along with a pore-scale mathematical model, were used to simulate and develop permeability and inertial resistance correlations that are valid for flow through a packed bed of spheres with large particle sizes. To the best of the author's knowledge, Chapter 3 presents the first 3D pore-scale model of flow through a packed bed focused on large particles.*

*Chapter 3 also proposed new constants for the Ergun and Forchheimer correlations to calculate the pressure gradient through a packed bed of large spheres (particle diameters 0.04–1.2 m) from low to high porosity (0.2–0.7). The results can assist engineers to accurately estimate the pressure gradient in porous structures with a wide range of porosities and macro-scale particle sizes.*

*Chapter 3 is published as:*

***Leyla Amiri**, Seyed Ali Ghoreishi-Madiseh, Ferri P. Hassani, and Agus P. Sasmito. "Estimating pressure drop and Ergun/Forchheimer parameters of flow through packed beds of spheres with large particle diameter." Powder Technology (2019).*

# CHAPTER 3

## 3. Estimating pressure drop and Ergun/Forchheimer parameters of flow through packed bed of spheres with large particle diameters


## Abstract

Characterization of flow through packed bed of spheres with large particle diameters (O ~ m) is important in industrial applications, such as mining, geothermal, oil and gas, and construction industries. In this study, a three-dimensional pore-scale mathematical model of packed bed of spheres with large particle diameters considering uniform and non-uniform particle size distributions is developed and validated against experimental data. It was found that the available correlations fail to predict flow behavior in packed bed with larger particle sizes. Hence, Ergun and Forchheimer theories along with pore-scale mathematical model are utilized to simulate and develop permeability (Carman-Kozeny) and inertial resistance (Forchheimer) correlations which are valid for flow through packed bed of spheres with large particle sizes, i.e. sphere diameter from 0.04 to 1.2 m and porosity between 0.2 to 0.7. The developed correlation can be used in either analytical or volume-averaged computational models which is useful for industrial/practical.

### 3.1. Introduction

The behavior of fluid flow in porous structure of packed bed with large particle sizes is very important for a large variety of engineering applications, such as mining, geothermal, oil and gas and construction industries. For example, in oil and gas industry, the flow of the gas/oil is governed by the pressure and the porous structure of the broken rocks due to drilling and fracturing. In construction industry, rock pile for foundation and associated seepage flow can be very important for the structural strength of the infrastructure. In typical underground mining operations, the drilling and blasting creates broken rocks structure in the stope which drives ventilation air to leak through the broken rocks. Understanding the gas leakage characterization and pressure drop through this caved-zone is one of the most essential tasks which directly influences the safety in underground operations as well as the required fan power for circulating the air. The reliable estimation of the pressure gradient through a body of broken rock (i.e., porous structure) is fundamentally important to the design of the ventilation fans. In other words, the permeability of a packed bed of broken rocks significantly affects the ventilation conditions in the underground working environment. Although the permeability of porous media plays a fundamental role, its accurate prediction is still not well understood. The specific characteristics (e.g., permeability and porosity) of each structure of porous media must be carefully assessed to conduct a cost-effective analysis for these systems (i.e., the pressure gradient dictates the flowrate). Due to the importance of porous media and its numerous associated applications, fluid flow and heat transfer in porous media has been vigorously studied (Nield and Bejan 2006, Kaviany 2012). Many studies have shown that the pressure gradient of fluid across a porous media can vary significantly, depending on the characteristics of the solid particles (e.g., particle shape and size, porosity, and packing arrangement) and the fluid properties (e.g., density, viscosity, and velocity).

Essentially, the pressure gradient of flow through a porous medium is caused by the frictional drag (Vafai and Tien 1981) which can be characterized by the empirical Darcy law based on viscous force $\left[\frac{\mu \mathbf{U}}{K}\right]$. This assumption is typically valid within low fluid velocity (Eq.3.1).

$$\nabla p = -\frac{\mu}{K}\mathbf{u} \tag{3.1}$$

Where $\mu$, **U** and $K$ are the dynamic viscosity, physical velocity, and permeability, respectively (Nield and Bejan 2006). The $\nabla p$ shows the pressure gradient and will be negative concerning the fluid flow direction. Although Darcy introduced a one-dimensional empirical model to calculate the pressure gradient through porous media for laminar flow (Liu, Afacan et al. 1994), many studies have demonstrated that the Darcy law is only valid for estimating fluid behavior dominated by the viscous effect. Meaning that, the Darcy law is not valid at higher velocities that the pressure drop becomes quadratic with velocity resulting from an increase in the inertia $[\beta \rho \mathbf{u}^2]$ (Eq. 3.2).

$$\nabla p = -\left(\frac{\mu}{K}\mathbf{u} + \beta \rho \mathbf{u}^2\right) = -\frac{1}{K}\left(1 + \frac{\beta K \rho \mathbf{u}}{\mu}\right)\mu \mathbf{u} = -\frac{1}{K}(1 + F_0)\mu \mathbf{u} \tag{3.2}$$

Where $\beta$ and $\rho$ are the inertial resistance coefficient (also known as the non-Darcy coefficient) and fluid density, respectively. Experimental data specify that the pressure drop in a porous medium is caused by a linear combination of fluid flow velocity $[\mu \mathbf{U}/K]$, namely Darcy term, and square of the fluid flow velocity $[\beta \rho \mathbf{U}^2]$, namely Forchheimer term, whereas the square term is proportional to the inertial effects occurred through the porous structure (Koekemoer and Luckos 2015). Also, $\left[F_0 = \frac{\beta K \rho \mathbf{u}}{\mu}\right]$ is known as Forchheimer number. In addition, it is important to seek correlations between packed bed characteristics and the viscous and inertial resistance forces under various conditions. Allen et al. (Allen, von Backström et al. 2013), Erdim et al. (Erdim, Akgiray et al. 2015), Vollmari et al. (Vollmari, Oschmann et al. 2015), Anbar et al. (Anbar, Thompson et

al. 2018), Bufe and Brenner (Bufe and Brenner 2018), and the others (Hicks 1970, Cicéron, Comiti et al. 2002, Montillet, Akkari et al. 2007, Vollmari, Jasevičius et al. 2016) reviewed and summarized models for spherical and non-spherical particles in fixed bed; however, none of these focused on large particle sizes.

In the flow through porous media, two well-known equations, Ergun correlation and Forchheimer equation are widely used to predict pressure drop as a function of velocity. Other different correlations basically have been developed based on these two equations (Dukhan, Bağcı et al. 2014). While in fluidized bed, some other correlations are commonly used, such as Wen-Yu or De Felice based correlations (Vejahati, Mahinpey et al. 2009).

- **Ergun correlation**

The pressure gradient across a packed bed is generally estimated using the semi-empirical Ergun correlation (Eq.3.3) (Ergun and Orning 1949, Du Plessis 1994, Feng, Dong et al. 2015) matched to experimental data from packed beds that comprise small or micro-sized particles. First and second Ergun constants for Darcy-Forchheimer flow in Eq.3.3, respectively, A and B vary with fluid velocity through porous media and may not accurately estimate the pressure gradient (Macdonald, El-Sayed et al. 1979, Cheng 2011, Dumont, Woudberg et al. 2016). Thus, the Ergun correlation should be validated as a function of the Reynolds number (Hicks 1970). The generality of constants A and B are widely debated. Many researchers claim that these values are different for each packed bed and should be empirically determined for each case (Lacroix, Nguyen et al. 2007, Montillet, Akkari et al. 2007, du Plessis and Woudberg 2008, du Plessis, Liebenberg et al. 2013).

$$\frac{\Delta p}{\mathrm{L}} = \nabla p = -\left(\frac{\boldsymbol{A} \times (1-\varepsilon)^2 \mu \mathbf{U}}{d^2 \times \varepsilon^3} + \frac{\boldsymbol{B} \times (1-\varepsilon) \rho \mathbf{U}^2}{d \times \varepsilon^3}\right) \tag{3.3}$$

From Eq. 3.2 and Eq. 3.3, correlations for the viscous and inertial resistance coefficient can be obtained:

$$\text{Viscous resistance coefficient} \quad (\alpha) = \frac{\mathbf{1}}{K} = \frac{\boldsymbol{A} \times (1-\varepsilon)^2}{d^2 \times \varepsilon^3} \tag{3.4}$$

$$\text{Inertial resistance coefficient} \quad (\beta) = \frac{\mathbf{1}}{\eta} = \frac{B \times (1-\varepsilon)}{d \times \varepsilon^3} \tag{3.5}$$

where the constants A and B are 150 and 1.75, respectively, in the original Ergun correlation. $\nabla p$ is the pressure loss per unit length ($\Delta p$/L). According to Eqs. 3.4 and 3.5, the permeability ($K$) and the passability (η) parameters can be determined by the inverse of viscous resistance coefficient (α) and the inverse of inertial resistance coefficient (β), respectively. The square root of the permeability is assumed to be the proper characteristic length for defining the Reynolds number (Eq. 3.6).

$$\mathrm{Re_k} = \frac{\text{inertial forces}}{\text{viscous forces}} = \frac{\boldsymbol{\rho} \mathbf{U}}{\mu} \sqrt{K} \tag{3.6}$$

It should be noted that the Ergun correlation is only valid to precisely calculate the pressure gradient through porous media with a uniform particle size (UPS) packing arrangement and porosity (ε) (i.e, the volume available to the fluid for passing through the pores as a ratio of the total volume (Lacroix, Nguyen et al. 2007, Choi, Kim et al. 2008)) between 0.35 and 0.55; it is not able to predict the fluid pressure gradient through all kind of porous structures (Allen, von Backström et al. 2013). Numerous correlations have been established that are valid only for a packed bed with small particle size (e.g., $3.2\times10^{-3}$ m (Baghapour, Rouhani et al. 2018), $1.59\times10^{-}$

$^{3}$ m (Thabet and Straatman 2018), 9.0 $\times 10^{-3}$ m (Das, Deen et al. 2018)). For packed beds, discrepancies may be related to the implemented correlations for estimating pressure drop within the porous media.

- **Forchheimer correlation**

For describing the pressure drop in porous medium, Forchheimer equation (Eq. 3.7) is also used. Forchheimer equation is an empirical correlation developed by using analogy with pipe flow with coefficients as correction factors to account for viscosity and inertial terms.

$$\frac{\Delta p}{\mathrm{L}} = \nabla p = -\left(\frac{\mu \mathbf{U}}{K} + F\frac{\rho \mathbf{U}^2}{\sqrt{K}}\right) \tag{3.7}$$

$F$ is Forchheimer coefficient that accounts for inertia drag. Forchheimer equation uses the following equation (Eq. 3.8) for the permeability as a function of particle size and porosity:

$$K = \frac{d^2 \times \varepsilon^3}{36k(1-\varepsilon)^2} \tag{3.8}$$

where $k$ is the Carman-Kozeny constant. The viscous resistance coefficient ($\alpha$=1/$K$) and inertial resistance coefficient ($\beta = \frac{F}{\sqrt{K}}$) determine the porous structure and must be determined to calculate the pressure gradient through porous media analytically.

$$F = \beta\sqrt{K} \tag{3.9}$$

$$F_o = Re_k F \tag{3.10}$$

where $F$ is Forchheimer coefficient, $F_o$ is the Forchheimer number. Although Kaviany (Kaviany 2012) stated that $k$ is identically 5, for spherical particles, the other researches (Lacroix, Nguyen et al. 2007, Montillet, Akkari et al. 2007, du Plessis and Woudberg 2008, du Plessis, Liebenberg et al. 2013) claimed that $k$ is a function of tortuosity, porosity and particle size. It should be noted

that the coefficients for Forchheimer correlation including $F$ and $k$ can be also obtained by utilizing the $\alpha$ and $\beta$ from Ergun correlation.

A comprehensive literature review and comparison of Ergun and Forchheimer equations correlations performed by Erdim et al. (Erdim, Akgiray et al. 2015). It is problematic to apply theses correlations to a packed bed of broken rock, which is relatively large, asymmetric, and irregular. Most published studies are based on packed beds with spherical particles (Erdim, Akgiray et al. 2015, Baghapour, Rouhani et al. 2018, Thabet and Straatman 2018); few consider non-spherical particles (du Plessis and Woudberg 2008, Ozahi, Gundogdu et al. 2008, Li and Ma 2011, Mayerhofer, Govaerts et al. 2011, Rong, Zhou et al. 2015, Partopour and Dixon 2017, Das, Deen et al. 2018). In their comprehensive review, Allen et al. (Allen, von Backström et al. 2013) presented limitations of the Ergun and Forchheimer correlations for estimating the pressure gradient in porous media.

It is also essential to predict the fluid flow behavior and associated pressure gradient through different porous media (Shitzer and Levy 1983) since they determine the power required to maintain the constant mass flow rate and the rate of heat exchange between two phases in a porous medium. Numerous models have been developed to estimate the fluid pressure gradient in porous media composed of granular particles. Given that the permeability of a fixed packed bed influences the fluid pressure gradient, it is necessary to assess the variation among models for packed beds.

It is generally recognized that the pressure gradient through packed beds filled by spheres or semi-spheres should be calculated by means of semi-empirical models. Otherwise, the modified Ergun or Forchheimer correlations should be used by evaluating viscous and inertial resistance coefficient (Nemec and Levec 2005). Several projects have been undertaken to study fluid flow behavior and heat transfer in porous structures at the nano- and micro-scale (Mahdi, Mohammed

et al. 2015, Wang, Lin et al. 2016, Kasaeian, Daneshazarian et al. 2017, Turrado, Fernández et al. 2018). Models developed using the Ergun correlation are valid only for specific conditions and can differ significantly (Table 3.1).

Table 3.1. Original and modified constants used in Ergun/Forchheimer correlations for media with different porosities and particle sizes

| | **Model** | **Constant A** | **Constant B** | **Porosity ε** | **Particle size (mm)** |
|---|---|---|---|---|---|
| Ergun-based studies | (Ergun and Orning 1949) | 150 | 1.75 | 0.35–0.55 | – |
| | (Happel 1958) | 165 | – | 0.2–0.78 | – |
| | (Dudgeon 1966) | 326–287 | 1.24–1.58 | 0.37–0.38 | 15.97–21.33 |
| | (England and Gunn 1970) | 180 | 2.0 | 0.35 | – |
| | (Kyan, Wasan et al. 1970) | 236–184 | 14.1–12.1 | 0.68–0.83 | 0.42–0.03 |
| | (Rumpf and Gupte 1971) | 162–124 | 1.49–1.09 | 0.36–0.64 | 0.67 |
| | (Reichelt 1972) | 200 | 2.0 | 0.36 | 9.71–24.5 |
| | (Macdonald, El-Sayed et al. 1979) | 124–162 | 1.09–1.49 | 0.37–0.64 | 0.68 |
| | (du Plessis and Woudberg 2008) | 170–200 | 1.35–2.00 | 0.2–0.8 | – |
| | **Model** | **Carman-Kozeny coefficient** | | **Porosity ε** | **Particle size (mm)** |
| Forchheimer-based studies | (Beavers and Sparrow 1969) | 5 | | 0.35–0.55 | - |
| | (England and Gunn 1970) | 5 | | 0.35 | - |
| | (Fand, Kim et al. 1987) | 5.12–5.33 | | 0.35 | 2–3.7 |
| | (Comiti and Renaud 1989) | 3.89 | | 0.31–0.46 | 1.12–4.99 |
| | (Rode, Midoux et al. 1994) | 5.11–5.28 | | 0.4 | 2.5–3.2 |
| | (Bağcı, Dukhan et al. 2014) | 2.82–3.69 | | 0.35 | 1-3 |

Many researchers have asserted that the constants in these equations need to be calculated empirically for different packed beds because they depend on many factors, including the particle size and shape in addition to packing method and size distribution of particles in the packed bed (Jiang, Khadilkar et al. 2002). The authors agree that unique constant value of Ergun and Forchheimer equations are not valid for all cases; however, the same values can be used for the

similar beds. Large particles are common in the mining, geothermal, oil and gas and construction industries, yet no quantitative data have been published on porous media containing large particles (e.g., particle diameter > 10 cm) and macroscale particles (Table 3.1). For example, the properties of the caved zone with the particle size larger than 10 cm in the gob of longwall mining operation—including permeability and porosity—can directly affect air and methane leakage in the ventilation (Karacan 2010) is not directly available.

Accurate measurement of porosity and permeability is not an easy task because the caved zone is not accessible to carry out conventional direct tests. Recent investigations by the authors assessed the seasonal thermal energy storage capacity of rock for supplying a portion of the energy demands in mine ventilation system in deep underground mines (Amiri, Ghoreishi-Madiseh et al. 2017, Ghoreishi-Madiseh, Amiri et al. 2017, Ghoreishi-Madiseh, Sasmito et al. 2017, Amiri, Ghoreishi-Madiseh et al. 2018). Data pertaining to characteristics of the rock structure did not exist or were not accessible at most mine sites. These limitations encouraged the authors to develop a numerical model in quantitative agreement with experimental results from the literature. There is a fundamental need to develop a pressure gradient model for porous media composed of large particles, which should be able to estimate the inertial and viscous resistance coefficients of a packed bed filled with large particle like rocks. Therefore, the objectives of this study are to: (i) generate a three-dimensional (3D) computational pore-scale model (PSM) of a packed bed of large spheres; (ii) evaluate the effect of packing arrangement (i.e., Uniform Particle Size (UPS) versus non-Uniform Particle Size (n-UPS)) on the pressure gradient of the air passing through the packed bed of spheres; (iii) propose modified coefficients for the Ergun correlation and Forchheimer equation.

### 3.2. Model development

First, two sets of PSMs were generated, one using the UPS packing arrangement and one using the n-UPS packing arrangement (Figure 3.1). Next, the analytical model was utilized to calculate the initial value for the viscous ($\alpha, k$) and inertial ($\beta, F$) resistance coefficients. After that, for simplicity and saving times, a volume-averaged model (VAM) was created and the calculated value of $\alpha, k$ and $\beta, F$ were entered into the model. Finally, the results of VAM and analytical model was compared to ensure that the assumption of $\alpha, k$ and $\beta, F$ at the VAM was accurate. This procedure is shown in the flowchart given in Figure 3.1. Accordingly, the following steps were followed to reach the stated objective. In step 1, a wide range of Reynolds number ($Re_k$) values was input to both above mentioned PSMs and their associated pressure gradient was recorded. In step 2, viscous ($\alpha, k$) and inertial ($\beta, F$) resistance coefficients in addition to the permeability ($K$) were calculated using analytical model (Eqs. 3.13-3.16). In step 3, the porosity ($\varepsilon$) and viscous ($\alpha, k$) and inertial ($\beta, F$) resistance coefficients were implemented into VAM to assess the accuracy and validity of the data from the PSM. Also, the two sets of model outputs were analyzed to find potential errors generated by using the original values for constants A and B for the Ergun and Forchheimer correlations (Table 3.1). In step 4, $\alpha, k$ and $\beta, F$ were obtained, calibrated and then input to VAM again. Steps 3 and 4 were repeated till the difference between the obtained results from analytical model and VAM was less than 5%.

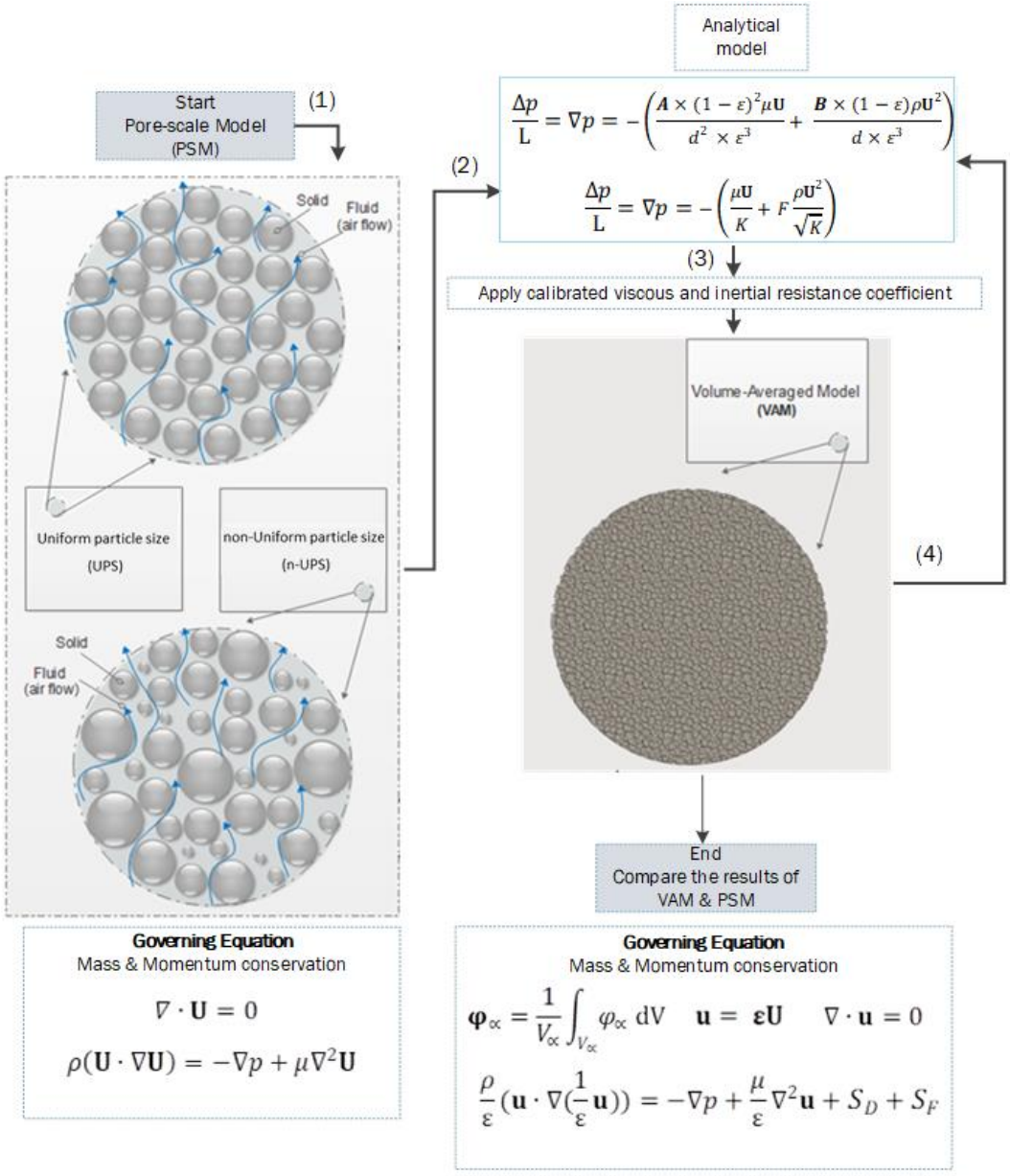


Figure 3.1. Schematic of research methodology: pore-scale, analytical and volume-averaged models

The structure and computational domain of UPS and n-UPS packing arrangements are presented in Figure 3.2. All cubes sides were approximately 16*d* in length in order to satisfy the length scale of the representative elementary volume (Das, Deen et al. 2017). The 3D model of the packed bed of spheres was created in EDEM software and transported to a DesignModeler and ANSYS workbench to label, mesh, and assign the boundary conditions.

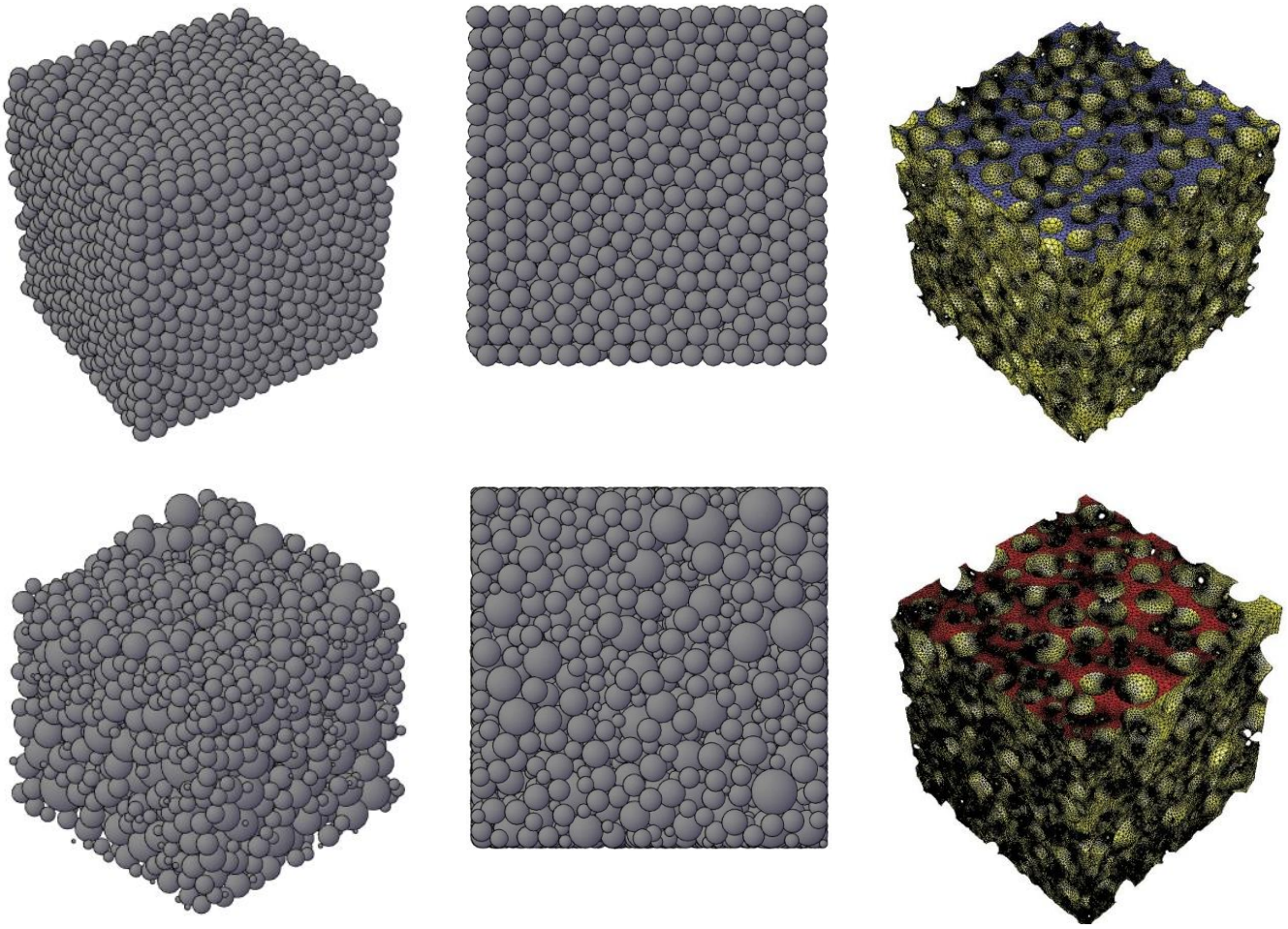

Figure 3.2. 3D representation of computational domains for the uniform particle size (UPS, top) and non-uniform particle size (n-UPS, bottom)

Generating a packed bed of large particles is not straightforward, particularly for the n-UPS model, and becomes increasingly complicated as the particle size and porosity of the bed decrease. Face-centered cubic UPS arrangements is used to generate randomly packed bed of spheres. In this study, the n-UPS geometries are created based on a normal size distribution with mean diameter of 0.55, 0.7, 0.85, 1.00 and 1.20 m and standard deviation between 0.35 and 0.65 (Figure 3.3). The normal size distribution was utilized as the structure of numerous natural porous media can be described by such a distribution (Bear 2013).

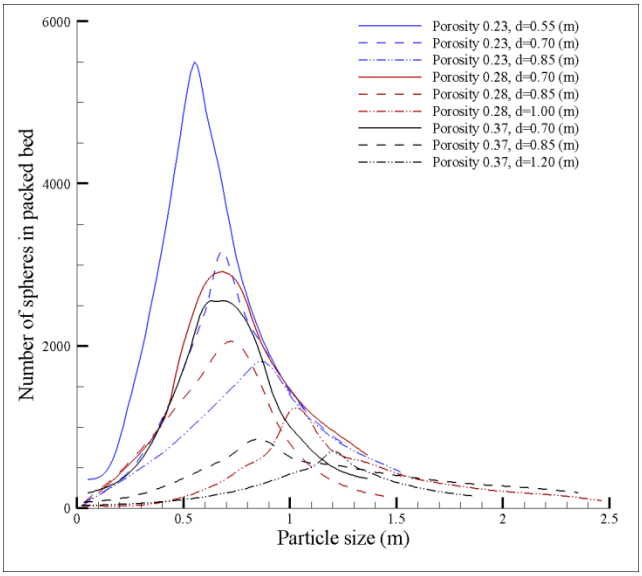


Figure 3.3. Gaussian distributions of the number of particle sizes in n-UPS pore-scale model

The particle diameter is a vital parameter to determine flow behavior through the packed bed of particles. However, the identification of average particle diameter is not a straightforward task when the packed bed is comprised of non-uniform particles, as the case for packed bed of rocks with a wide range of size distribution. For the non-uniform particle size distribution, the average particle diameter is not constant even for the same combination of non-uniform spherical particles, depending on which average particle diameters function considered (Li and Ma 2011, Chikhi, Coindreau et al. 2014). According to the literature, the number average diameter is more appropriate function for packed bed of rocks characterization than the other available ones. Thus, in the present study the number average diameter function is used to calculate average particle diameter $d_{ave}$ as follows:

$$d_{ave} = \sum d_i n_i = \frac{\sum d_i f_i}{\sum f_i} \tag{3.11}$$

where the parameter $n_i$ is size distribution function by number of the particles and $f_i$ is the number of spherical particles within the given size $d_i$.

The boundary conditions for the model in this study can be written as: (i) top of the packed bed of spheres is defined as inlet and various air velocities are prescribed; (ii) bottom of the packed bed of spheres is set as a pressure outlet; and (iii) the no-slip wall is applied at the side boundaries. Also, in PSM, the no-slip wall is assigned at the surface of particles. Since knowledge of the porosity of the packed bed is not complete, supplementary parameters such as packing method and particle size need to be clearly defined [29]. Any bed can be filled using UPS or n-UPS packing arrangements (Figure 3.2). The average diameter of sphere particles varies from 0.04 to 1.20 m in the present study, whereas the porosity (ε) of the packed beds ranges between 0.23 and 0.70. It should be noted that increasing the porosity decreases the density of the system.

### 3.2.1. Governing equations

The mass and momentum governing equations conditional on appropriate boundary conditions are used here. The steady conservation equations for mass and momentum for the PSM, VAM, and analytical model are presented and described below.

- ***Pore-scale model***

In the pore-scale model, laminar fluid is taken into consideration and the conservation of mass (Eq. 3.12) and momentum (Eq. 3.13) are given by:

$$\nabla \cdot \mathbf{U} = 0 \tag{3.12}$$

$$\rho(\mathbf{U} \cdot \nabla \mathbf{U}) = -\nabla p + \mu \nabla^2 \mathbf{U} \tag{3.13}$$

Where $\rho$, $\mathbf{U}$, and $\mu$ are the fluid density, physical velocity, and dynamic viscosity, respectively (Nield and Bejan 2006, Barzegar Gerdroodbary, Jahanian et al. 2015, Amini, Karimi-Sabet et al.

2016). The PSM has made it possible to understand the fluid flow behavior in porous medium at the pore scale.

- ***Volume-averaged model***

The method of volume averaging makes the boundary value problem simpler (Eqs. 3.12 and 3.13) by taking only the large scale behavior of the flow into consideration. This can be developed by averaging the governing equations over a sufficiently large volume V, called representative elementary volume (REV) of a porous medium (Whitaker 1986). If REV is correctly chosen, adding extra volume around it will not have a meaningful effect on the results (Nield and Bejan 2006). The details of the system are illustrated in Figure 3.3. The smallest macroscopic length scales, $d_{\text{Fluid}}$ and $d_{\text{Solid}}$, are an average pore and particle diameter, respectively, while the largest macroscopic length scale, $L$, is the characteristic length of flow domain. Also, the macroscopic length scales, $l$, is the characteristic length of REV. In most cases, the volume averaged method (Eq. 3.12) is valid when $l \geq 5d_{\text{Fluid}}$, $l \geq 5d_{\text{Solid}}$ and $l \ll L$ are satisfactory (Whitaker 1986). Since, in this study, $l$ is large enough compared to $d_{\text{Fluid}}$ and $d_{\text{Solid}}$ showed in Figure 3.4, this constraint was satisfied in all cases.

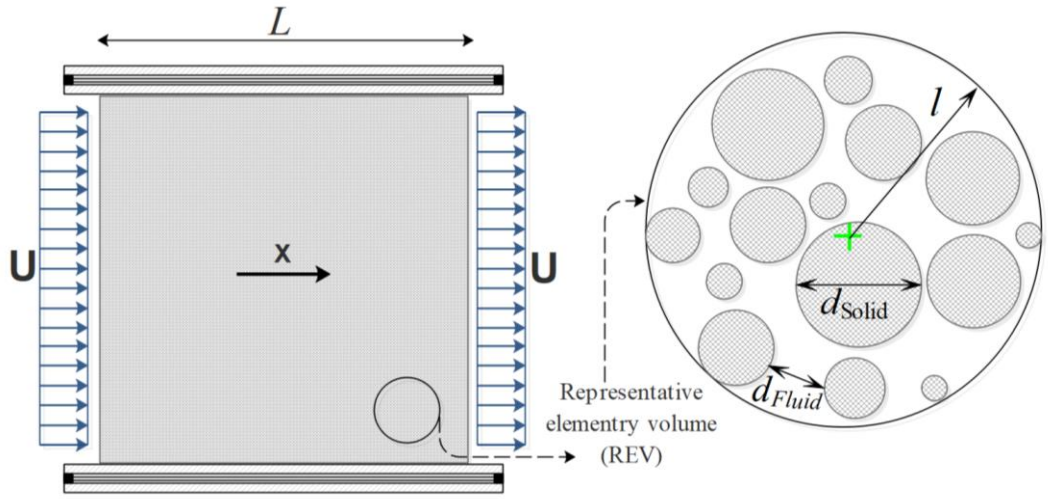


Figure 3.4. Schematic of the representative elementary volume (REV) and range of the length scales. Not to scale

By using the volume-averaged method, a 3D VAM model was governed by the conservation equations of mass and momentum:

$$\boldsymbol{\varphi}_{\propto} = \frac{1}{V_{\propto}} \int_{V_{\propto}} \varphi_{\propto} \, \mathrm{dV} \tag{3.14}$$

Where $\propto$ shows the phases, $s$ for solid phase (particles) and $f$ for fluid phase (air).

$$\mathbf{u} = \boldsymbol{\varepsilon}\mathbf{U} \tag{3.15}$$

$$\nabla \cdot \mathbf{u} = 0 \tag{3.16}$$

$$\frac{\rho}{\varepsilon}(\mathbf{u} \cdot \nabla(\frac{1}{\varepsilon}\mathbf{u})) = -\nabla p + \frac{\mu}{\varepsilon}\nabla^2\mathbf{u} + S_D + S_F \tag{3.17}$$

Derived from the volume averaging method **u** is the superficial velocity (Eq. 3.9), where V is a REV of a porous medium. Where $S_D$ and $S_F$ are the Darcy term and Forchheimer term, respectively (Nield and Bejan 2006, Barzegar Gerdroodbary, Jahanian et al. 2015, Amini, Karimi-Sabet et al. 2016).

$$S_D = -(\mu\mathbf{u}/K) \tag{3.18}$$

$$S_F = -(\beta\rho|\mathbf{u}|\mathbf{u}) \quad (3.19)$$

Permeability ($K$) is a measure of the ability of the porous medium to let fluids pass through the medium. To obtain an accurate $K$ and β, comprehensive computational and experimental analyses must be conducted. In the current study, we calculated these two important values for different packed bed of spheres of differing porosity and particle size.

- ***Analytical model***

Fluid flow through porous media was simulated by considering the Darcy and Forchheimer terms (Figure 3.1). The term $[\mu\mathbf{U}/K]$ in Eq. 3.1 prevails in the Darcy regime when $Re_k$ is very low. However, for flow with higher $Re_k$ in porous media, both viscous and inertial effects have to be considered. The only difficulty is the non-linear behavior of the fluid flow in a packed bed, which is addressed by Forchheimer. The term $[\beta\boldsymbol{\rho}\mathbf{U}^2]$ in Eq. 3.2 becomes the principal term in the Forchheimer regime at higher Reynolds numbers. Also, when the pressure gradient versus flow velocity has a nonlinear relationship, the inertial coefficient becomes the dominant factor in assessing the fluid flow behavior.

### 3.3. Numerical methods

A large packed bed filled by spherical particles was created using EDEM software, then the model was developed by importing the bed geometry into Ansys 17.2 software. The influence of particle size and arrangement (UPS versus n-UPS) and porosity on the permeability of the packed bed was subsequently analyzed. To conduct the mesh independence test, the initial UPS and n-UPS models were created with approximately $6.5\times10^5$ and $1.1\times10^6$ nodes, respectively. Subsequent UPS and n-UPS models were developed with more nodes (up to $3.2\times10^6$ and $5.2\times10^6$ nodes, respectively)

until the deviation between the last two models with a fine mesh size was 1%. To optimize computational costs, two sets of computational domains were solved: a packed UPS bed with average $2.9\times10^6$ nodes and a packed n-UPS bed with average $4.82\times10^6$ nodes. The computational model was established using the Semi-Implicit Pressure-Linked Equation (SIMPLE) algorithm, second-order upwind discretization, and the Algebraic Multi-grid (AMG) method. It should be noted that convergence (residual of $10^{-6}$) was reached by approximately 15 and 45 iterations for the UPS and n-UPS models, respectively.

Here, the Ergun and Forchheimer correlations is used to develop engineering tools based on experimental data for spheres and valid for a wide range of $Re_k$. The packed bed porosity is also considered in the sensitivity analysis to check the functional dependence of the pressure gradient. The sensitivity analysis results confirmed that even relatively small changes in bed characteristics like porosity and particle size can have a significant impact on the resistance of the porous media and would make it complicated to estimate the fluid flow behavior accurately for different beds with different packing arrangements (Macdonald, El-Sayed et al. 1979, Nemec and Levec 2005, du Plessis and Woudberg 2008, Wu, Yu et al. 2008). Consequently, the effect of different characteristics of a packed bed such as porosity and particle size on constants A and B (Eq. 3.3) was investigated using information in the literature in addition to the new computational data simulated in the current and previous projects (Ergun and Orning 1949, Nemec and Levec 2005, du Plessis and Woudberg 2008, Amiri, Ghoreishi-Madiseh et al. 2018).

## 3.4. Results and Discussion

### 3.4.1. Validation of pore-scale CFD model using experimental data

In spite of high-accuracy of CFD model output because of its significant advancement within the past few years, it is fundamental to validate the model results with the experimental data prior to applying them for further examination of the fluid flow behavior through the packed beds. Consequently, we created a packed bed of spherical particles imitating the experimental setup implemented by (Allen 2014) whereby golf balls of diameter 42.6 mm were utilized to develop the packed bed (470 mm width by 500 mm height) with the porosity of 0.376. To the best of our knowledge, no investigation is focused on experimental and numerical analysis of large-scaled packed beds. Therefore, we used the results of the study by Allen (2014), presenting the largest particle size studied available in literature to date, to validate our model. As appeared in Figure 3.5-a, the simulated data are in reasonably good agreement with the value of pressure gradient in the experimental data with the deviation up to 7% is noticed at higher $Re_k$ which is well satisfactory in the prediction of pressure drop through the packed beds. It demonstrates that the methodology used in this research is acceptable to develop the packed bed filled with large size of particles (e.g. broken rock). The deviation can be ascribed to an assortment of reasons, for example, arrangement of the particles in the bed, variations in the surface roughness (i.e. dimples on a golf ball), and slight difference (i.e. 2.5%) in the porosities of the simulation and the experimental setup.

The correlation proposed by Allen et al. (Allen, von Backström et al. 2013, Allen, von Backström et al. 2015) is further tested to predict flow through packed bed with larger particle diameters and compared with the results from PSM. Figure 5b shows that the proposed correlation deviates significantly as compared to the PSM results, especially at higher particle sizes. Notably, the deviation increases from 7% to 12% (Figure 3.5b) to 46% (Figure 3.5b-3.4) when the particle

diameter is increased from 0.04 to 0.1 to 1.2 m, respectively. Hence, it can be deduced that there is a fundamental need to develop new Ergun/Forchheimer correlation for flow through packed bed of particles with large particle diameters.

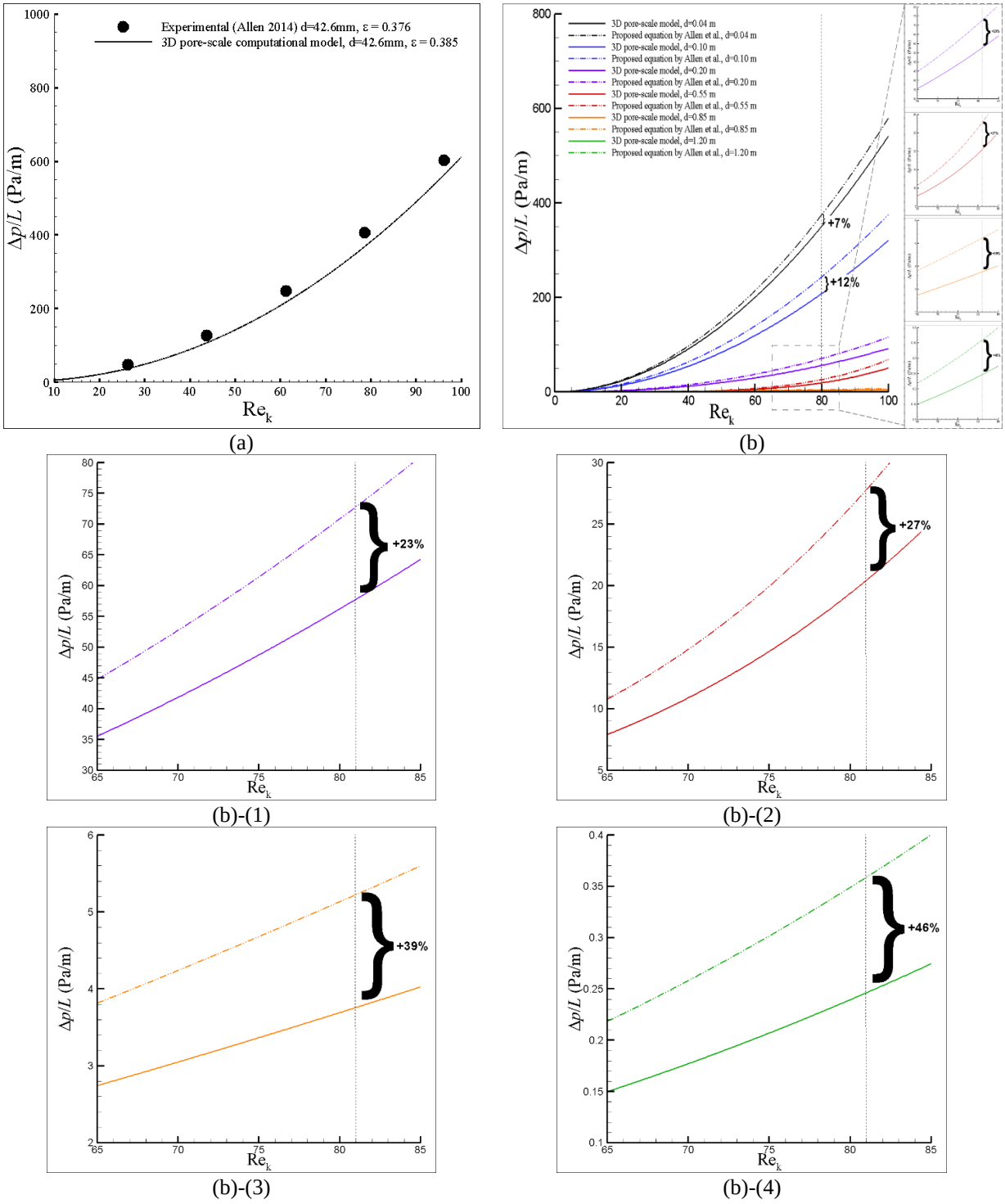


Figure 3.5. (a) Validation of the pore-scale model with the experimental data (Allen 2014) at particle size diameter of 0.04 m; (b) Comparison of the simulation results for packed bed with larger particles (1) 0.20 m, (2) 0.55 m, (3) 0.85 m, and (4) 1.2 m against correlations from (Singh, Saini et al. 2006, Allen 2014).

### 3.4.2. Comparison of pressure gradient with available correlations

Most of the complexity in estimating the pressure gradient for porous media derives from its dependence on the porosity and packing arrangement. The PSM of UPS and n-UPS packing arrangements are simulated and compared with available correlations, i.e. Ergun et al (Ergun and Orning 1949, Macdonald, El-Sayed et al. 1979, du Plessis and Woudberg 2008), du Plessis et al. (Ergun and Orning 1949, Macdonald, El-Sayed et al. 1979, du Plessis and Woudberg 2008) and Macdonald et al. (Ergun and Orning 1949, Macdonald, El-Sayed et al. 1979, du Plessis and Woudberg 2008). Here several features are apparent; foremost among them is the available correlations (Ergun and Orning 1949, Macdonald, El-Sayed et al. 1979, du Plessis and Woudberg 2008) fail to predict flow characteristics for both packing arrangements, especially at higher $Re_k$; see Figure 3.6 – 3.8. Notably, Macdonald correlation gives rise to the highest deviation by more than 100% at higher $Re_k$, followed by du Plessis and Ergun correlations, respectively. This, again, highlight the importance and necessity of developing new correlation for packed bed with large particle sizes.

Comparing UPS and n-UPS packing arrangements, at lower $Re_k$ (Darcy regime), the UPS and n-UPS arrangements do not show significant pressure different. As $Re_k$ is increased to Darcy-Forchheimer regime, the pressure starts to increasingly deviate by up to 10% at higher $Re_k$. This postulates that the n-UPS arrangement with normal distribution can be safely assumed as UPS arrangement. Further investigation is underway to evaluate the effect of different particle size distributions, e.g. exponential, poisson, binomial and bernoulli and compaction.

Looking at the effect of particle size and porosity, it is obvious that reducing porosity increases pressure requirement due to reduced flow path and increased flow resistance. On closer inspection, at same porosity, increasing particle size decreases pressure drop. This can be explained by the

fact that larger particle size gives rise to larger spacing in between particles and lower flow resistance. At lower $Re_k$, pressure gradient increases linearly with $Re_k$ as it is viscous dominating flow (Darcy); while at higher $Re_k$, the relations becomes quadratic due to additional of inertia force from pore-scale eddies in between particles (Darcy-Forchheimer). It is also shown that, the pressure gradient data for the PSM with fixed porosities of 0.23 (Figure 3.6), 0.28 (Figure 3.7), and 0.37 (Figure 3.8) gave reasonably good agreement behavior as compared to experimental data in other studies (Macdonald, El-Sayed et al. 1979, Nemec and Levec 2005, Choi, Kim et al. 2008, du Plessis and Woudberg 2008, du Plessis, Liebenberg et al. 2013).

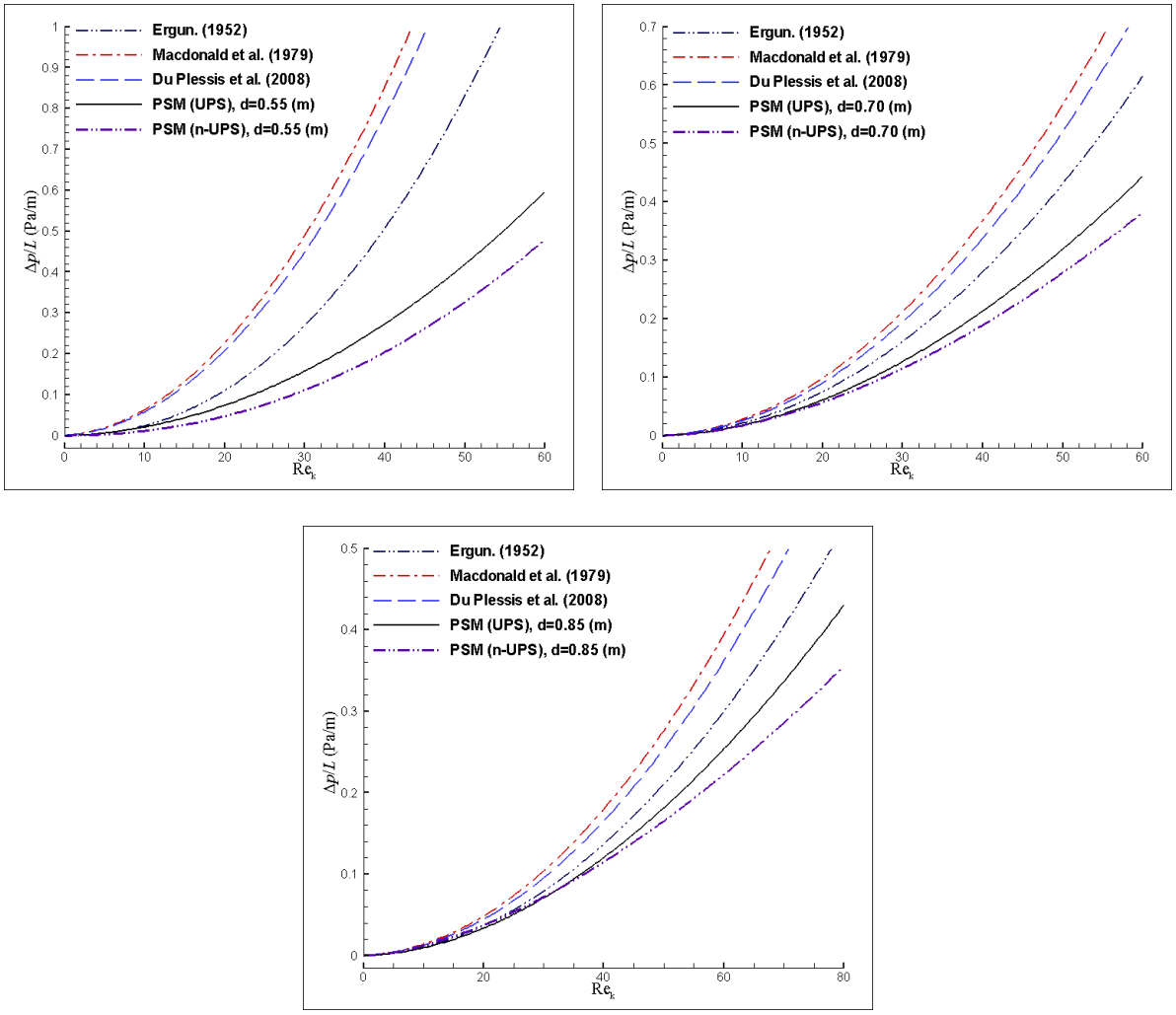


Figure 3.6. Comparison of pressure gradient ($\Delta p/L$) versus Reynolds number ($Re_k$) from pore-scale model results of UPS and n-UPS packing arrangements with three available correlations from literature at porosity 0.23 and particle size: (a) 0.55; (b) 0.7; and (c) 0.85 m.

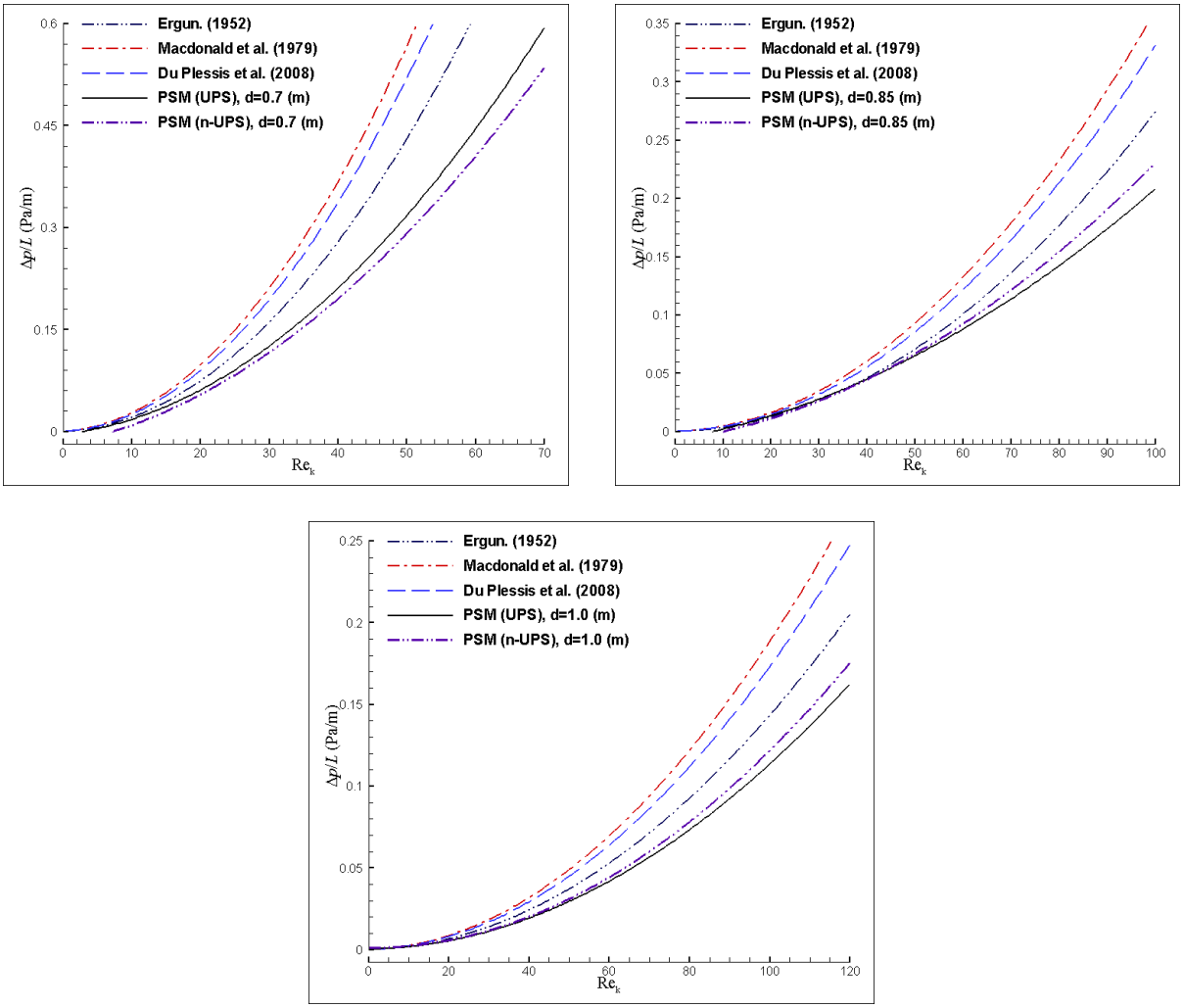


Figure 3.7. Comparison of pressure gradient ($\Delta p/L$) versus Reynolds number ($Re_k$) from pore-scale model results of UPS and n-UPS packing arrangements with three available correlations from literature at porosity 0.28 and particle size: (a) 0.7; (b) 0.85; and (c) 1 m.

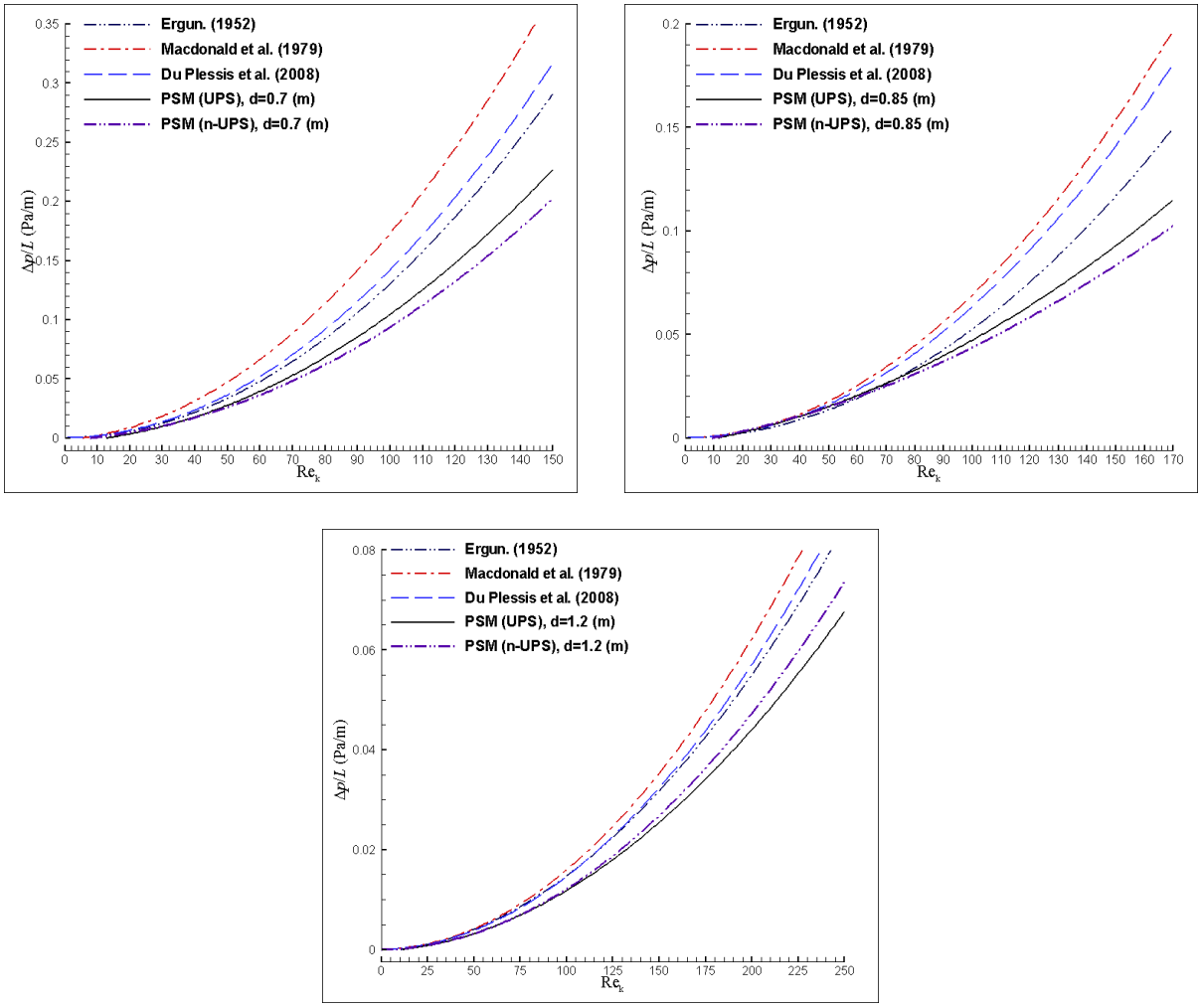


Figure 3.8.Comparison of pressure gradient ($\Delta p/L$) versus Reynolds number ($Re_k$) from pore-scale model results of UPS and n-UPS packing arrangements with three available correlations from literature at porosity 0.37 and particle size: (a) 0.57; (b) 0.85; and (c) 1.2 m.

### 3.4.3. The modified values of Ergun and Forchheimer correlations obtained by pore-scale model versus various models from the literature.

Figure 3.9 compares the values of (a) constants A and B for Ergun correlation as well as (b) coefficients *F* and *k* for Forchheimer equation calculated in this study with published values (Ergun and Orning 1949, Macdonald, El-Sayed et al. 1979, du Plessis and Woudberg 2008). The coefficients of the viscous and the inertial term in the Ergun correlation and Forchheimer equation are shown to be related. Ergun proposed the constant values A (150), B (1.75), and *k* (4.16) (Ergun

and Orning 1949). However, Macdonald et al., (Macdonald, El-Sayed et al. 1979) suggested constant values A (157-180), B (1.49-1.77), and *k* (4.36-5.00) at porosities ranging from 0.34 to 0.48. Recently, the empirical values for the granular representative unit cell model reported as (174-178), (1.88-1.75), and (4.83-4.94), respectively, for A, B, and *k* at the same porosities ranging, by (du Plessis and Woudberg 2008). However, as can be seen in Figure 3.9a, according to the results presented in this study, proposed modified constants A (121–164) and B (1.41–1.78) can be effectively applied into Ergun formulation to more accurately determine the pressure gradient across a packed bed filled with large spherical particle size of 1.0 m. Furthermore, as Figure 3.9b illustrated, anticipated Forchheimer correction factors *k* (3.4–4.5) and *F* (1.4-0.25) can be successfully used in Forchheimer equation to more accurately calculate the pressure drop across a packed bed filled with large particle size of 1.0 m.

a

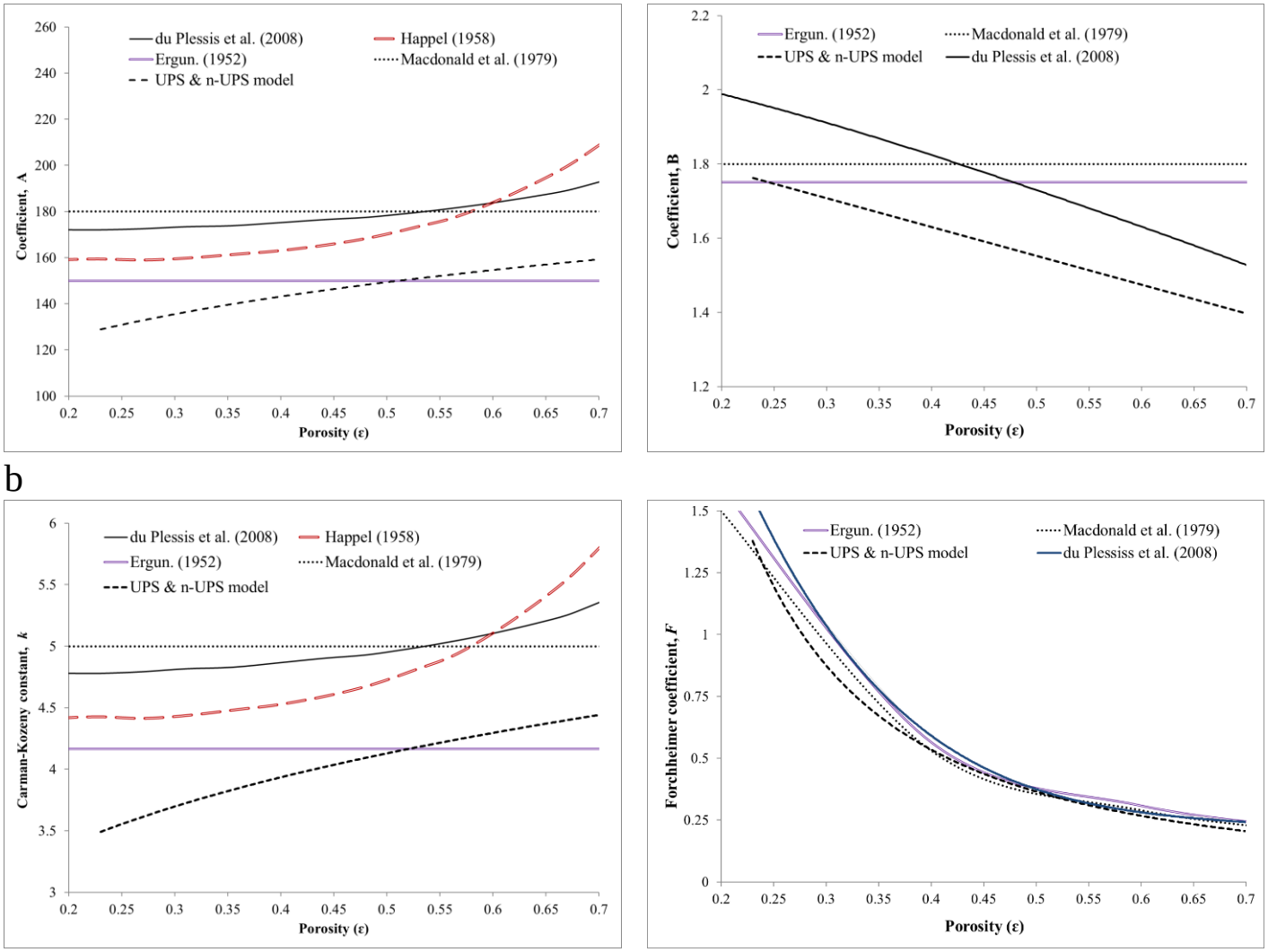


b




Figure 3.9. Comparison of the values of (a) the constants A and B from the Ergun correlation; and (b) the Forchheimer coefficients (*F* and *k*), with values from literature

### 3.4.4. Proposed charts for predicting Ergun constants and Forchheimer coefficients

The unique feature of the presented model is its broad applicability over a wide range of porosities, as well as large particle sizes. By obtaining results from the PSM, VAM, and analytical model, and by validating them with available data in literature, we propose the following charts to predict A and B Ergun constants (Figure 3.10a) as well as F and *k* (Figure 3.10b) as a function of porosity ε and particle diameter d (m) which is expected to be valid for a range of porosity values between

0.2 and 0.7 and particle size between 0.04 m and 1.20 m. The values presented by Figure 3.10 are in very good agreement both quantitatively and qualitatively with computational results with R-squared values ($R^2 > 0.98$).

The constant A in Ergun equation varies from 105 to 150, while constant B ranges from 1.45 to 1.95, depending on the porosity and particle size. Similarly, the Forchheimer coefficient ($F$), varies from 0.2 to 2.2 which is highly affected by the porosity and is marginally affected by particle size. The Carman-Kozeny coefficient, on the other hand, is affected by both porosity and particle size with range values from 3.0 to 4.4.

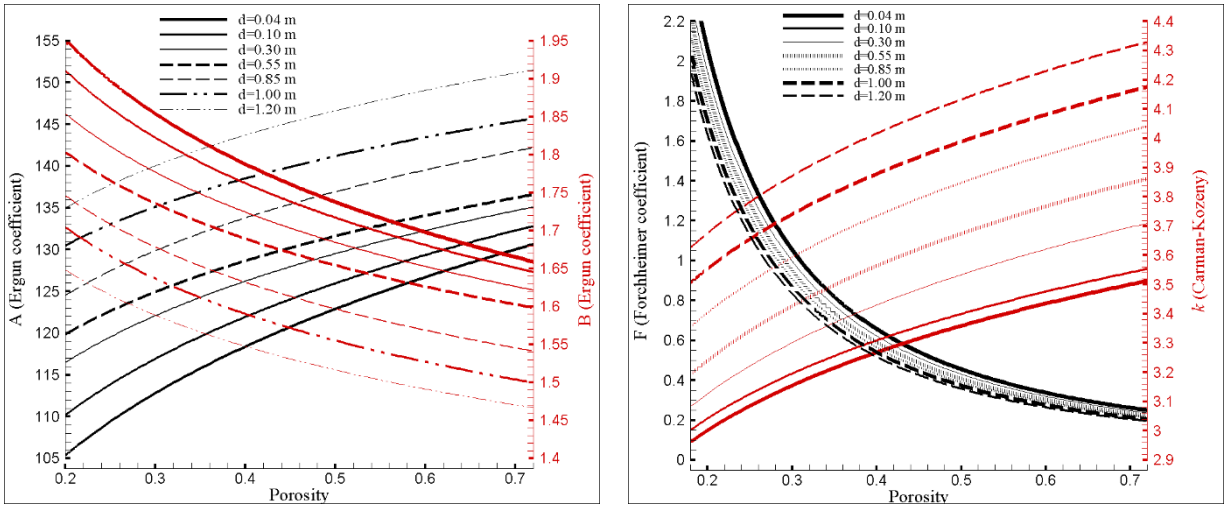


(a) (b)

Figure 3.10. Proposed values of (a) the constants A and B for the Ergun correlation; and (b) the Forchheimer coefficients ($F$ and $k$), developed in this study.

Thus, the value of Ergun coefficients A and B can be obtained from Figure 3.10a and applied in Ergun correlation (Eq. 3.3) to predict the pressure drop. Similarly, Figure 3.10b can be used to predict the essential coefficients of Forchheimer correlation (Eq. 3.4) and estimate the pressure loss accordingly.

### 3.4.5. Pressure gradient versus $Re_k$ in pore-scale and volume-averaged models

In essence, PSM is computationally expensive and impractical. The volume-averaged model (VAM), on the other contrary, is computationally less demanding and is widely used for practical application of porous media flow. To ensure the validity of the proposed constant values of the Ergun and Forchheimer correlations, the volume-averaged models were simulated with different porosities and viscous and inertial resistance coefficients. The results are in very good agreement with PSM and analytical model (Figure 3.11). Some differences are evident at high porosity, which can be explained by the high $Re_k$. Since simplicity and low computational cost and time are important characteristics of any numerical study, the VAM can be used to estimate the pressure gradient with the great reliability and accuracy for the similar porous structures. In all cases, the standard errors for the estimated versus analytical data are less than 5%.

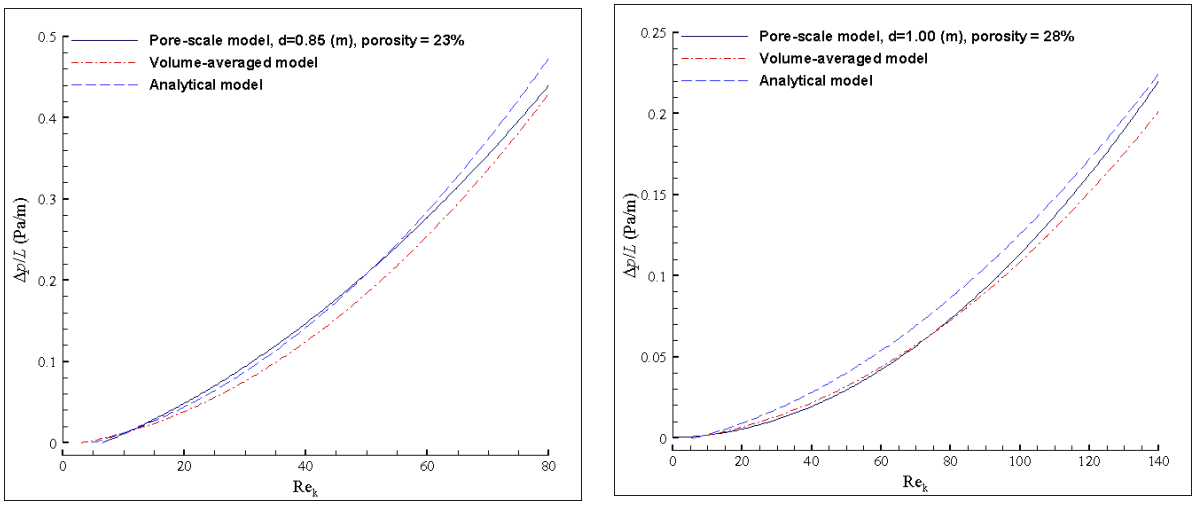

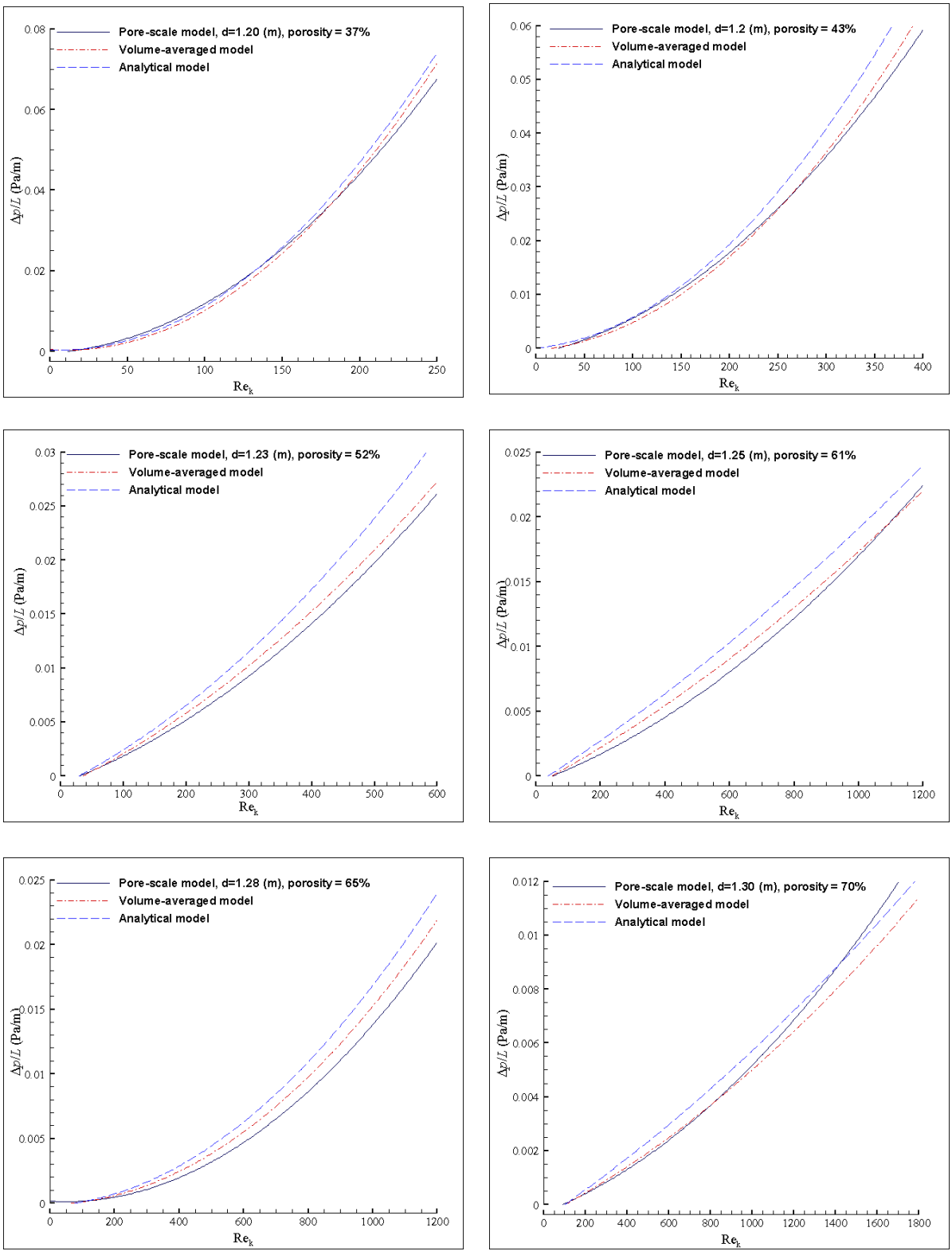


Figure 3.11. Comparison of pressure gradient ($\Delta p/L$)) versus Reynolds number ($Re_k$) between the results from pore-scale model and volume-averaged model at different porosities.

### 3.4.6. Permeability and inertial resistance

Figure 3.12 shows the permeability (Fig. 3.12a) and inertial resistance (Fig. 3.12b) as functions of porosity and particle size that can be directly used to calculate pressure drop in practical applications. In general, reducing porosity and particle size decreases permeability and increases inertial resistance. Notably, at porosity 0.3, reducing particle size from 1.2 to 0.5 to 0.2 m decreases the permeability from $10^{-4}$ to $10^{-5}$ to $10^{-6}$, respectively; while the inertial resistance increases from $10^{2}$ to $5\times10^{2}$ to$10^{4}$, respectively.

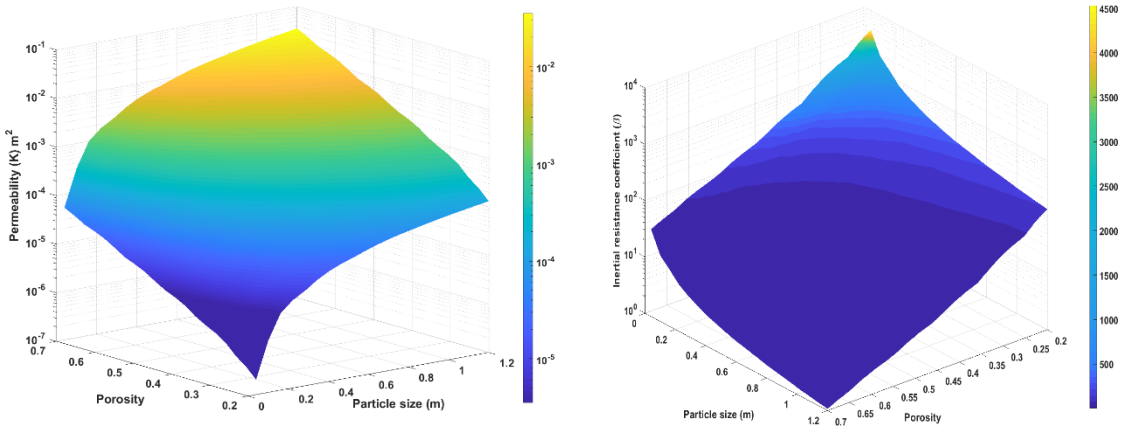


(a) (b)

Figure 3.12. Proposed (a) Permeability ($K$); and (b) Inertial resistance coefficient ($\beta$) as a function of the particle size and porosity

Based on these results, one can predict pressure loss in practical application, for example, the fan power required to provide an adequate mass flow rate in an underground mine ventilation network when the air has to pass through the blasted rocks. In packed beds of spheres with the same porosity (0.23) and particle diameters of 0.55, 0.70, and 0.85 m, the permeabilities were $5.13\times10^{-5}$, $8.04\times10^{-5}$, $1.1\times10^{-4}$ m$^2$, respectively. In a packed bed of spheres with the same of particle size (0.7 m) and porosities of 0.23, 0.28, and 0.37 are, respectively, the permeabilities were $8.04\times10^{-5}$, $1.66\times10^{-4}$, and $4.80\times10^{-4}$. Comparison of these values again confirms that both the porosity and

the particle size should be taken into consideration when calculating the pressure gradient in porous structures. By obtaining the permeability $K$ and inertial resistance coefficient $\beta$ from Figure 3.12, respectively, the Ergun coefficients, A and B along with the Forchheimer coefficient $F$ and $k$ can be determined.

### 3.5. Conclusion

It is essential to accurately predict the pressure gradient of air passing through a packed bed of large particles in various industry applications, such as mining, geothermal, oil and gas and construction. To the best of the authors' knowledge, this paper presents the first 3D PSM of flow through packed bed focused on large (in the scale of meters) particles. New constant values for the Ergun and Forchheimer correlations were proposed as functions of porosity and particle size. These modified values can be directly used to calculate the pressure gradient through a packed bed of large spheres (particle diameters from 0.04 to 1.2 m) in two different packing arrangements (UPS and n-UPS) from low to high porosity (0.2 – 0.7). The proposed correlations were successfully used to predict flow characteristic in volume-averaged CFD model with much lesser computational cost as compared to PSM. Permeability and inertial resistance were also presented as functions of porosity and particle size. The results can assist engineers to accurately estimate the pressure gradient in porous structures with a wide range of porosities and large-scale particle sizes. The outcome of this study may also lead to a starting point, as an alternative solution for estimating the friction factor which represents the fundamental contributions of fluid flow in porous media that govern the pressure gradient and its associated cost in said industries.

## 3.6. Nomenclature

Abbreviations**:**

| | |
|---|---|
| PSM | Pore-scale model |
| VAM | Volume-averaged model |
| UPS | Uniform particle size |
| n-UPS | non-Uniform particle size |
| REV | Representative elementary volume |

Symbols:

| | |
|---|---|
| $\rho$ | Density |
| $f_k$ | Friction factor |
| $D_f$ | Dimension factor |
| **u** | Superficial velocity |
| **U** | Average velocity |
| $p$ | Pressure |
| $\varepsilon$ | Porosity |
| $\mu$ | Dynamic viscosity of the fluid |
| $d$ | Particle diameter |
| $K$ | Permeability |
| η | Passability |
| Re | Reynolds number |
| $Re_k$ | local Reynolds number |
| $k$ | Carman-Kozeny constant |
| $F_o$ | Forchheimer number |
| $F$ | Forchheimer coefficient |
| A, B | Constants in the Ergun correlation |
| $\alpha$ | Viscous resistance coefficient |
| $\beta$ | Inertial resistance coefficient |

## 3.7. References


Allen, K. G. (2014). Rock bed thermal storage for concentrating solar power plants, Stellenbosch: Stellenbosch University.

Allen, K. G., T. W. von Backström and D. G. Kröger (2013). "Packed bed pressure drop dependence on particle shape, size distribution, packing arrangement and roughness." Powder Technology 246: 590-600.

Amini, Y., J. Karimi-Sabet and M. N. Esfahany (2016). "Experimental and numerical simulation of dry pressure drop in high-capacity structured packings." Chemical Engineering & Technology 39(6): 1161-1170.

Amiri, L., S. A. Ghoreishi-Madiseh, A. P. Sasmito and F. P. Hassani (2017). "Evaluation of Heat Transfer Performance between Rock and Air in Seasonal Thermal Energy Storage Unit." Energy Procedia 142: 576-581.

Amiri, L., S. A. Ghoreishi-Madiseh, A. P. Sasmito and F. P. Hassani (2018). "Effect of buoyancy-driven natural convection in a rock-pit mine air preconditioning system acting as a large-scale thermal energy storage mass." Applied Energy 221: 268-279.

Anbar, S., K. E. Thompson and M. Tyagi (2018). "The Impact of Compaction and Sand Migration on Permeability and Non-Darcy Coefficient from Pore-Scale Simulations." Transport in Porous Media: 1-21.

Baghapour, B., M. Rouhani, A. Sharafian, S. B. Kalhori and M. Bahrami (2018). "A pressure drop study for packed bed adsorption thermal energy storage." Applied Thermal Engineering 138: 731-739.

Barzegar Gerdroodbary, M., O. Jahanian and M. Mokhtari (2015). "Influence of the angle of incident shock wave on mixing of transverse hydrogen micro-jets in supersonic crossflow." International Journal of Hydrogen Energy 40(30): 9590-9601.

Bear, J. (2013). Dynamics of fluids in porous media, Courier Corporation.

Bufe, A. and G. Brenner (2018). "Systematic Study of the Pressure Drop in Confined Geometries with the Lattice Boltzmann Method." Transport in Porous Media 123(2): 307-319.

Cheng, N.-S. (2011). "Wall effect on pressure drop in packed beds." Powder Technology 210(3): 261-266.

Choi, Y. S., S. J. Kim and D. Kim (2008). "A Semi-empirical Correlation for Pressure Drop in Packed Beds of Spherical Particles." Transport in Porous Media 75(2): 133-149.

Cicéron, D., J. Comiti and R. P. Chhabra (2002). "Pressure drops for purely viscous non-newtonian fluid flow through beds packed with mixed-size spheres." Chemical Engineering Communications 189(10): 1403-1414.

Das, S., N. G. Deen and J. A. M. Kuipers (2018). "Multiscale modeling of fixed-bed reactors with porous (open-cell foam) non-spherical particles: Hydrodynamics." Chemical Engineering Journal 334: 741-759.

du Plessis, G. E., L. Liebenberg and E. H. Mathews (2013). "Case study: The effects of a variable flow energy saving strategy on a deep-mine cooling system." Applied Energy 102(0): 700-709.

Du Plessis, J. P. (1994). "Analytical quantification of coefficients in the Ergun equation for fluid friction in a packed bed." Transport in porous media 16(2): 189-207.

du Plessis, J. P. and S. Woudberg (2008). "Pore-scale derivation of the Ergun equation to enhance its adaptability and generalization." Chemical Engineering Science 63(9): 2576-2586.

Dukhan, N., Ö. Bağcı and M. Özdemir (2014). "Experimental flow in various porous media and reconciliation of Forchheimer and Ergun relations." Experimental Thermal and Fluid Science 57: 425-433.

Dumont, E., S. Woudberg and J. Van Jaarsveld (2016). "Assessment of porosity and biofilm thickness in packed beds using porous media models." Powder Technology 303: 76-89.

Erdim, E., Ö. Akgiray and İ. Demir (2015). "A revisit of pressure drop-flow rate correlations for packed beds of spheres." Powder Technology 283: 488-504.

Ergun, S. and A. A. Orning (1949). "Fluid flow through randomly packed columns and fluidized beds." Industrial & Engineering Chemistry 41(6): 1179-1184.

Feng, J., H. Dong and H. Dong (2015). "Modification of Ergun's correlation in vertical tank for sinter waste heat recovery." Powder Technology 280: 89-93.

Ghoreishi-Madiseh, S. A., L. Amiri, A. P. Sasmito and F. P. Hassani (2017). "A conjugate natural convection model for large scale seasonal thermal energy storage units: application in mine ventilation." Energy Procedia 105: 4167-4172.

Ghoreishi-Madiseh, S. A., A. P. Sasmito, F. P. Hassani and L. Amiri (2017). "Performance evaluation of large scale rock-pit seasonal thermal energy storage for application in underground mine ventilation." Applied Energy 185: 1940-1947.

Hicks, R. E. (1970). "Pressure Drop in Packed Beds of Spheres." Industrial & Engineering Chemistry Fundamentals 9(3): 500-502.

Jiang, Y., M. Khadilkar, M. Al-Dahhan and M. Dudukovic (2002). "CFD of multiphase flow in packed-bed reactors: I. k-Fluid modeling issues." AIChE Journal 48(4): 701-715.

Karacan, C. Ö. (2010). "Prediction of Porosity and Permeability of Caved Zone in Longwall Gobs." Transport in Porous Media 82(2): 413-439.

Kasaeian, A., R. Daneshazarian, O. Mahian, L. Kolsi, A. J. Chamkha, S. Wongwises and I. Pop (2017). "Nanofluid flow and heat transfer in porous media: a review of the latest developments." International Journal of Heat and Mass Transfer 107: 778-791.

Kaviany, M. (2012). Principles of heat transfer in porous media, Springer Science & Business Media.

Koekemoer, A. and A. Luckos (2015). "Effect of material type and particle size distribution on pressure drop in packed beds of large particles: Extending the Ergun equation." Fuel 158: 232-238.

Lacroix, M., P. Nguyen, D. Schweich, C. Pham Huu, S. Savin-Poncet and D. Edouard (2007). "Pressure drop measurements and modeling on SiC foams." Chemical Engineering Science 62(12): 3259-3267.

Li, L. and W. Ma (2011). "Experimental Study on the Effective Particle Diameter of a Packed Bed with Non-Spherical Particles." Transport in Porous Media 89(1): 35-48.

Liu, S., A. Afacan and J. Masliyah (1994). "Steady incompressible laminar flow in porous media." Chemical engineering science 49(21): 3565-3586.

Macdonald, I., M. El-Sayed, K. Mow and F. Dullien (1979). "Flow through porous media-the Ergun equation revisited." Industrial & Engineering Chemistry Fundamentals 18(3): 199-208.

Mahdi, R. A., H. Mohammed, K. Munisamy and N. Saeid (2015). "Review of convection heat transfer and fluid flow in porous media with nanofluid." Renewable and Sustainable Energy Reviews 41: 715-734.

Mayerhofer, M., J. Govaerts, N. Parmentier, H. Jeanmart and L. Helsen (2011). "Experimental investigation of pressure drop in packed beds of irregular shaped wood particles." Powder Technology 205(1): 30-35.

Montillet, A., E. Akkari and J. Comiti (2007). "About a correlating equation for predicting pressure drops through packed beds of spheres in a large range of Reynolds numbers." Chemical Engineering and Processing: Process Intensification 46(4): 329-333.

Nemec, D. and J. Levec (2005). "Flow through packed bed reactors: 1. Single-phase flow." Chemical Engineering Science 60(24): 6947-6957.

Nield, D. A. and A. Bejan (2006). Convection in porous media, Springer.

Ozahi, E., M. Y. Gundogdu and M. Ö. Carpinlioglu (2008). "A modification on Ergun's correlation for use in cylindrical packed beds with non-spherical particles." Advanced Powder Technology 19(4): 369-381.

Partopour, B. and A. G. Dixon (2017). "An integrated workflow for resolved-particle packed bed models with complex particle shapes." Powder Technology 322: 258-272.

Rong, L. W., Z. Y. Zhou and A. B. Yu (2015). "Lattice–Boltzmann simulation of fluid flow through packed beds of uniform ellipsoids." Powder Technology 285: 146-156.

Shitzer, A. and M. Levy (1983). "Transient behavior of a rock-bed thermal storage system subjected to variable inlet air temperatures: Analysis and experimentation." Journal of Solar Energy Engineering 105(2): 200-206.

Singh, R., R. Saini and J. Saini (2006). "Nusselt number and friction factor correlations for packed bed solar energy storage system having large sized elements of different shapes." Solar Energy 80(7): 760-771.

Thabet, A. and A. G. Straatman (2018). "The development and numerical modelling of a Representative Elemental Volume for packed sand." Chemical Engineering Science 187: 117-126.

Turrado, S., J. R. Fernández and J. C. Abanades (2018). "Determination of the solid concentration in a binary mixture from pressure drop measurements." Powder Technology 338: 608-613.

Vafai, K. and C. Tien (1981). "Boundary and inertia effects on flow and heat transfer in porous media." International Journal of Heat and Mass Transfer 24(2): 195-203.

Vollmari, K., R. Jasevičius and H. Kruggel-Emden (2016). "Experimental and numerical study of fluidization and pressure drop of spherical and non-spherical particles in a model scale fluidized bed." Powder Technology 291: 506-521.

Vollmari, K., T. Oschmann, S. Wirtz and H. Kruggel-Emden (2015). "Pressure drop investigations in packings of arbitrary shaped particles." Powder Technology 271: 109-124.

Wang, Y., C. L. Lin and J. D. Miller (2016). "3D image segmentation for analysis of multisize particles in a packed particle bed." Powder Technology 301: 160-168.

Whitaker, S. (1986). "Flow in porous media I: A theoretical derivation of Darcy's law." Transport in Porous Media 1(1): 3-25.

Wu, J., B. Yu and M. Yun (2008). "A resistance model for flow through porous media." Transport in Porous Media 71(3): 331-343.

# Connecting Text

*The outcomes from Chapter 3 led to initiation of a study to seek an alternative solution for estimating the friction factor (the fundamental contributions of fluid flow in porous media) that determines the pressure gradient and its associated cost in mining, geothermal, oil and gas, and construction industries. Thus, the main objective of Chapter 4 is to develop a new friction factor correlation of flow through broken rock that can be used directly in the Atkinson equation.*

*Chapter 4 has been submitted for publication as:*

***Leyla Amiri**, Seyed Ali Ghoreishi-Madiseh, Ferri P. Hassani, and Agus P. Sasmito. "Friction Factor Correlation for Airflow through Broken Rocks and Its Applications in Mine Ventilation."*

# CHAPTER 4

# 4. Friction factor correlation for airflow through broken rocks and its applications in mine ventilation


## Abstract

The Atkinson equation along with its friction factor is commonly used to estimate pressure requirement in mine ventilation. However, friction factor correlation of flow through broken rock, typically found in blasted stope, gob, rock pit or block caving rock deposits etc, is currently unavailable. Also, it is impractical to conduct direct measurements of flow resistance in an inaccessible broken rock zone. This paper aims to develop a new friction factor correlation of flow through broken rock that can be used directly in Atkinson equation. The proposed correlation is valid for broken rock with diameter between 0.04 – 1.2 m and porosity range from 0.23 to 0.7.


### 4.1. Introduction

In the recent years, there has been considerable interest in the concept of optimizing the underground mine ventilation system, owing to the providing larger amount of airflow rate to battle the impacts of higher-temperature environments experienced with increment the depth of underground mines. The most empirical aspect of designing a modern mine ventilation network is to estimate pressure losses by passing the air through the underground opening areas as well as caved zones. A significant amount of energy is typically being used to circulate air through underground mine. It is not uncommon that some portions of the energy are used to ventilate air through broken/fractured rock, such as air leakage in a stope after blasting, block-caved mines,

gob area in coal mine, or large scale rock-pit thermal energy storage, such as in Creighton mine, Sudbury. The required fan power can be obtained by accurately estimating the pressure drop through the broken rock and the amount of ventilated air to generate mine (system) characteristic curve. The fan operating point can be graphically obtained from the intersection point between fan characteristic curve (from the manufacturer) and mine characteristic curve. Underground mine ventilation network analysis has not been much changed since 1935 when McElroy conducted the study of the engineering factors in the underground mine ventilation. The concept of utilizing the Atkinson equation presented as a promising method to estimate pressure drops in underground mine openings by (McElroy 1935).

The Atkinson equation (Eqs. 4.1 and 4.2) is a well-known method to determine the pressure drop in the airways and to generate mine characteristic curve when designing the ventilation system in an underground mine (McPherson 2012).

$$\Delta p = RQ^2 \tag{4.1}$$

where $\Delta p$ represents the pressure drop through the airway, $R$ is the airway resistance, and $Q$ is the volumetric mass flowrate. This equation was proposed by Atkinson in 1890 as a mathematical tool in solving airflow problems in the airways in mines. Since the pressure loss is directly affected by the airway resistance, the effect of the various physical conditions of the airways on the pressure loss as well as power requirements for constant quantities of flow can be readily examined through the Atkinson formula. The fan power requirement, in the underground ventilation system, is basically determined by airflow, since the pressure losses are proportional to the second order of volumetric airflow rate. If volumetric airflow rate is kept constant, then the required fan power changes directly by varying the airway resistance, which should be determined by using different developed methods. It is worth mentioning that it is not an easy task and varies significantly by even small changes in the physical characteristics of the system. This challenging task will be

extensively addressed in this paper. The total airflow rate may be increased by increase the fan power only, however in some cases boosting the airflow rate without changing the airway resistance often result in huge fan power increases; thus, the only practical way is a reduction of the airway resistance through physical characteristics of the porous zone (e.g., permeability) in underground mine ventilation system. In summary, he Atkinson, which is the simplified version of Eq. 4.2, indicates that by estimating the airway's resistance and measuring the volumetric mass flow rate, the pressure drop, and associated fan power can be calculated. It is worth to mention that mine ventilation engineers usually work with the volumetric mass flowrate rather than air flow velocities, thus the Eq. 4.1 seems to be more common equation for estimating the pressure losses. The volume of air flow as well as the associated friction losses are mainly two key parameters to find the optimum design of ventilation system. Hence, a proper balance between these parameters is the essential requirement to optimize the total associated cost to underground mine ventilation system.

It should be noted that, by varying the amount of the air flowrate in Eq. 4.1, the mine characteristic curve can be graphically generated. This equation, which is the simplified version of Eq. 4.2, indicates that by estimating the airway's resistance and measuring the volumetric mass flow rate, the pressure drop, and associated fan power can be calculated. Also, by varying the amount of the air flowrate in Eq. 4.1, the mine characteristic curve can be graphically generated. Of all the parameters in Atkinson's equation (Eq. 4.2a), the airway resistance, represented by the Atkinson friction factor (or Chezy-Darcy friction factor), $f$, or *k*-factor ($k = \frac{1}{2}\rho f$) is the most challenging parameter to be accurately estimated. Noted, the Atkinson friction factor, $f$, is equal to 4 times of the Fanning friction factor, thus a correlating factor has been taken into calculation to derive the following equation:

$$\Delta p = 4fL\frac{\text{per}}{4A}(\frac{1}{2}\rho v^2) = fL\gamma\left(\frac{1}{2}\rho v^2\right) = kL\gamma(\rho v^2) \quad (4.2a) \qquad \gamma = \frac{\text{per}}{A} \quad (4.2b)$$

Here, $L$ (m) is the length of the airway, $\gamma$ ($\text{m}^{-1}$) is the geometric characteristics, defined in Eq. 4.2b, where per (m) is the perimeter of the airway, $A$ ($\text{m}^2$) is the cross-section area of the airway, $v$ ($\text{m/s}$) is air velocity and $\rho$ ($\text{kg/m}^3$) is air density (Figure. 4.1). For typical mine ventilation airways, the friction factor, *f*, has already been established either from Moody chart or from mine ventilation database, see for example in page 138 of textbook (McPherson 2012). In flow through broken rock, unfortunately, no such friction factor data or correlation is available in literature that can be directly used to estimate pressure drop in Atkinson equation. In other applications, such as mechanical or chemical engineering, some friction factor correlation for porous media is available, however, it is derived based on Ergun or Darcy-Forchheimer equation which cannot be directly plugged into Atkinson formula. Moreover, all of the correlations were derived based on much smaller particle size ($O \sim 10^{-3}$m).

As there is no specific friction factor correlation for flow through broken rocks in literature, the friction factor value may deviate by up to 70% depending upon the air flow movement through the porous media (Allen 2014). Hence, the Atkinson friction factor ($f$) of each specific packed rock bed needs to be established, which will enable mine ventilation engineers to perform more accurate estimation on the required fan power for the ventilation system.

In essence, the friction factor varies according to the fluid velocity and this relation can be described in a linear trend for the Darcy regime (Kaviany 2012). From first principle, we can thus postulate that the drag force ($F_d$) of a fluid on the rock in a packed bed is proportional to the cross-section area, $A_c$ ($\text{m}^2$) and the pressure drop, indicated as follows:

$$F_d = A_c \Delta p \tag{4.3}$$

By applying volume averaging theory for porous media in which the fluid-solid momentum is described at a small length scale, which is much smaller than the linear dimension of the system, yet larger than the linear dimension of the rock (Kaviany 2012), Equation 4.4 can be obtained as a function of the area of the rocks (i.e. spheres) and the kinetic energy of the fluid:

$$F_d = f_{por}\, A_s(\frac{1}{2}\rho v^2) \tag{4.4}$$

$$A_s = SV = SA_cL \tag{4.5}$$

$$S = \varepsilon/d_H = 6(1-\varepsilon)/d \tag{4.6}$$

where $f_{por}$ is the porous media friction factor of broken rock, which can be assumed as porous media, and includes the inertia and pressure distribution over the surface of the rocks as well as shear effects caused by velocity gradients (viscous force). $A_s$ ($m^2$) is the total surface area of the particles in broken rock bed, $V$ ($m^3$) is the total volume, $S$ ($m^{-1}$) is the specific surface area based on the solid volume, $d_H$ (m) is the hydraulic diameter, $d_H$ (m) is the particle diameter, and $L$ (m) is the length of fractured zone (Kaviany 2012). Then Equation 4.7 is obtained by combining Equations 4.4-4.6. For further details refer to (Wentz Jr and Thodos 1963, Kaviany 2012).

$$\Delta p = f_{por} L \frac{1}{d_H}\frac{1}{\varepsilon^2}\left(\frac{1}{2}\rho v^2\right) = f_{por} L\alpha \left(\frac{1}{2}\rho v^2\right) \tag{4.7}$$

By comparing Equations 4.2 and 4.7, one can see their similarity of these two. The only difference is on the geometric characteristics' parameters of a macroscale airway channel and porous structure in broken rock, respectively, $\gamma$ (c.f. Eq. 4.2) and $\alpha$ (c.f. Eq. 4.7). In a packed bed of

spherical particles, the geometric characteristic parameter $\alpha$ can be related to rock diameter $d$ (m) and the porosity $\varepsilon$ of the bed as (Ergun 1952, Kaviany 2012):

$$\alpha = {}^{1}/_{\varepsilon^2 d_H} = 6(1-\varepsilon)/d\varepsilon^3 \tag{4.8}$$

As the main focus of this study is developing the friction factor in the porous zone in underground mine environments like stopes filled with broken rock, this study is carried out by considering Equation 4.7 which is developed based on the porous structure. It should be noted that the relationship between $f$ in Atkinson equation and $f_{por}$ in Ergun equation can be obtained by taking the geometric characteristics of any specific bed into consideration; it will be discussed later in this paper.As the main focus of this study is developing the friction factor in the porous zone in underground mine environments like stopes filled with broken rock, this study is carried out by considering Equation 4.8 which is developed based on the porous structure. It should be noted that the relationship between $f$ in Atkinson equation and $f_{por}$ in Ergun equation can be obtained by taking the geometric characteristics of any specific bed into consideration; it will be discussed later in this paper.

The pressure losses in straight airways, of as uniform cross-sectional area as is normal for this particular type, are considered as strictly friction pressure losses and are so calculated. Any departure from this condition of straight airway of approximately uniform area is considered to involve shock losses which may be calculated approximately as friction losses by means of certain allowances but which should preferably be calculated separately as shock losses.

As mentioned earlier, although several porous media friction factor correlations are available in literature, they are all derived from Ergun equation which cannot be directly used in Atkinson equation. The friction factor correlations for porous media from the literature can be categorised into two main groups: spherical shaped particles and non-spherical shaped particles (Carman 1937,

Hicks 1970, Tallmadge 1970, Allen 2014). Most of the correlations are only valid within a specific range of Reynolds numbers and porosities (c.f. Table 4.1). Moreover, most of them were developed as a function of Reynolds number ($Re = \rho v d/\mu$), while a limited number of correlations include the effect of porosity and geometrical characteristics of the bed in their studies (e.g. (Fried and Idelchik 1989), (Montillet, Akkari et al. 2007), and (Singh, Saini et al. 2006)). Another important point is that these studies consider particle diameters in the order of $O \sim 10^{-3}$m, which is far from the typical range present in mining applications (i.e. particle diameter $O \sim 1$m). In fact, a deep understanding of the air flow's behavior through the porous media and the pressure drop's dependence on the porosity and the size of the particles is needed for mining applications where there is a definite lack of information on the friction factor and its corresponding pressure drop.

Table 4.1 Various friction factor correlations for porous media

| **Correlation** | **Validity** | **Ref.** |
|---|---|---|
| $f_{por} = \frac{150}{Re} + 1.75$ | $Re < 3{,}000$ | (Ergun 1952) |
| $f_{por} = \frac{180}{Re} + \frac{2.68}{Re^{0.1}}$ | $0.1 < Re < 60{,}000$ | (Carman 1937) |
| $f_{por} = \frac{6.8}{Re^{0.2}}$ | $300 < Re < 60{,}000$ | (Hicks 1970) |
| $f_{por} = \frac{150}{Re} + \frac{4.2}{Re^{0.17}}$ | $0.1 < Re < 100{,}000$<br>$0.35 < \varepsilon < 0.88$ | (Tallmadge 1970) |
| $f_{por} = \frac{160}{Re} + \frac{3.1}{Re^{0.1}}$ | $0.01 < Re < 40{,}000$<br>$0.36 < \varepsilon < 0.42$ | (Brauer 1971) |
| $f_{por} = 0.061\omega^{0.2}(\frac{1000}{Re} + \frac{60}{Re^{0.5}} + 12)$ | $10 < Re < 2500$<br>$3.8 < \omega < 50$<br>$\omega = bed\ diameter/particle\ diameter$<br>$6.3mm < d < 15.8mm$ | (Montillet, Akkari et al. 2007) |
| $f_{por} = 4.466Re^{-0.2}\varepsilon^{-2.945}$ | $Re < 2500$<br>$0.3 < \varepsilon < 0.6$<br>$125mm < d < 186mm$ | (Singh, Saini et al. 2006) |

The behaviour and characteristic of air flow through broken rock is extremely complicated to understand due to the complex flow structure through the pore geometry and non-linearity of pressure, shear and inertia forces. Some experimental studies were conducted by some researchers to quantify porous media friction factor using laboratory-scale packed bed of simulated particles in wind tunnel. However, simulating rock bed particle with large diameter typically found in mining would have been impractical, whilst direct measurement in underground mine in broken rock zone can be prohibitive due to safety concern. Computational fluid dynamics (CFD) has, in few decades, emerged as a useful tool to help quantifying flow characteristic in porous media. There are two main approaches of using CFD in porous media: pore-scale and volume averaging models. The former is carried out by modelling the real complex porous structure in pore scale level, while the latter is conducted by implementing volume averaging theory using the representative elementary volume (REV) to simplify the flow properties into Ergun (or Darcy-Forchheimer) equation in the conservation equation of momentum. In our earlier work (Amiri, Ghoreishi-Madiseh et al. 2019), we developed volume average Ergun properties of flow through broken rock, i.e. permeability and inertia coefficient, from pore-scale CFD model that can be used in volume averaged CFD model. To extend our work for practical used in mine ventilation industry, we aim to develop Atkinson friction factor correlation for airflow through broken rock that can be directly used in Atkinson equation and/or mine ventilation network software such as VNetPC, Ventsim or Vuma. We utilize pore-scale CFD model of packed rock bed to simulate the complex flow structure and generate database of characteristic curve of pressure-Reynolds which will be used to develop Atkinson friction factor correlation. The rock diameter is varied from 0.04 to 1.2 m with porosity range 0.23 to 0.7 typically found in underground mines.

The air velocity varies though the pores in a porous media and different regimes (Darcy and Darcy-Forchheimer regimes) can be found in one packed bed of particles in different part of such porous media. Such variations in velocities are rarely happened within underground mine airways with the constant cross-sectioned area. These fluctuations in air velocities occur mostly where gas (e.g., air, methane, etc.) passes/leaks through packed bed of fractured rocks due to change in the opening areas through the porous media. In such circumstances, the estimation of air leakage and pressure losses play significant roles to calculate the proper fan power requirement to provide enough ventilated air in underground openings. Since, these mentioned factors are very complicated to be obtained, the numerical analysis appears to be inevitable.

From mining engineers' point of view, there has always been a practical preference for a widely applicable correlation, similar to Atkinson equation, that could be utilized for a packed bed of broken rocks in underground mine as a rule of thumb to estimate the amount of air/gas leakage as well as the fan power requirement. It should be noted that such a practical equation for these special circumstances has not been proposed yet.

### 4.2. Model description

The pressure drop of air passing through a packed rock bed arises from the resistance to flow through the pores. In this study, all generated particles in the packed beds are assumed to be spherical; even though in situ rock bed particles exhibit a considerable variability in shape, with few spherical particles. Particles are considered as impermeable rock. Uniform and non-uniform particle size distributions of rocks are evaluated. The schematic and computational domain of the pore-scale model (PSM) is shown in Figure 4.1. The cross-sectional of the domain is 20 m length by 20 m width by 20 m height. The 3D PSM model was generated in EDEM software and then imported to ANSYS workbench for labelling, meshing, and assigning the boundary conditions.

The boundary conditions for the PSM can be summarized as: (1) top surface is defined as inlet and various air velocities are prescribed, (2) bottom surface is set as a pressure outlet, (3) the sides and the cut surface of particles are assigned as a no-slip wall (Figure. 4.1). We also refer to (Amiri, Ghoreishi-Madiseh et al. 2019) for the detailed information of the model. Laminar flow is assumed within the PSM and the conservation of mass (Eq. 4.9) and momentum (Eq. 4.10) equations are given by (Nield and Bejan 2006):

$$\nabla \cdot \mathbf{u} = 0 \tag{4.9}$$

$$\rho(\mathbf{u} \cdot \nabla \mathbf{u}) = -\nabla p + \mu \nabla^2 \mathbf{u} \tag{4.10}$$

Where $\rho$, $\mathbf{u}$, and $\mu$ are the fluid density, physical velocity, and dynamic viscosity, respectively. The $\nabla p$ denotes the pressure drop over the length of the broken rock zone. It should be noted that an impermeable wall with a no-slip condition were assumed for the solid surfaces in the PSM. Apart from pore scale-based computational fluid dynamics (CFD) model, pressure drop through porous media can also be estimated analytically using Darcy-Forchheimer equation (Eq. 4.11).

$$\frac{\Delta p}{L} = \nabla p = -\left(\frac{\mu U}{K} + \frac{F \rho U^2}{\sqrt{K}}\right) \tag{4.11}$$

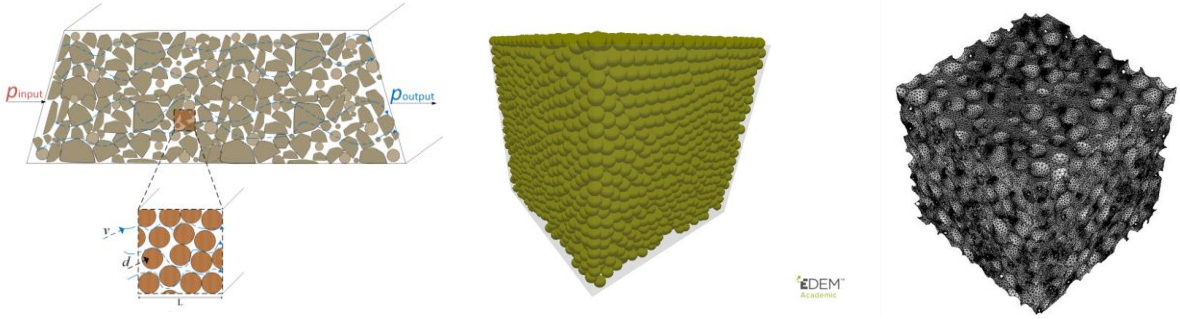


Figure 4.1. Schematic and computational domain of realistic and simplified proposed packed bed of broken rocks

Packed bed of spherical particles may better represent sand and gravel products, rather than caved broken rock, however the main purpose of this study is to investigate the applicability of CFD

models to predict the airflow through the pores. Thus, the motivation behind the current study isn't to check whether a packed bed of spherical particles is a proper representation of a fractured rock in underground environment. Instead, its main purpose is to confirm whether a CFD technique can reliably estimate the pressure drop and airflow behaviour within the pores in such a large-scale porous media for a real geometry and particle size, when the geometrical characteristics (e.g., bed dimensions, particle size, porosity) of the packed bed are given. It is worth mentioning that in mining environment, unlike the other industries, where the explicit information about fractured zone is rare, the outcome of the current study would be very helpful. Practically speaking, mining professionals usually design the ventilation system based on the available values from other mines, without making any direct measurements. Luckily, CFD methods are developed to help with evaluating fluid flow and heat transfer in such an inaccessible environment.

### 4.3. Results and Discussions

#### 4.3.1. Validation of pore-scale CFD model using experimental data

Despite high-accuracy of CFD model results due to its remarkable development within the past few years, it is essential to validate the model output with the experimental data prior to applying them for further investigation of the fluid flow behaviour through the packed beds. Hence, we developed a packed bed of spherical particles imitating the experimental setup implemented by (Allen 2014) whereby golf balls of diameter 42.6 mm were used to create the packed bed (470 mm width by 500 mm height) with the porosity of 0.376. To the best of our knowledge, no study is reported on experimental and numerical analysis of large-scaled packed beds. Therefore, we used the results of the study by Allen (2014), presenting the largest particle size studied in literature to date, to validate our model. As shown in Figure 4.2, the simulated data are in reasonably good agreement with the value of $f_{\mathrm{por}}$ in the experimental data. The highest deviation of about 9.46%

occurs in low local Reynold number which can be ascribed to difficulty in measuring the low flow rate in the experimental setup. By increasing $Re_k$, the deviation reduces to 4.93% which is highly satisfactory in the prediction of pressure drop through the packed beds. It indicates that the methodology used in this study is acceptable to generate the packed bed filled with large size of particles (e.g. broken rock). The deviation can be attributed to a variety of reasons such as variations in the surface roughness, arrangement of the particles in the bed, and slight difference (i.e. 2.5%) in the porosities of the simulation and the experimental setup. It is, therefore, hoped that the scale-up pore-scale CFD model helps to provide an in-depth analysis of the fluid flow phenomena that happens within the pores of the broken rock beds. The effect of porosity on the fluid velocity distribution in packed beds are examined by (Suekane, Yokouchi et al. 2003). The velocity distribution at $Re_k$ of about 43 is shown in Figure 4.3. Accordingly, the well agreement between experimental data and simulated results would offer an advanced novel technique to understand air flow in fractured rocks.

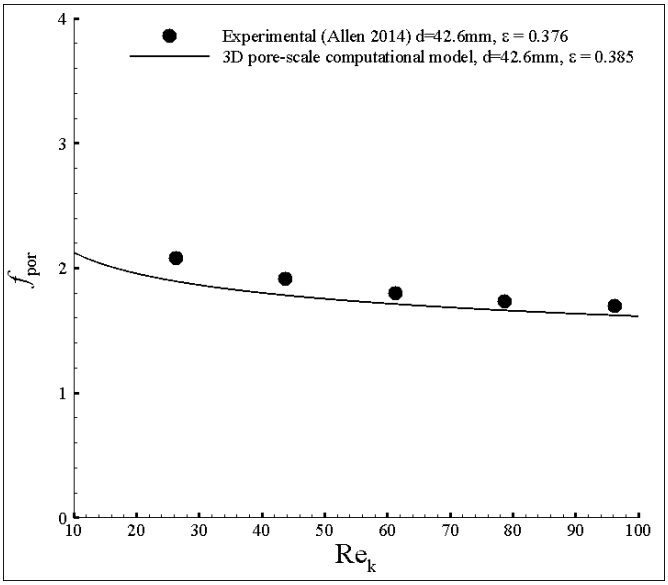


Figure 4.2. Validation of the simulation results (pore-scale CFD model) and the experimental data of (Allen 2014)

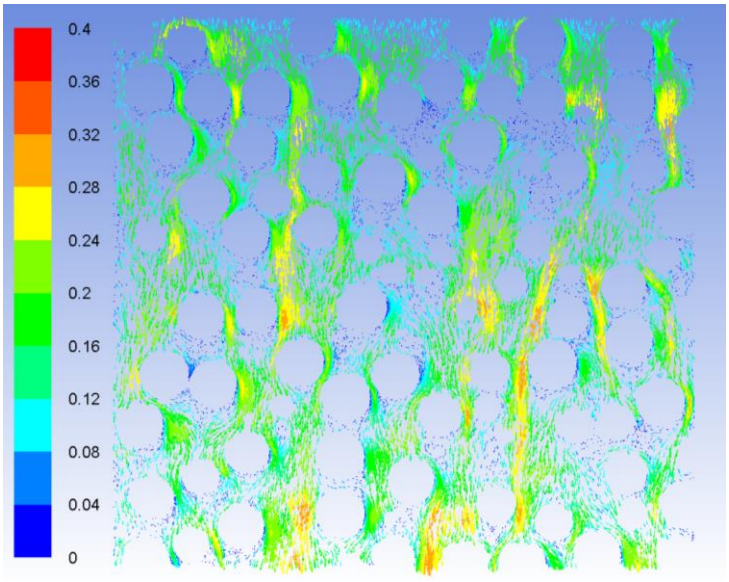


Figure 4.3. Velocity vectors in pore-scale model with porosity 0.385 and particle size 42.6 mm

### 4.3.2. Development of the new porous media friction factor, $f_{por}$, correlation

Friction factor for porous media, $f_{\mathrm{por}}$, is found to be a function of viscous (shear) and inertia forces which can be represented by non-dimensional terms: local Reynolds number, $\mathrm{Re_k}$, and Forchheimer coefficient, $F$. The functional relationship for $f_{\mathrm{por}}$ can therefore be written as:

$$f_{por} = f(Re_K, F) \tag{4.12}$$

Thus, all of the calculated data are converted into dimensionless groups, defined as:

$$\mathrm{Re_k} = \frac{\rho \mathrm{U}}{\mu}\sqrt{K} \tag{4.13}$$

$$F = \beta\sqrt{K} \tag{4.14}$$

$$F_o = Re_k F \tag{4.15}$$

where $\mathrm{F_o}$ is the Forchheimer number. Permeability, K ($\mathrm{m^2}$), and inertial resistance coefficient, $\beta$ ($\mathrm{m^{-1}}$), can be calculated by following correlations (Eqs. 4.16 and 4.17) in which the original Ergun constant values, A and B, are 150 and 1.75 respectively.

$$K = \frac{d^2 \times \varepsilon^3}{A \times (1-\varepsilon)^2} \tag{4.16}$$

$$\beta = \frac{B \times (1-\varepsilon)}{d \times \varepsilon^3} \tag{4.17}$$

However, the authors postulated in previous paper (Amiri, Ghoreishi-Madiseh et al. 2019) that these Ergun values shouldn't be considered as a constant value for all porous media. So, the effect of porosity ε and particle size $d$ (m) should be taken into consideration (Amiri, Ghoreishi-Madiseh et al. 2019). Also, it can be noted that the permeability of any packed bed has a direct relation with the particle size and porosity of the system (Amiri, Ghoreishi-Madiseh et al. 2019). Thus, the adopted A and B can be read from proposed chart in Figure 4.4.

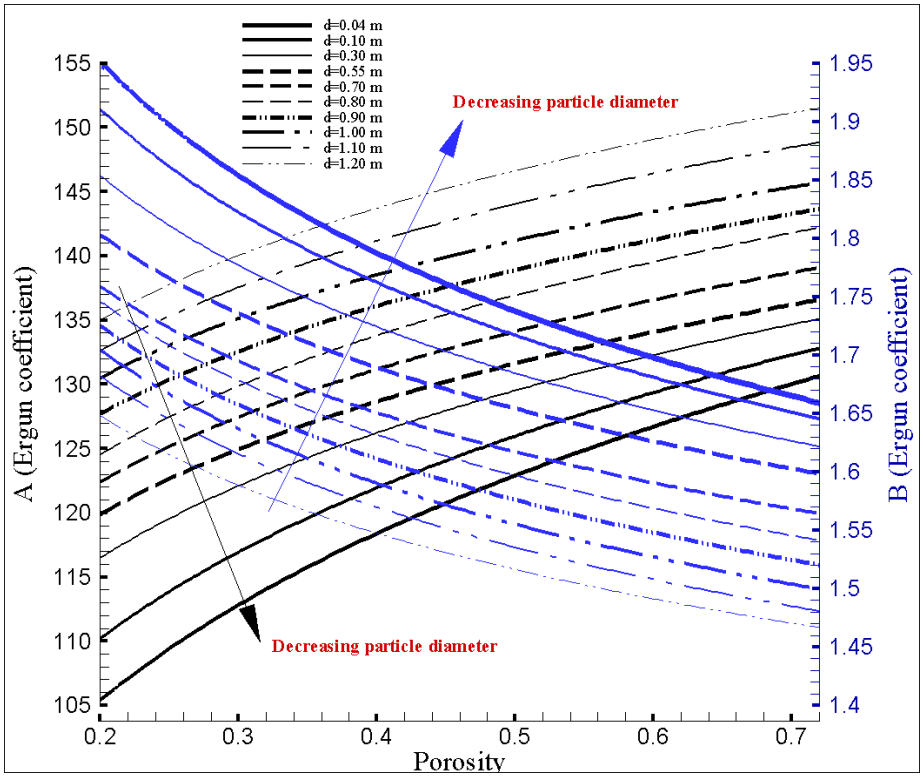


Figure 4.4. Values of the constants A and B from the Ergun correlation at different porosities and particle size predicted by the pore-scale model.

Data from Figures 4.5 and 4.6 are employed to calculate the statistical correlation with the help of multivariate regression analysis. The correlation is developed for $f_{\text{por}}$ by following the method given by (Singh, Saini et al. 2006). From the presented data, the average slope of the data simulated

by PSM for packed beds, with porosity ranging from 0.23 to 0.70, is calculated. Afterward, the variation of the function $f_{\mathrm{por}}/(5.6/\mathrm{Re_K})$ with $F$ of the packed rock bed is measured. So, the following correlation is proposed to determine the porous media friction factor value, $f_{\mathrm{por}}$, as a function of $\mathrm{Re_K}$ and $F$. The correlation is expected to be valid for particle diameter ranging from 0.04 to 1.20 m and porosity values ranging from 0.23 to 0.70 and to fit well to the calculated pore-scale CFD data:

$$f_{por} = \frac{5.6}{Re_K} + (Re_K F)^{0.12} \tag{4.18}$$

The friction factor value is plotted against the local Reynolds number ($Re_K$) and is indicated in Figure 4.5 for broken rocks of spherical particles porosities ($\varepsilon$) ranging from 0.23 to 0.70 with a constant particle diameter ($d$) of 0.55 m. It is apparent that the friction factor decreases with increasing porosity values for a given local Reynolds number and a given particle size. This behaviour is due to the fact that the total specific surface area in the bed decreases with increasing porosity. Also, the results show that as porosity increases, the friction factor value decreases due to the probability of decrease in tortuousness in streamlines. To further study the effects of particle size, the friction factor value is plotted against the local Reynolds number ($Re_K$) with a constant porosity of 0.28 for particle sizes ranging from 0.04 m to 1.2 m (c.f. Figure 4.6). The results reveal that as particle size rises, the friction factor value decreases. This may be due to the reduction of the tortuousness value of the fluid passing through the packed bed, as well as the total specific surface area. Therefore, it is reasonable to expect a higher pressure drop in a packed bed with smaller particle sizes as well as a lower porosity value. Thus, it can be concluded that the $Re$, particle diameter, and porosity of the packed bed are the main factors which strongly affect the pressure drop and friction factor value. Therefore, effects of these parameters are needed to be taken into account when developing the new correlations.

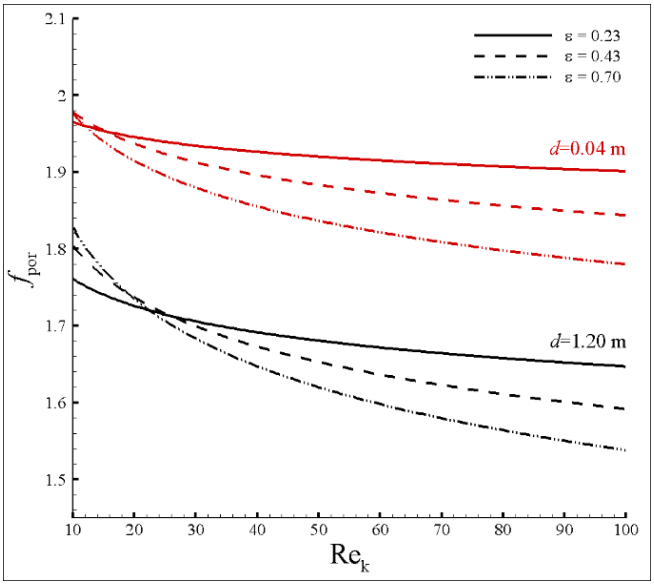


Figure 4.5. The friction factor for porous media value plotted against the local Reynolds number for broken rock with porosity 0.23-0.70 at constant rock diameter 1.20 m and 0.04 m

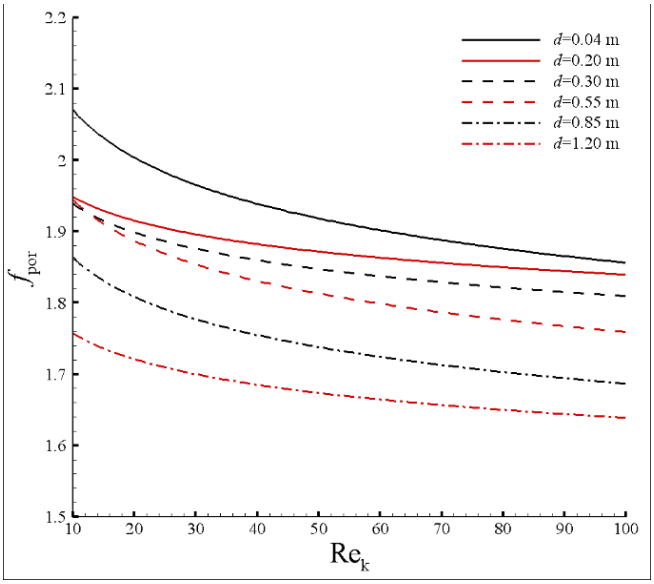


Figure 4.6. The friction factor for porous media value plotted against the local Reynolds number for broken rock with diameter 0.04-1.20 m at constant porosity 0.28

The proposed porous media friction factor correlation, $f_{por}$ in Equation 4.18, is further verified against one calculated from the pore scale CFD model, as depicted from Figure 4.5. Here, the simulated pore scale CFD results are in a good agreement with the results calculated by the proposed correlation (Equation 4.18) over the range of Reynolds number considered. On closer

inspection, the average absolute percentage deviation between the pore scale CFD model and calculated results are less than 7%, which can be attributed to the error in multiple regression analysis. Therefore, it can be deduced that the proposed friction factor correlation, $f_{por}$ in Equation 4.18, can accurately predict the porous media friction factor for airflow through broken rock which later can be used to estimate pressure drop and fan power.

Now, let us compare our proposed porous media friction factor correlation (Equation 4.18) against correlations available in literature from Table 4.1. It is worth mentioning that the available correlations in literature were developed based on much smaller particle diameters. Some correlations are only function of Reynolds number; some others have limited validity range in terms of porosity and/or particle diameter. Figure 4.6 shows the comparison of proposed correlation with correlations from literature. It is apparent that the friction factor correlations from literature deviate significantly as compared to our proposed correlation by up to 40%. It should be noted that a large deviation of some points can be the result of having large particle size 0.04-1.2 m in the packed rock bed of this study which is different from the studies in the literature. As discussed above, even the friction factor correlations considering the porosity value of the bed may lead to significant errors due to the exclusion of the effect of particle size. Thus, the fundamental need to improve the accuracy of the predicted friction factor and pressure drop in the packed bed composed of large particles motivates us to perform this study. These finding highlight the importance of geometrical and flow parameters, such as porosity $\varepsilon$, particle size diameter $d$, viscosity $\mu$, density $\rho$, and velocity $v$, which are represented by non-dimensional parameters ($Re_K$ and $F$) in the porous media friction factor correlation.

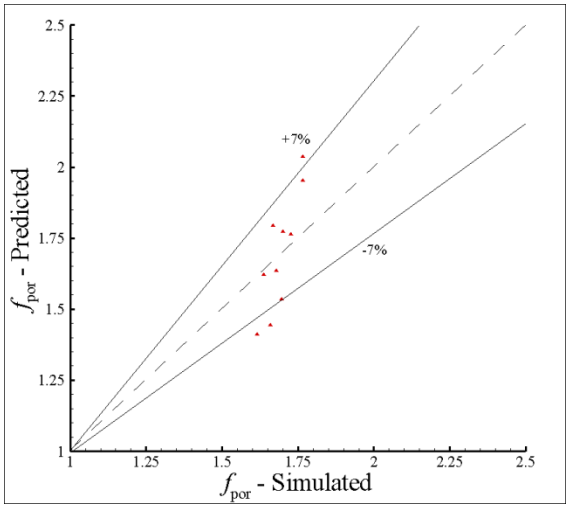


Figure 4.7. Comparison of porous media friction factor, $f_{por}$, from proposed correlation (Eq. 4.18) and pore scale CFD model

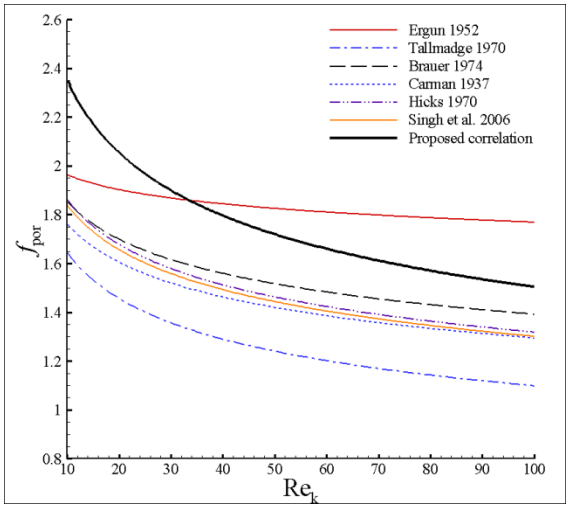


Figure 4.8. Comparison of porous media friction factor, $f_{por}$, correlations from literature and proposed correlation (Eq. 4.18) for rock diameter 0.55 at constant porosity 0.37

### 4.3.3. Development of the new Atkinson friction factor, *f*, correlation for broken rock and its application in underground mine: case study a stope filled with broken rock

The amount of pressure drop through the caved zone (gob) in the longwall operation or the fragmented ore in a stope after blasting has a significant effect on the underground mine ventilation system. The permeability of the stope section is a critical parameter in predicting the gas or air leakage into the mine environment (Ren and Edwards 2000). Furthermore, an accurate prediction of pressure drop helps to understand the behaviour of gas (e.g. methane, air) passing through the stope filled with fragmented rock. A correct prediction of pressure drop can also reveal the amount of gas or air leakage through the ventilation system, which is important in an underground mining environment. Although its importance is recognized, direct measurement of the pressure drop and permeability is not practical due to the inaccessibility of stopes in the majority of cases.

Thus far, we have developed a new porous media friction factor correlation, $f_{por}$, and verify its validity for packed rock bed with diameter range from 0.04 to 1.2 m and porosity from 0.23 to 0.7. In mine ventilation practice, however, the Ergun equation is not commonly used, instead Atkinson

equation is the one used and implemented in most of mine ventilation software. Therefore, the proposed porous media friction factor, $f_{por}$, in Equation 4.18 cannot be directly used into the software. Here, we extend our proposed $f_{por}$ into a more general Atkinson friction factor, *f*, so it can be directly used in mine ventilation practice. By comparing Equation 4.2a and 4.6, we can apply geometric characteristic correction, and thus the Atkinson friction factor, *f*, in Equation 4.18 can be obtained as:

$$f = f_{\mathrm{por}} \frac{\alpha}{\gamma} \tag{4.19}$$

For demonstration purpose, a case study is carried out to show the application of proposed Atkinson friction factor correlations (Eq. 4.19) in a stope which has a cross-sectional of 20 m by 20 m and height of 20 m. This stope is assumed to be filled with the large particles size 0.85 m (i.e. broken rocks). Figure 4.8 shows the predicted Atkinson friction factor for the stope with specific geometrical characteristics. It is seen that the Atkinson friction factor for broken rock is about two to three order of magnitude higher than typical Atkinson friction factor found in ventilation airways which makes sense as pressure drop in broken rock is much higher than in airways.

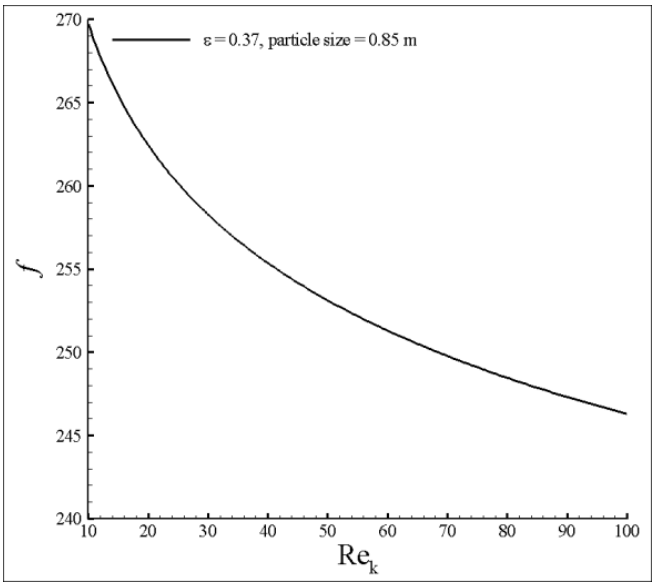


Figure 4.9. The Atkinson friction factor value plotted against the local Reynolds number for a stope of 20 m ×20 m ×20 m filled with broken rock diameter 0.85 m and porosity 0.37

The Atkinson friction factor in Figure 4.10 along with friction factor correlations in literature from Table 4.1 (corrected using geometric characteristic $\alpha/\gamma$) are used to calculate the pressure drop through broken rock using well-known Atkinson equation (Equation 4.2). The results are summarized in Figure 4.10. Here, several features are apparent; foremost among them is that the proposed correlation yields better agreement to the 3D pore-scale computational model within 7% errors at higher local Reynolds number.

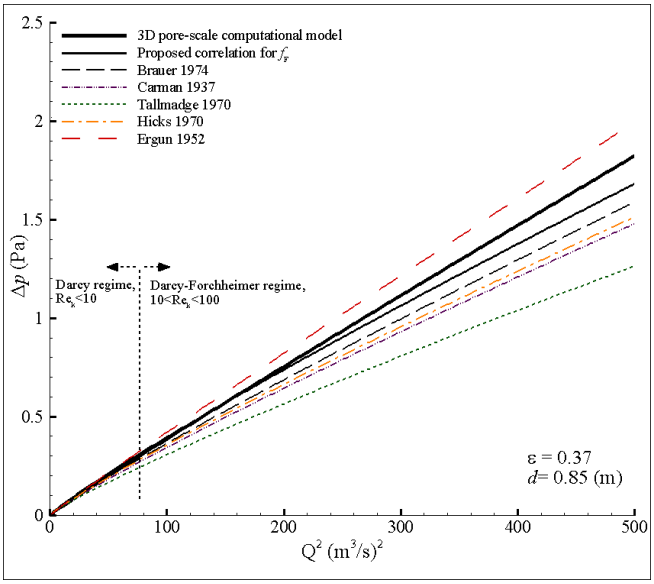


Figure 4.10. Comparison of simulated and predicted pressure drop over the 20 m height of the stope with the calculated data from previous correlations

Closer inspection reveals that the correlations from literature deviate up to 34% with increasing magnitude at higher Reynolds number (see Figure 4.11). From a linear regression of the data presented, it is found that the slopes of all lines are between 0.0029 and 0.0043. These slopes can be considered as the air path resistance *R* from the Atkinson equation (Eq.4.1). This result is in line with the observation that the effect of the air velocity passing through the pores on the pressure drop is important when the local Reynolds number is relatively high in the Darcy-Forchheimer regime (Nield and Bejan 2006). The results demonstrate that the proposed Atkinson friction factor correlation, *f*, in Equation 4.18 can be successfully used to predict pressure drop using mine ventilation Atkinson equation in a broken rock zone in underground mine.

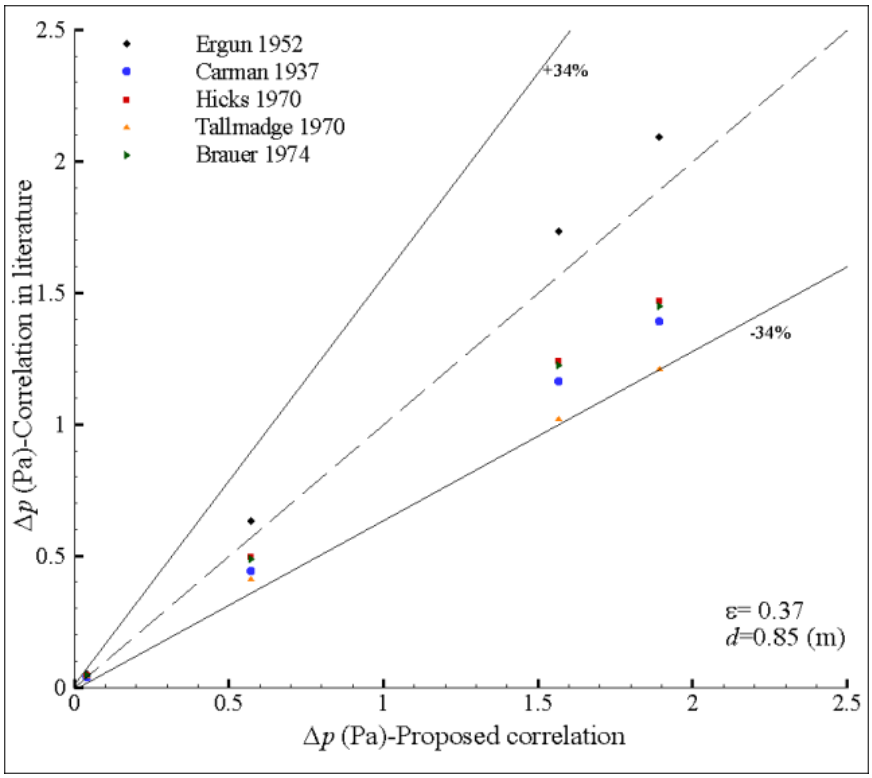


Figure 4.11. Comparison of numerical and predicted results with the pressure drop correlations from the literature

### 4.4. Conclusions

A study is conducted to evaluate the applicability of existing friction factor correlations for porous media to be implemented in typical broken rock in underground mine ventilation. The correlations are compared against three-dimensional pore scale-based computational fluid dynamics model. It was found that the available friction factor correlations deviate significantly as compared to pore scale CFD model. Therefore, there is a need to develop a new friction factor correlation for broken rock with large diameter. We further derive and develop a new Atkinson friction factor correlation based on Ergun or Darcy-Forchheimer equations with the help of pressure-Reynolds database generated from pore-scale computational model. The proposed correlation is functions of geometrical characteristics ($\alpha/\gamma$) and leading forces (shear and inertia) summarized in non-dimensional parameters, i.e. local Reynolds number and Forchheimer coefficient. A reasonable

agreement is shown between numerical results and one from the proposed correlation. The average deviation between the numerical and predicted values of the friction factor is ±7%. Hence, the developed correlation can accurately predict the Atkinson friction factor and its corresponding pressure drop for packed beds of broken rock in the specified range of geometric and flow parameters.

## 4.5. References


Allen, Kenneth Guy. (2014). Rock bed thermal storage for concentrating solar power plants. Stellenbosch: Stellenbosch University.

Amiri, Leyla, Sasmito, Agus P., Ghoreishi-Madiseh, Seyed Ali , & Hassani, Ferri P. . (2019). Estimating pressure loss and Ergun parameters in packed rock bed with large diameter in mining applications. Submitted - Scientific Report.

Brauer, Heinz. (1971). Grundlagen der Einphasen-und Mehrphasenströmungen (Vol. 2): Sauerländer.

Carman, Philip Crosbie. (1937). Fluid flow through granular beds. Trans. Inst. Chem. Eng., 15, 150-166.

Ergun, Sabri. (1952). Fluid flow through packed columns. Chem. Eng. Prog., 48, 89-94.

Fried, Erwin, & Idelchik, IE. (1989). Flow resistance, A Design Guide for Engineering, Hemisphere Publ: Co.

Hicks, RE. (1970). Pressure drop in packed beds of spheres. Industrial & Engineering Chemistry Fundamentals, 9(3), 500-502.

Kaviany, Maasoud. (2012). Principles of heat transfer in porous media: Springer Science & Business Media.

McPherson, Malcolm J. (2012). Subsurface ventilation and environmental engineering: Springer Science & Business Media.

Montillet, A, Akkari, E, & Comiti, J. (2007). About a correlating equation for predicting pressure drops through packed beds of spheres in a large range of Reynolds numbers. Chemical Engineering and Processing: Process Intensification, 46(4), 329-333.

Nield, Donald A, & Bejan, Adrian. (2006). Convection in porous media (Vol. 3): Springer.

Ren, TX, & Edwards, JS. (2000). Three-dimensional computational fluid dynamics modelling of methane flow through permeable strata around a longwall face. Mining technology, 109(1), 41-48.

Singh, Ranjit, Saini, RP, & Saini, JS. (2006). Nusselt number and friction factor correlations for packed bed solar energy storage system having large sized elements of different shapes. Solar Energy, 80(7), 760-771.

Suekane, Tetsuya, Yokouchi, Yasuo, & Hirai, Shuichiro. (2003). Inertial flow structures in a simple-packed bed of spheres. AIChE journal, 49(1), 10-17.

Tallmadge, JA. (1970). Packed bed pressure drop—an extension to higher Reynolds numbers. AIChE journal, 16(6), 1092-1093.

Wentz Jr, Charles A, & Thodos, George. (1963). Pressure drops in the flow of gases through packed and distended beds of spherical particles. AIChE journal, 9(1), 81-84.

# Connecting Text

*In Chapter 5, using the vast volume of large broken rocks as a thermal energy storage mass was investigated with the help of outcomes from previous chapters regarding calculating the permeability and pressure drop. Seasonal thermal energy storage is a cost-effective solution to improve cooling and heating efficiencies, thereby reducing associated costs. The effect of natural convection and a variety of heat transfer mechanisms in the proposed storage system was modelled and simulation results and field-data measurements were compared. For the range of porosities studied (0.45–0.20), these parameters had a small effect on the outlet air temperature and the thermal storage phenomenon. The novel model also compared forced and natural convection and incorporated the effects of design factors (e.g., air trench positions and flow rate of ventilated air) on energy savings.*

*Chapter 5 is published as:*

***Leyla Amiri**, Seyed Ali Ghoreishi-Madiseh, Agus P. Sasmito, and Ferri P. Hassani. "Effect of buoyancy-driven natural convection in a rock-pit mine air preconditioning system acting as a large-scale thermal energy storage mass." Applied Energy 221 (2018): 268-279.*

# CHAPTER 5

## 5. Effect of buoyancy-driven natural convection in a rock-pit mine air preconditioning system acting as a large-scale thermal energy storage mass


## Abstract

Underground mining is among the most energy-intensive industries and ventilation comprises a significant portion of the energy demands of this important industry. Using the vast volume of broken rock, left in a decommissioned mine pit, as a thermal energy storage mass has enormous potential to lower ventilation-related energy costs in deep underground mines. This approach facilitates moderating seasonal air temperature variations. Seasonal thermal energy storage is a cost-effective solution to improve cooling and heating process efficiencies, thereby reducing associated costs. Temperature gradients observed in the proposed storage system suggest the presence of a natural convection heat transfer mechanism that is buoyancy-driven. The effect of natural convection and a variety of heat transfer mechanisms were modeled and simulation results and field-data measurements were compared. The conjugate heat transfer and fluid flow model that was developed considers the porous rock mass in the rock-pit along with the air (i.e. fluid) blanketing the top surface. The effects of rock size, permeability and porosity were studied. It was observed that, for the range of porosities (from 0.45 to 0.20), these parameters have a small effect on the outlet air temperature and the performance of thermal storage phenomenon. The novel model compares forced (from ventilation fan) and natural (result of buoyancy) convection. Further,

it incorporates the effect of design factors, such as air trench positions and flow rate of ventilated air, on energy savings.

## 5.1. Introduction

Energy intensity is a major hurdle to future development of the global mining industry. It derives from two major issues: 1) the insatiable demand of the mining industry for energy for electricity, heating, and cooling; and 2) unpredictable fossil fuel prices caused by numerous political and economic factors. Mining is among the most energy-intensive industries, along with chemical, petroleum, and base metals (Masnadi, Grace et al. 2015, Yu, Gao et al. 2016). This enormous energy need is accompanied by a long-term trend for fossil fuel prices to rise. Therefore, energy costs constitute a growing portion of the total operating costs of mining operations, which will be exacerbated by the introduction of carbon taxes by major industrial countries (Ploeg and Withagen 2014). The unreliable nature of the energy market is a fundamental risk source, making operating costs difficult to predict. These major issues have motivated the mining industry to seek new sources and technologies to help improve the energy efficiency, reduce the energy demand, and the shrink carbon footprint of operations (Bharathan, Sasmito et al. 2017).

Among the energy-intensive activities at a mine, ventilation (fresh air, air heating and cooling) is a top contributor. Studies have shown that 40% of the overall electricity consumption in a typical underground mine is due to ventilation (Karacan 2007, Gan 2015) which roughly results in 60% of the total operating costs in these mines (Karacan 2007, Bharathan, Sasmito et al. 2017). In Canada and other countries such as the USA and Australia, the quality and quantity of the ventilation air is regulated. For example, the fresh air flow required in hard rock mines in the province of Ontario in Canada is regulated at 0.06 m3/s per kW of diesel engine power at a (wet

bulb globe) air temperature below 27°C. To ensure good air quality, especially in the deepest galleries and work faces, underground mine operators typically require enormous amount of fresh air (100–1000 m3/s). Over the past few years, several studies have focused on cost-effective ventilation solutions for underground mines (Kurnia, Xu et al. 2016).

Ventilation energy demands are in form of electricity (needed to run main/booster/auxiliary fans for air delivery or mechanical refrigeration for cooling) or thermal heat (sourced from fossil fuels such as natural gas, propane, or diesel)(Chatterjee, Zhang et al. 2015). In extremely cold climates, like winter in Canada and many areas in the USA, intake air must be preheated to above 0°C before sinking down the main ventilation shaft(s). In summer, air temperature should be maintained below 27°C (wet bulb globe) with a cooling system (Mayala, Veiga et al. 2016). Preheating and cooling practices incur account for 50–80% of annual ventilation operating costs (US$4–15 million), depending on the mine depth, production, temperature and the air flow rate.

Ventilation costs cannot be eliminated, but they can be effectively reduced by employing renewable energy sources at mine site (Ghoreishi-Madiseh, Hassani et al. 2015, Ghoreishi-Madiseh, Sasmito et al. 2017). For example, seasonal thermal energy storage (STES) involves collecting thermal energy (heat or cold, depending on the outside temperature) when it is available for future use. Storing thermal energy in waste rock is an elegant approach to improve the performance of the mine ventilation system. To create a STES system, huge volumes of waste rock are dumped into a decommissioned pit to create a large seasonal heat storage mass. This massive STES unit provides the mining operation with a “natural heat exchanger”. The amount of sensible thermal energy stored in the STES system depends on the temperature difference between the air and rock mass. By passing ventilation air through the broken rock mass, seasonal temperature

oscillations can be moderated, resulting in 50–80% reduction in ventilation costs (Sylvestre 1999, Ghoreishi-Madiseh, Sasmito et al. 2017, He, Luo et al. 2017).

As a natural and renewable energy storage technique, STES can help deep underground mines meet refrigeration and air preheating requirements and reduce associated greenhouse gas emissions. For example, employing STES at the Creighton mine in Sudbury, Ontario reduced seasonal variations in the temperature of the intake fresh air passing through the natural heat exchanger unit (Ghoreishi-Madiseh, Amiri et al. 2017). As mining extends to depths beyond current norms in the Creighton mine, implementation of STES has improved energy management, and has led to considerable savings in capital/operating costs.

Since large-scale STES systems have been deployed, ventilation engineers have gained engineering tools with which they can assess STES system capacity and improve system performance. Their research initiated development of empirical relations that are backed by extensive amount of field data but lack the means of predicting the capability of system to satisfy a growing ventilation demand (Envers 1986, Stachulak 1991). Another serious shortcoming of empirical models is that they cannot be applied to assess temperatures and air velocities inside the rock-pit over time (Ghoreishi-Madiseh, Sasmito et al. 2017). To overcome such limitations, researchers have proposed using three-dimensional (3D) models capable of simulating heat transfer and fluid flow in large-scale STES units (Sylvestre 1999, Schafrik 2015, Ghoreishi-Madiseh, Sasmito et al. 2017, He, Luo et al. 2017). These 3D models enable engineers to achieve a better understanding of the heat exchange phenomena in the rock-pit and to improve the storage capacity of STES units.

To analyze the storage and extraction of heat in such large-scale STES units, it is necessary to establish a clear understanding of heat exchange and fluid mechanics in the porous structure of the

rock-pit. This approach is based on assuming a homogeneous porous medium (i.e. solid rock mass and fluid air) (Pruess 1985, Zhu, Fox et al. 1999, Berrada, Loudiyi et al. 2017). Using a volume averaging technique, researchers have been able to derive amenable fluid flow and heat transfer equations for porous media (Whitaker 1977, Vafai and Tien 1981, Vafai and Tien 1982, Carbonell and Whitaker 1984, Ghoreishi-Madiseh, Hassani et al. 2013, Yan, Wieberdink et al. 2015).

Interphase exchange of heat plays an important role in the performance of STES systems. The local thermal equilibrium (LTE) assumption can be made when the solid phase and the fluid inside the pores are thermally equilibrated in microscopic (pore) scale (Zhang, Xiao et al. 2015). However, this assumption is not valid when interphase exchange of heat cannot be neglected and the local thermal non-equilibrium (LTNE) methodology should be taken into consideration (DeGroot and Straatman 2011). Building upon recent heat and fluid flow models for porous media (Ghoreishi-Madiseh, Hassani et al. 2013), Ghoreishi-Madiseh et al. (Ghoreishi-Madiseh, Sasmito et al. 2017) developed a 3D numerical model for large-scale STES systems that they compared and validated with field data collected at the ventilation trenches and ambient air temperature data. This study highlighted that in some cases, LTE is not a valid assumption. Accordingly, a LTNE approach was proposed underlying the importance of heat interphase heat exchange.

However, there are other potentially important mechanisms that have not yet been studied. For example, most STES systems are large—hundreds of metres in each length—and exhibit relatively large temperature differences (20–40°C). The performance of a given STES system depends on several factors, which can be classified as controllable and uncontrollable. The present study primarily considered controllable factors such as number of active trenches, air flow rate through each trench and through the whole system, and pressure drop and air speed in the rock-pit and ventilation trenches. The significance of uncontrollable factors, such as wind speed in the vicinity

of the pit, air leakage in closed trenches, solar radiation, and ice formation will be examined in future studies by the authors.

According to the findings of (Nield and Bejan 2006) and Ghoreishi-Madiseh et al. (Ghoreishi-Madiseh, Sasmito et al. 2017), large STES systems are viable candidates for exhibiting sizeable buoyancy-driven fluid flow, especially in the gravitational direction. To visualize the situation, assume warm summer air (~20°C) drawn by ventilation fans into the rock-pit to exchange thermal energy with the cold broken rock mass (~0°C). The buoyancy effect pushes the air through the rock mass because the air becomes more dense while cools. Buoyancy will also induce natural circulation of the air that is inside the rock-pit. In the winter, the reverse is expected to happen: the buoyancy force lifts the air, making heat exchange less effective. Therefore, a salient point in the study of large-scale STES systems is to investigate the effects of fan-driven forced convection versus the effects of buoyancy-driven (natural) convection. So far, to the best of the authors' knowledge, the effects of buoyancy-driven fluid flow on the thermal efficiency of large-scale STES systems have not been investigated.

To conduct this type of research, equations of heat transfer and fluid flow inside the rock-pit (i.e. porous medium) should be coupled with the air (i.e. fluid) blanketing the top surface. This so called "conjugate" modeling is necessary and considered as an important feature of the current research. The conjugate heat transfer and fluid flow model can qualitatively and quantitatively evaluate the significance of natural convection. The performance of STES system will be studied in three canonical cases:

1. In the absence of gravity, so there is zero buoyancy everywhere

2. In a non-conjugate model that ignores the presence of fluid air on the top of the rock-pit: buoyancy can act in the porous rock-pit but there will be no circulation of air on the top of the rock-pit
3. In a conjugate model where buoyancy can act in the porous rock-pit and the overlying air.

Thermal storage performance of the large-scale STES is then evaluated using the developed model and the potential energy savings are quantified and discussed.

## 5.2. Model development

The 3D mathematical model of rock-pit STES developed by (Ghoreishi-Madiseh, Sasmito et al. 2017) was extended to take into account overlying ambient air to allow for conjugate fluid flow and heat transfer, and to capture the development of natural convection flow caused by temperature differences within the ambient air and broken rock. The physical domain of the rock-pit STES system comprises a porous, conical cavity that represents an abandoned open-pit mine filled with broken rock, and the ambient air overlying the rock-pit (Fig. 5.1). This allows natural convection to develop due to temperature differences between the rock-pit and ambient air. The diameter of the rock-pit is 697 m and the maximum depth is 330 m (Fig. 5.1). The thickness of the rock-pit at the bottom-most point is 133 m (Sylvestre 1999). The volume of the broken rock in the STES is a porous zone (porosity 0.4) with a mean rock diameter of 1.2 m created by past mining activities (Sylvestre 1999). The ventilation air is forced to flow through the porous medium rock-pit by ventilation fans installed on six trenches located at the bottom of the rock-pit. The trenches are connected with ventilation shafts to continuously provide fresh air to the underground mine.

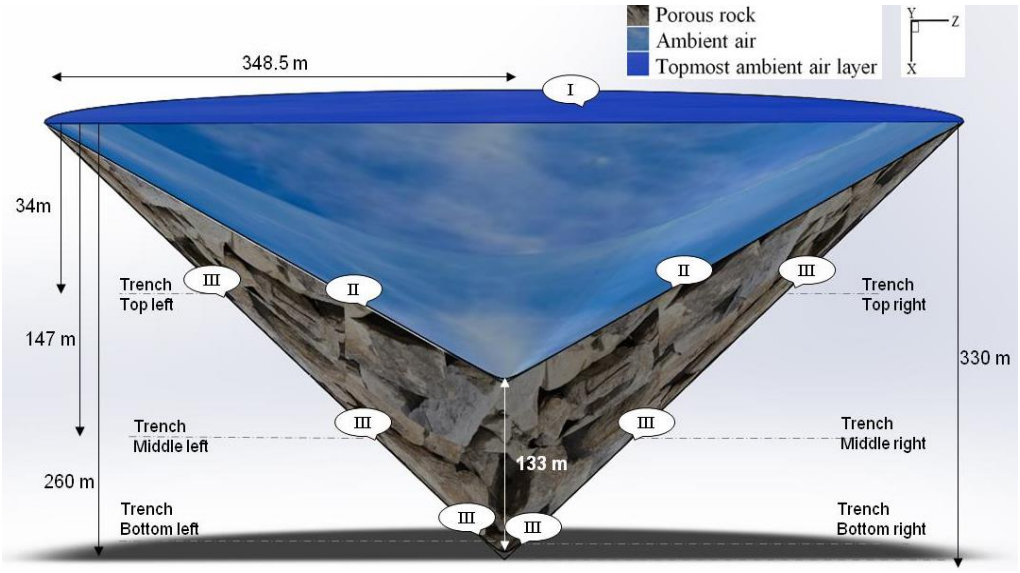


Figure 5.1. Schematics and 3D representation of the computational domain of STES system and its boundary conditions; (I) pressure inlet at top ambient air, (II) wall at surrounding surface and the bottom of rock-pit, and (III) exhaust fan at trenches

### 5.2.1. Governing equations

Temperature at the overlying (top) boundary of air is set as a sinusoidal function to represent the seasonal ambient air temperature profile. The lowest and highest temperature values are assumed to be –20°C (i.e. minimum winter daily average) and +20°C (i.e. maximum summer daily average), respectively. This temperature gradient between the rock-pit and ambient leads to natural convection flow. The mathematical model comprises two components: the rock-pit and ambient air.

- *Rock-pit*

The porous rock-pit is assumed to have a laminar and transient flow regime while its interphase heat is deemed to experience LTNE (Ghoreishi-Madiseh, Sasmito et al. 2017) effects. Partial differential equations of conservation of mass, momentum and energy are used in the mathematical modelling, in which all terms are clearly stated: accumulated mass and balanced mass are

explained by Eq.5.1 (conservation of mass); accumulated momentum, inertia force term, pressure and viscous force, dilated volume caused by different factors such as compressibility factor of gas, gravitational force, and the friction loss factor (Darcy) are explained by Eq.5.2 (conservation of momentum); accumulated energy in air, convective heat transfer mechanism, conductive heat transfer mechanism and interphase exchange of energy among fluid-phase and solid-phase are explained by Eq.5.3 (conservation of energy in a fluid-phase); and accumulated energy in rock-pit, conductive heat transfer mechanism, and interphase exchange of energy among rock-pit and air are explained by Eq.5.4 (conservation of energy in a solid-phase). Average-volume theory is considered for fundamental variables such as velocity and temperature which are driven by superficial variables.

$$\partial \varepsilon \rho_{\mathrm{f}} / \partial t + \nabla \cdot \left( \rho_{\mathrm{f}} \langle \mathbf{u} \rangle \right) = 0 \tag{5.1}$$

$$\partial \left( \varepsilon \rho_{\mathrm{f}} \mathbf{u} \right) / \partial t + \nabla \cdot (\rho_{\mathrm{f}} \langle \mathbf{u} \rangle \otimes \langle \mathbf{u} \rangle) = -\nabla \langle p \rangle \mathbf{I} + \nabla \cdot \left[ \mu_{\mathrm{f}} \left( \nabla \langle \mathbf{u} \rangle + \left( \nabla \langle \mathbf{u} \rangle \right)^{\mathrm{T}} \right) - \frac{2}{3} \mu_{\mathrm{f}} \left( \nabla \cdot \langle \mathbf{u} \rangle \right) \mathbf{I} \right] + \rho_{\mathrm{f}} \mathbf{g} - \frac{\mu_{\mathrm{f}}}{\kappa} \langle \mathbf{u} \rangle \tag{5.2}$$

$$\partial \left( \varepsilon \rho_{\mathrm{f}} c_{\mathrm{p,f}} \langle T \rangle_{\mathrm{f}} \right) / \partial t + \nabla \cdot \left( \rho_{\mathrm{f}} c_{\mathrm{p,f}} \langle \mathbf{u} \rangle \langle T \rangle_{\mathrm{f}} \right) = \nabla \cdot \left( \varepsilon k_{\mathrm{f}} \nabla \langle T \rangle_{\mathrm{f}} \right) + h_{\mathrm{fs}} A_{\mathrm{fs}} \left( \langle T \rangle_{\mathrm{s}} - \langle T \rangle_{\mathrm{f}} \right) \tag{5.3}$$

$$\partial \left( (1-\varepsilon) \rho_{\mathrm{s}} c_{\mathrm{p,s}} \langle T \rangle_{\mathrm{s}} \right) / \partial t = \nabla \cdot \left( (1-\varepsilon) k_{\mathrm{s}} \nabla \langle T \rangle_{\mathrm{s}} \right) + h_{\mathrm{fs}} A_{\mathrm{fs}} \left( \langle T \rangle_{\mathrm{f}} - \langle T \rangle_{\mathrm{s}} \right) \tag{5.4}$$

where $\partial$ is the partial differential symbol, ε is porosity, $\rho$ is density, subscript f pertains to the fluid, $t$ indicates time, ∇ is the representative of the Nabla symbol, subscript s indicates the solid phase, ‹**u**› is the superficial fluid velocity, $p$ is the pressure, **I** is the identity or second order unit tensor, $\mu$ is the dynamic viscosity of the fluid, **g** is gravitational acceleration, $\kappa$ is thermal conductivity, $c_p$ is the specific heat, and $T$ is the temperature.

The heat transfer coefficient $h$ is given by (Nield and Bejan 2006):

$$1/h_{fs} = d_p/Nu_{fs}k_f + d_p/\beta k_s \tag{5.5}$$

where the Nusselt number among broken rock and air ($Nu_{fs}$) is defined as (Nield and Bejan 2006):

$$Nu_{fs} = (0.255/\varepsilon)\,\mathrm{Pr}^{1/3}\,\mathrm{Re}^{2/3} \tag{5.6}$$

where Pr is the Prandtl number and Re is Reynolds number.

The specific surface area, $A_{fs}$, is taken into consideration by the interphase mass transfer defined as (Nield and Bejan 2006):

$$A_{fs} = 6(1-\varepsilon)/d_p \tag{5.7}$$

where $d_p$ is the diameter of the rock.

*- Ambient air*

In the ambient air, transient turbulent fluid flow and heat transfer with buoyancy are considered. The turbulent mass, momentum, and energy transport equations subject to appropriate boundary conditions are solved. Several temperature-dependent thermophysical properties of air are also taken into account. Conservation equations for turbulent mass, momentum, energy, and species in vector form are:

$$\partial\rho_f/\partial t + \nabla\cdot\rho_f\mathbf{U} = 0 \tag{5.8}$$

$$\partial(\rho_f\mathbf{U})/\partial t + \nabla\cdot\rho_f\mathbf{UU} = -\nabla p\mathbf{I} + \nabla\cdot\left[(\mu+\mu_t)\left(\nabla\mathbf{U}+(\nabla\mathbf{U})^T\right)\right] + \frac{2}{3}\nabla\cdot\left[(\mu+\mu_t)(\nabla\cdot\mathbf{U})\mathbf{I} - \rho_f k\mathbf{I}\right] + \rho_f\mathbf{g} \tag{5.9}$$

$$\partial(\rho_f\mathbf{U})/\partial t + \nabla\cdot\rho_f\mathbf{UU} = -\nabla p\mathbf{I} + \nabla\cdot\left[(\mu+\mu_t)\left(\nabla\mathbf{U}+(\nabla\mathbf{U})^T\right)\right] + \frac{2}{3}\nabla\cdot\left[(\mu+\mu_t)(\nabla\cdot\mathbf{U})\mathbf{I} - \rho_f k\mathbf{I}\right] + \rho_f\mathbf{g} \tag{5.10}$$

where **U** is the turbulent air velocity (**U** = **u**+**u**' where **u** is the mean velocity and **u**' is the fluctuating velocity components), $k$ is the turbulent kinetic energy, $\kappa_{eff}$ is thermal conductivity of the fluid, $\mu_t$ is turbulent viscosity (defined in Eq. 5.14), and $\mathrm{Pr}_t$ is the turbulent Prandtl number. The density follows incompressible ideal gas law as a function of pressure and temperature, given by:

$$\rho_f = \left((p_{\text{op}} + p)M\right)/RT \tag{5.11}$$

where $p_{\text{op}}$ is the Operating Pressure, M is the molecular weight of the gas and R is known as the universal gas constant.

Turbulent flow in the current model was studied numerically to determine which of four turbulence models (k-ε, k-ω, Reynolds Stress Model and Spalart-Allmaras) is best suited to predict the temperature of the air leaving the STES system and approximate experimental data. All four models were in close agreement (< 1% relative difference) with experimental data (Fig. 5.2).

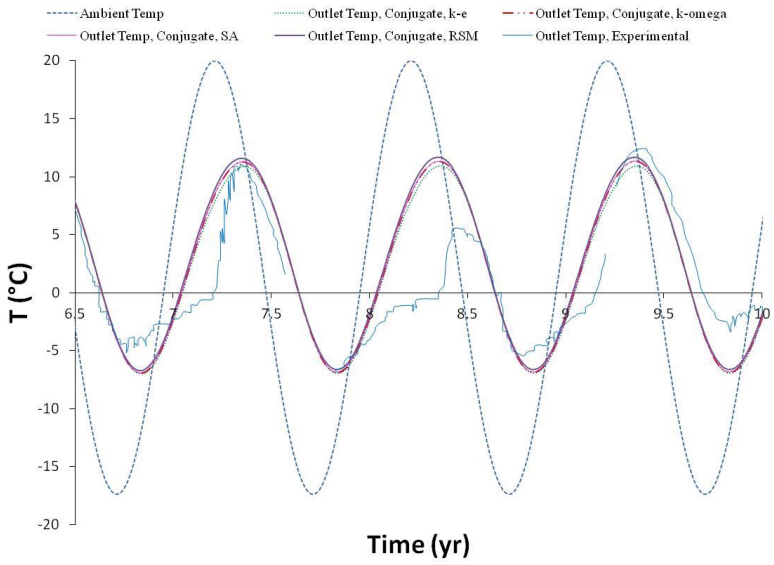


Figure 5.2. Validation of simulated and measured (Fava 2012 ) outlet temperature after exchanging heat with the fractured rock mass

Therefore, the most commonly used turbulent model, k-ε, was selected to minimize computational costs. In addition, published literature on numerical modeling of turbulence inside porous media has largely recommended the use of the k–ε model, in which turbulence is characterized by the turbulent kinetic energy (k) and its rate of dissipation (ε), which is coupled to the turbulent viscosity (Avramenko and Kuznetsov 2006, Teruel 2009, Nimvari, Maerefat et al. 2012).

$$\partial\left(\rho_{\mathrm{f}} k\right)/\partial t+\nabla\cdot\left(\rho_{\mathrm{f}}\mathbf{U}k\right)=\nabla\cdot\left[\left(\mu+\frac{\mu_t}{\sigma_k}\right)\nabla k\right]+G_k+G_B-\rho_{\mathrm{f}}\varepsilon, \tag{5.12}$$

$$\partial\left(\rho_{\mathrm{f}}\varepsilon\right)/\partial t+\nabla\cdot\left(\rho_{\mathrm{f}}\mathbf{U}\varepsilon\right)=\nabla\cdot\left[\left(\mu+\frac{\mu_t}{\sigma_\varepsilon}\right)\nabla\varepsilon\right]+C_{1\varepsilon}\frac{\varepsilon}{k}\left(G_k+C_{3\varepsilon}G_B\right)-C_{2\varepsilon}\rho_{\mathrm{f}}\frac{\varepsilon^2}{k}, \tag{5.13}$$

where $\mu_t$ indicates turbulent viscosity given by:

$$\mu_t=\rho_{\mathrm{f}}C_\mu\frac{k^2}{\varepsilon}, \tag{5.14}$$

$G_k$ denotes the turbulent kinetic energy initiated by velocity gradients, $G_B$ indicates the turbulent kinetic energy generated by buoyancy, $C_{1\varepsilon}$, $C_{2\varepsilon}$, $C_{3\varepsilon}$, $C_\mu$, $\sigma_k$, and $\sigma_\varepsilon$ are constants with values of 1.44, 1.92, 1.44, 0.09, 1 and 1.3, respectively, while $\sigma_k$ and $\sigma_\varepsilon$ are the turbulent Prandtl numbers for $k$ and $\varepsilon$, respectively.

### 5.2.2. Boundary conditions

The boundary conditions are listed as bellow:

- *at top layer of ambient air (I – Fig. 5.1):* pressure ($p_{\mathrm{top}}$) is assumed as equal to the ambient pressure (101,325 Pa), whereas the temperature ($T_{\mathrm{top}}$) is expected as a time-dependent function in accordance to Eq.5.15:

$$p_{\mathrm{top}}=p_{\mathrm{amb}},\ T_{\mathrm{top}}=T_{\mathrm{amb}}=25\times\left(\sin\left(2\pi\left(t-7884000\right)\right)/31536000\right) \tag{5.15}$$

where 7,884,000 is related to the number of seconds in quarter of a year and 31,536,000 is the number of seconds in a year.

- *at side and bottom pit walls (II – Fig. 5.1):* no slip boundary condition is considered as well as zero heat flux condition.

$$\mathbf{u}=\mathbf{0},\ \mathbf{n}\cdot\nabla T=\mathbf{0} \tag{5.16}$$

at the trench outlet (III – Fig. 5.1): the exhaust ventilation fan pressure (7,120 Pa) is assumed:

$$p_{out} = p_{fan},\ \mathbf{n} \cdot \nabla T = 0 \tag{5.17}$$

It should be noted that the specified boundary conditions are defined based on the accurate and detailed experimental data collected from Creighton mine.

Ghoreishi-Madiseh et al. (Ghoreishi-Madiseh, Sasmito et al. 2017) examined the sensitivity of the models to the parameterisation of the thermophysical properties at the Creighton mine site (Table 5.1). The specific heat and the thermal conductivity were allowed to vary from 750 to 1,750 J/kg K and from 0.5 to 4 W/mK (typically found in mining applications), respectively. It was noted that increasing specific heat reduced the oscillation of outlet temperature (after exchanging heat with the fractured rock mass). Results from the initial model (Ghoreishi-Madiseh, Sasmito et al. 2017) illustrated that, as expected, the best storage capacity would be achieved with a rock material that has high specific heat. Interestingly, the effect of thermal conductivity on the proposed model is much more minimal. Thus, results show that the sensitivity of the STES performance to thermal conductivity is much lower than for specific heat. The results of both models were calculated after 5 years of simulation time.

Table 5.1. Thermophysical properties of the model (based on mean values in Canadian metal mines reported in (Sylvestre 1999))

| | Property | Unit | Value |
|---|---|---|---|
| Rock mass | Initial temperature, $T_0$ | °C | 0 |
| | Density | kg/m$^3$ | 3,000 |
| | Specific heat $c_P$ | J/kgK | 1,000 |
| | Thermal conductivity | W/mK | 2.68 |
| | Permeability of porous rock-pit | m$^2$ | 0.0011 |
| | Average rock diameter | m | 1.2 |
| | Porosity | - | 0.4 |
| Air | Density | kg/m$^3$ | Ideal-gas |
| | Specific heat $c_P$ | J/kgK | 1,006.4 |
| | Thermal conductivity $k$ | W/mK | 0.0242 |
| | Viscosity | Kg/ms | $1.79\times10^{-5}$ |

### 5.2.3. Numerical methodology

The geometry shown in Fig. 5.1 was generated in Solidworks software; ANSYS workbench was used for meshing, determining boundary conditions as well as the computational domain. To conduct the grid independence test, the mesh size was decreased by 20% in each run and then the difference in the results of the outlet air temperature of two sequential runs were calculated until the resulting difference between them was $10^{-6}$ (or less). Mesh sizes were fined at the interface of rock-pit and ambient air in addition to the areas close to the ventilation trenches to resolve the boundary layer, while a relatively larger sized mesh was generated in the middle of the rock-pit and ambient air to reduce computational costs. According to the results of the mesh independence analysis, the computational design was solved with approximately 80,000 nodes for the non-conjugate model and 951,000 nodes for the conjugate model.

Using finite volume solver ANSYS Fluent 15, the mathematical models given by Eqs. 5.1–5.14, together with appropriate boundary conditions and constitutive relations comprising eight dependent variables ($u$, $v$, $w$, $p$, $k$, $\varepsilon$, $T_f$, and $T_s$) were solved. A user-defined function code was developed in C language to consider the interphase heat transfer (Eqs. 5.5–5.7) and to apply the

ambient temperature (Eq. 5.15). The equations were then discretized and iteratively solved using second-order upwind discretization scheme and Semi-Implicit Pressure-Linked Equation (SIMPLE) algorithm, respectively. The iterative procedure was repeated till relative residuals of $10^{-6}$ were achieved (i.e. approximately converging after 20 iterations at each time step of 86,400 seconds). For a simulation of 5 years, it took approximately 18 and 24 h for non-conjugate model and conjugate model development, respectively, on a workstation with two quad-core processors (2.6 GHz) and 64 GB RAM.

### 5.2.4. Validation and sensitivity analysis

The proposed model was validated with outlet air temperature data collected from Creighton mine by (Fava 2012 ). Dry bulb temperature data are based on readings of sensors installed in the side of each ventilation trench of the STES unit (solid blue line in Fig. 5.2). The validation was carried out by curve-fitting the weather temperature recorded at the site for boundary condition of temperature at the surface of the rock-pit. The temperature of the air in the ventilation trenches and the temperature of the ambient air follow the same frequency, but differ in phase and amplitude (Fig. 5.2). Incorporating this ambient curve-fit temperature into the model, the outlet air temperature in the trenches was compared with the measured data and very good agreement has been found both qualitatively and quantitatively (Fig. 5.2).

### 5.2.5. Conjugate vs. non-conjugate model comparison

To evaluate effects of buoyancy as well as air-to-porous rock conjugated modeling, the 3D canonical model (Fig. 5.1) was compared with the conjugate model without gravity and with the

non-conjugate model in two folds. The first part studied the effect of buoyancy force in the absence of gravity, by considering the following two trench configurations:

- 6 active trenches (symmetric with 3 active trenches on each side)
- 4 active trenches (symmetric with 2 active trenches on each side at 147 and 260 m depth)

It is assumed that air is drawn through each active trench by identical ventilation fans. The second part investigated the effect of total air flow rates of 240, 360, and 480 $m^3/s$.

## 5.3. Results and discussion

This section will include assessment and analysis of the performance of the STES system and its associated energy savings.

### 5.3.1. Comparison of conjugate with/without buoyancy force and non-conjugate models

Fig. 5.3 shows the resulting temperature contours of the rock-pit, with properties of Table 5.1, at the summer and winter of the 3rd year of system operation with and without buoyancy force. Comparing the velocity vectors when buoyancy is included and excluded emphasizes the significance of buoyancy-driven fluid movement. When buoyancy is included, the velocity vectors differ between summer and winter. In summer, buoyancy helps to push air down into the center of the pit (Fig. 5.4a). In winter, the reverse occurs: an upward buoyancy-induced force heats the layer of air in the vicinity of the rock, creating an up-draft on the rock surface and a down-draft in the center of the pit (Fig. 5.4b). When buoyancy is excluded, the velocity vectors for summer and winter time are identical (Figs. 5.4c and 5.4d).

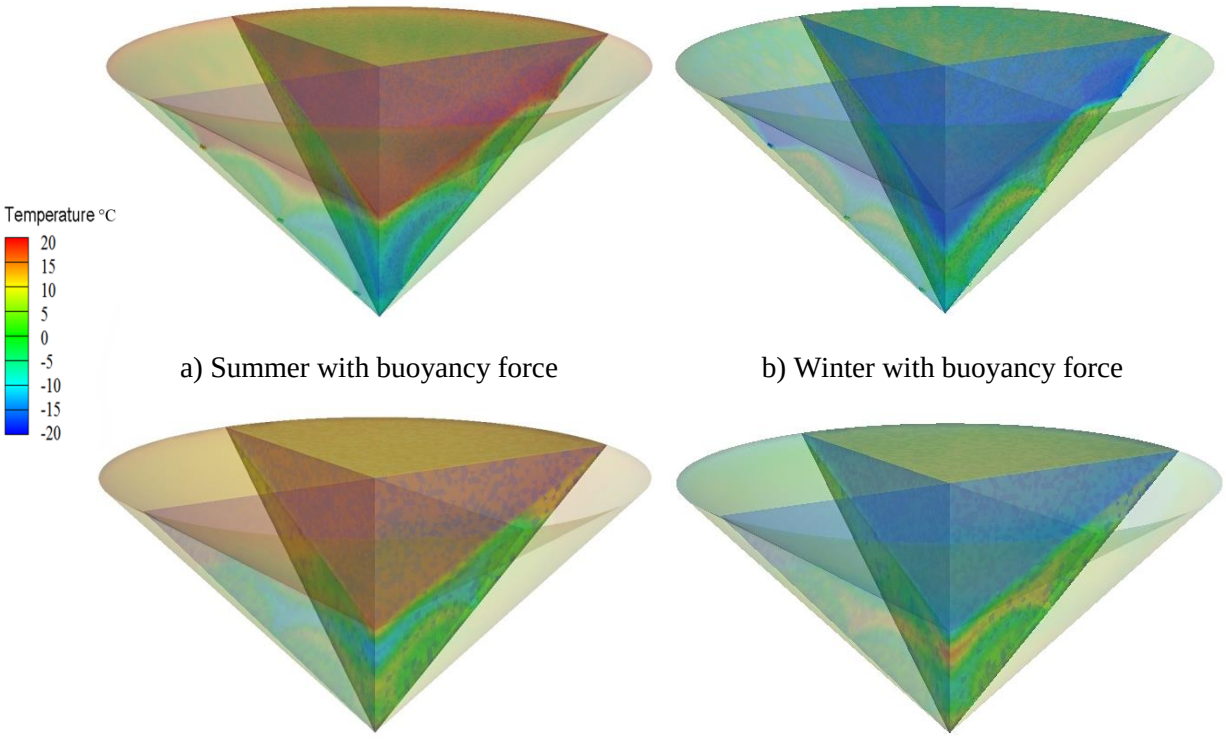


a) Summer with buoyancy force

b) Winter with buoyancy force

c) Summer without buoyancy force

d) Winter without buoyancy force

Figure 5.3. Temperature contours of the rock-pit in Year 3 (summer and winter) with and without buoyancy force

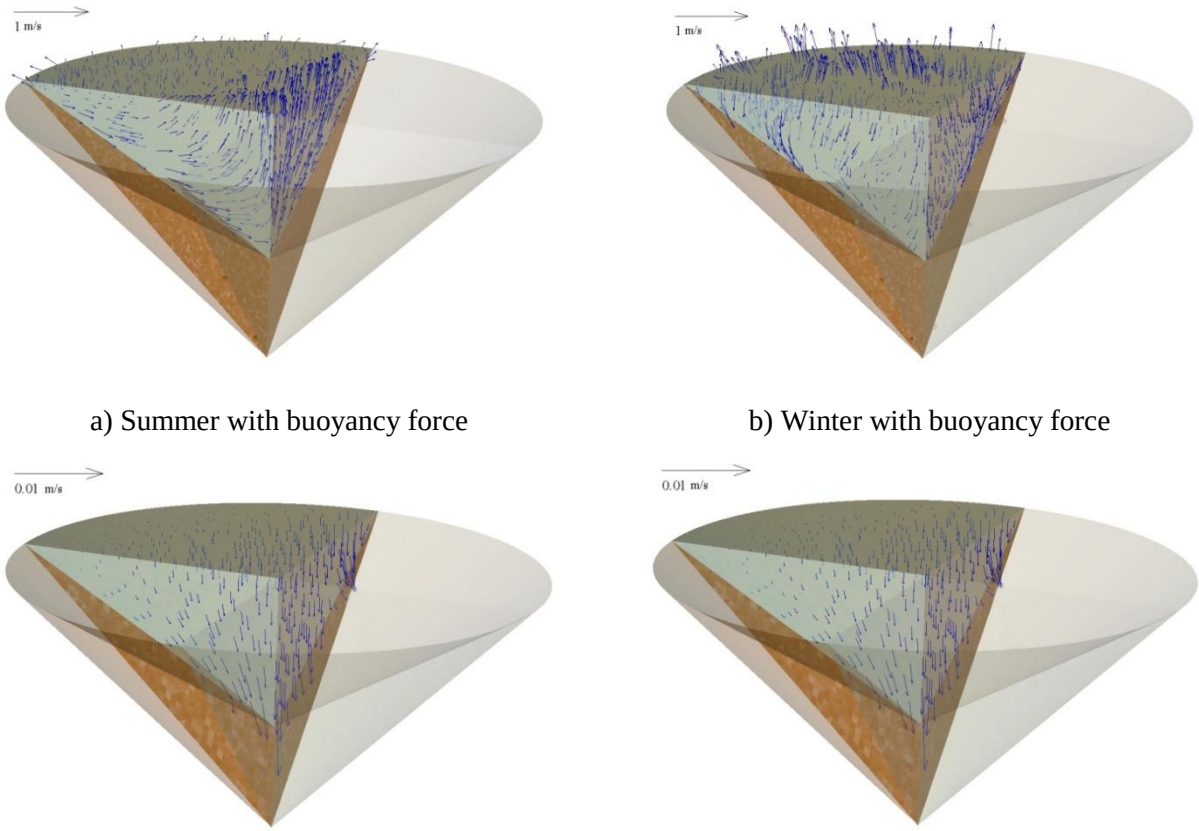


a) Summer with buoyancy force

b) Winter with buoyancy force

c) Summer without buoyancy force

d) Winter without buoyancy force

Figure. 5.4. Velocity vectors in the air at the top of the quarter of the rock-pit in Year 3 (summer and winter) with and without buoyancy force

Natural convection occurs when the air adjacent to the rock-pit surface is moved by buoyancy forces induced by temperature-related density differences of at least 20°C between the rock surface and bulk air (Fig. 5.5).

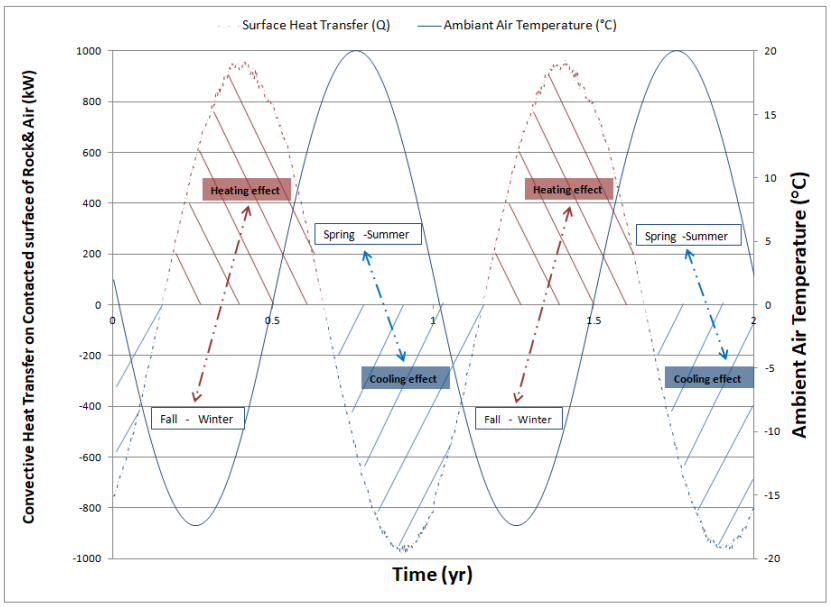


Figure 5.5. Convective heat transfer at contact surface between rock-pit and air, and ambient air temperature at mine site for conjugate model with 6 trenches and air flow of 240 $m^3/s$

It is worth to mention that in spite of the complicated convection theory, the heat transfer convection rate is related to the temperature difference, and is determined by Newton's Law as shown in Eq. 5.18.

$$\dot{Q}(W) = hA_s(T_s - T_\infty) \tag{5.18}$$

where $h$ is the convection heat transfer coefficient in $w/m^2$°C, $A_s$ is the surface area through which convection heat transfer takes place (rock-pit surface), $T_s$ is the surface temperature, and $T_\infty$ is the temperature of the surrounding ambient air that is sufficiently far from the rock surface.

At the rock-air interface, the air temperature is very close to the rock-pit surface temperature. Natural convection heat transfer on a surface is an experimentally defined parameter that be subject to on all variables influencing convection (e.g., geometry of the surface, orientation), as well as the thermo-physical properties of bulk fluid (in this case air). While natural convection is a well-established heat transfer component, the complexities of bulk fluid movement make it hard to be

presented through simple analytical relations. Some analytical solutions have been developed for natural convection, but they cannot be applied as a general solution because they are developed for canonical cases with specific geometries under many simplifying assumptions. Therefore, in this study, according to its very specific and complex geometry, the heat transfer coefficient value ($0.061\ w/m^2$℃ ) was calculated in FLUENT. Although small, this heat transfer coefficient should not be neglected because when multiplied by the large rock-pit surface area (~$8.2x10^5\ m^2$) and the sizeable temperature difference between surface and the air (~10°C), it yields a 1,000 kW naturally-convected heat transfer rate which is approximately 10% of the total energy savings. Thus, natural convection improves system efficiency by its heating effect in fall and winter and its cooling effect in warm seasons (Fig. 5.5). The difference in temperature between rock and bulk air improves system performance, even with a very low heat transfer coefficient.

In winter of Year 1, the simulated mass-average outlet air temperature was similar for conjugate models with and without buoyancy force and for the non-conjugate model (Fig. 5.6). After Year 1, it was lowest in summer and winter for the conjugate model with buoyancy. The other two models tracked each other more closely, with similar winter minima and higher summer maxima for the conjugate model without buoyancy. Outlet temperature patterns stabilized after Year 3. There was a 2–3 month phase shift between the conjugate and non-conjugate models with buoyancy force and the ambient temperature, but the model without a buoyancy force was aligned with ambient temperature. Thus, effect of the buoyancy force cannot be neglected: it leads to a considerable decrease in heat transfer among the rock-pit and air, in both conjugate and non-conjugate models with buoyancy force in summer and winter.

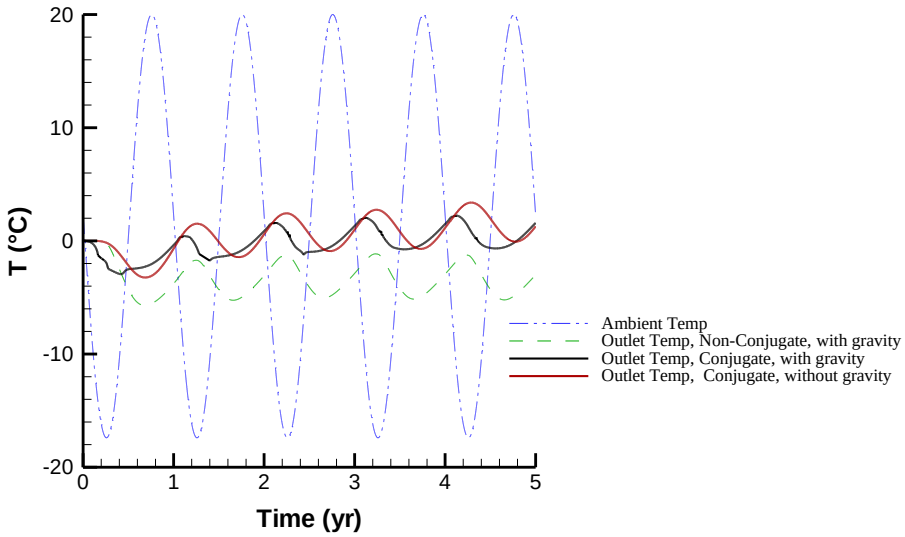


Figure 5.6. Ambient air temperature at Creighton mine and average outlet air temperature for non-conjugate model, and conjugate model with and without considering buoyancy effects for 6 trenches and air flow of 240 $m^3/s$

Compared to the 6-trench design in Fig. 5.6, when only 4 trenches were used to draw ventilation air into the mine, outlet temperatures from the conjugate models (with and without buoyancy) were similar, whereas the non-conjugate model outlet temperatures were relatively low (Fig. 5.7). Fewer active trenches led to higher Reynolds numbers in parts of the rock-pit that experience air movement. Forced convection heat transfer induced by ventilation fans gained significance over buoyancy-induced natural convection. Based on the difference between conjugate and non-conjugate (with buoyancy) results, it was necessary to use the conjugate model to simulate buoyancy-induced air circulation on top of the rock mass. Having confirmed the applicability and accuracy of the conjugate model, the STES analyses in subsequent work was carried out using the conjugate natural convection model. The average air velocity (0.002 m/s) through the porous rock (Fig. 5.4) yielded a Reynolds number of approximately 0.001. This low value means that the Darcy regime dominates the fluid flow inside the porous rock-pit (Zeng and Grigg 2006, Nagel, Beckert et al. 2016).

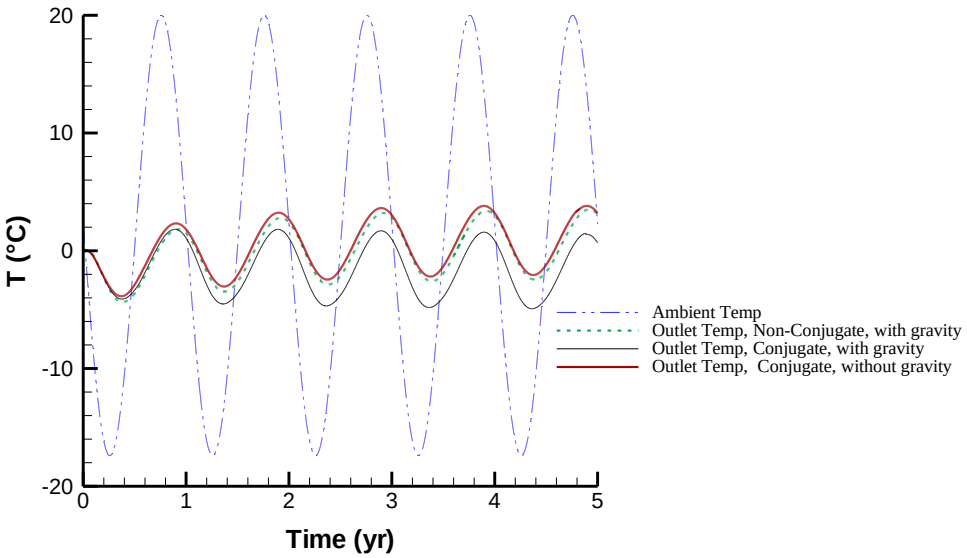


Figure 5.7. Ambient air temperature at Creighton mine and average outlet air temperature for non-conjugate model, and conjugate model with and without considering buoyancy effects for 4 trenches and air flow of 240 $m^3/s$

### 5.3.2. Effect of position of trenches on outlet air temperature

Fig. 5.8 highlights the importance of ventilation trench location (see Fig. 5.1 for depths below surface). The outlet air temperature of the pair of top trenches was similar to ambient air temperature, which is not surprising, since ambient air travels its shortest path through the broken rock mass to reach this trench. Ambient air travelling toward the pairs of middle and bottom trenches had more time to exchange heat with the rock-pit and therefore, its temperature approached that of the rock mass.

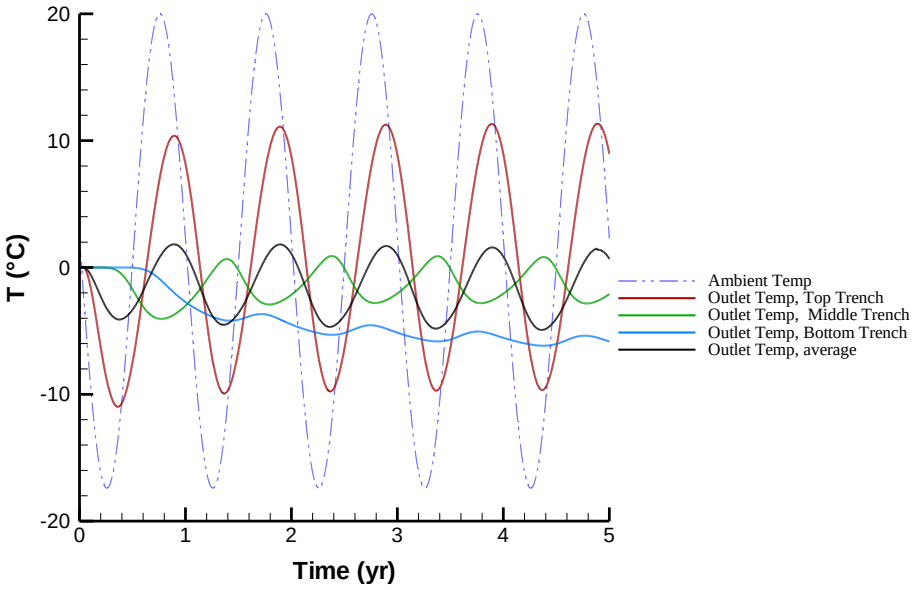


Figure 5.8. Ambient air temperature at Creighton mine and average outlet air temperature from conjugate model with considering buoyancy force for 3 pairs of trenches and air flow of 240 $m^3/s$

When just two pairs of trenches (147 and 260 m depth) were used, outlet air temperature was closer to that of the rock mass (Fig. 5.9). The performance of STES unit was improved: by eliminating the uppermost pair of ventilation trenches, the deeper ventilation trenches stored and released more heat. Opening more ventilation trenches in the bottom of the rock-pit allowed the underground ventilation system to pass more air through the bottom of the rock-pit, resulting in a larger heat exchange rate. In winter, this trench configuration pulled more air from deep in the rock-pit and supported the circulation of the cold air to deeper levels of the mine. This could potentially provide greater cooling capacity during summer. However, it should be noted that in order to provide the same flow rate for both 6- and 4-trench configurations, it is necessary to increase fan power. Thus, the number of trenches should be determined by conducting a cost and benefit analysis that compares the economics of saving heating/cooling energy, as well as the cost of running ventilation fans. A comprehensive study of the Creighton mine will help optimize the number and the location of ventilation trenches.

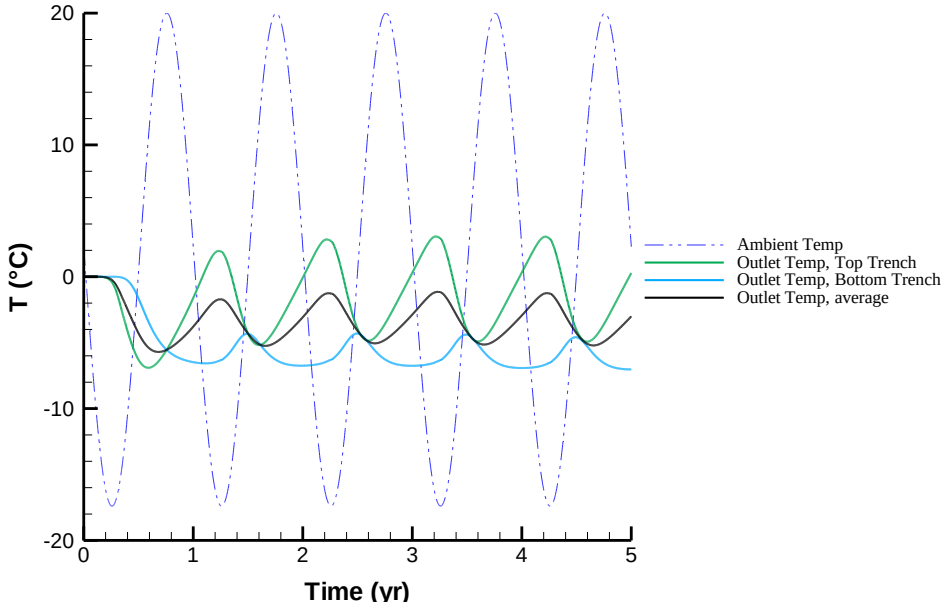


Figure 5.9. Ambient air temperature at Creighton mine and average outlet air temperature from conjugate model with considering buoyancy force for 2 pairs of trenches and air flow of 240 $m^3/s$

### 5.3.3. Effect of volumetric air flow rate on performance of large-scale STES unit

Auto-compression and the geothermal gradient, coupled with heat generation from mining machines are the main sources of heat load in underground mines. As a result, more cooling loads are required in mine thermal management (Sasmito, Kurnia et al. 2015). The effects of volumetric air flow rate must be understood so as to boost the cooling/heating load. Theoretically, increasing air flow enhances the rate of heat exchange among the ventilated air and the porous rock mass. Increasing the flow rate from 240 to 360 $m^3/s$ will slightly improve the outlet air temperature oscillation, whereas an increase from 360 to 480 $m^3/s$ will more dramatically increase the annual oscillation (Fig. 5.10). Thus, increasing the flow rate makes the outlet temperature approach ambient temperature (i.e. higher flow rate means less temperature difference). Particularly, temperature increases/decreases about 2 °C and 1 °C in summer/winter, respectively, when flow rate is raised to 480 $m^3/s$. While increasing flow rate by 50% amplifies fluctuation of outlet air

temperature causing an adverse effect on the thermal capacity of the STES system, the energy savings are effectively increased due to the higher flow rate of the air that is preconditioned. Is it worth increasing the flow rate? To answer this essential question, the effect of flow rate on the energy savings will be discussed in the following section.

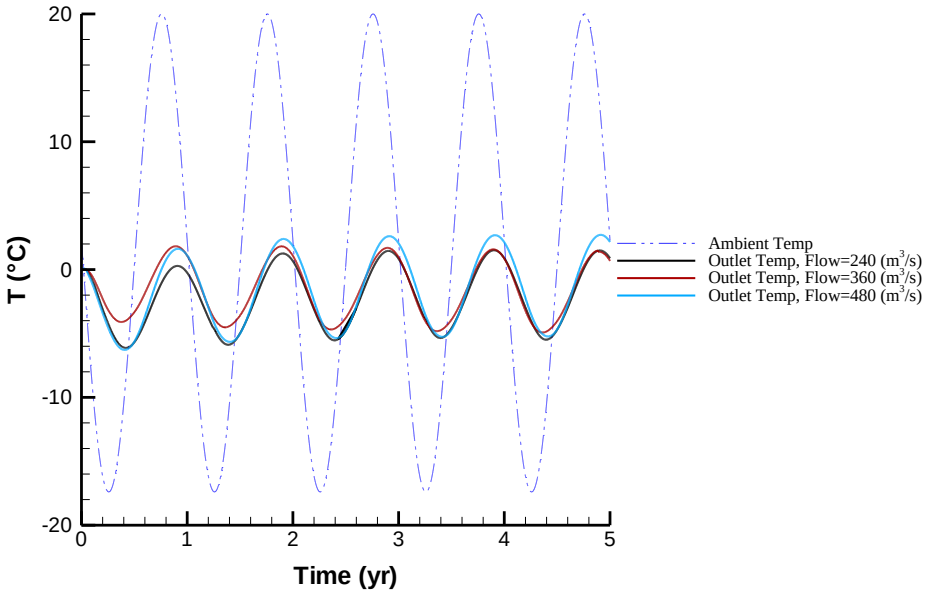


Figure 5.10. Ambient air temperature at mine site and average outlet air temperature for Conjugate model with 6 trenches and different flow rate (240, 360 and 480 ($m^3/s$))

### 5.3.4. Effect of rock size, permeability and porosity

To study the effects of physical properties of rock mass on the performance of thermal storage system, Figs. 5.11 and 5.12 are given which include 6 different rock types as shown in Table 5.2.

Table 5.2. Rock size, porosity and permeability of 6 different rock types

| Rock type | Rock size (m) | Porosity | Permeability ($m^2$) |
|---|---|---|---|
| A | 1.25 | 0.45 | $2.5 \times 10^{-3}$ |
| B | 1.20 | 0.40 | $1.1 \times 10^{-3}$ |
| C | 1.05 | 0.35 | $4.1 \times 10^{-4}$ |
| D | 0.90 | 0.30 | $2.3 \times 10^{-4}$ |
| E | 0.75 | 0.25 | $6.9 \times 10^{-5}$ |
| F | 0.60 | 0.20 | $1.8 \times 10^{-5}$ |

According to Fig. 5.11, changing the porosity of rock (from 0.45 to 0.2) has some, but not significant, effects on the performance of the storage system. These effects can be better understood by noting that decreasing porosity from 0.45 to 0.20 has almost linearly reduced the air flow rate from 792 to 396 $m^3/s$, respectively (Fig. 5.12). At the same time, decreasing rock size (from 1.25 to 0.60 m), permeability (from $2.5 \times 10^{-3}$ to $1.84 \times 10^{-5}\ m^2$) and porosity (from 0.45 to 0.20), has yielded to marginal effects on the outlet temperature, i.e. less than 1°C. Therefore, it can be deduced that from the design point of view, to maximize storage capacity and minimize the fan power, it is suggested to use larger rocks to achieve higher porosity and permeability.

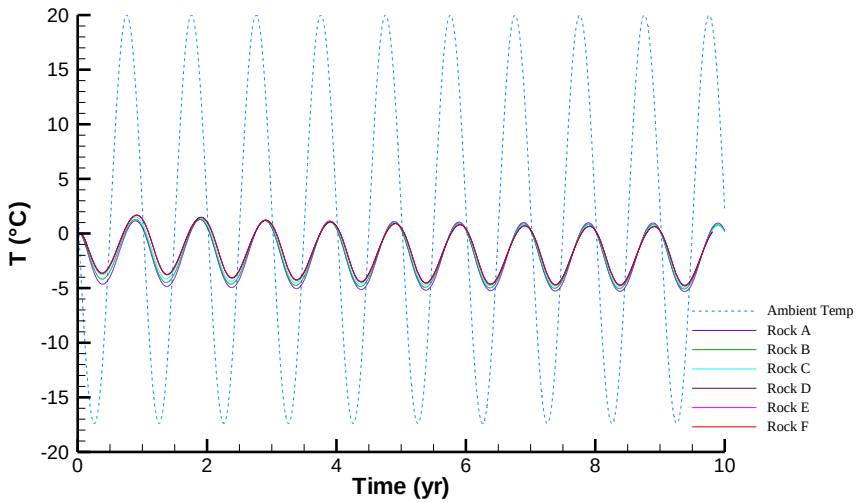


Figure 5.11. Effect of rock size, porosity and permeability on average outlet air temperature

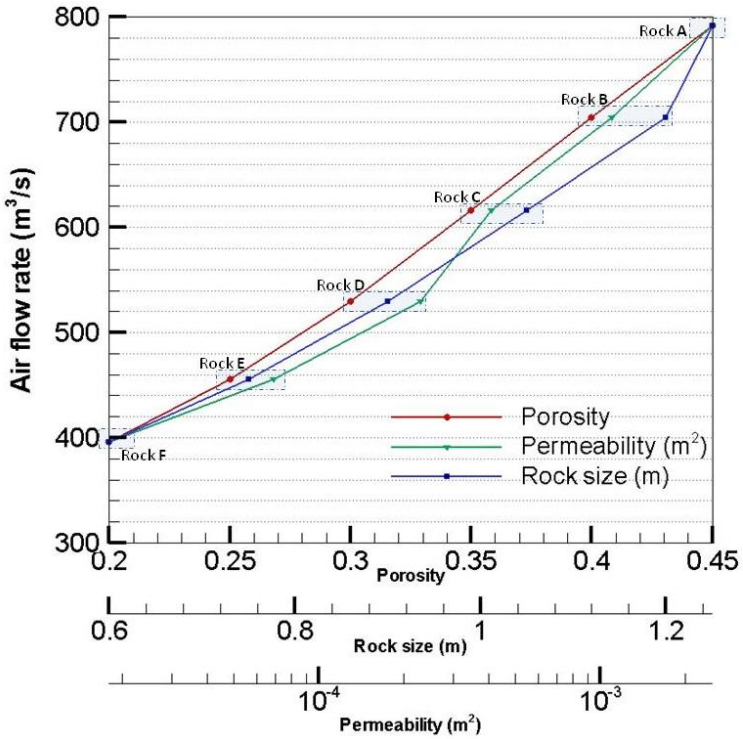


Figure 5.12. Effect of changing rock properties (i.e. porosity, rock size and permeability) on air flow rate $(m^3/s)$

### 5.3.5. Energy savings

Effects of having 6 and 4 active ventilation trenches (i.e. air draw points) are shown in Fig. 5.13. It is worth mentioning that, heating demand in summer and cooling requirement in winter are zero (Fig. 5.13). It is found that on average, approximately 11.8 and 11.1 GWh/year of heating energy can be saved for 4 and 6 trench configurations, respectively. The savings in cooling are even greater; 24.5 GWh/yr for 4 trenches and 18.9 GWh/year for 6 trenches. In overall, the total savings are found to be total of 36.3 GWhr/yr for 4 trenches and 30.0 GWh/year energy for 6 trenches. Thus, the total savings for the 4-trench configuration are roughly 20% higher than the 6-trench configuration. In other words, by deactivating the closer-to-surface trenches, higher rates of heat exchange are achieved as air is forced to pass through a longer pass through the porous rock to

reach the deeper trenches. However, it is important to remember that drawing more air through the rock-pit requires more fan power. Therefore, there is a limit to increasing the savings by drawing more air into the STES unit.

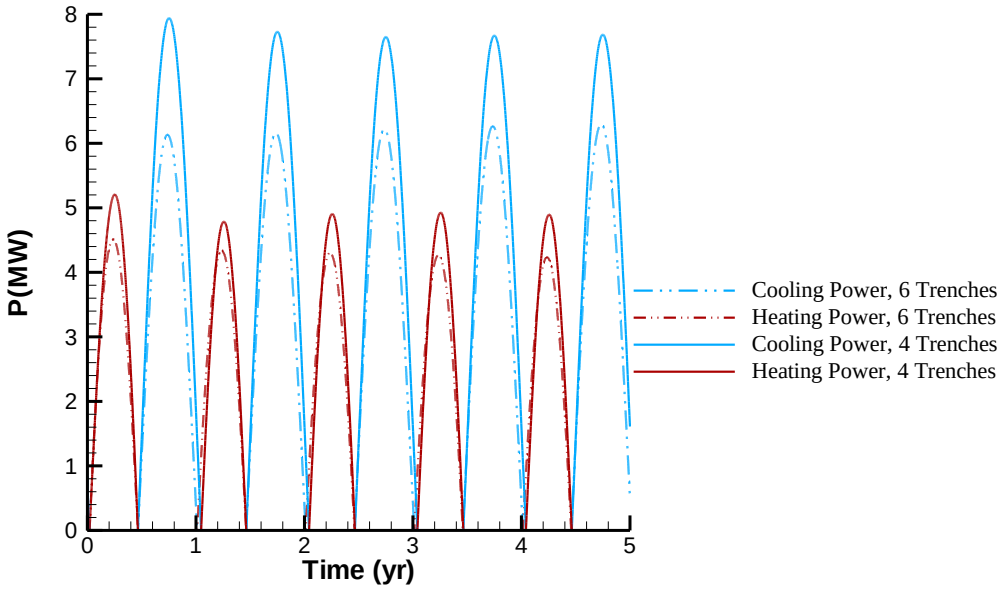


Figure 5.13. Heating and cooling power for conjugate model for 4- and 6-trench configuration with air flow rate of 240 $m^3/s$

As shown in Fig. 5.14, which investigates the impact of air flow rate on heat exchange between rock and air, the highest energy savings are achieved in the case with an air flow rate of 480 $m^3/s$ and 6 trenches. Increasing the flow rate by 50% (from 240 to 360 $m^3/s$) increased the savings by approximately 74%. However, a 100% increase in flow rate (from 240 to 480 $m^3/s$) increased the savings by 128%. These significant economic savings will be even more if carbon tax credits associated with use of the STES system are to be considered.

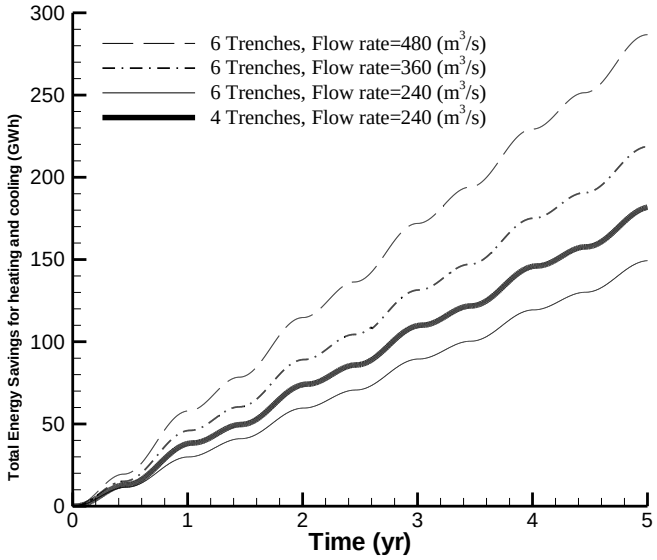


Figure 5.14. Total energy savings with three air flow rates and 4- or 6-trench configurations

Assuming natural gas is the main source of heat in the mine site (i.e. 422 tons $CO_2$ eq per GWh (Walmsley, Walmsley et al. 2014)), implementation of an STES unit is estimated to reduce the total carbon footprint by 5,612 and 4,262 t $CO_2$ per year for the 4- and 6-trench configurations, respectively. This reduction would be even more if the electricity was produced by burning oil or coal.

## 5.4. Conclusions

Preheating and cooling account for 50–80% of annual ventilation operating costs at underground mines. The STES system at Creighton mine in Ontario, Canada is a precious asset that offers natural cooling and heating for ventilating deeper mine levels. STES is a cost-effective strategy to enhance cooling and heating process efficiencies, thereby reducing associated costs. In areas with sizeable seasonal temperature oscillations, this type of natural heat exchanger can be used for cooling/heating purposes in underground mine ventilation systems. A conjugate heat transfer and fluid flow model was developed to better understand the performance of large-scale STES units

for application in mine ventilation. Simulation results were compared and validated based on field measurement at ventilation trenches and ambient air temperature. Temperature gradients observed in the proposed storage system suggest the presence of natural convection effects driven by buoyancy. Effects of buoyancy forces on the fluid flow and heat exchange regimes inside the rock-pit were studied, resulting in comparison of forced convection versus natural convection heat transfer mechanisms. The model was also used to study the effects of number and position of ventilation trenches along with the fresh air flow rate. Increasing air flow rate from 240 to 480 $m^3/s$ and reducing the number of active trenches from 6 to 4 and will improve energy savings. However, determining whether these changes lead to reductions in energy costs requires consideration of costs associated with fan power. For the range of porosities studies in this research (0.2-0.45), the porosity effects on the performance of thermal storage phenomenon were not found to be significant.

### 5.5. Nomenclature

Abbreviations:

LTE Local Thermal Equilibrium

LTNE Local Thermal Non-Equilibrium

STES Seasonal Thermal Energy Storage

Symbols:

ρ density

ρf density of fluid

dp diameter of the broken rock

μ dynamic viscosity of the fluid

GB generation of turbulent kinetic energy due to buoyancy

Gk generation of turbulent kinetic energy due to mean velocity gradients

f fluid phase

| | |
|---|---|
| u | fluid velocity |
| g | gravitational acceleration |
| h | heat transfer coefficient |
| I | identity or second order unit tensor |
| ∇ | Nabla symbol |
| $Nu_{fs}$ | Nusselt between air and rock |
| ∂ | Partial differential symbol |
| ε | porosity |
| p | pressure |
| pop | Operating Pressure |
| $p_{top}$ | air pressure at the top of the ambient air |
| M | molecular weight of the gas |
| R | universal gas constant |
| Pr | Prandtl number |
| $Pr_t$ | turbulent Prandtl number |
| Re | Reynolds number |
| cp | specific heat |
| s | solid phase |
| $A_{fs}$ | specific surface area |
| $A_s$ | surface area through which convection heat transfer takes place (rock-pit surface) |
| ‹u› | superficial fluid velocity |
| t | time |
| T | temperature |
| Ts | surface temperature |
| T∞ | temperature of the surrounding ambient air that is sufficiently far from the rock surface |
| $T_{top}$ | temperature at top of the ambient air |
| κ | thermal conductivity |
| $κ_{eff}$ | thermal conductivity of the fluid |

k turbulent kinetic energy

σk turbulent Prandtl number for k

σε turbulent Prandtl number for ε

μt turbulent viscosity

## 5.6. References


Avramenko, A. and A. Kuznetsov (2006). "Renormalization group model of large-scale turbulence in porous media." Transport in porous media 63(1): 175-193.

Berrada, A., K. Loudiyi and I. Zorkani (2017). "System design and economic performance of gravity energy storage." Journal of Cleaner Production 156(Supplement C): 317-326.

Bharathan, B., A. P. Sasmito and S. A. Ghoreishi-Madiseh (2017). "Analysis of energy consumption and carbon footprint from underground haulage with different power sources in typical Canadian mines." Journal of Cleaner Production 166(Supplement C): 21-31.

Carbonell, R. G. and S. Whitaker (1984). Heat and mass transfer in porous media. Fundamentals of transport phenomena in porous media, Springer: 121-198.

Chatterjee, A., L. Zhang and X. Xia (2015). "Optimization of mine ventilation fan speeds according to ventilation on demand and time of use tariff." Applied Energy 146(Supplement C): 65-73.

DeGroot, C. T. and A. G. Straatman (2011). "Closure of non-equilibrium volume-averaged energy equations in high-conductivity porous media." International Journal of Heat and Mass Transfer 54(23): 5039-5048.

Envers, P. (1986). "Controlled air through efficient system at inco." Canadian Mining Journal 107(7): 12-14.

Fava, L., Millar, D., Anderson, B., Schafrik, S., O'Connor, D., Allen, C., (2012 ). Modeling of the Natural Heat Exchange Area at Creighton Mine for Operational Decision Support. 14th US/North American Mine Ventilation Symposium.

Gan, G. (2015). "Simulation of dynamic interactions of the earth–air heat exchanger with soil and atmosphere for preheating of ventilation air." Applied Energy 158(Supplement C): 118-132.

Ghoreishi-Madiseh, S., F. Hassani, A. Mohammadian and P. Radziszewski (2013). "A transient natural convection heat transfer model for geothermal borehole heat exchangers." Journal of Renewable and Sustainable Energy 5(4): 043104.

Ghoreishi-Madiseh, S. A., L. Amiri, A. P. Sasmito and F. P. Hassani (2017). "A Conjugate Natural Convection Model for Large Scale Seasonal Thermal Energy Storage Units: Application in Mine Ventilation." Energy Procedia 105(Supplement C): 4167-4172.

Ghoreishi-Madiseh, S. A., F. Hassani and F. Abbasy (2015). "Numerical and experimental study of geothermal heat extraction from backfilled mine stopes." Applied Thermal Engineering 90: 1119-1130.

Ghoreishi-Madiseh, S. A., A. P. Sasmito, F. P. Hassani and L. Amiri (2017). "Performance evaluation of large scale rock-pit seasonal thermal energy storage for application in underground mine ventilation." Applied Energy 185: 1940-1947.

Goldemberg, J. (2000). World Energy Assessment: Energy and the challenge of sustainability, United Nations Pubns.

He, W., X. Luo, D. Evans, J. Busby, S. Garvey, D. Parkes and J. Wang (2017). "Exergy storage of compressed air in cavern and cavern volume estimation of the large-scale compressed air energy storage system." Applied Energy 208(Supplement C): 745-757.

Karacan, C. Ö. (2007). "Development and application of reservoir models and artificial neural networks for optimizing ventilation air requirements in development mining of coal seams." International Journal of Coal Geology 72(3–4): 221-239.

Kurnia, J. C., P. Xu and A. P. Sasmito (2016). "A novel concept of enhanced gas recovery strategy from ventilation air methane in underground coal mines – A computational investigation." Journal of Natural Gas Science and Engineering 35: 661-672.

Maria, E. and T. Tsoutsos (2004). "The sustainable management of renewable energy sources installations: legal aspects of their environmental impact in small Greek islands." Energy conversion and management 45(5): 631-638.

Masnadi, M. S., J. R. Grace, X. T. Bi, C. J. Lim and N. Ellis (2015). "From fossil fuels towards renewables: Inhibitory and catalytic effects on carbon thermochemical conversion during co-gasification of biomass with fossil fuels." Applied Energy 140(Supplement C): 196-209.

Mayala, L. P., M. M. Veiga and M. B. Khorzoughi (2016). "Assessment of mine ventilation systems and air pollution impacts on artisanal tanzanite miners at Merelani, Tanzania." Journal of Cleaner Production 116(Supplement C): 118-124.

Mendu, V., T. Shearin, J. E. Campbell, J. Stork, J. Jae, M. Crocker, G. Huber and S. DeBolt (2012). "Global bioenergy potential from high-lignin agricultural residue." Proceedings of the National Academy of Sciences 109(10): 4014-4019.

Midilli, A., I. Dincer and M. Rosen (2007). "The role and future benefits of green energy." International journal of green energy 4(1): 65-87.

Nagel, T., S. Beckert, C. Lehmann, R. Gläser and O. Kolditz (2016). "Multi-physical continuum models of thermochemical heat storage and transformation in porous media and powder beds—A review." Applied Energy 178(Supplement C): 323-345.

Nield, D. A. and A. Bejan (2006). Convection in porous media, Springer Science & Business Media.

Nimvari, M. E., M. Maerefat and M. K. El-Hossaini (2012). "Numerical simulation of turbulent flow and heat transfer in a channel partially filled with a porous media." International Journal of Thermal Sciences 60: 131-141.

Ploeg, F. and C. Withagen (2014). "Growth, renewables, and the optimal carbon tax." International Economic Review 55(1): 283-311.

Pruess, K. (1985). "A practical method for modeling fluid and heat flow in fractured porous media." Society of Petroleum Engineers Journal 25(01): 14-26.

Salam, P. A., S. Kumar and M. Siriwardhana (2010). "Report on the status of biomass Gasification in Thailand and Cambodia." Prepared for: Energy Environment Partnership (EEP)(Mekong Region. Asian Inst Technol, Bangkok, Thailand).

Sasmito, A. P., J. C. Kurnia, E. Birgersson and A. S. Mujumdar (2015). "Computational evaluation of thermal management strategies in an underground mine." Applied Thermal Engineering: 1144-1150.

Schafrik, S. (2015). The use of packed sphere modelling for airflow and heat exchange analysis in broken or fragmented rock, Laurentian University of Sudbury.

Sims, R. E. (2003). Bioenergy options for a cleaner environment: in developed and developing countries, Elsevier.

Stachulak, J. (1991). "Ventilation strategy and unique air conditioning at Inco Limited." CIM(Canadian Mining and Metallurgical) Bulletin 84(950): 41-45.

Statistics, N. C. f. H. S. D. o. V., U. S. N. V. S. Division, U. S. N. O. o. V. Statistics and U. S. B. o. t. C. V. S. Division (1979). Vital statistics of the United States, United States Bureau of the Census.

Stigka, E. K., J. A. Paravantis and G. K. Mihalakakou (2014). "Social acceptance of renewable energy sources: A review of contingent valuation applications." Renewable and Sustainable Energy Reviews 32: 100-106.

Sylvestre, M. J.-G. (1999). Heating and Ventilation Study of Inco's Creighton Mine.

Teruel, F. E. (2009). "A new turbulence model for porous media flows. Part I: Constitutive equations and model closure." International Journal of Heat and Mass Transfer 52(19): 4264-4272.

Vafai, K. and C. Tien (1981). "Boundary and inertia effects on flow and heat transfer in porous media." International Journal of Heat and Mass Transfer 24(2): 195-203.

Vafai, K. and C. Tien (1982). "Boundary and inertia effects on convective mass transfer in porous media." International Journal of Heat and Mass Transfer 25(8): 1183-1190.

Walmsley, M. R., T. G. Walmsley, M. J. Atkins, P. J. Kamp and J. R. Neale (2014). "Minimising carbon emissions and energy expended for electricity generation in New Zealand through to 2050." Applied Energy 135: 656-665.

Whitaker, S. (1977). "Simultaneous heat, mass, and momentum transfer in porous media: a theory of drying." Advances in heat transfer 13: 119-203.

Yan, B., J. Wieberdink, F. Shirazi, P. Y. Li, T. W. Simon and J. D. Van de Ven (2015). "Experimental study of heat transfer enhancement in a liquid piston compressor/expander using porous media inserts." Applied Energy 154(Supplement C): 40-50.

Yu, S., S. Gao and H. sun (2016). "A dynamic programming model for environmental investment decision-making in coal mining." Applied Energy 166(Supplement C): 273-281.

Yue, D., F. You and S. W. Snyder (2014). "Biomass-to-bioenergy and biofuel supply chain optimization: overview, key issues and challenges." Computers & Chemical Engineering 66: 36-56.

Zeng, Z. and R. Grigg (2006). "A Criterion for Non-Darcy Flow in Porous Media." Transport in Porous Media 63(1): 57-69.

Zhang, P., X. Xiao, Z. N. Meng and M. Li (2015). "Heat transfer characteristics of a molten-salt thermal energy storage unit with and without heat transfer enhancement." Applied Energy 137: 758-772.

Zhu, Y., P. J. Fox and J. P. Morris (1999). "A pore-scale numerical model for flow through porous media." International journal for numerical and analytical methods in geomechanics 23(9): 881-904.

# Connecting Text

*The outcomes of the previous chapters shape the idea of using waste rock as an energy storage material and exhaust hot air as a heat transfer fluid. The poor efficiency of conventional diesel engines means they lose a significant amount of heat through the exhaust. Chapter 6 presents a validated numerical study that focuses on the coupling of a waste heat recovery system to a diesel exhaust stream, offering a performance assessment for application of the proposed rock-pile waste heat storage system in a remote, off-grid community located in northern Canada.*

*Chapter 6 is published as:*

***Leyla Amiri**, Marco Antonio Rodrigues de Brito, Durjoy Baidya, Ali Fahrettin Kuyuk, Seyed Ali Ghoreishi-Madiseh, Agus P Sasmito, and Ferri P. Hassani. "Numerical investigation of rock-pile based waste heat storage for remote communities in cold climates." Applied Energy 252 (2019): 113475.*

# CHAPTER 6

## 6. Numerical investigation of rock-pile based waste heat storage for remote communities in cold climates


## Abstract

Remote communities in arctic climates are solely dependent on diesel generators for continuous power supply due to their detached loci from national power gridlines or natural gas pipelines. Moreover, to get along with the harsh, long winters, these communities directly or indirectly depend on fossil-fuel based heating systems. Due to the lower efficiency of the conventional diesel engines, these generators discard a significant amount of heat through the exhaust. Occasionally, during the wintertime, this waste heat from the exhaust is used directly as a heat source after recovery. However, during summer, when the heating demand is lower or nil, this heat is commonly discarded, and its energy potential wasted. A rock-pile based seasonal thermal energy storage is a viable solution that can sustainably resolve this issue. This paper presents a validated numerical study that focuses on the coupling of a waste heat recovery system to a diesel exhaust stream offering a performance assessment of the proposed rock-pile waste heat storage system in a remote, off-grid community located in northern Canada. It examines the impacts of local thermal equilibrium versus non-equilibrium approaches as well as temperature-dependent properties, variation of air mass flow rate, particle size and finally the thermo-physical properties on the proposed model. The presented results show that air should be treated as an ideal gas and that the local thermal non-equilibrium approach should be used for its considerably higher accuracy.

Techno-economic assessment of the system resulted in a relatively short payback period of less than six years.

### 6.1. Introduction

Communities located on isolated cold areas of the globe that have a permanent settlement with at least ten inhabitants, are deemed “off-grid” or “remote” if they are not connected to the electrical grid or a natural gas pipeline. There are around 300 of such communities in Canada only, including both Aboriginal and non-Aboriginal establishments, such as villages and small cities, as well as mining camps and other campsites for longstanding commercial operations (i.e., forestry and fishing) (Royer 2013). For all these communities, affordable energy provision is a common challenge which often makes them solely dependent on fossil fuel based power generation, mainly diesel generators (Knowles 2016). To cope with the cold winter conditions in Canada, these communities usually also rely upon fossil fuels for heating purposes either directly by burning heating (heavy) oil (or sometimes even diesel) (Royer 2013), or indirectly by the use of electric heating (Brooks and Frost 2012). The latter requires even higher generation capacities to assure the availability of electricity for heating during the winter season. Furthermore, recurrent transportation of goods to these remote areas (inclusive of fuel) are not as common as in their non-remote counterparts and face additional environmental challenges. This leads to significantly high shipping costs(Brooks and Frost 2012), which are carried along to energy provision costs. For instance, in Nunavut where several remote Canadian communities are located, electricity costs are ten times greater than the Canadian average (Knowles 2016). Besides the financial costs, another disadvantage of such high fossil fuel dependency is the environmental impact to the community caused by the emission of greenhouse gases and other diesel related pollutants (Lovekin and Heerema 2019).

A diesel generator is a combination of an internal combustion engine (typically a diesel engine) and an electric generator. Even with the best available technology. this diesel engine has an efficiency of only about 35%. That means that typically, up to 65% of the total energy input is discarded in the form of heat through jacketwater, intercooler, exhaust gases and so on(Bari and Hossain 2013). As a result, it can be approximated that in these generators, from every 3kW of fuel energy consumed, only 1kW becomes electricity, and the other 2kW are wasted (Ghoreishi-Madiseh, Kuyuk et al. 2019), from which half (1kW) is present on the exhaust gas (Bari and Hossain 2013). The popularity of the diesel engine has resulted in increasing concern with environmental policies and energy savings technologies and led the engine to become a constant object of study(Hossain and Bari 2013). Waste heat recovery of the exhaust streams of a diesel generator can be an indirect way of saving a considerable amount of primary fuel and decreasing the system's impact on global warming (Pandiyarajan, Pandian et al. 2011). Although several studies investigate the potentials of waste heat recovery (WHR) systems, the usual focus is on the use of the heat for power generation through organic Rankine cycles (Hossain and Bari 2013, Zhang, Wang et al. 2013, Feru, de Jager et al. 2014, Di Battista, Mauriello et al. 2015, Xu, Rathod et al. 2017, Alshammari, Pesyridis et al. 2018) or thermoelectric generators (Love, Szybist et al. 2012, Wang, Luan et al. 2014, Orr, Akbarzadeh et al. 2016, Fernández-Yañez, Armas et al. 2018) mainly due to the flexibility of electrical power.

As a consequence, the direct use of heat from exhaust WHR is still not commonly seen as a practical employment of this energy (Ghoreishi-Madiseh, Kuyuk et al. 2019). Moreover, conversion of heat to different forms of energy has significant associated losses, and in a scenario where demand exists, direct heating can be a potential asset. For instance, for a remote, cold village

with their huge shipping costs, even recovering a fraction of the discarded heat can lead to significant savings in heating fuel (Mokkapati and Lin 2014).

One major challenge that often arises in implementing an alternative energy solution is the mismatch between demand and supply. In case of combined heating and power generation, lower heating demand in the summer time also enhances the challenge(Erlund and Zevenhoven 2018). Any WHR system faces problems because of this difference between the periods of availability and demand of the heating energy (Hasnain 1998). To confront this issue, a common approach is the employment of a seasonal thermal energy storage techniques that store the surplus of the recovered waste heat during low heat demand periods in a suitable storage medium for several months to use when the heating demand is peaked (Ghoreishi-Madiseh, Kuyuk et al. 2019). Such techniques are commonly employed on solar energy-based district/space heating systems(Chapuis and Bernier 2009, Forsberg 2012, Singh, Deshpandey et al. 2015, Templeton, Hassani et al. 2016, McCartney, Başer et al. 2017, Dahash, Ochs et al. 2019) and less frequently in powerplants, for combined heat and power (CHP) applications (Forsberg 2012, McDaniel and Kosanovic 2016, Tiskatine, Aharoune et al. 2017, Ghoreishi-Madiseh, Kuyuk et al. 2019) or even in alternative mine ventilation systems (Ghoreishi-Madiseh, Sasmito et al. 2017). Thermal Energy Storage (TES) systems are widely classified in three main types; sensible, latent and chemical heat storage. In sensible heat storage, the energy is stored by the rise or drop of the storage media temperature, in latent heat storage, phase-change processes are used to store or release heat and finally chemical heat storage is based on the use of endothermal or exothermal chemical reactions to store/release heat (Tian and Zhao 2013). Among these, sensible heat storage is the cheapest and easiest to implement, causing it to be the only competitive one for district applications (Tian and Zhao 2013, Welsch, Göllner-Völker et al. 2018) and for that will be focused here. These systems can also be

categorized regarding their charging/discharging time as diurnal (for short-term), or seasonal (for long-term applications) (Fisch, Guigas et al. 1998).

The main types of large-scale thermal energy storage systems include boreholes, aquifers and rock beds. The last one presenting several important advantages, namely suitability for high-temperature applications (Hasnain 1998) and dispensing the need for an extra heat exchanger as air is used as the heat transfer fluid (Barton 2013). Moreover, they are economic and clean for the use of naturally occurring rocks as storage media (Tiskatine, Aharoune et al. 2017). Several relevant studies have concentrated on rock bed or packed bed thermal storage systems. Hasnain mentioned that the performance of a packed bed heat storage system depends on many parameters as shape and size of the selected rock, the porosity of the bed (or void fraction) and thermal properties of the rock (Hasnain 1998). Hänchen et al. developed a numerical model for heat transfer in a packed bed of rocks for short term heat storage from a concentrated solar powerplant and analyzed the effects of parameters as air mass flow and bed dimensions. Results showed that higher flow and lower heights of the bed lead to better capacity but lower the overall system efficiency (Hänchen, Brückner et al. 2011). Zanganeh et al. numerically modeled and experimentally validated industrial-scale packed beds for Concentrated Solar Powerplant (CSP) use and achieved 95% overall thermal efficiency even with thin insulation layers (Zanganeh, Pedretti et al. 2012, Zanganeh, Pedretti et al. 2015). Barton performed simulations of TES in a rock bed driven by air flow and showed the importance of using a two-way charge/discharge schedule(Barton 2013). Zanganeh et al. also studied the possibility of adding phase change materials to a rock bed in order to obtain a more constant temperature output and achieve stabilization with only 1.33% of the total storage volume in Phase Change Material (PCM) (Zanganeh, Commerford et al. 2014). Cascetta et al. used Ansys CFD module Fluent to simulate

heat transfer in a packed bed using a local thermal non-equilibrium model and suggested that an internal layer of insulation could lead to a better performance of the system (Cascetta, Cau et al. 2016). Abnay et al. did a study on thirteen rock samples to identify thermo-physical properties more significant to the rocks' lifetime (Abnay, Eddemani et al. 2016). Ghoreishi-Madiseh et al proposed a large scale Seasonal Thermal Energy Storage (STES) system for underground mine ventilation purposes using a large mass of rock (or rock-pit) as the storage media and successfully showed that the technique has potential to reduce the intense energy consumption for heating and cooling in the mining industry (Ghoreishi-Madiseh, Sasmito et al. 2017). Later, they also analyzed in more detail the natural convection effects in such system (Amiri, Ghoreishi-Madiseh et al. 2018). Lastly, Tiskatine et al. studied deeply the viability of different rock types for solar powerplant applications and determined that several varieties are appropriate for high-temperature applications (up to 650°C) identifying gabbro rock as the best one (Tiskatine, Aharoune et al. 2017). However, these studies are based on simplified assumptions which limit the accuracy of modeling the real heat transfer phenomenon occurring in packed beds. Such assumptions are made either by using a Local Thermal Equilibrium (LTE) approach, with a one-phase transient energy equation, by discarding natural convection, or by assuming a simplified radial uniform temperature pattern. Also, most of the existing studies focus on solar (CSP) applications and to the best of authors' knowledge, so far, direct recovery and storage of waste heat from exhaust gases of diesel generators has not been investigated. As demonstrated by previous studies, it is essential to capture the interphase heat exchange within porous media; this means that using a LTE method that considers perfect thermal equilibrium between the solid and fluid phase might not be appropriate (Ghoreishi-Madiseh, Sasmito et al. 2017). On the other hand, the Local Thermal Non-Equilibrium (LTNE) approach uses two energy equations for a more realistic two-phase energy balance and

that is why it should be considered in highly transient systems and whenever the heat exchange in one of the phases is dominant (Gandomkar and Gray 2018). Therefore, this paper proposes a novel concept of coupling a conical shape, rock-plie based large-scale STES system with a diesel exhaust heat recovery system in remote communities on Arctic regions like the northmost of Canada. Depending on the feasibility, such a concept can be applied in both small villages and large commercial operations like mine sites.

To exemplify the proposed concept, a remote community named Kwadacha of northern British Columbia has been selected. This is a non-commercial establishment that depends mainly on diesel generators for electricity generation. Considering a well-established off-the-shelf waste heat recovery system in place, the proposed study seeks to mitigate the seasonal mismatch between demand and supply of heat using a rock-pile seasonal waste heat storage. Therefore, all the heat that is generally discarded during summer can be stored and later used during peak months of heat demand on winter, adding up to the instant heat recovery rate. For that, a numerical model has been created on Ansys Fluent to represent the rock-pile and to study its heat transfer characteristics. The effect of LTNE versus the LTE approach has been taken into consideration, based on principles for forced convection in porous media (Nield and Bejan 2006). Then, the model has been validated against experimental data of a previous study (Hänchen, Brückner et al. 2011). Hence, mass-flow for the discharge period, the particle size of the rock, porosity and permeability of the structure and distinct rock types are also analyzed. Finally, a simple cost estimation is performed to confirm the viability of the proposed system.

## 6.2. Model description

Table 6.1. General information of the community selected for the case study

| **General Overview** | |
|---|---|
| Community | Kwadacha |
| Location | British Columbia, CA |
| Community record status | Active off-grid |
| Community type | Settlement |
| Community classification | Indigenous |
| Indigenous category | First Nation |
| Population | 332 |
| Residential accounts | 127 |
| Main Power Source | Diesel |
| Power generation Capacity (kW) | 1800 |
| Annual average fossil fuel power generation (MWh/year) | ~3000 |
| Average Winter Temperature (°C) | -7 |
| Average Summer Temperature (°C) | 9 |
| Estimated overall annual heat demand (GJ/year-house) | 66 |

A typical remote Canadian community called Kwadacha and located in British Columbia was selected for this study. The pile has been sized based on a storage period of about six months and the average recoverable available heat from the exhaust stream of diesel generators, which is estimated based on literature(Baidya, de Brito et al. 2019). The available waste heat was calculated in accordance to the manufacturer's catalogs of diesel generator. The average energy consumption of the community is obtained from the Government of Canada's database (Canada 2017), as well as some other essential parameters reported in Table 6.1. The pile size is the one estimated to be able to hold the amount of energy available in the exhaust stream, on an assumed continuous operation of the generators during summer months, by means of raising the temperature of the rock up to the temperature of the heat source (around 400°C). Limestone has been initially selected as a storage material for its abundance. For the base case, the thermo-physical properties have been assumed as shown in Table 6.2. The proposed system would employ large rock sizes that have not been processed or crushed, meaning it could be waste rock from a neighbor industrial operation.

A truncated cone geometry with a standard angle of repose of 37° has been chosen for its ease of construction and lower cost in a remote environment. This way the rock could be moved and piled by a truck on the spot. The schematic can be seen in Figure 6.1. A concrete dome is intended to be used as a protective means against weather conditions. The lateral walls of the pile have a layer of thermally insulating material to prevent heat from escaping. Although the insulation is considered perfect for the most part of this study where the numerical model is involved, a heat loss analysis, as well as the corresponding insulation required, are evaluated on the economic feasibility part of this study. The direct impact of insulation and losses on the temperature distribution of the pile shall be deeply investigated in prospective studies from this group.

It is important to mention that in the proposed scenario, the waste heat recovery system using the rock-pile does not intend to substitute the commonly employed fossil-fueled conventional heating system. Such conventional heating systems usually consist of fossil-fueled boilers that distribute heated water to the residential and commercial areas. The system has been designed to work storing the heat directly from the diesel generators' exhaust air and subsequently supplying said energy as an additional heat source for the conventional system. For heat extraction, ambient air has been circulated through the system and later sent to original the heating system. This allows the WHR/STES system to be able to take advantage even of small temperature gradients as any low-grade heat will be further upgraded by the conventional system using fossil fuels before being delivered to the households. The 3D geometry was developed on Solidworks and as for the numerical simulations, all the partial differential equations have been solved using finite volume solver Ansys Fluent 17.1.

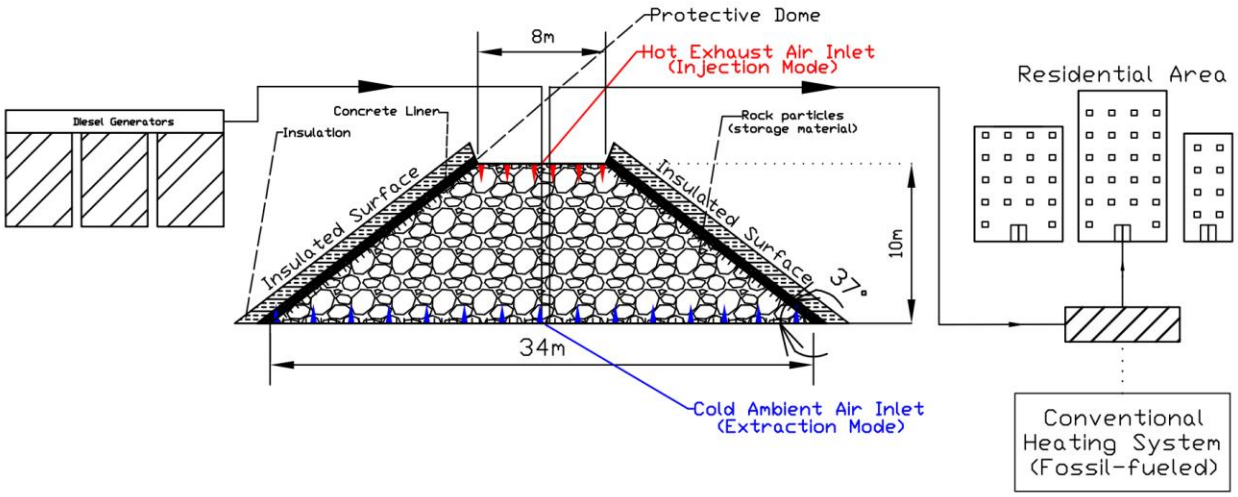


Figure 6.1. Diagram of the proposed rock-pile STES system

Table 6.2. Thermo-physical properties of the system for the base case

| Domain | Parameter | Value |
|---|---|---|
| Solid rock | Material | Limestone |
| | $\rho_s$ (kg/m³) | 2600 |
| | $c_{p,s}$ (J/kg-°C) | 920 |
| | $k_s$ (W/m-K) | 2.2 |
| | Volume needed (m³) | 3,830 |
| | Mass needed (tonnes) | ~$10^4$ |
| | $\varepsilon$ | 0.4 |
| | $d_p$ (m) | 0.1 |
| | K (m²) | $1.25\times10^{-5}$ |
| Exhaust air | $\rho_f$ (kg/m³) | Ideal-gas |
| | $c_{p,f}$ (J/kg-°C) | 1066 |
| | $k_s$ (W/m-K) | 0.0242 |

### 6.2.1. Governing equations

Fluid flow and heat transfer in the system have been modeled according to porous media theory (Nield and Bejan 2006). The equations for conservation of mass, momentum and energy are as shown in Eqs. 6.1-6.5. In this study, two different approaches have been used to determine the heat transfer for the porous media, namely local thermal equilibrium (LTE) and local thermal non-equilibrium (LTNE). The first one assumes that a thermal equilibrium occurs for both phases at all instants (i.e., it assumes the rock and neighbor fluid are always at the same temperature) leading to one equation to be solved for energy conservation as an equivalent "one-phase" system.

Meanwhile, the second one uses the assumption that an energy balance always happens between phases. This means the temperatures are calculated based on an energy balance between the two phases (i.e., it considers the heat transfer happening between solid and fluid) leading to two separate equations for energy conservation. For all that, it can be expected that the LTNE method gives a more realistic result since it consists of more accurate modeling of the actual physical phenomena happening within the porous media. However, depending on the application, LTE might give a result that is just accurate enough for practical means. Note that the bold small characters represent vectors and I represents the identity matrix.

- Mass conservation (continuity)

$$\frac{\partial(\varepsilon\rho_f)}{\partial t} + \nabla\cdot\left(\rho_f\langle\boldsymbol{u}\rangle\right) = 0 \tag{6.1}$$

- Momentum conservation

$$\frac{\partial(\varepsilon\rho_f\boldsymbol{u})}{\partial t} + \nabla\cdot\left(\rho_f\langle\boldsymbol{u}\rangle\times\langle\boldsymbol{u}\rangle\right) = -\nabla P\boldsymbol{I} + \nabla\cdot\left[\mu_f(\nabla\langle\boldsymbol{u}\rangle + (\nabla\langle\boldsymbol{u}\rangle)^T) - \frac{2}{3}\mu_f(\nabla\cdot\langle\boldsymbol{u}\rangle)\boldsymbol{I}\right] + \rho_f\boldsymbol{g} - \frac{\mu_f}{k_f}\langle\boldsymbol{u}\rangle \tag{6.2}$$

- Energy conservation (**LTE**)

$$\frac{\partial(\varepsilon\rho_{eff}Cp_{eff}T)}{\partial t} + \nabla\cdot\left(\rho_{eff}Cp_{eff}\boldsymbol{u}T\right) = \nabla\cdot(k_{eff}\nabla T) \tag{6.3}$$

- Energy conservation (**LTNE**)

$$\frac{\partial(\varepsilon\rho_f Cp_f T_f)}{\partial t} + \nabla\cdot\left(\rho_f Cp_f\langle\boldsymbol{u}\rangle T_f\right) = \nabla\cdot(\varepsilon k_f\nabla T) + h_{fs}A_{fs}(T_s - T_f) \tag{6.4}$$

$$\frac{\partial[(1-\varepsilon)\rho_s Cp_s T_s]}{\partial t} = \nabla\cdot[(1-\varepsilon)k_f\nabla T] + h_{fs}A_{fs}(T_f - T_s) \tag{6.5}$$

Where Eq. 6.4 and Eq. 6.5 represent the energy balance for the fluid and solid phases respectively and $h_{fs}$ is the corrected heat transfer coefficient, a parameter crucial to the correct implementation of the LTNE method. With that in mind, its calculation is done using Eqs. 6.6-6.9, according to

(Nield and Bejan 2006). For that, a UDF is developed in C programming language) and implemented in Fluent to compute said parameter in each iteration.

$$h_{fs} = a_{fs} h^* \tag{6.6}$$

$$\frac{1}{h^*} = \frac{d_p}{k_f Nu_{fs}} + \frac{d_p}{\beta_f k_s} \tag{6.7}$$

$$Nu_{fs} = (\frac{0.255}{\varepsilon}) Pr^{1/3} Re^{2/3} \tag{6.8}$$

$$a_{fs} = 6(1-\varepsilon)/d_p \tag{6.9}$$

To consider a temperature-dependent density the ideal-gas model was used. Thus, density was obtained by the relation in Eq. 6.10.

$$\rho_f = P/RT_f \tag{6.10}$$

Finally, the parameter here denominated storage efficiency was calculated by:

$$\eta = \frac{Q_{ext}}{Q_{sto}} \tag{6.11}$$

### 6.2.2. Boundary conditions

The boundary conditions applied are presented in Table 6.3. These are used throughout the paper unless otherwise specified. Inlets have fixed mass flow, outlets have fixed pressure and walls have zero velocities (**u** = 0) and zero temperature gradients ($\boldsymbol{n} \cdot \nabla T = 0$). Note that the flow direction is from top to bottom on the charging cycle and it is inverted on the discharging cycle. This is found to be the most efficient way of operating the system as it takes advantages of both geometric and buoyancy effects on the flow. Initial temperature of the pile before charging is assumed to be 10 °C. It is important to note that for the greatest part of this work the heat losses through the storage walls are neglected as the main goal is to evaluate the impact specific thermodynamic and physical parameters on the charging and discharging cycles. However, heat losses are considered on the

economic evaluation of the system in section 6.3.7. The boundary conditions of the cycles are also represented in detail in Figure 6.2.

Table 6.3. Boundary conditions used on numerical simulation (base case)

| Cycle | Location | Condition |
|---|---|---|
| Charging (6 months) | Inlet (Top) | $\dot{m}$ = 1.75 kg/s; $T_f$ = 400°C |
| | Outlet (Bottom) | Gauge pressure = 0 |
| | Pile Walls | No slip condition (**u** = 0) and zero heat flux ($\boldsymbol{n} \cdot \nabla T = 0$) |
| Discharging (6 months) | Inlet (Bottom) | $\dot{m}$ = 1.75kg/s; $T_f$ = 7°C |
| | Outlet (Top) | Gauge pressure = 0 |
| | Pile Walls | No slip condition (**u** = 0) and zero heat flux ($\boldsymbol{n} \cdot \nabla T = 0$) |

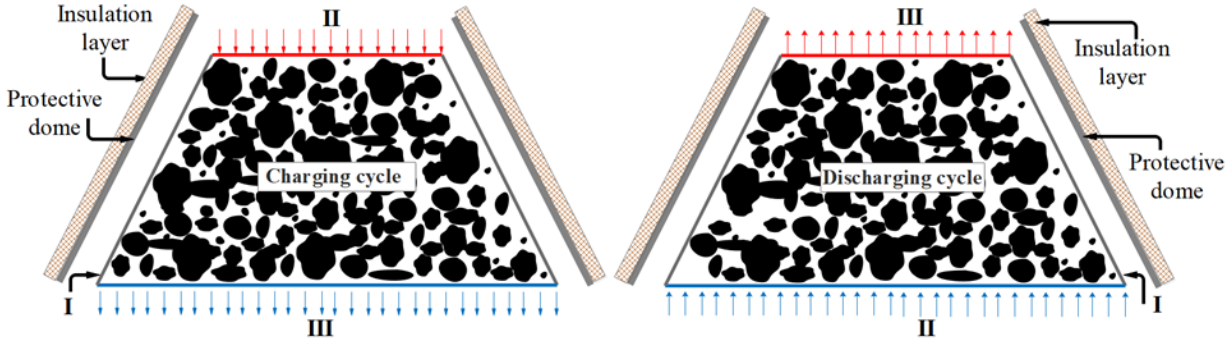


Figure 6.2. Schematics of the computational domain of TES system and its boundary conditions; (I) wall at lateral surface, (II) mass flow inlet at top and bottom in charging and discharging cycle, respectively, and (III) pressure outlet at bottom and top in charging and discharging cycle, respectively.

### 6.2.3. Numerical methodology

The 3D mesh of the model was created on the Ansys *Meshing* assistant. To perform a mesh independence analysis, the initial model has been designed with approximately 68,000 nodes and then next models have been developed with a higher number of nodes up to 143,240 until the result difference between the finer models was observed to be as low as 2%. Given the results of the mesh independence analysis, the model was solved with about 124,360 nodes to reduce computational costs. Fluid flow through the porous rock-pile domain is considered to be transient and laminar. To solve the numerical model, the Semi-Implicit Pressure-Linked Equation

(SIMPLE) method was used with the second-order upwind discretization scheme and the Algebraic Multi-grid (AMG) algorithm. Iterations were performed until residuals of about $10^{-6}$ were reached (i.e., approximately converging after 50 iterations at each time step of averagely 5,400 s).

## 6.3. Results and discussion

### 6.3.1. Model validation

If one intends to use the proposed model to predict the outcome of a real STES system and its applications, it is essential to make sure that it correctly captures the fluid flow and the interphase heat transfer phenomena within the porous domain. To that end, the model has been resized and adapted to match the packed bed thermal energy storage experimental setup presented and utilized by (Hänchen, Brückner et al. 2011). The operational parameters of the rescaled system have also been changed to match the pilot thermal energy storage system setup used in their experiments. By comparing the obtained numerical results with the original experimental data, the ability of the numerical model developed in this study to simulate real-life fluid flow and heat transfer within porous media shall be evaluated. Thus, both temperature distribution and pressure difference along the rock bed have been compared to validate heat transfer and fluid flow, respectively. Figure 6.3 depicts the validation of the temperature distribution along the rock bed, and Figure 6.4 shows the validation of pressure drop across the system. Note that pressure drop for fluid flow across porous media is a critical outcome for the evaluation of the performance of the system and is significantly hard to predict. Both the LTE and the LTNE approach were used in the numerical simulations for this section aiming to evaluate and display the difference between them in predicting heat transfer for a packed bed thermal energy storage system and the implication of using LTNE over LTE.

Both have an outcome that has very good agreement with the experimental data, with the LTNE method being a noticeably closer match. This shows that for this application, utilizing LTNE will lead to significantly more accurate results. For that reason, the LTNE approach is chosen for all the further simulations performed in this study unless otherwise specified.

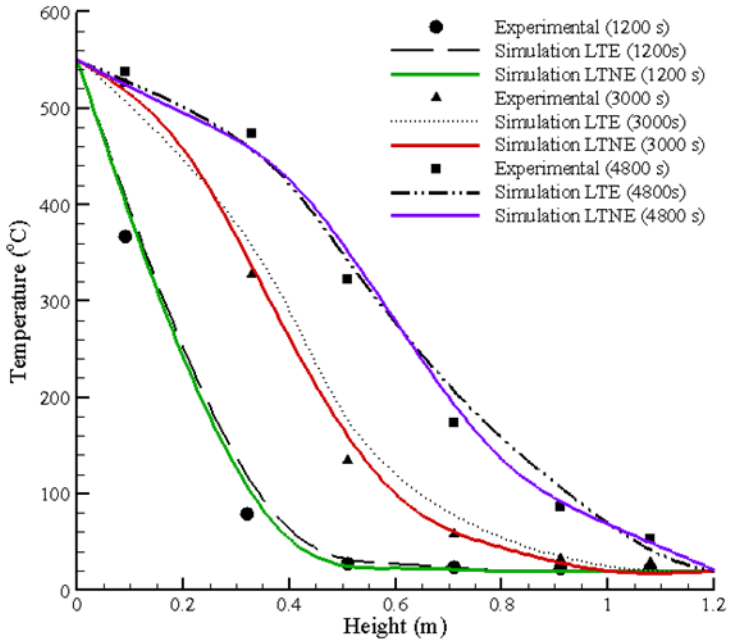


Figure 6.3. Validation of porous media heat transfer of the proposed numerical model, comparison of temperature along the vertical axis of the setup presented on (Hänchen, Brückner et al. 2011)

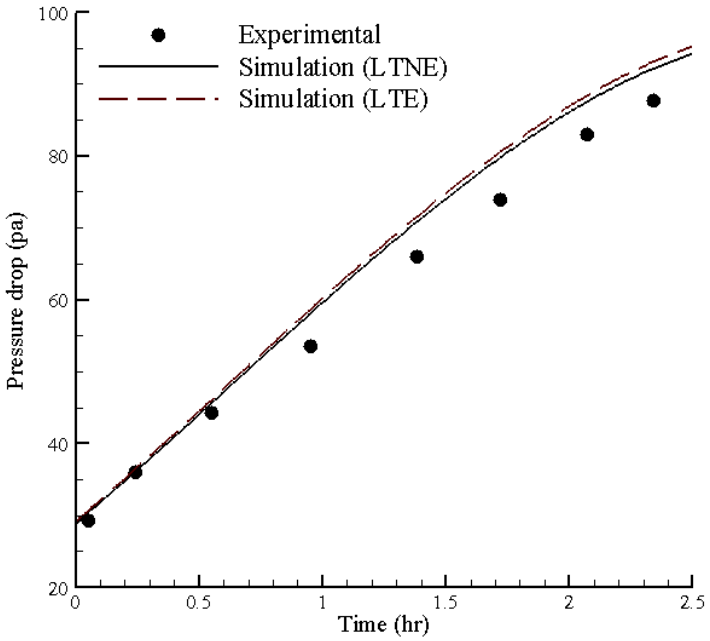


Figure 6.4. Validation of porous media fluid flow of the proposed numerical model, comparison of pressure drop along the rock bed of setup presented on (McCartney, Başer et al. 2017)

### 6.3.2. Local Thermal Equilibrium vs. Local Thermal non-Equilibrium approach

Simulations of the base model have been run initially for the LTE and subsequently for the LTNE method to evaluate the impact of the thermal equilibrium approach in the porous media heat transfer within the rock-pile. Figure 6.5 displays the mass-flow averaged inlet and outlet temperatures for both approaches. A significant difference in outlet temperature can be noted. As seen in the previous section, it is expected that the LTNE method will lead to significantly more accurate results for this application. The situation, in this case, is that the heat transfer happening within the pile is slower than the air temperature variation, which leads to a non-equilibrium of temperature between the solid rock and the fluid flow. This means that the LTE method will not be able to capture the temperature distributions within the rock bed fully. Hence, for its higher accuracy, the LTNE method has been selected to conduct all further simulations throughout this

study. Figure 6.6 shows the temperature distribution (on the left) within the rock-pile 60 days after the beginning of each cycle, as well as the velocity vectors (on the right) for the LTNE approach.

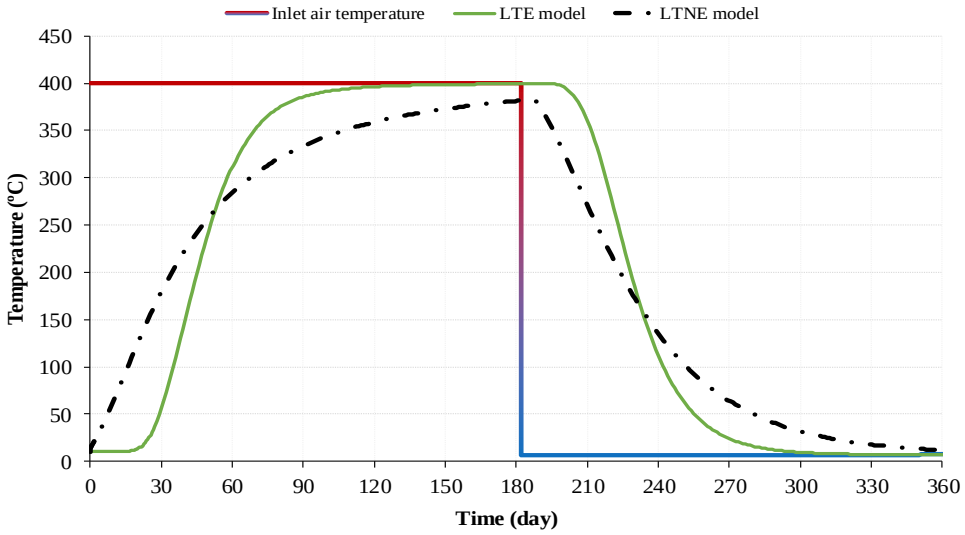


Figure 6.5. The mass-weighted average outlet temperature of air for the LTE and LTNE models, $\dot{m}$ = 1.75 (kg/s) for both cycles.

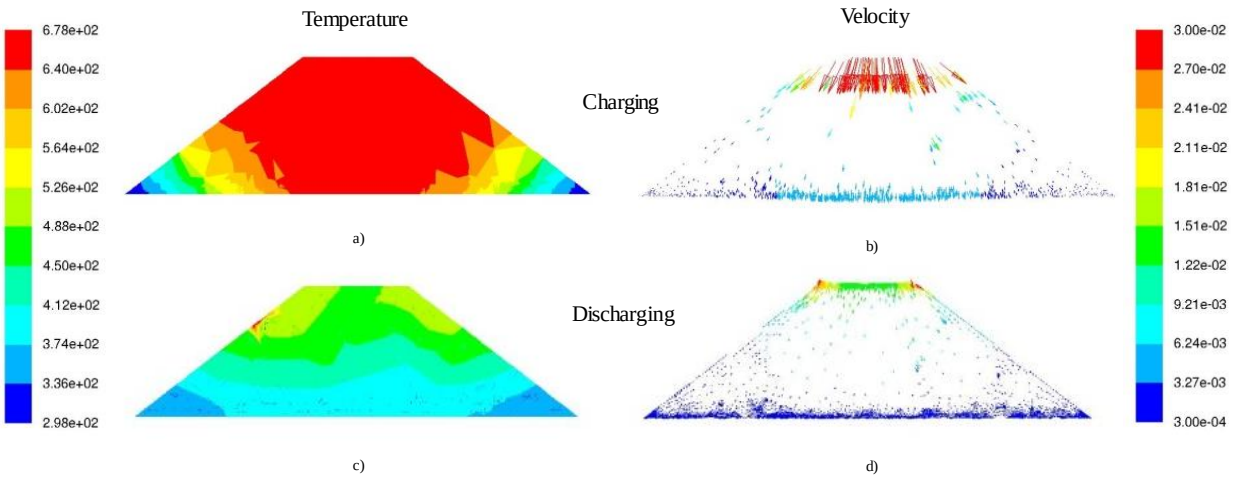


Figure 6.6. For LTNE model: a) Temperature contours-60 days after charging starts; b) Velocity vectors-60 days after charging starts; c) Temperature contour-60 days after discharging starts; d) Velocity vector-60 days after discharging starts.

### 6.3.3. Effect of temperature-dependent properties

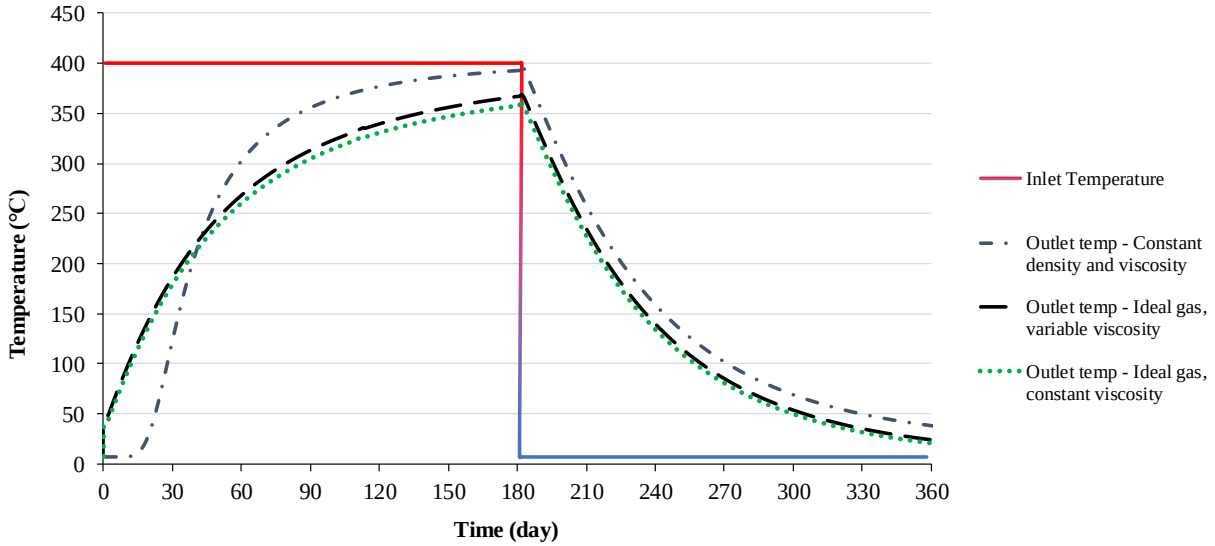


Figure 6.7. Comparison of outlet temperatures for different temperature-dependent scenarios on thermo-physical properties of air

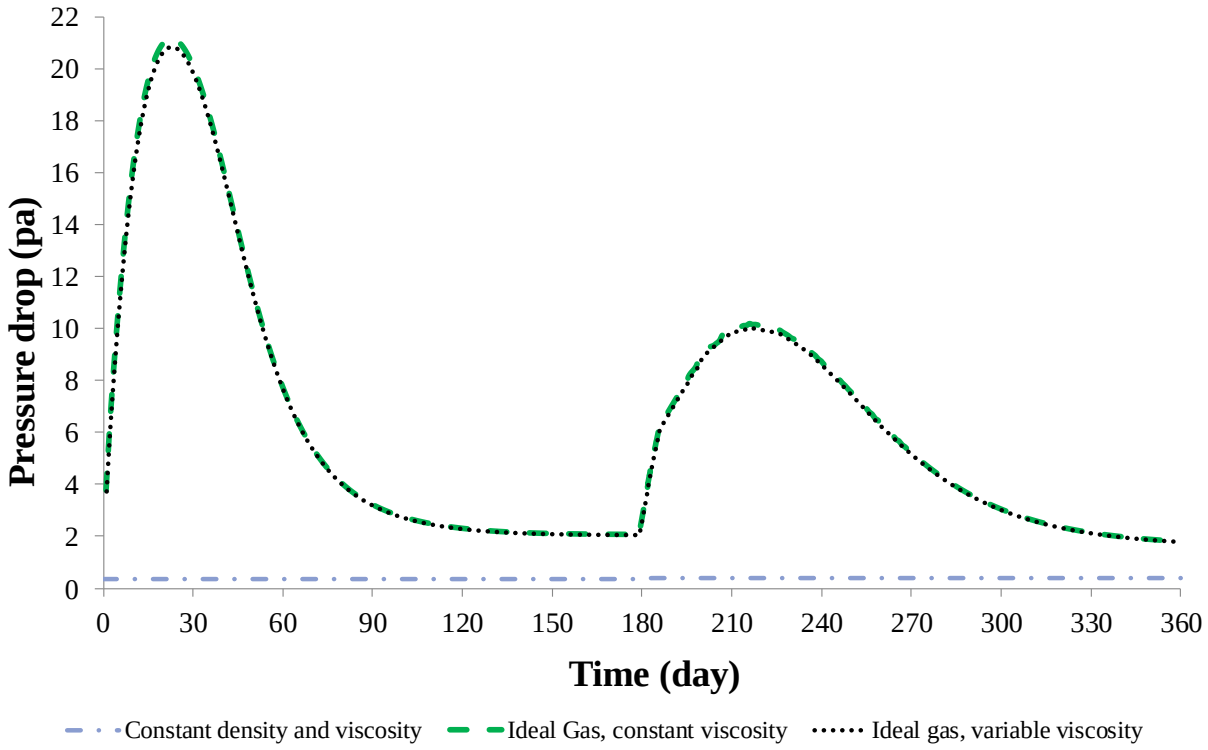


Figure 6.8. Comparison of pressure drop across rock-pile for different temperature-dependent scenarios on thermo-physical properties of air

A question that often arises from the study of fluid flow over porous media is what is the impact of the assumption that thermo-physical properties are constant. As the airflow here is subjected to a massive temperature difference (about 350°C), it is crucial to investigate the effect of temperature-dependent properties. For that, two parameters that have a greater change in the temperature range analyzed here are selected for a more in-depth investigation. Such parameters are density and viscosity, the first for its very high variation within the given temperature difference (almost 50%) and the former for its expected greater influence on the fluid flow and pressure drop. Figure 6.7 shows the effect of the distinct approaches used on the outlet temperature of the airflow, while Figure 6.8 shows the effect of those on the pressure drop across the rock-pile with time. It becomes clear that using a constant density approach leads to incorrect results, proving that an ideal-gas approach is essential when simulating the porous fluid flow and heat transfer. This should be expected as (Nield and Bejan 2006) suggests that pressure drop is directly related to the fluid density, besides, buoyancy effects are expected to take place within the porous domain, which will not exist if a constant density is used.

On the other hand, variable viscosity seems to have a very subtle effect on both the flow and the heat exchange. Therefore, all further simulations are performed with Ideal gas density and a constant viscosity. It is worth mentioning that using temperature-dependent properties significantly affects the stability (ability to converge) of the model creating additional challenges for a higher accuracy. For that, it is important to find the optimum approach for each model that gives enough accuracy while still able to achieve convergence.

### 6.3.4. Effect of mass flow on discharge

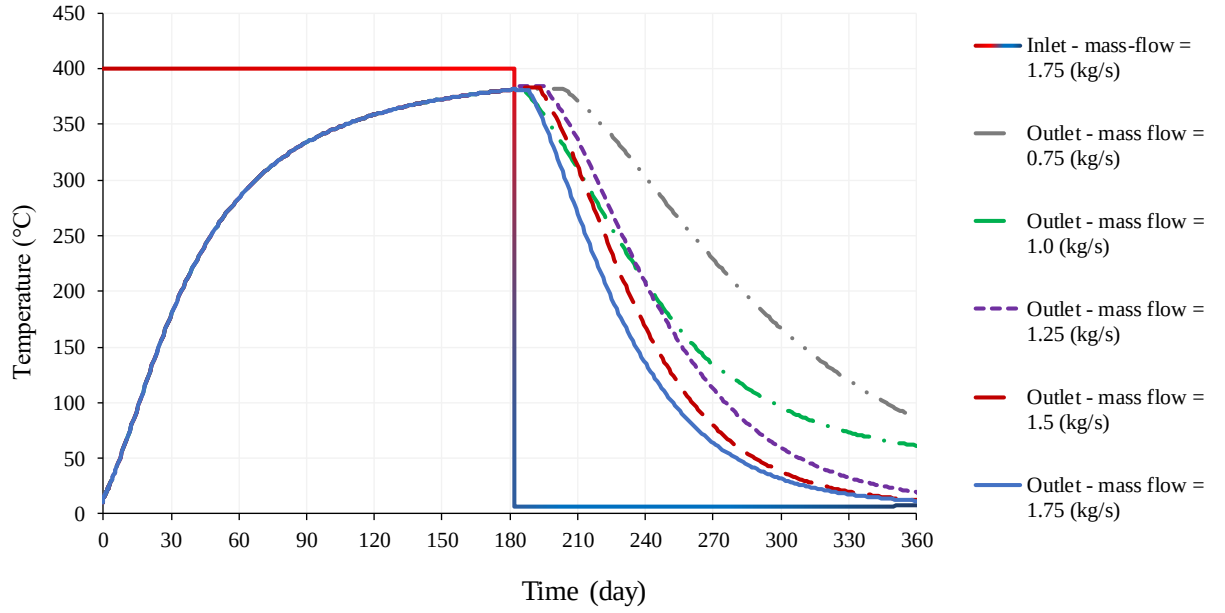


Figure 6.9. Mass-weighted average outlet air temperature for model with $\dot{m}$ = 1.75 (kg/s) for charging and $\dot{m}$ = 1.75; 1.5; 1.25; 1.00 and 0.75 (kg/s) for the discharging cycle

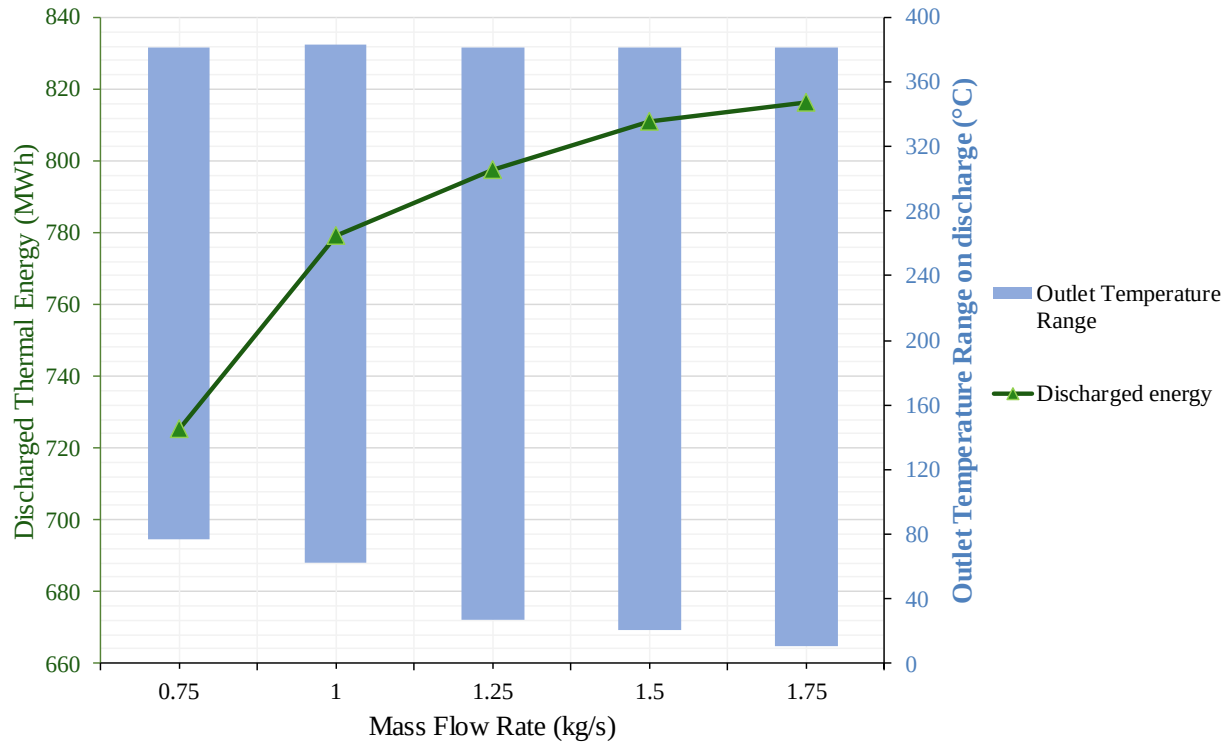


Figure 6.10. Total extracted energy and outlet temperature range for distinct mass flow rates during 6 months of discharge

Even though with the base operational conditions the system is successfully able to store around 840MWh, outlet temperature drops very fast on the discharging cycle. To mitigate that, the impact of distinct mass flows of air is investigated. Seeking a subtler drop on said temperature (and consequently on the net heat flux), several smaller mass flows are employed to extract the heat. Figure 6.9 depicts the mass-weighted averaged outlet temperatures for air for the base charge cycle ($\dot{m}$ = 1.75 kg/s) and varying discharging mass flows. Different air flows also impact on the total amount of energy that can be extracted in six months; these are shown in Figure 6.10 along with temperature ranges obtained for each case. Even though the smaller mass flow has resulted in a range with higher temperatures even at the end of the discharging cycle, the $\dot{m}$ = 1.75 kg/s case culminated in the best value for total heat extracted. This is caused by the higher velocities within the rock mass due to a larger mass flow. Accordingly, higher convection coefficients are obtained resulting in a better overall rate of heat transfer. With that, it can be said that there is a trade-off relationship between the range of temperatures for the outlet discharging air and the total energy extracted in a 6-month cycle. Ideally, a variable speed fan can be employed along with a control system to adapt the operating parameters and conform to specific heat requirements.

### 6.3.5. Effect of particle size, porosity and permeability

Physical properties of the rock used as storage material are also important parameters known to have a significant impact on the fluid flow over porous media. Seeing that the permeability is directly related to the velocity of the fluid within the domain, and given that it is dependent on both particle size and porosity (Nield and Bejan 2006), six different relatable rock scenarios are taken from (Amiri, Ghoreishi-Madiseh et al. 2018) and used for a more in-depth analysis on the physical properties of the rock medium. The properties for each scenario are described in Table 6.4.

Table 6.4. Cases selected from (Amiri, Ghoreishi-Madiseh et al. 2018) for more in-depth analysis on physical properties of the rock domain

| Case | $d_p$ (m) | ε | K (m²) |
|---|---|---|---|
| A | 1.25 | 0.45 | $2.50\times10^{-3}$ |
| B | 1.2 | 0.4 | $1.10\times10^{-3}$ |
| C | 1.05 | 0.35 | $4.10\times10^{-4}$ |
| D | 0.9 | 0.3 | $2.30\times10^{-4}$ |
| E | 0.75 | 0.25 | $6.90\times10^{-5}$ |
| F | 0.6 | 0.2 | $1.80\times10^{-5}$ |

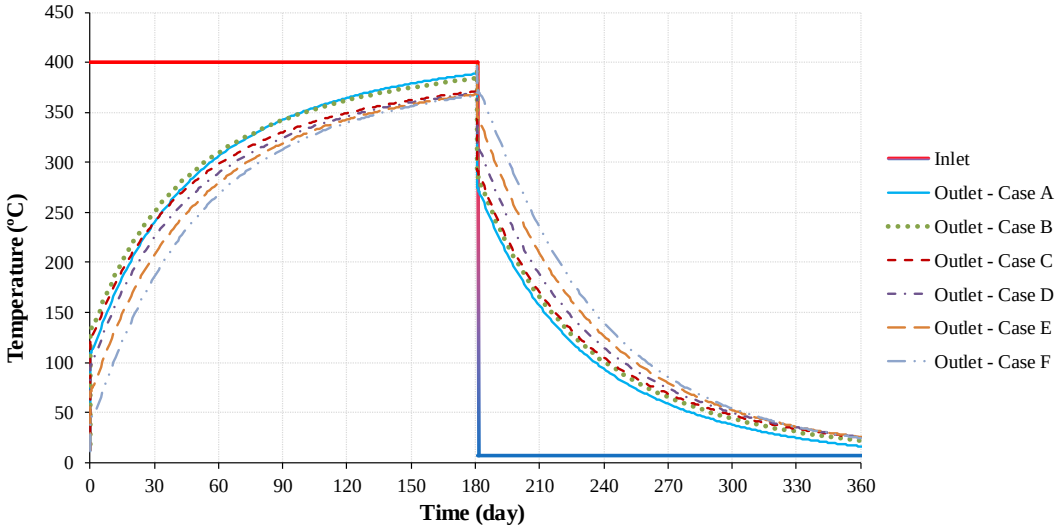


Figure 6.11. Airflow temperatures for distinct porosity-permeability scenarios

It is possible to see in Figure 6.11 that the change in the rock physical properties has a modest impact on the outlet temperature of the system. Overall temperature difference (between inlet and outlet) drops with the increase of porosity and permeability. Thus, total heat exchange and consequently heat stored and will be higher for a lower permeability. Such an effect is a consequence that a domain with a higher permeability will allow the fluid to navigate faster, reducing the time necessary for heat exchange between phases. On the other hand, with higher porosity and permeabilities the pressure drops across the system increase significantly, as shown in Figure 6.12. Still, the pressure drop is considerably low, due to the small velocities involved,

and as displayed in Figure 6.13 energy stored, extracted and storage efficiency (defined as the ratio of energy extracted/stored) significantly increases. With that in mind, it can be said that smaller rocks should be preferred if one seeks higher thermal storage capacity.

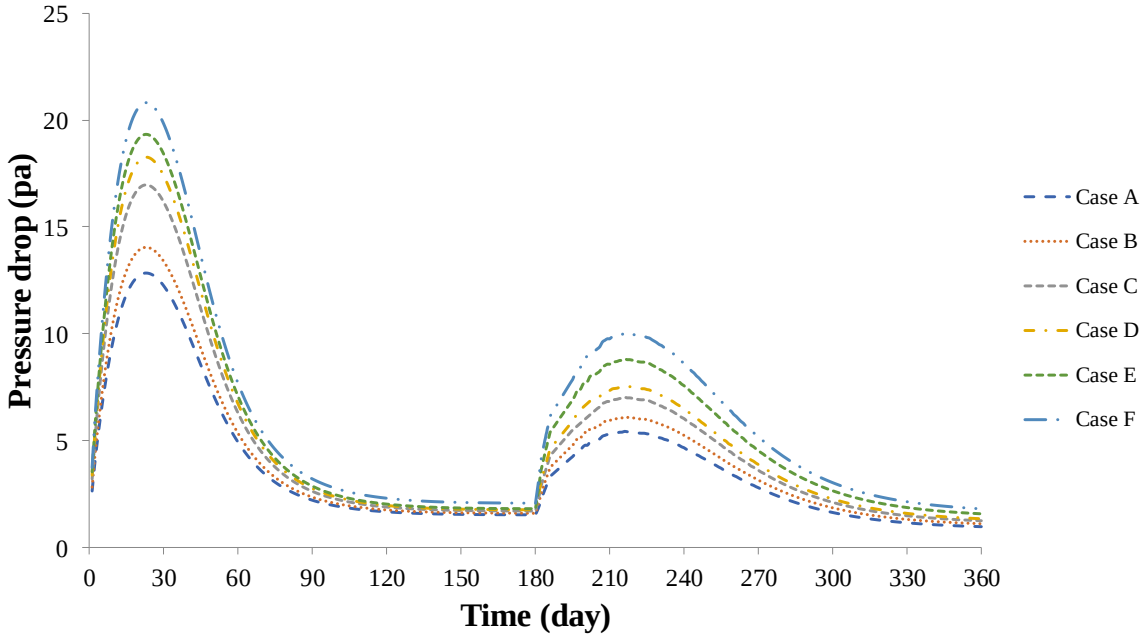


Figure 6.12. Pressure drop across rock-pile for distinct porosity-permeability scenarios

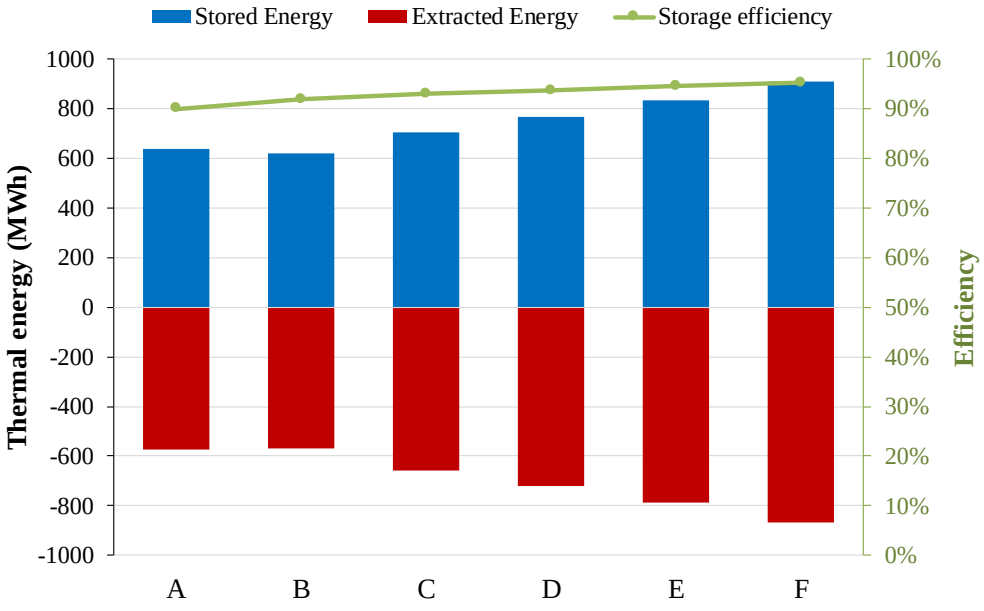


Figure 6.13. Energy stored (positive) and extracted (negative) for distinct porosity-permeability scenarios

### 6.3.6. Effect of rock thermo-physical properties

Table 6.5. Thermo-physical properties of four distinct rock types used in the analysis

| Properties | Limestone (base case) | Sandstone | Granite | Gabbro |
|---|---|---|---|---|
| ρ (kg/m³) | 2600 | 2400 | 2600 | 2900 |
| $c_p$ (J/Kg-K) | 920 | 775 | 820 | 980 |
| $k_s$ (W/m-K) | 2.2 | 2.3 | 2.8 | 2.2 |

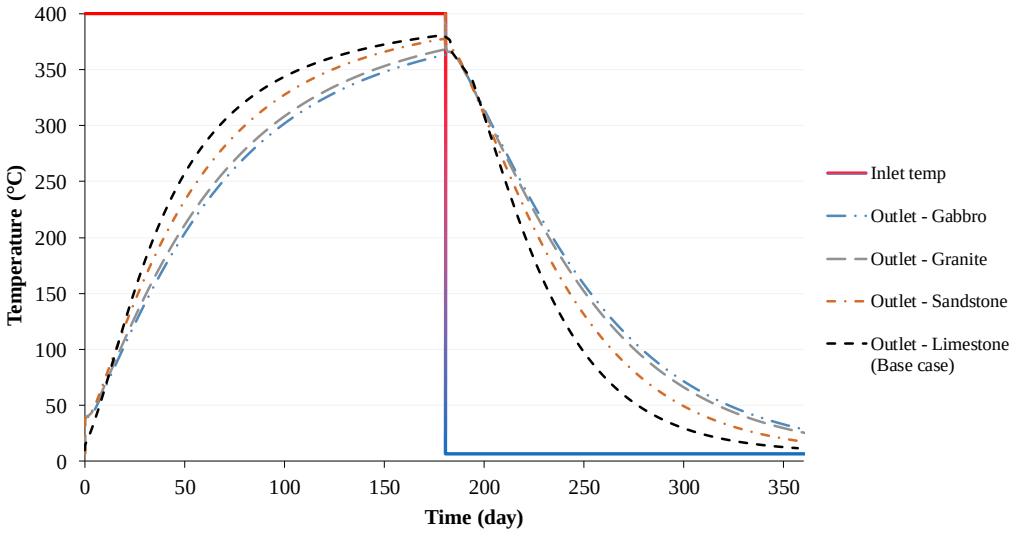


Figure 6.14. Airflow temperatures for distinct rock type scenarios

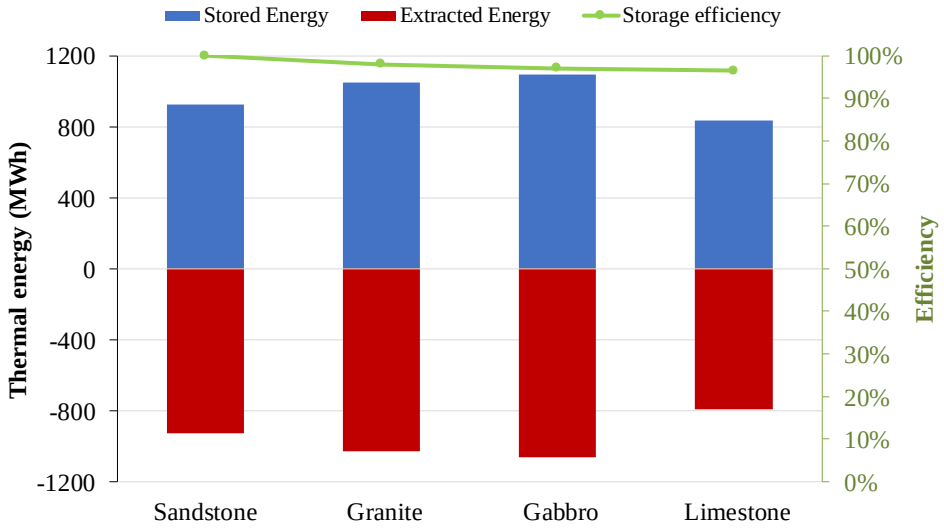


Figure 6.15. Energy stored (positive) and extracted (negative) for distinct rock type scenarios

Lastly, to evaluate the impact of employing different rock types to create the pile, three additional rock types are selected and their properties are taken from (Tiskatine, Aharoune et al. 2017). The case F from Table 6.4 was used for the simulations in this section. Temperatures for the charging and discharging cycles are shown in Figure 6.14, while total energy stored, extracted and storage efficiency are displayed in Figure 6.15. Note that a larger thermal conductivity will allow a faster heat exchange leading to higher temperature differences in flow and resulting in higher heat flux.

Meanwhile larger density and $c_p$ (mainly) will directly affect the heat storage capacity of the system. This is evidenced by the results as Gabbro with its higher specific heat and density was able to store the most heat. Thus agreeing with the affirmation made by (Tiskatine, Aharoune et al. 2017) that Gabbro is the best material, concerning thermal performance, for use in STES systems. Limestone on the other hand initially selected here for its abundance and lower cost turns out not to be amongst the best options for storage medium regarding performance. Still, it manages to store the approximate design value of energy. It is important to remember that the volume of the pile is kept constant for all the analyzed scenarios and walls are considered insulated all the time.

### 6.3.7. Cost estimation

From the above-mentioned results, it is proved that the system successfully achieved the proposed task of working as a STES system for a remote arctic community. Being able to store (with limestone as media and base parameters) around 840MWh and release up to 811 MWh (in the optimum scenario with $\dot{m} = 1.75$ kg/s) of thermal energy which can be extracted during the winter and used for several heating purposes within the community. However, for it to be

successfully employed in such scenarios, it is essential to check whether the system is financially justified.

Although heat losses have been neglected in the numerical investigations implemented in this study, it is important to consider such losses on the economic evaluation of the system as they might, from an operational perspective, severely impact the performance of the system. For that, heat losses were considered at a minimum reasonable value of 10% for the base case and the corresponding thermal insulating layer needed was determined using conductive and convective thermal resistance principles according to the literature (Cengel 2014). The insulating material selected was glass wool, one of the most inexpensive insulating materials employed in the industry (Villasmil, Fischer et al. 2019). More details about the protective dome and the insulating layer are given in Table 6.5. The fraction of the volume of insulation to the overall volume of the system is found to be about 14%, which agrees with the trend shown in literature for such material (Villasmil, Fischer et al. 2019). Data regarding costs and material properties were taken from literature and company catalogs (Cengel 2014, Villasmil, Fischer et al. 2019). Average values of environmental parameters over the winter for the locale were obtained from the Canadian Government (Canada 2018). Seeking a conservative approach, the temperature conditions for the insulation design were considered the worst possible over the winter: maximum temperature inside the dome wall (400°C) and minimum ambient winter temperature (-25°C).

Table 6.6. Heat loss and designed insulation details

| Property | Value | Property | Value |
|---|---|---|---|
| Energy capacity (kWh/Year) | 816,340 | Discharge mass flow rate (kg/s) | 1.75 |
| Energy density (MJ/ $m^3$) | 940 | Design $\Delta T$ for insulation (K) | 425 |
| Heat losses | 10% | Insulation material | Glass wool |
| Energy extracted after losses (kWh/Year) | 736,232 | Insulation thickness (cm) | 95 |
| Protective dome material | Concrete | Insulation cost | C$ 110,724 |
| Protective dome thickness (cm) | 10 | Thermal conductivity of insulation (W/m-K) | 0.038 |
| Protective dome cost | C$ 15,269.98 | $V_{Insulation}/V_{Total}$ | 14% |
| Thermal conductivity of dome (W/m-K) | 0.8 | Dome and insulation cost | C$ 125,994 |

Considering the new parameters which include the heat losses and the cost of the protective and insulative layers, the cost estimation was performed for the base case with the optimum mass flow. The simple payback can be seen in Table 6.6 along with some other important values. Costs for labor and equipment used are from a well-known industry standard for mining cost estimations. The simple payback analysis considers how long the cumulative financial savings from the use of the system will take to compensate for the initial implementation cost of the system.

The correspondent cost estimation showed that the expected payback period would be about 5.83 years, which represents a 38% increase from the one obtained disregarding insulation needs. Still, the system shows a favorable payback for a STES system of the kind. This project also saves carbon tax that represents 7.5% of the overall savings providing substantial environmental leverage for the communities which depend on fossil-fuel for power generation. Mainly when considering that the Government of British Columbia has stated an almost 42% increase on the current carbon tax by 2021 (Xu, Rathod et al. 2017). It is also noteworthy that systems based on renewable low-grade heat sources, like solar thermal energy concentrators, coupled to common thermal energy

storage methods, usually lead to very long payback periods (up to 20 and even 40 years) (Ucar and Inalli 2006, Karacavus and Can 2009). This shows the advantages of implementing rock-pile thermal energy storage along with waste heat recovery systems, which has a much higher-grade heat available in larger quantities and readily accessible allowing for the heat to be recovered and stored at lower costs.

Table 6.7. Economic evaluation of the system

| Property | Value | Property | Value |
|---|---|---|---|
| Rock Piling (tpd) | 1000 | Diesel Equivalent Savings (Liter/year) | 83,190 |
| Supplies and Labour (C$/tonne) | 47.03 | Energy Savings (kWh/year) | 734,611 |
| Fan Owning and Installation (2.2kW Axial) | C$ 6,550.00 | Annual Diesel Savings | C$ 95,710.17 |
| Pile Tonnage (tonne) | 10,000 | eCO2 (kg/year) | 222,117 |
| Days Needed for Piling (days) | 10 | Carbon Tax (C$/tonne) | 35.00 |
| Total cost of piling | C$ 476,892.40 | Carbon Tax Savings | C$ 7,774.11 |
| Overall cost of system | C$ 602,886.52 | Overall Annual Savings | C$ 103,484.28 |
| Diesel Cost (C$/kWh) | 0.13 | Simple Payback (years) | 5.83 |

## 6.4. Conclusion

The present work establishes a numerical study to store the waste heat from the exhaust of diesel generators in a rock-pile based seasonal thermal energy storage during summer and provide heating during harsh winter when it is needed. Evaluation of the concept has been done by scoping its application in a remote community, located in the cold climate zone of northern Canada. The heat transfer model for the rock-pile has been validated with a relevant experimental setup. Comparison between LTE and LTNE was performed and LTNE has led the model to a more realistic outcome resulting in LTNE being selected for further analysis. Examination of the effects

of temperature-dependent properties of air has shown more significant variation in results in the case of using variable density and negligible effects have been observed in the case of variable viscosity. An approach to estimate the suitable mass flow of air (1.75 kg/s) with ideal gas density and constant viscosity for higher heat extraction has suggested that possible employment of a fan with variable speed along with a control system could help ameliorate the performance of the system to comply with the instant heat requirements. Investigation on the effects of particle size, porosity and permeability has advocated for smaller rock size (and consequently lower porosity and permeability) leading to higher heat transfer rates and higher thermal storage capacities while still having a considerably small pressure drop. On the context of thermal performance, although most of the rock types seem to have a good outcome, due to its higher specific heat and density, Gabbro-based rock-pile shows better overall thermal storage performance. The proposed rock-pile based seasonal thermal energy storage holds the potential to be a greener solution for the heating demand of the remote communities in the cold climatic conditions (mainly when coupled with EHR) by reducing the burning of fossil fuels and the associated carbon tax. Furthermore, the calculated payback of less than six years gives the system the necessary economical sustainability for practical applications in said communities.

### 6.5. Nomenclature

*Abbreviations*

| | |
|---|---|
| **CSP** | Concentrated solar powerplant |
| **EHR** | Exhaust heat recovery |
| **LTE** | Local thermal equilibrium |
| **LTNE** | Local thermal non-equilibrium |
| **ORC** | Organic Rankine Cycle |
| **PCM** | Phase change material |
| **RC** | Rankine cycle |
| **STES** | Seasonal thermal energy storage |
| **SWHS** | Seasonal waste heat storage |
| **TES** | Thermal energy storage |
| **UDF** | User-defined function |
| **WHR** | Waste heat recovery |

*Symbols*

| | |
|---|---|
| $a_{fs}$ | Specific surface area ($m^{-1}$) |
| $\beta$ | Coefficient of thermal expansion ($K^{-1}$) |
| $c_{p,f}$ | Isobaric specific heat of fluid (J/kg-K) |
| $\rho_f$ | Density of fluid ($kg/m^3$) |
| $k_f$ | Thermal conductivity of fluid (W/m-K) |
| $c_{p,s}$ | Isobaric specific heat of solid (J/kg-K) |
| $\rho_s$ | Density of solid ($kg/m^3$) |
| $k_s$ | Thermal conductivity of solid (W/m-K) |
| $c_{p,eff}$ | Effective isobaric specific heat (J/kg-K) |
| $\rho_{eff}$ | Effective density ($kg/m^3$) |
| $k_{eff}$ | Effective thermal conductivity (W/m-K) |
| $\varepsilon$ | Porosity or Void fraction (non-dimensional) |
| $d_p$ | Solid particle average diameter (m) |
| $K$ | Permeability of rock mass ($m^2$) |
| $h_{fs}$ | Corrected convection heat transfer coefficient ($W/m^2$-K) |
| $h^*$ | Ancillary convection coefficient (W/m-K) |
| $\boldsymbol{I}$ | Identity matrix |
| $\boldsymbol{g}$ | Gravity vector ($m/s^2$) |
| $Pr$ | Prandtl number (non-dimensional |
| $Re$ | Reynolds number |
| $Nu_{fs}$ | Nusselt number of porous fluid flow |
| $T_s$ | Temperature of solid (°C) |
| $T_f$ | Temperature of fluid (°C) |
| $t$ | Time (s) |
| $\mu_f$ | Dynamic viscosity of fluid (Pa.s) |
| $\boldsymbol{u}$ | Superficial fluid velocity vector (m/s) |
| $P$ | Pressure (Pa) |

## 6.6. References


Abnay, B., A. Eddemani, A. Aharoune, A. Ihlal, L. Bouirden, R. Tiskatine and L. Gourdo (2016). "Experimental evaluation of thermo-mechanical performances of candidate rocks for use in high temperature thermal storage." Applied Energy 171: 243-255.

Alshammari, F., A. Pesyridis, A. Karvountzis-Kontakiotis, B. Franchetti and Y. Pesmazoglou (2018). "Experimental study of a small scale organic Rankine cycle waste heat recovery system for a heavy duty diesel engine with focus on the radial inflow turbine expander performance." Applied Energy 215: 543-555.

Amiri, L., S. A. Ghoreishi-Madiseh, A. P. Sasmito and F. P. Hassani (2018). "Effect of buoyancy-driven natural convection in a rock-pit mine air preconditioning system acting as a large-scale thermal energy storage mass." Applied Energy 221: 268-279.

Bari, S. and S. N. Hossain (2013). "Waste heat recovery from a diesel engine using shell and tube heat exchanger." Applied Thermal Engineering 61(2): 355-363.

Barton, N. G. (2013). "Simulations of air-blown thermal storage in a rock bed." Applied Thermal Engineering 55(1-2): 43-50.

Brooks, M. R. and J. D. Frost (2012). "Providing freight services to remote arctic communities : Are there lessons for practitioners from services to Greenland and Canada's northeast?" Research in Transportation Business & Management 4: 69-78.

Canada, N. R. (2017). The Atlas of Canada - Remote communities Energy Database.

Cascetta, M., G. Cau, P. Puddu and F. Serra (2016). "A comparison between CFD simulation and experimental investigation of a packed-bed thermal energy storage system." Applied Thermal Engineering 98: 1263-1272.

Chapuis, S. and M. Bernier (2009). "Seasonal storage of solar energy in borehole heat exchangers." Eleventh International IBPSA Conference: 599-606.

Dahash, A., F. Ochs, M. B. Janetti and W. Streicher (2019). "Advances in seasonal thermal energy storage for solar district heating applications: A critical review on large-scale hot-water tank and pit thermal energy storage systems." Applied Energy 239: 296-315.

Di Battista, D., M. Mauriello and R. Cipollone (2015). "Waste heat recovery of an ORC-based power unit in a turbocharged diesel engine propelling a light duty vehicle." Applied Energy 152: 109-120.

Erlund, R. and R. Zevenhoven (2018). Hydration of Magnesium Carbonate in a Thermal Energy Storage Process and Its Heating Application Design. 11.

Fernández-Yañez, P., O. Armas, A. Capetillo and S. Martínez-Martínez (2018). "Thermal analysis of a thermoelectric generator for light-duty diesel engines." Applied Energy 226: 690-702.

Feru, E., B. de Jager, F. Willems and M. Steinbuch (2014). "Two-phase plate-fin heat exchanger modeling for waste heat recovery systems in diesel engines." Applied Energy 133: 183-196.

Fisch, M. N., M. Guigas and J. O. Dalenbäck (1998). "A review of large-scale solar heating systems in Europe." Solar energy 63(6): 355-366.

Forsberg, C. W. (2012). "Gigawat-year geothermal energy storage coupled to nuclear reactors and large concentrated solar thermal systems."

Gandomkar, A. and K. E. Gray (2018). "Local thermal non-equilibrium in porous media with heat conduction." International Journal of Heat and Mass Transfer 124: 1212-1216.

Ghoreishi-Madiseh, S. A., A. F. Kuyuk, M. A. R. Brito, D. Baidya, Z. Torabigoodarzi and A. Safari (2019). "Application of Borehole Thermal Energy Storage in Waste Heat Recovery from Diesel Generators in Remote Cold Climate Locations." Energies: 13-13.

Ghoreishi-Madiseh, S. A., A. P. Sasmito, F. P. Hassani and L. Amiri (2017). "Performance evaluation of large scale rock-pit seasonal thermal energy storage for application in underground mine ventilation." Applied Energy 185: 1940-1947.

Hänchen, M., S. Brückner and A. Steinfeld (2011). "High-temperature thermal storage using a packed bed of rocks–heat transfer analysis and experimental validation." Applied Thermal Engineering 31(10): 1798-1806.

Hasnain, S. (1998). "Review on sustainable thermal energy storage technologies, Part I: heat storage materials and techniques." Energy conversion and management 39(11): 1127-1138.

Hossain, S. N. and S. Bari (2013). "Waste heat recovery from the exhaust of a diesel generator using Rankine Cycle." Energy Conversion and Management 75: 141-151.

Karacavus, B. and A. Can (2009). "Thermal and economical analysis of an underground seasonal storage heating system in Thrace." Energy and Buildings 41(1): 1-10.

Knowles, J. (2016). Power Shift: Electricity for Canada's Remote Communities, Conference Board of Canada.

Love, N. D., J. P. Szybist and C. S. Sluder (2012). "Effect of heat exchanger material and fouling on thermoelectric exhaust heat recovery." Applied Energy 89(1): 322-328.

Lovekin, D. and D. Heerema (2019). The True Cost of Energy in Remote Communities: Understanding diesel electricity generation terms and economics, PEMBINA Institute: 7-7.

McCartney, J. S., T. Başer, N. Zhan, N. Lu, S. Ge and K. Smits (2017). "Storage of solar thermal energy in borehole thermal energy storage systems."

McDaniel, B. and D. Kosanovic (2016). "Modeling of combined heat and power plant performance with seasonal thermal energy storage." Journal of Energy Storage 7: 13-23.

Mokkapati, V. and C. S. Lin (2014). "Numerical study of an exhaust heat recovery system using corrugated tube heat exchanger with twisted tape inserts." International Communications in Heat and Mass Transfer 57: 53-64.

Nield, D. A. and A. Bejan (2006). Convection in porous media, Springer.

Orr, B., A. Akbarzadeh, M. Mochizuki and R. Singh (2016). "A review of car waste heat recovery systems utilising thermoelectric generators and heat pipes." Applied Thermal Engineering 101: 490-495.

Pandiyarajan, V., M. C. Pandian, E. Malan, R. Velraj, R. V. Seeniraj, M. Chinna Pandian, E. Malan, R. Velraj and R. V. Seeniraj (2011). "Experimental investigation on heat recovery from diesel engine exhaust using finned shell and tube heat exchanger and thermal storage system." Applied Energy 88(1): 77-87.

Royer, J. (2013). Status of remote/off-grid communities in Canada. Ottawa, Natural Resources Canada: 44-44.

Singh, P. L., S. D. Deshpandey and P. C. Jena (2015). "Thermal performance of packed bed heat storage system for solar air heaters." Energy for sustainable development 29: 112-117.

Templeton, J. D., F. Hassani and S. A. Ghoreishi-Madiseh (2016). "Study of effective solar energy storage using a double pipe geothermal heat exchanger." Renewable Energy 86: 173-181.

Tian, Y. and C. Y. Zhao (2013). "A review of solar collectors and thermal energy storage in solar thermal applications." Applied Energy 104: 538-553.

Tiskatine, R., A. Aharoune, L. Bouirden and A. Ihlal (2017). "Identification of suitable storage materials for solar thermal power plant using selection methodology." Applied Thermal Engineering 117: 591-608.

Wang, T., W. Luan, W. Wang and S. T. Tu (2014). "Waste heat recovery through plate heat exchanger based thermoelectric generator system." Applied Energy 136: 860-865.

Welsch, B., L. Göllner-Völker, D. O. Schulte, K. Bär, I. Sass and L. Schebek (2018). "Environmental and economic assessment of borehole thermal energy storage in district heating systems." Applied Energy 216: 73-90.

Xu, B., D. Rathod, S. Kulkarni, A. Yebi, Z. Filipi, S. Onori and M. Hoffman (2017). "Transient dynamic modeling and validation of an organic Rankine cycle waste heat recovery system for heavy duty diesel engine applications." Applied Energy 205: 260-279.

Zanganeh, G., M. Commerford, A. Haselbacher, A. Pedretti and A. Steinfeld (2014). "Stabilization of the out fl ow temperature of a packed-bed thermal energy storage by combining rocks with phase change materials." Applied Thermal Engineering 70(1): 316-320.

Zanganeh, G., A. Pedretti, A. Haselbacher and A. Steinfeld (2015). "Design of packed bed thermal energy storage systems for high-temperature industrial process heat." Applied Energy 137: 812-822.

Zanganeh, G., A. Pedretti, S. Zavattoni, M. Barbato and A. Steinfeld (2012). "Packed-bed thermal storage for concentrated solar power–Pilot-scale demonstration and industrial-scale design." Solar Energy 86(10): 3084-3098.

Zhang, H. G., E. H. Wang and B. Y. Fan (2013). "Heat transfer analysis of a finned-tube evaporator for engine exhaust heat recovery." Energy Conversion and Management 65: 438-447.

# Connecting Text

*The outcomes of the previous chapters shape the idea of using waste rock as an energy storage material and hot exhaust air as a heat transfer fluid. Accordingly, the main objective of Chapter 7 is to understand the porous structure of such packed rock beds which is required for their design. The pressure drop across a rock bed directly affects its heat exchange performance, because additional fan power is required to circulate air during periods of storage/extraction. In this chapter, the fluid flow behavior inside a packed rock bed thermal energy storage system is investigated by developing a transient, 3D computational fluid dynamics and heat transfer model that accounts for interphase energy balance during energy conservation, using a local thermal non-equilibrium approach. It also offers useful information for evaluating the performance of packed beds of large rocks.*

*Chapter 7 has been submitted for publication as:*

***Leyla Amiri**, Seyed Ali Ghoreishi-Madiseh, Agus P. Sasmito, and Ferri P. Hassani. "Numerical study of volume averaged porous media heat transfer and fluid flow model for thermal energy storage in packed rock beds."*

# CHAPTER 7

## 7. Numerical study of volume averaged porous media heat transfer and fluid flow model for thermal energy storage in packed rock beds


## Abstract

Thermal energy storage in packed rock beds helps to reduce energy costs and carbon footprints on an industrial, commercial and residential scale. Fluid flow and heat transfer in large packed rock beds used in mining applications such as heating/cooling of mine intake air or ventilation of block-caved mines have recently received significant attention. Understanding the porous structure of such packed rock beds is a necessity in the design of such systems. The pressure drop across a rock bed directly affects its heat exchange performance, as it requires additional fan power to circulate air during periods of storage/extraction. In this study, the fluid flow behavior inside a packed rock bed thermal energy storage system is investigated by developing a transient three-dimensional computational fluid dynamics and heat transfer model that accounts for interphase energy balance using a local thermal non-equilibrium approach. It seeks to offer useful information for evaluating the performance of packed bed of large rocks and in caved zones. System performance is evaluated for a wide range of distinct parameters such as porosity, fluid velocity and the aspect ratio of the bed. The latter is further analysed in a variety of combinations with other system characteristics. The impact of all these parameters on the most important performance factors, such as pressure drop, heat transfer rate, total energy stored/extracted, are investigated. The findings show that while the total thermal energy storage capacity of the system is not significantly affected by fluid

mass flow rate, lower mass flow rates can result in longer charge/discharge times. Also, the aspect ratio is found to directly impact the pressure gradients along the bed but has no major effect on total energy stored. Finally, it is shown that porosity has the greatest impact on both fluid flow and heat transfer, while thermal capacity is deemed to be the most important thermo-physical factor in thermal energy storage performance.

## 7.1. Introduction

Increasing population and economic growth in the past years has significantly amplified fossil fuel dependency and its impact on the environment (Krishan and Suhag 2018). This has led industries to search for alternatives to fossil fuel and more environmentally friendly solutions for energy generation. With the increase in usage of renewable and alternative technologies, energy storage has gained great importance (Sorgulu and Dincer 2018, Sarbu and Dorca 2019). Thermal energy storage (TES) allows for energy to be stored in the form of heat in times of low or null demand and used later whenever demand rises (Sarbu and Dorca 2019). These systems help to reduce energy costs and carbon footprint on an industrial, commercial and residential scale, being even deemed vital in some applications (Abdel-Salam, Aly et al. 1991, Dincer 2002). Such technologies are mostly used in solar energy applications, mainly concentrated solar power plants (CSP)(Zanganeh, Pedretti et al. 2012, Tian and Zhao 2013, Mertens, Alobaid et al. 2014, Sorgulu and Dincer 2018) and solar district heating (Raftery, Shier et al. 1980, Dincer and Dost 1996, Schmidt, Mangold et al. 2004, Singh, Deshpandey et al. 2015, Dahash, Ochs et al. 2019), but waste heat storage systems can also take great advantage of their use (Zanganeh, Pedretti et al. 2015, Ghoreishi-Madiseh, Safari et al. 2018, Ghoreishi-Madiseh, Fahrettin Kuyuk et al. 2019). Among the three main types of TES systems: Chemical heat storage (based on thermochemical reactions);

Latent heat storage (using phase change materials) and sensible heat storage (simply based on temperature increase/decrease of medium) (Sarbu and Dorca 2019), the latter is currently the cheapest and easiest one to implement (Dincer 2002). For that reason, it is the most promising one for immediate use in large/industrial scale (Welsch, Göllner-Völker et al. 2018). That happens as it generally implements low-cost materials (e.g., air and broken rock) (Galione, Pérez-Segarra et al. 2015) and it often dispenses the need of intermediate heat exchangers (Zanganeh, Pedretti et al. 2015).

It has been shown previously that, rock bed storage systems frequently are more cost-effective than similar water-based systems for heating (Raftery, Shier et al. 1980). Still, other advantages of such systems can be bolded. They are more environmentally friendly than their counterparts as they use naturally occurring storage medium, they can usually withstand very high temperatures, they also have a high heat transfer coefficient between phases when in use, but low conductivity of heat when air flow is not present (Dincer and Dost 1996). Despite being used mostly for solar applications, due to its flexibility, packed rock bed TES can be employed in a wide range of energy-intensive industries. A good example is the development of the application for mine sites, where an opportunity exists in storing sensible thermal energy in packed rock beds created with broken rock. In those, packed rock beds and air are adopted as the storage media and heat transfer fluid (HTF), respectively, which has been shown as a favorable approach for TES systems (Ghoreishi-Madiseh, Sasmito et al. 2015, Amiri, Ghoreishi-Madiseh et al. 2017, Ghoreishi-Madiseh, Amiri et al. 2017, Ghoreishi-Madiseh, Sasmito et al. 2017, Amiri, Ghoreishi-Madiseh et al. 2018).

The performance of TES systems depends on many parameters which are not easy to obtain through analytical correlations. As packed rock bed storage efficiency depends on many designing

and operating factors, computational modeling can be considered a proper way to study and optimize these systems. Hence it is essential to have computational models to evaluate the performance of TES systems. Many studies have focused on the heat and mass transfer inside the packed beds (Esence, Bruch et al. 2017). Abdel-Salam et al. developed a one dimensional numerical model in cylindrical coordinates based on forward upwind methods to evaluate temperature distribution in a packed bed and found that increasing the bed length would raise the storage capacity without affecting the charging rate (Abdel-Salam, Aly et al. 1991). Arias et al. used finite difference models with variable number of sections to evaluate their capacity of representing the stratification phenomena observed in experiments (Arias, McMahan et al. 2008). Hänchen et al. developed a 1D numerical model for two-phase conservation of energy within a rock bed and compared it to experimental tests in a pilot-scale to validate it (Hänchen, Brückner et al. 2011). Zanganeh et al. used a transient quasi-one-dimensional numerical model to analyse two-phase heat transfer within a packed bed heat storage for industrial processes and evaluated the impact of several construction parameters on its performance. Barton developed a one-dimensional model for airflow within a porous rock bed medium and used it to study the effect of different charging and discharging flow direction schedules (Barton 2013). Kuravi et al. studied a large-sized packed bed (created with bricks) circulating air as a HTF with experiments and a 1D energy model and confirmed the viability of its fluid flow and heat transfer for solar applications (Kuravi, Trahan et al. 2013). Finally, Cascetta et al. presented a comparison between numerical and experimental results and obtained good agreement for simulations with experimental temperatures as inputs (Cascetta, Cau et al. 2016).

Two of the most important factors which should be taken into consideration for designing and operating porous media storage systems are: (1) the power required to circulate the HTF, and (2)

the heat transfer rate between the solid and fluid phases inside of the packed bed. The former determines operating cost, while the latter is directly related to storage capacity and rate. Besides, other case specific factors could affect the performance of the system. For that, understanding the porous structure of such packed rock beds and its importance is a necessity in the design of such systems. Some studies have focused on evaluating influential parameters. A high rate of heat transfer between solid and fluid has demonstrated to be a key factor to achieve a good performance on TES systems (Agrawal, Gautam et al. 2018). The performance of packed beds of rocks and sand was studied experimentally and numerically by (Mertens, Alobaid et al. 2014) and (Rodat, Bruch et al. 2015). They presented the influence of various design and operating conditions on TES performance such as air velocity and temperature. Air mass flow has been shown to enhance interphase heat transfer rates decreasing charging time (Abdel-Salam, Aly et al. 1991), while some suggested that air density would not directly affect said heat transfer (Barton 2013). It has also been stated that volumetric heat capacity would play a major role on overall system performance (Hänchen, Brückner et al. 2011). Regarding insulation, a thickness of about 16-20cm was found to be enough to retain low energy losses for intermediate temperatures (Zanganeh, Pedretti et al. 2015). Studies have also shown that for short-term (diurnal) cycles, a 95% overall thermal efficiency is achievable (Zanganeh, Pedretti et al. 2012). A study has also been performed to evaluate rock suitability for use on TES, regarding chemical, mechanical and thermo-physical properties and found that some rocks are not thermally stable (like foliated rocks) being unsuitable. Finally, it has been stated that there is no absolute optimum design to a rock bed TES system, meaning every unit needs to be planned directed towards the requirements for cost and performance of the specific application.

It is worthwhile to mention that most of the available experimental data are documented from laboratory-scale models. Few studies investigate fluid flow and heat transfer in large-size packed rock beds as the ones with potential for implementation in mining applications. Only recently, uses like heating/cooling of mine intake air or ventilation of block-caved mines have received significant attention (Ghoreishi-Madiseh, Sasmito et al. 2017, Amiri, Ghoreishi-Madiseh et al. 2018). In such systems the pressure drop across the rock bed is extremely important as it requires additional fan power to circulate the air, leading to significantly high costs that could affect the viability of the system.

Even though several studies have modelled heat transfer and fluid flow in a packed bed of rocks, most of them present restrictions including reduction of one or more dimension, simplification from interphase energy balance (obtained by the Local Thermal Non-Equilibrium method, or LTNE) to a less realistic Local Thermal Equilibrium (LTE), or even neglection of pressure drops. The current study considers a hot inlet air (120 ℃) for charging the TES system that is captured from the exhaust stream of a power plant. The novel concept proposed here is the use of large rocks (possibly waste rock from mining operations) as storage medium while using hot exhaust gases as the heat source of the TES. The latter containing energy commonly discarded to the ambient air on establishments employing diesel based power plants, as the ones present on remote communities in Canada (Ghoreishi-Madiseh, Safari et al. 2019). The main goal of this research is to investigate the characteristics of waste heat storage by means of packed rock beds for space heating purposes in cold-climate remote communities. Such task is achieved employing a three-dimensional, transient model, based on the LTNE approach. By which fluid flow and heat transfer inside the packed rock bed TES system are investigated in depth with a computational fluid dynamics (CFD) analysis. The impact of several parameters on the performance of the large-sized,

rock bed waste heat storage for remote communities is evaluated for distinct system dimensions, i.e., aspect ratios (AR). Which to the best knowledge of the authors has not been performed before.

### 7.2. Model description

The thermal storage system proposed here is based on a conical geometry with a truncated top. Such shape is chosen as it facilitates construction, achieved through piling by trucks of the rock selected, respecting a maximum angle of repose. Thus, this system has been referred to as a rock-pile TES (Ghoreishi-Madiseh, Safari et al. 2018) and is represented in Figure 7.1. Note that the directions of the flow and fluid inlet are inverted for charging (top to bottom) and discharging (bottom to top) to take advantage of the stratification of temperature within the HTF as previously pointed in literature (Arias, McMahan et al. 2008).

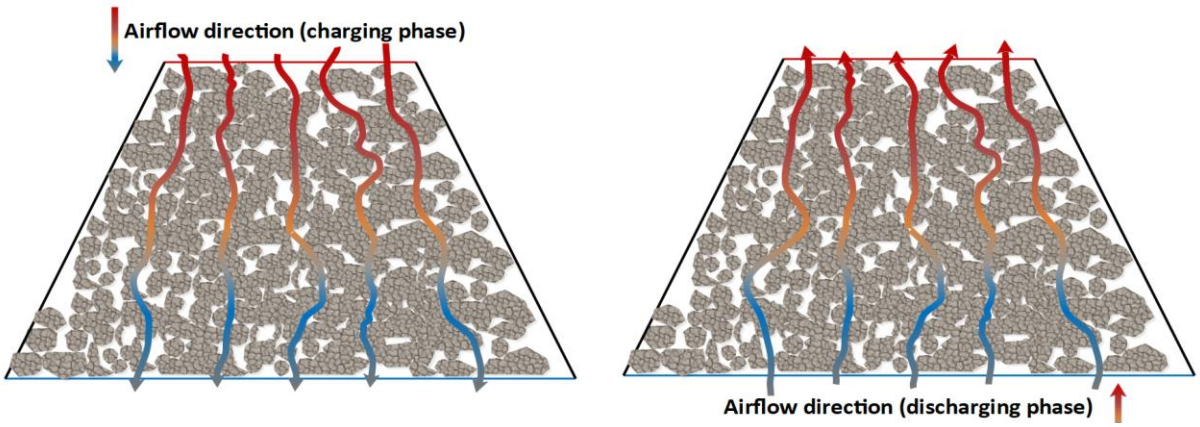


(a) (b)

Figure 7.1. Packed-bed with air and rocks in (a) charging and (b) discharging modes

When fluid flows through the packed bed, several heat transfer mechanisms will be present. To fully understand the operation of the proposed system, it is important to be aware of all the heat transfer mechanisms involved which are indicated in Figure 7.2. One of the main advantages of this technology is the fact that a high heat transfer rate can be achieved during operation due to the

large total interphase heat transfer area. While in non-operating periods, with the absence of flow the heat conduction and consequently dispersion and heat losses can be maintained at lower levels than other similar TES technologies. It worth noting that here the solid phase is assumed to have constant thermo-physical properties along the bed.

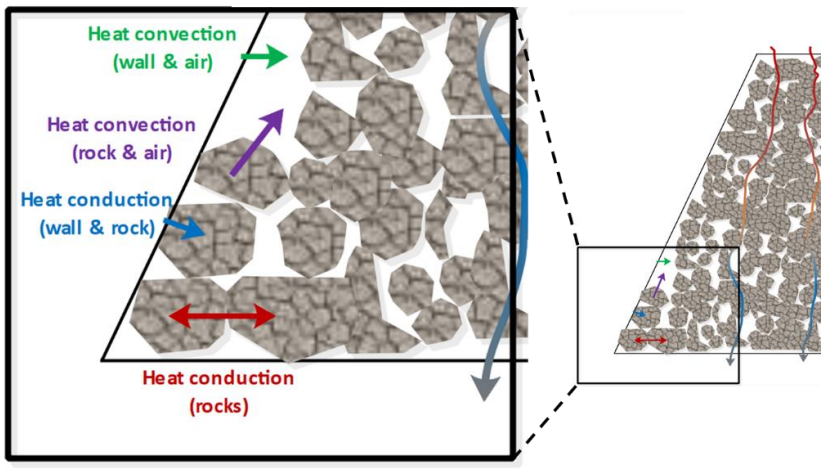


Figure 7.2. Various heat transfer mechanisms happening in a rock bed thermal energy storage system

In this study, the volume-averaging method is used to develop a volume-averaged model (VAM). Such model allows the investigation of the mass and heat transfer through a packed bed, with low computational cost and time, by considering the macroscale fluid flow behavior in the porous media. Empirical correlations are used to estimate the viscous and inertial resistance coefficients as inputs to the VAM. A representative elementary volume (REV) of the porous structure is shown in Figure 7.3. It should be noted that for the volume-averaging method to be suitable, the relations $l \geq 5d$ and $l \ll L$ should be satisfied (Whitaker 1986, Nield and Bejan 2006); where $d$ is an average pore diameter, $L$ and $l$ are the characteristic length of flow domain and of the REV, respectively.

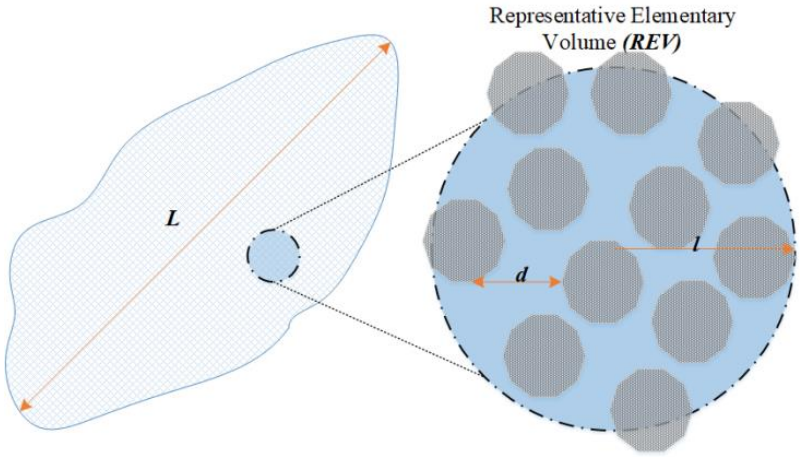


Figure 7.3. A porous media representative elementary volume (REV).

The 3D computational VAM is created in *ANSYS* Design Modeler and then meshed and solved by *ANSYS Fluent 17.2*. The presented numerical model is solved with a Semi-Implicit Method for Pressure-Linked Equation (SIMPLE). Basically, two different methods can be used in terms of the energy conservation equation in a porous media: A Local Thermal Equilibrium (LTE) approach and a Local Thermal non-Equilibrium (LTNE) approach. When the thermal properties of the fluid and the solid are not the close and the flow conditions through the system are highly transient, the latter model should be used. In said method, since the variation of the local rate of temperature for fluid and solid are different, two separate energy equations are then solved. Hence, the heat transfer phenomena for both fluid and solid phases can be examined in the proposed thermal energy storage system. Accordingly, the following mass, momentum, and energy conservation equations (respectively) were then solved by the finite-volume analysis under LTNE conditions.

$$\nabla \cdot \mathbf{u} = 0 \tag{7.1}$$

$$\rho(\mathbf{u} \cdot \nabla \mathbf{u}) = -\nabla p + \nabla \cdot \left(\mu\left[\left(\nabla \mathbf{u} + \nabla \mathbf{u}^{\mathrm{T}}\right)\right]\right) + \rho g - \alpha\mu\mathbf{u} - \beta\rho\mathbf{u}^2 \tag{7.2}$$

$$\frac{\partial(\varepsilon\rho c_p T)_f}{\partial t} + \nabla \cdot (\rho c_p \mathbf{u} T)_f = \nabla \cdot (\varepsilon k \nabla T)_f + h_{fs} A_{fs}(T_s - T_f) \tag{7.3}$$

$$\frac{\partial((1-\varepsilon)\rho c_p T)_s}{\partial t} = \nabla \cdot ((1-\varepsilon)k\nabla T)_s + h_{fs}A_{fs}(T_f - T_s) \quad (7.4)$$

Where $\alpha$ and $\beta$ are the viscous and inertial resistance coefficient as given by Eq.7.5 and Eq.7.6, respectively. Note that α represents the inverse of the permeability of the medium (K) In the current study, the well-known Ergun correlation (Ergun and Orning 1949) is used to estimate α and β, for different porous structures with a range of porosities ($\varepsilon$) from 0.2 to 0.5 and a particle size ($d$). It should be mentioned that comprehensive numerical and experimental studies must be conducted to obtain these values, and only then should the validity of the Ergun correlation be assessed for each specific packed bed.

$$\alpha = \frac{150 \times (1-\varepsilon)^2}{d^2 \times \varepsilon^3} \quad (7.5)$$

$$\beta = \frac{1.75 \times (1-\varepsilon)}{d \times \varepsilon^3} \quad (7.6)$$

Therefore, within the context of TES, a 3D VAM is proposed to study the main outcomes of the system as pressure drop/fan power requirements, total energy storage, charging rate and temperature profiles of the bed as a function of thermodynamic and physical parameters for different geometries (i.e., aspect ratios).

### 7.2.1. Heat transfer coefficient (HTC) in the packed bed

As previously mentioned, in the thermal energy storage systems, the determination of the convective heat transfer coefficient (HTC) between fluid and solid is extremely important. Hence, it is fundamental to assume appropriate correlations to accurately estimate the performance of such systems. Here, the correlations used are as given by (Nield and Bejan 2006), which are presented in Eq.7.7 to Eq.7.9.

$$h = 6h^*(1-\varepsilon)/d_p \quad (7.7)$$

$$\frac{1}{h^*} = \frac{d_p}{Nu_{fs}k_f} + \frac{d_p}{10k_s} \tag{7.8}$$

$$Nu_{fs} = \frac{0.255}{\varepsilon} Pr^{1/3} Re^{2/3} \tag{7.9}$$

### 7.2.2. Geometry and aspect ratio

The design of TES systems is a trade-off between pressure and thermal losses, as well as constructional limitations. According to the literature, an optimum aspect ratio ($\gamma = H/D_{upper}$) of height ($H$) to upper diameter ($D_{upper}$) for a truncated cone TES system should be more than one (Esence, Bruch et al. 2017). However, it should be noted that the design of each specific system can be affected by different technical and economic limitations. Thus, three different geometries with aspect ratios ranging from 1.0 to 1.35 are created with an identical volume of 1830 $m^3$. The height ($H$) of the truncated cones are 10 m, 12 m, and 13.5 m as illustrated in Figure 7.4(a), Figure 7.4 (b) and Figure 7.4(c), respectively. The upper diameter in all geometries is 10 m and the lower diameter ($D_{lower}$) changes from 20 to 16 m.

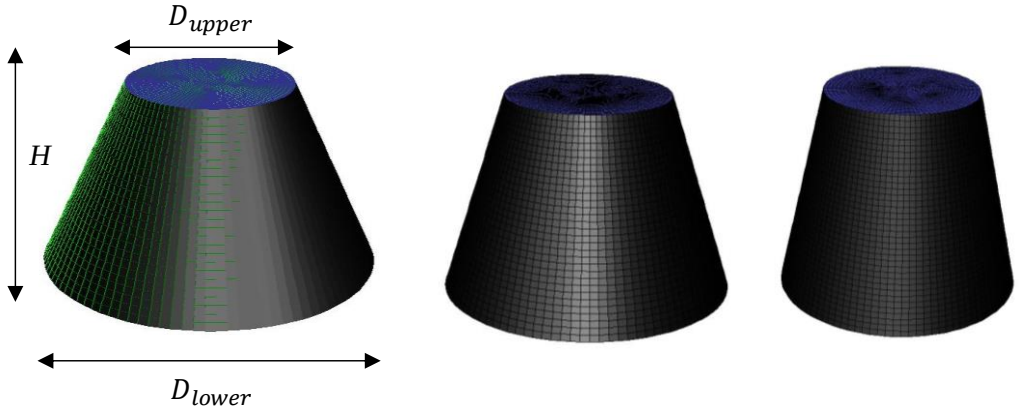


(a) (b) (c)

Figure 7.4. The developed packed bed geometries with different aspect ratios (γ): (a) 1.0, (b) 1.2, and (c) 1.35

### 7.2.3. Thermophysical properties

In this study, the rock thermophysical properties are considered constant, while the air thermophysical properties are defined as functions of temperature. Thermophysical properties of the storage medium in this study are summarized in Table 7.1.

Table 7.1. Thermophysical properties of the storage medium (Rock)

| **Property** | $\mathbf{c_{p,s}}$ | $\boldsymbol{\rho_s}$ | $\mathbf{k_s}$ | $\mathbf{d_p}$ |
|---|---|---|---|---|
| Value | 1000 (J/kg.K) | 3000 (kg/m$^3$) | 2.68 (W/m.K) | 0.8, 1.0 and 1.2 (m) |

As the proposed TES in this study aims to be charged with high-temperature exhaust air around 120 ℃ and discharged with ambient-temperature in winter around 7℃, it is crucial to correlate the air properties (i.e., density, thermal conductivity, and viscosity) with temperature. Several correlations have been proposed to calculate the air thermal properties as a function of temperature. In this study the following equations (Eq.7.10-7.12) were used, which are valid in a range of -73℃ – 200℃ (McQuillan, Culham et al. 1984).

$$\rho_f = \frac{351.99}{T} + \frac{344.84}{T^2} \tag{7.10}$$

$$\mu_f = \frac{1.4592T^{3/2}}{109.10 + T} \tag{7.11}$$

$$\mathrm{k}_f = \frac{2.3340 \times 10^{-3}\mathrm{T}^{3/2}}{164.54 \times \mathrm{T}} \tag{7.12}$$

Where $\rho_f$ is air density (kg/m³), $\mu_f$ is air viscosity ($10^{-6}$N.s/m²), $\mathrm{k}_f$ is air thermal conductivity (W/m.K), and T is the air temperature (Kelvin). Thus, User-defined functions (UDF) written in C language were used to account for the air thermal properties as a function of temperature.

### 7.2.4. Boundary conditions

In the current study, the transient fluid flow between the air and the solid parts is taken into consideration. In the charging phase, velocity inlet and pressure outlet boundary conditions were applied at the top and bottom of the system, respectively. Meanwhile, during discharging phase the boundaries were inverted and the ambient air (i.e., cold air) was injected from the bottom of the TES system. During the storage and extraction phases, buoyancy effects may occur due to the presence of hot and cold air in the packed bed. In order to take advantage of buoyancy in this study, hot inlet air at a constant temperature of 120 ℃ is injected through the top of the packed bed, while the system is fed from the bottom by cold air during the discharging phase. Additionally, there is a no-slip condition with no heat flux (insulated) boundary condition at the side walls.

### 7.2.5. Mesh independency test

To ensure mesh independent results, meshes with three different refinement levels were developed containing $8.5 \times 10^4$, $1.54 \times 10^5$and $2.86 \times 10^5$ elements respectively. The mesh containing about $1.54 \times 10^5$ elements resulted in a 2% deviation in terms of pressure drop and outlet temperature compared to the mesh with around $2.86 \times 10^5$ elements. The deviation in results was found to be about 9% between the coarsest mesh (containing $8.5 \times 10^4$ elements) and the finest one ($2.86 \times 10^5$ elements). Thus, the intermediate mesh consisting of around $1.54 \times 10^5$elements was chosen for all the further numerical investigations.

## 7.3. Results and discussion

### 7.3.1. Model validation

An essential step on the use of a heat transfer and fluid flow model on the prediction of real case system performance is the validation of its results against outcomes of an experimental system. It

is essential to prove that the proposed model is able to capture the real phenomena experienced by the porous media domain while used as TES. Here, the pilot-test data presented by (Hänchen, Brückner et al. 2011) is used for experimental validation. Dimensions are rescaled, and the boundary conditions are readjusted to conform with the heat storage system proposed there. Hence, the model is run considering both the LTE and LTNE approaches. This is performed seeking the best match for the numerical model and the experimental results. The results are shown in Figure 7.5(a) for temperature distribution within the rock bed at different points in time, allowing for the validation of heat transfer. While Figure 7.5(b) depicts a comparison of pressure drop development across the bed with time, allowing validation of fluid flow. Both temperature and pressure can be seen to agree well with the experimental results. It is important to note that although LTE and LTNE results are very similar for pressure drop, they are significantly different for temperature distribution across the bed, with LTNE being closer to the experimental ones. This is particularly true as temperatures develop with time. For that reason, the LTNE method, despite being more computationally intensive, is chosen for all the following simulations presented in this study.

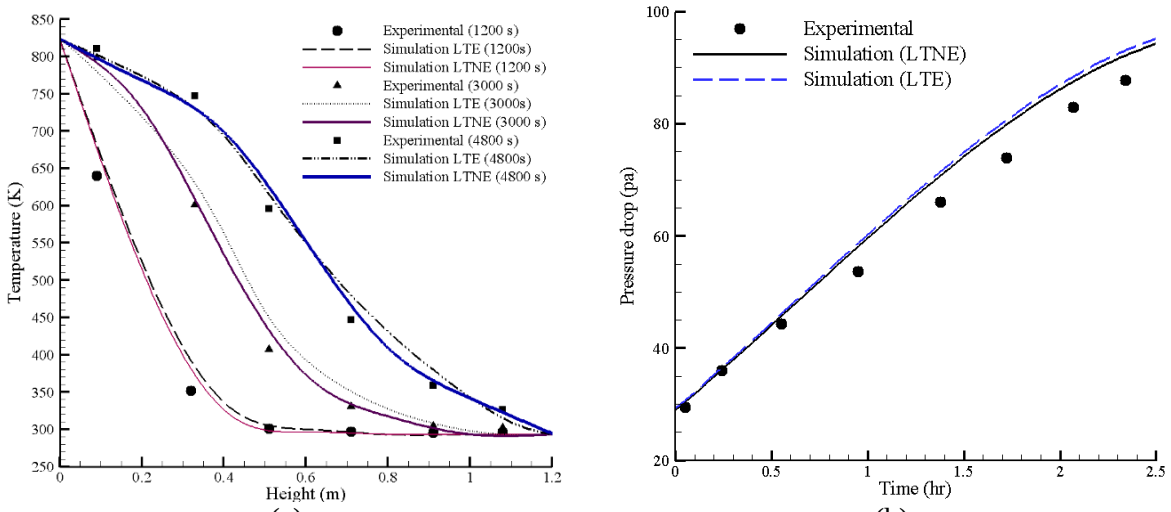


(a) (b)

Figure 7.5. Validation of the proposed model for both LTE and LTNE approaches against experimental results from (Hänchen, Brückner et al. 2011): a) Comparison of temperature along the vertical axis; b) comparison of pressure drop along the rock bed

### 7.3.2. Parametric analysis

- **Aspect ratios (rock bed shape)**

Dimensions of the packed rock bed are expected to have an influence on the fluid flow behaviour and velocity profiles inside the porous domain, consequently affecting the heat transfer ratio and thermal energy storage capacity of the rock bed. Due to that, the distinct geometries previously presented are used throughout the study to show the impact of several parameters in the fluid flow and heat transfer of rock beds of different dimensions. The velocity profiles within the TES system during the storage phase for all the geometries are illustrated in Figure 7.6 for an inlet velocity of 0.05m/s, a porosity of 0.2 and an average particle size of 1.0m (here considered the base case). It can be seen that outlet air velocity is the lowest in the geometry with the lowest aspect ratio as it has larger outlet area. It should be noted that increasing the Reynolds number results in an increase in both energy efficiency and the exploitation rate during the storage and extraction phase by increasing the mass flow rate (Bruch, Molina et al. 2017). Given that increasing air velocity through the system decreases the residence time of the hot HTF inside the bed, consequently

reducing the opportunity for heat exchange. Then it is important noting that in order to improve heat exchange rate within the system an optimum fluid velocity should be found for each application.

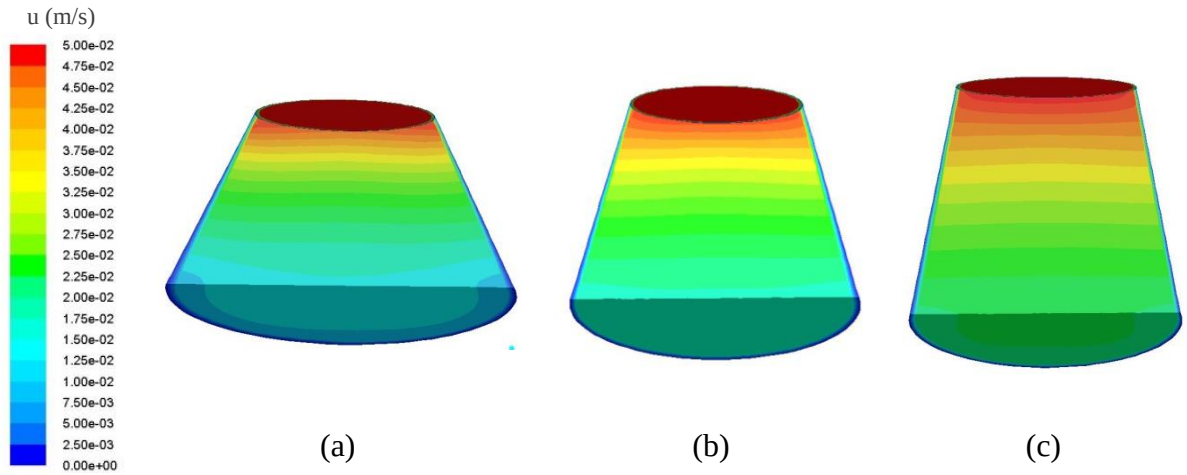


Figure 7.6. Velocity contour for a constant air velocity inlet of 0.05 m/s and porosity of 0.2 for geometries with different aspect ratios (γ): (a) 1.0, (b) 1.2, and (c) 1.35

- **Effect of porosity, particle size and fluid velocity**

Simulations were performed with distinct porosities, particle diameter and velocities for all the aspect ratios. The air velocity at the inlet is varied between 0.01 m/s and 0.07 m/s. While the porosity is changed from 0.2 to 0.5. The outlet temperature is plotted along with the time for different aspect ratios and porosities in both charging, shown in Figure 7.7(a), (b) and (c), and discharging, depicted in Figure 7.7(d), (e) and (f) cycles. An increase in the outlet air temperature during the charging phase continued until the outlet temperature approached the constant inlet air temperature of 120 ℃ (i.e., the difference between the inlet and outlet air temperatures shrank to less than 1 ℃). The outlet temperature increases remarkably fast for higher fluid velocities (and consequently larger mass flow), becoming practically independent from the porosity of the bed and the aspect ratio. The same can be said for the discharging cycle where the drop in outlet temperature is equally fast.

These results can then be used to obtain the energy stored in the bed. It is found that the TES systems with porosities of 0.2, 0.35, and 0.5 have the capacity of storing energy up to 540, 450, and 350 GJ, respectively. This stored heat can be extracted during cold seasons, when demand is high, for several heating purposes. As displayed in Figure 7.8, the increase in porosity within the packed bed leads to a significant decrease in the total heat stored in the rock which is expected due to the decrease in volume of heat storage media. On the other hand, aspect ratio and rock particle size are not seen to have significant effect in the stored/extracted capacity, reason why Figure 7.8 only shows results for one case of each. It was also found that while the total thermal energy storage capacity of the system slightly increases for higher mass flow rates, lower velocities can provide a longer charging/discharging period for the TES system. Finally, it can be concluded that the total thermal energy stored in the rock bed is almost identical for different geometric aspect ratios and Reynolds numbers, being almost completely dependent of storage material volume.

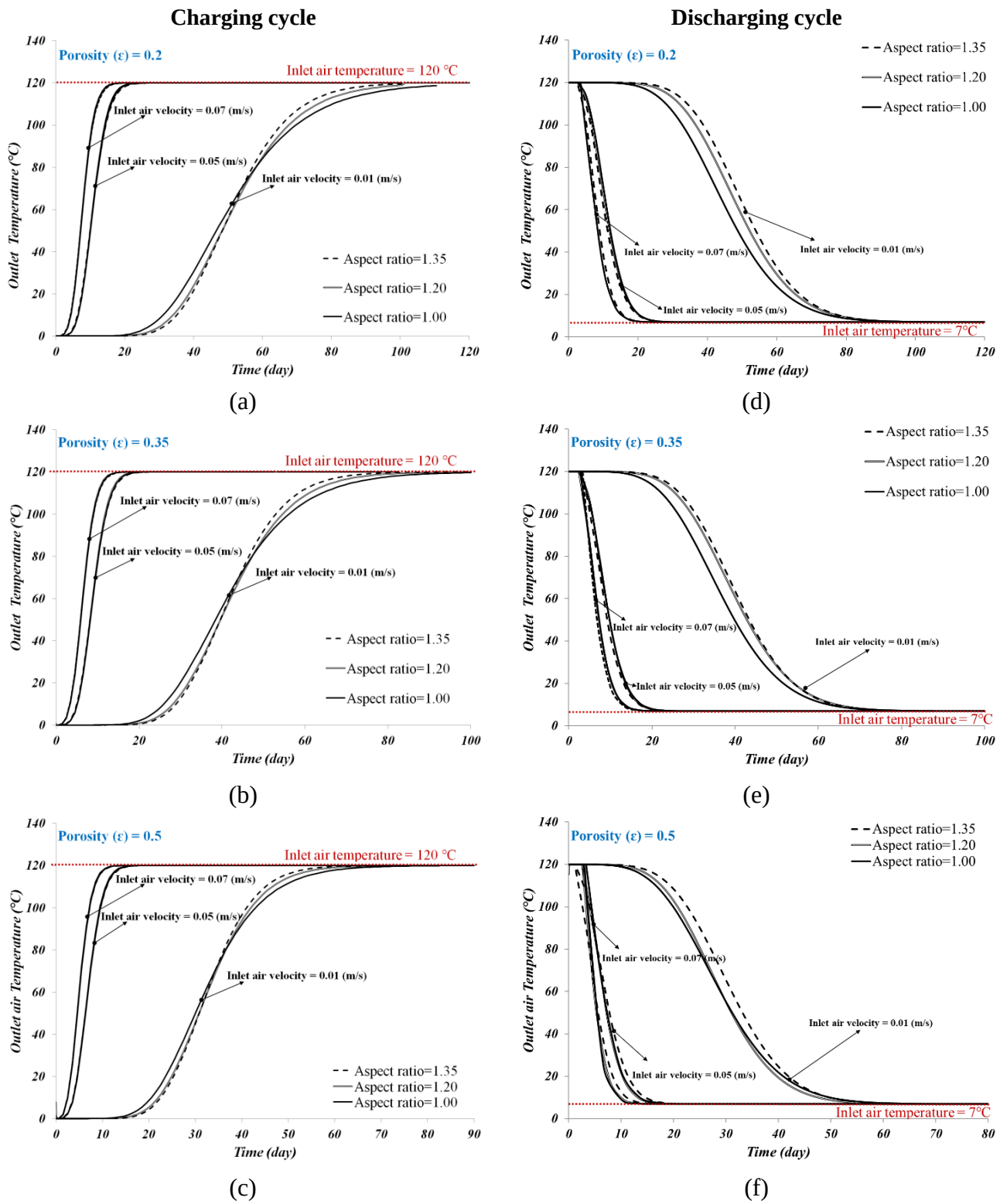


Figure 7.7. Simulated outlet air temperature (°C) in Charging mode (left column) and Discharging (right column) versus time for different aspect ratios and porosities: (a) and (d) ε = 0.2; (b) and (e) ε = 0.35; and (c) and (f) ε = 0.5

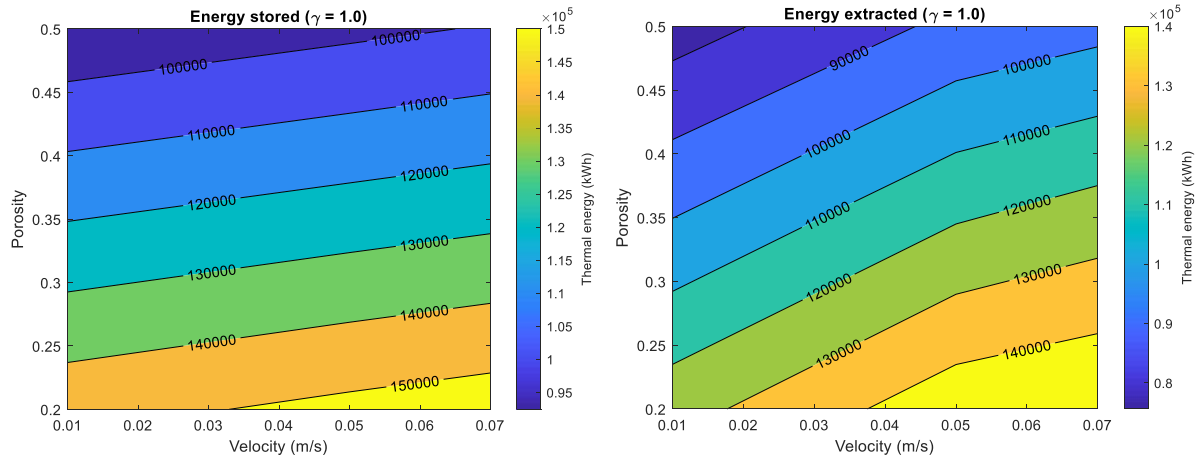


(a) (b)

Figure 7.8. Contours of energy stored (a) and energy extracted (b) from the VAM simulation for AR = 1.0 and dp = 1.0m

To evaluate the impact of these parameters on the pressure drop through the bed, a range of Reynolds numbers from 100 to 750 were applied and the pressure loss inside the packed bed was calculated numerically. The results can be seen in Figure 7.9 that show the development of pressure gradient across the bed with Reynolds number. In addition, Figure 7.10 shows contours for maximum pressure gradient across the system against aspect ratio and inlet velocity for a constant particle size of 1.0m. Figure 7.9 shows that even though pressure drop increases with velocity for all scenarios, the growth is very subtle for higher porosities, being even an order of magnitude lower than that for a low porosity (and consequently low permeability). The same happens for the slight increase in pressure difference seen in larger aspect ratios, which only becomes significant at lower porosities. Perhaps this effect can be more clearly identified in Figure 7.10 as it shows the maximum pressure gradient contours growing rapidly with velocity as opposed to γ but being considerably low except for the lowest porosity. This implies that the pressure drop is significantly more affected by the permeabiliy of the system (consequence of porosity and particle size) than the aspect ratio of the geometry. It should also be noted that a higher fluid velocity results in a

higher pressure drop through the system. Meaning more power will be necessary from the fans for two aspects, to provide a higher mass flow rate and to overcome the higher pressure drop that comes with it.

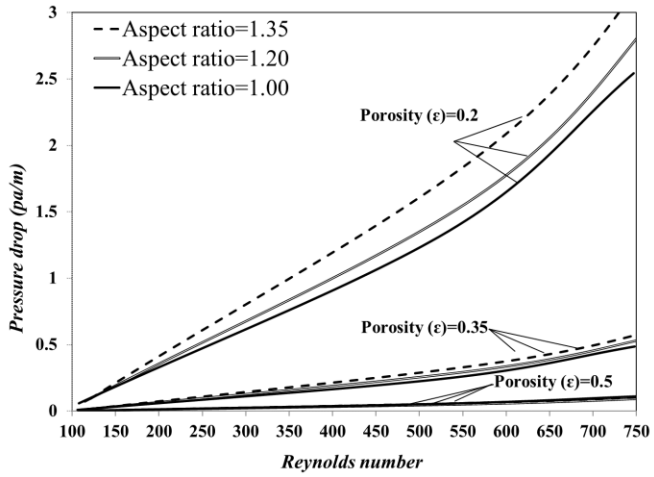


(a) $d_p = 0.8m$

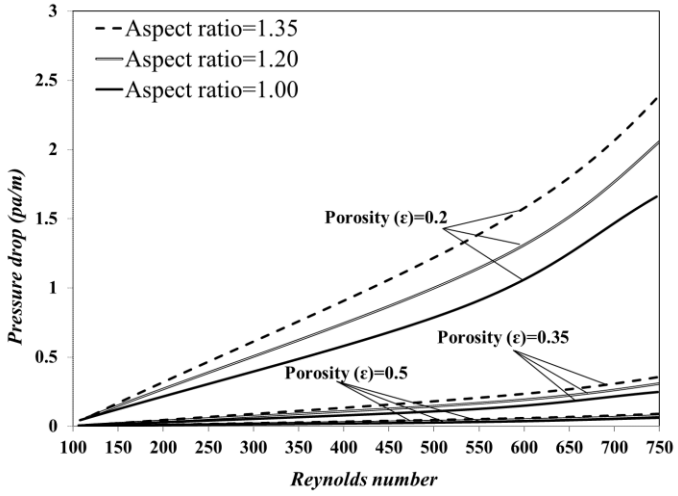


(b) $d_p = 1.0m$

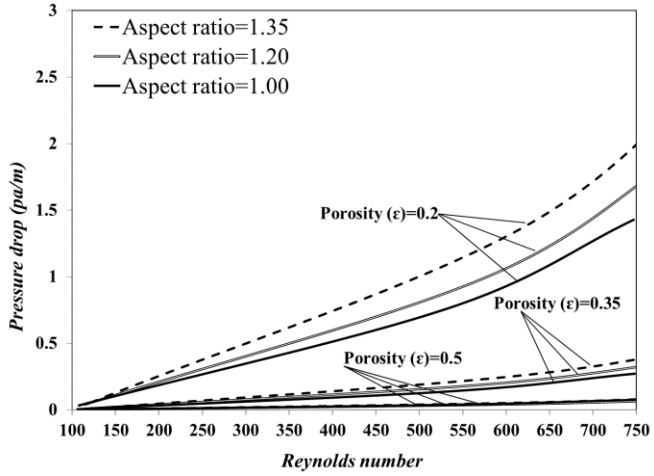


(c) $d_p = 1.2m$

Figure 7.9. Pressure gradient ($\Delta p/L$) versus Reynolds number (Re) from the volume-averaged model (VAM) for different porosities and aspect ratios with (a) particle diameter 0.8m, (b) 1.0m, and (c) 1.2m

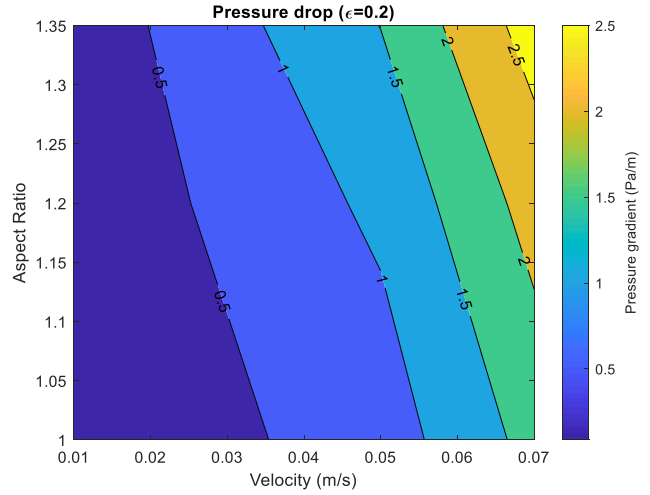


(a) ε = *0.2*

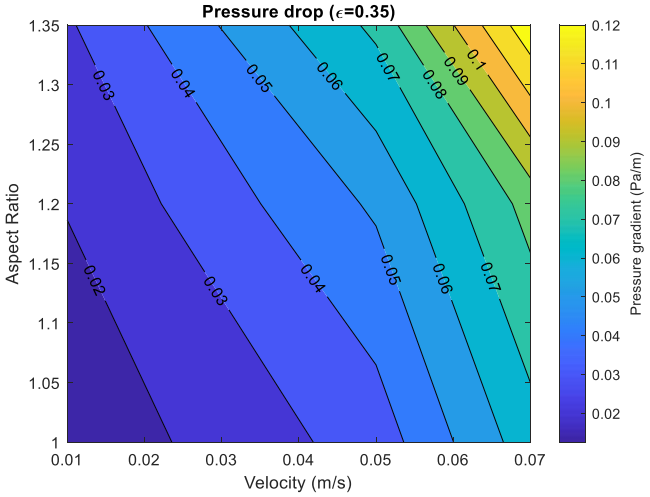


(b) ε = *0.35*

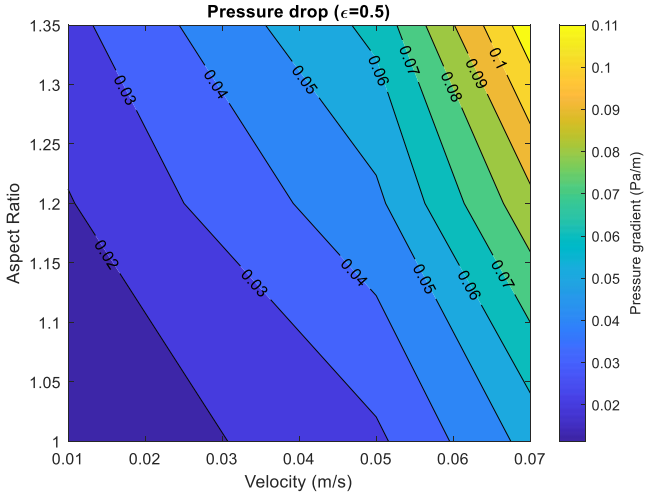


(c) ε = *0.5*

Figure 7.10. Pressure gradient ($\Delta p/L$) versus Aspect ratio and inlet velocity from the volume-averaged model (VAM) for different porosities: (a) ε = 0.2, (b) ε = 0.35, and (c) ε = 0.5

- **Effect of rock thermophysical properties**

Bearing in mind that for a constant volume of rock, the TES capacity of the packed bed could be enhanced by its natural ability to store heat (i.e., ρ and cp) different rock types were investigated. Five types of rock are selected and their thermophysical properties are taken from literature (Tiskatine, Aharoune et al. 2017) and given in Table 7.2. The results for outlet fluid temperature during the charging cycle can be seen in Figure 7.11. It is noticeable that the highest impacting factor is the thermal capacity of the rock (the product of density and specific heat). As shown, sandstone (lowest thermal capacity) quickly achieves its maximum temperature while Gabbro (highest thermal capacity) takes the longest time to be fully charged. This can also be noticed from the similarity between the Quartzite and the Granite temperature profiles, even with very distinct values for k. The thermal conductivity has a subtle effect on the charging rate, being slightly more accentuated for smaller aspect ratios. Except from that, the aspect ratio has a small impact on charging rate, mainly caused by the higher velocities of fluid within the bed (as previously mentioned in section 3.2.1). However, its effect on the total energy storage is virtually null, as shown in Figure 7.12.

Table 7.2. Properties of the distinct rock types analysed, taken from 37

| **Rock Type** | **Density** $(kg/m^3)$ | **Thermal conductivity** $(W/m.K)$ | **Specific heat** $(j/kg\ K)$ | **Thermal capacity** $(kJ/m^3.K)$ |
|---|---|---|---|---|
| Quartzite | 2600 | 5.0 | 830 | 2158 |
| Granite | 2600 | 2.8 | 820 | 2132 |
| Sandstone | 2400 | 2.3 | 775 | 1860 |
| Limestone | 2700 | 2.2 | 880 | 2376 |
| Gabbro | 2900 | 2.2 | 980 | 2842 |

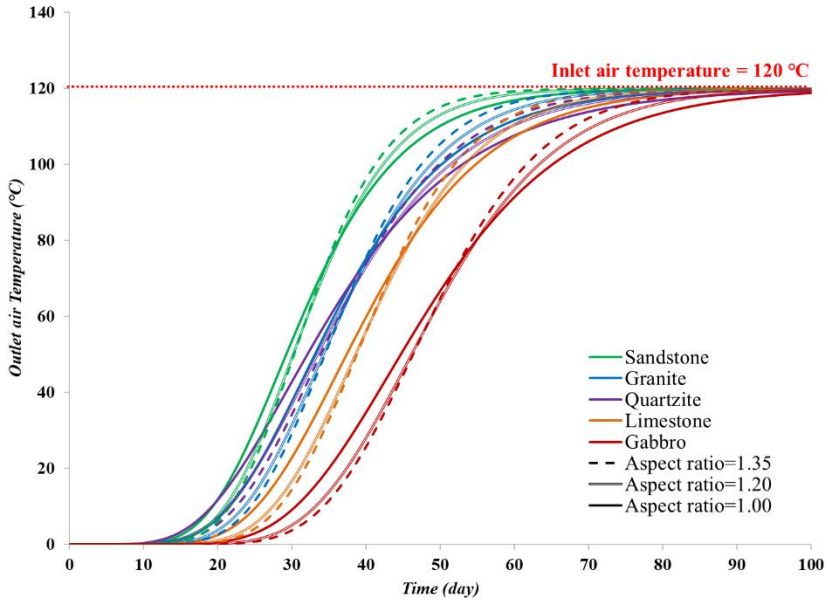


Figure 7.11. Simulated outlet temperature in charging phase for distinct rock types

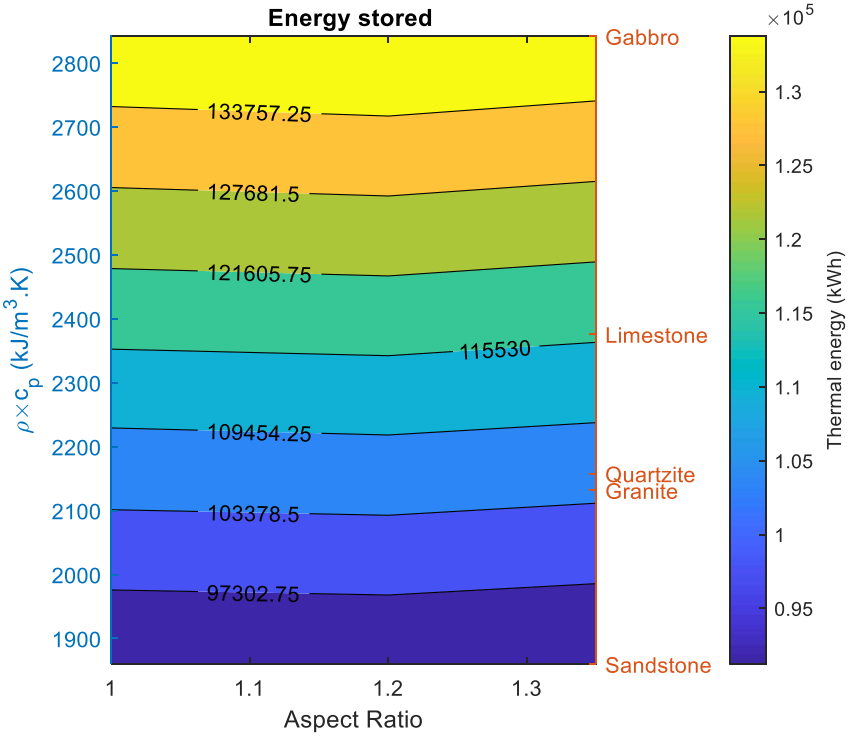


Figure 7.12. Total energy stored versus thermal capacity of the rocks simulated, and aspect ratio

- **Carbon emission reduction**

To further demonstrate the benefits of the system, the carbon footprint reduction introduced by its use is evaluated using emissions data from literature (ASHRAE 1993, Stritih, Zavrl et al. 2019). Assuming the system substitutes natural gas as a heating source, which has carbon emissions of approximately 510 tons of CO2,eq per GWh, the total amount of carbon footprint reduction is estimated. It is found that for the base properties the proposed TES (with a volume of 1,830m³ corresponding to 5,490 tonnes of rock) would be able to reduce emissions in about 156 tonnes of CO2,eq per year, for all the aspect ratios. This is equivalent to 85 tonnes of CO2,eq/m³ of rock per year or 28 tonnes of CO2,eq/tonne of rock per year. It should be noted that the carbon footprint reduction can be even larger if the heating is provided by burning oil (~730 tons of CO2,eq per GWh) or coal (~905 tons of CO2,eq per GWh) which are shown in detail in Table 7.3.

Table 7.3. Estimated carbon footprint reduction for heating using the proposed system (base properties)

| Unit | Natural gas | Oil | Coal |
|---|---|---|---|
| **Tonnes $CO_{2,eq}$/year** | 156 | 223 | 276 |
| **Tonnes $CO_{2,eq}$/($m^3$.year)** | 85 | 122 | 151 |
| **Tonnes $CO_{2,eq}$/(Tonne rock.year)** | 28 | 41 | 50 |

## 7.4. Conclusion

A transient 3D model was developed to analyse fluid flow and heat transfer in truncated cone TES packed rock beds. A considerable number of simulations was performed to account for the impact of all the distinct parameters (aspect ratio, HTF velocity, bed porosity, particle size and thermo-physical properties) and their combination in performance of the system. It is illustrated that packed bed properties, like porosity, play a crucial role in the performance of the TES system,

regarding both charging rate, energy stored/extracted, and pressure drop. The aspect ratio however, here evaluated in a series of combinations with other parameters, is shown not to have a significant effect in anything but the total pressure gradients across the system. Pressure drop through the porous media is also investigated by varying the HTF velocity. It is indicated that the pressure drop can be significantly raised by an increase in Reynolds number or a decrease in porosity. Particle size is also analysed and does not appear to significantly influence the heat transfer, having effect mostly on permeability and, as a result, on pressure drop. A few different rock types are investigated, and it is seen that the most important thermo-physical parameter for a rock bed in terms of heat storage is the thermal capacity. Some estimations of the environmental benefits of the system are also made showing that it could lead to a carbon footprint reduction (from heating systems) around 85-150 tonnes of CO2,eq per cubic meter of rock per year.

These results offer useful information for the design and evaluation of the performance of packed rock beds with large rocks and in caved zones. The proper range of packed bed properties could lead to considerable energy savings for establishments in remote, cold areas, both commercial (as mining operations) and non-commercial (as first nation dwellings) in applications such as heating for communal areas, domestic hot water provision or even mine ventilation.

### 7.5. References

Abdel-Salam, M., S. Aly, A. El-Sharkawy and Z. Abdel-Rehim (1991). "Thermal characteristics of packed bed storage system." International journal of energy research 15(1): 19-29.

Agrawal, P., A. Gautam, A. Kunwar, M. Kumar and S. Chamoli (2018). "Performance assessment of heat transfer and friction characteristics of a packed bed heat storage system embedded with internal grooved cylinders." Solar Energy 161: 148-158.

Amiri, L., S. A. Ghoreishi-Madiseh, A. P. Sasmito and F. P. Hassani (2017). "Evaluation of Heat Transfer Performance between Rock and Air in Seasonal Thermal Energy Storage Unit." Energy Procedia 142: 576-581.

Amiri, L., S. A. Ghoreishi-Madiseh, A. P. Sasmito and F. P. Hassani (2018). "Effect of buoyancy-driven natural convection in a rock-pit mine air preconditioning system acting as a large-scale thermal energy storage mass." Applied Energy 221: 268-279.

Arias, D. A., A. C. McMahan and S. A. Klein (2008). "Sensitivity of long-term performance simulations of solar energy systems to the degree of stratification in the thermal storage unit." International Journal of Energy Research 32(3): 242-254.

ASHRAE , H. F. S. (1993). "American Society of Heating, Refrigerating and Air Conditioning Engineers." Inc., Atlanta, GA.

Barton, N. (2013). "Simulations of air-blown thermal storage in a rock bed." Applied Thermal Engineering 55(1-2): 43-50.

Bruch, A., S. Molina, T. Esence, J. Fourmigué and R. Couturier (2017). "Experimental investigation of cycling behaviour of pilot-scale thermal oil packed-bed thermal storage system." Renewable energy 103: 277-285.

Cascetta, M., G. Cau, P. Puddu and F. Serra (2016). "A comparison between CFD simulation and experimental investigation of a packed-bed thermal energy storage system." Applied Thermal Engineering 98: 1263-1272.

Dahash, A., F. Ochs, M. B. Janetti and W. Streicher (2019). "Advances in seasonal thermal energy storage for solar district heating applications: A critical review on large-scale hot-water tank and pit thermal energy storage systems." Applied Energy 239: 296-315.

Dincer, I. (2002). "Thermal energy storage systems as a key technology in energy conservation." International journal of energy research 26(7): 567-588.

Dincer, I. and S. Dost (1996). "A perspective on thermal energy storage systems for solar energy applications." International Journal of Energy Research 20(6): 547-557.

Ergun, S. and A. A. Orning (1949). "Fluid flow through randomly packed columns and fluidized beds." Industrial & Engineering Chemistry 41(6): 1179-1184.

Esence, T., A. Bruch, S. Molina, B. Stutz and J.-F. Fourmigué (2017). "A review on experience feedback and numerical modeling of packed-bed thermal energy storage systems." Solar Energy 153: 628-654.

Galione, P., C. Pérez-Segarra, I. Rodríguez, S. Torras and J. Rigola (2015). "Numerical evaluation of multi-layered solid-PCM thermocline-like tanks as thermal energy storage systems for CSP applications." Energy Procedia 69: 832-841.

Ghoreishi-Madiseh, S. A., L. Amiri, A. P. Sasmito and F. P. Hassani (2017). "A Conjugate Natural Convection Model for Large Scale Seasonal Thermal Energy Storage Units: Application in Mine Ventilation." Energy Procedia 105(Supplement C): 4167-4172.

Ghoreishi-Madiseh, S. A., A. Fahrettin Kuyuk, M. A. Rodrigues de Brito, D. Baidya, Z. Torabigoodarzi and A. Safari (2019). "Application of Borehole Thermal Energy Storage in Waste Heat Recovery from Diesel Generators in Remote Cold Climate Locations." Energies 12(4): 656.

Ghoreishi-Madiseh, S. A., A. Safari, L. Amiri, D. Baidya, M. Antonio Rodrigues de Brito and A. Fahrettin Kuyuk (2018). "Investigation of viability of seasonal waste heat storage in rock piles for remote communities in cold climates." Energy Procedia.

Ghoreishi-Madiseh, S. A., A. Safari, L. Amiri, D. Baidya, M. A. R. de Brito and A. F. Kuyuk (2019). "Investigation of viability of seasonal waste heat storage in rock piles for remote communities in cold climates." Energy Procedia 159: 66-71.

Ghoreishi-Madiseh, S. A., A. P. Sasmito, F. P. Hassani and L. Amiri (2015). "Heat Transfer Analysis of Large Scale Seasonal Thermal Energy Storage for Underground Mine Ventilation." Energy Procedia 75: 2093-2098.

Ghoreishi-Madiseh, S. A., A. P. Sasmito, F. P. Hassani and L. Amiri (2017). "Performance evaluation of large scale rock-pit seasonal thermal energy storage for application in underground mine ventilation." Applied Energy 185: 1940-1947.

Hänchen, M., S. Brückner and A. Steinfeld (2011). "High-temperature thermal storage using a packed bed of rocks–heat transfer analysis and experimental validation." Applied Thermal Engineering 31(10): 1798-1806.

Krishan, O. and S. Suhag (2018). "An updated review of energy storage systems: Classification and applications in distributed generation power systems incorporating renewable energy resources." International Journal of Energy Research.

Kuravi, S., J. Trahan, Y. Goswami, C. Jotshi, E. Stefanakos and N. Goel (2013). "Investigation of a high-temperature packed-bed sensible heat thermal energy storage system with large-sized elements." Journal of Solar Energy Engineering 135(4): 041008.

McQuillan, F. J., J. R. Culham and M. M. Yovanovich (1984). Properties of dry air at one atmosphere (UW/MHTL 8406 G-01). Waterloo, Ontario, Microelectronics Heat Transfer Lab, University of Waterloo.

Mertens, N., F. Alobaid, L. Frigge and B. Epple (2014). "Dynamic simulation of integrated rock-bed thermocline storage for concentrated solar power." Solar Energy 110: 830-842.

Nield, D. A. and A. Bejan (2006). Convection in porous media, Springer.

Raftery, A., P. Shier and T. Obilade (1980). "Domestic space-heating and solar energy in Ireland." International Journal of Energy Research 4(1): 31-39.

Rodat, S., A. Bruch, N. Dupassieux and N. El Mourchid (2015). "Unique Fresnel demonstrator including ORC and thermocline direct thermal storage: operating experience." Energy Procedia 69: 1667-1675.

Sarbu, I. and A. Dorca (2019). "Review on heat transfer analysis in thermal energy storage using latent heat storage systems and phase change materials." International Journal of Energy Research 43(1): 29-64.

Schmidt, T., D. Mangold and H. Müller-Steinhagen (2004). "Central solar heating plants with seasonal storage in Germany." Solar energy 76(1-3): 165-174.

Singh, P. L., S. Deshpandey and P. Jena (2015). "Thermal performance of packed bed heat storage system for solar air heaters." Energy for sustainable Development 29: 112-117.

Sorgulu, F. and I. Dincer (2018). "Design and analysis of a solar tower power plant integrated with thermal energy storage system for cogeneration." International Journal of Energy Research.

Stritih, U., E. Zavrl and H. O. Paksoy (2019). "Energy Analysis and Carbon Saving Potential of a Complex Heating System with Solar Assisted Heat Pump and Phase Change Material (PCM) Thermal Storage in Different Climatic Conditions." European Journal of Sustainable Development Research 3(1): em0067.

Tian, Y. and C.-Y. Zhao (2013). "A review of solar collectors and thermal energy storage in solar thermal applications." Applied energy 104: 538-553.

Tiskatine, R., A. Aharoune, L. Bouirden and A. Ihlal (2017). "Identification of suitable storage materials for solar thermal power plant using selection methodology." Applied Thermal Engineering 117: 591-608.

Welsch, B., L. Göllner-Völker, D. O. Schulte, K. Bär, I. Sass and L. Schebek (2018). "Environmental and economic assessment of borehole thermal energy storage in district heating systems." Applied Energy 216: 73-90.

Whitaker, S. (1986). "Flow in porous media I: A theoretical derivation of Darcy's law." Transport in Porous Media 1(1): 3-25.

Zanganeh, G., A. Pedretti, A. Haselbacher and A. Steinfeld (2015). "Design of packed bed thermal energy storage systems for high-temperature industrial process heat." Applied Energy 137: 812-822.

Zanganeh, G., A. Pedretti, S. Zavattoni, M. Barbato and A. Steinfeld (2012). "Packed-bed thermal storage for concentrated solar power–Pilot-scale demonstration and industrial-scale design." Solar Energy 86(10): 3084-3098.

# CHAPTER 8

## 8. General Conclusions and Recommendations

### 8.1. Conclusions

This thesis discussed thermal energy storage systems for application in underground mine ventilation, as well as space heating in remote communities. The framework of this thesis comprised the development of a three-dimensional (3D) numerical model that evaluated the fluid flow and heat transfer behavior in packed beds of large particles.

A comprehensive literature review was conducted of thermal energy storage (TES) systems as a porous media, which summarized published methods to predict the pressure drop and heat transfer mechanisms in porous media. Published correlations were shown not to be valid to predict flow behavior in packed beds with larger particle sizes. An overview of the available renewable energy, as well as the energy demand in mine sites was provided. Finally, the history of using thermal energy storage in the mining industry summarized and the potential of using waste rock as a heat storage material discussed.

In the following chapters, flow through packed beds of spheres with large particle diameters (in the scale of metres) was characterized as a critical parameter for the design and operation TES systems in industrial settings, such as mining, geothermal, oil and gas, and construction industries. Therefore, it is essential to accurately predict the pressure gradient of air passing through a naturally generated packed bed in various industry applications. To the best of the author's knowledge, the first 3D pore-scale mathematical model of a flow through packed bed focused on large (in the scale of metres) particles is presented in this thesis. This model, which considered both uniform and non-uniform particle size distributions, was developed and validated against

experimental data. Then, it was used alongside Ergun and Forchheimer theories to simulate and develop permeability (Carman-Kozeny) and inertial resistance (Forchheimer) correlations that are valid for flow through packed bed of spheres with diameter from 0.04 to 1.2 m and porosity between 0.2 and 0.7. The proposed correlations were successfully used to predict flow characteristic in a volume-averaged computational fluid dynamics model with much lower computational cost compared to a pore-scale model. Permeability and inertial resistance were also presented as functions of porosity and particle size. The results can assist engineers to accurately estimate the pressure gradient in porous structures with a wide range of porosities and macro-scale particle sizes.

As a continuation of this study, the Atkinson equation, along with its friction factor, was investigated to estimate pressure requirements for mine ventilation. It should be noted that a friction factor correlation of flow through broken rock—typically found in blasted stope, gob, rock pit or block caving rock deposits—has not been published. Also, it is impractical to conduct direct measurements of flow resistance in an inaccessible broken rock zone. Thus, an important outcome of this study was the development of a new friction factor correlation of flow through broken rock that can be used directly in the Atkinson equation and that is valid for broken rock with diameters between 0.04 and 1.2 m and porosity ranging from 0.23 to 0.7.

In the Chapters 5, 6, and 7, two concepts of using thermal energy storage were studied.

1. Seasonal thermal energy storage (STES) system at Creighton mine in Ontario, Canada which offers natural cooling and heating for ventilating deeper mine levels
2. Using large rock to make a TES system coupled with the waste heat from diesel engine exhaust.

It was concluded that TES is a cost-effective strategy to enhance cooling and heating process efficiencies, thereby reducing associated costs.

For a first time, a full-scale conjugate heat transfer and fluid flow model was developed to better understand the performance of large-scale STES units for application in mine ventilation. Simulation results were compared and validated based on field measurement at ventilation trenches and ambient air temperature. Temperature gradients observed in the proposed storage system suggest the presence of natural convection effects driven by buoyancy. Effects of buoyancy forces on the fluid flow and heat exchange regimes inside the rock-pit were studied, resulting in comparison of forced versus natural convection heat transfer mechanisms. The model was also used to study the effects of number and position of ventilation trenches along with the fresh air flow rate. Increasing air flow rate and reducing the number of active trenches will improve energy savings. However, determining whether these changes lead to reductions in energy costs requires consideration of costs associated with fan power.

Other sections in this thesis focused on development of an unsteady 3D model to analyze fluid flow and heat transfer in truncated cone TES packed rock beds. Several simulations were performed to account for impacts of all the distinct parameters (aspect ratio, heat transfer fluid (HTF) velocity, bed porosity, particle size, and thermo-physical properties) and their combination in system performance. Packed bed properties like porosity played a crucial role in TES system performance in terms of charging rate, energy stored/extracted, and pressure drop. The aspect ratio, however, did not have a significant effect in anything but the total pressure gradients across the system.

Pressure drop through the porous media was also investigated by varying the HTF velocity. The pressure drop can be significantly increased by an increase in Reynolds number or a decrease in porosity. Particle size was also analyzed and did not appear to significantly influence the heat transfer, instead affecting permeability and as a result, pressure drop. A few rock types were investigated, which showed that the most important thermo-physical parameter for a rock bed in terms of heat storage is the thermal capacity. Some environmental benefits of the system were also estimated, showing that it could lead to a carbon footprint reduction (from heating systems) of approximately 85–150 tonnes of $CO_{2,eq}$ per cubic metre of rock per year.

### 8.2. Contributions to knowledge

This study presents informative tools to evaluate fluid flow and heat transfer behavior through a packed bed of large broken rocks. The outcome of this study has contributed to both scientific knowledge and particularly to TES systems in several ways. A few of the commendable contributions are as follows:

1. For the first time, fluid flow through a packed bed of large particles was comprehensively characterized to accurately predict the pressure gradient of air passing through a naturally generated packed bed in various industrial applications, such as mining, geothermal, oil and gas, and construction.
2. New constants for the Ergun and Forchheimer correlations were proposed, which can assist engineers to accurately estimate the pressure gradient in porous structures with a wide range of porosities and macro-scale particle sizes.
3. The results of this study can be used as a guideline to predict the permeability of packed bed of large spheres from low to high porosity as functions of porosity and particle size.

4. Study outcomes may also serve as a starting point to find an alternative solution for estimating the friction factor, which represents the fundamental contributions of fluid flow in porous media that govern the pressure gradient and its associated cost in mining, geothermal, oil and gas, and construction industries.
5. A conjugate heat transfer and fluid flow model was developed to better understand the performance of large-scale seasonal TES units for application in mine ventilation.
6. A novel concept was established which involved coupling a large-scale seasonal TES system with a diesel exhaust heat recovery system in remote communities in northern regions.
7. A comprehensive database was compiled to analyze fluid flow and heat transfer in large-scale TES packed rock beds.

### 8.3. General Recommendations

This study focused on the development of thermal energy storage systems to enhance the accuracy of prediction of fluid flow and heat transfer behaviour in packed bed of large particles. The following recommendations are offered for future research:

1- Developing a pilot-scale TES unit is recommended to examine effects of designing and operating factors.
2- A detailed investigation of particle shape and roughness and tortuosity factor in packed bed of particles could help to predict more accurate fluid flow and heat transfer mechanism in such a porous media.
3- Developing a pore-scale model of packed bed of large rocks to study the heat transfer between fluid and solid at pore scale level.

4- An investigation of the geometrical parameters such as size distribution models, and number of particles would be helpful to find the optimum point for both the flow and heat transfer performances of the TES systems.

## References


Abdel-Salam, M., S. Aly, A. El-Sharkawy and Z. Abdel-Rehim (1991). "Thermal characteristics of packed bed storage system." International journal of energy research **15**(1): 19-29.

Abdelaziz, E., R. Saidur and S. Mekhilef (2011). "A review on energy saving strategies in industrial sector." Renewable and sustainable energy reviews **15**(1): 150-168.

Abnay, B., A. Eddemani, A. Aharoune, A. Ihlal, L. Bouirden, R. Tiskatine and L. Gourdo (2016). "Experimental evaluation of thermo-mechanical performances of candidate rocks for use in high temperature thermal storage." Applied Energy **171**: 243-255.

Achenbach, E. (1995). "Heat and flow characteristics of packed beds." Experimental Thermal and Fluid Science **10**(1): 17-27.

Agalit, H., N. Zari, M. Maalmi and M. Maaroufi (2015). "Numerical investigations of high temperature packed bed TES systems used in hybrid solar tower power plants." Solar Energy **122**: 603-616.

Agrawal, P., A. Gautam, A. Kunwar, M. Kumar and S. Chamoli (2018). "Performance assessment of heat transfer and friction characteristics of a packed bed heat storage system embedded with internal grooved cylinders." Solar Energy **161**: 148-158.

Al-Sumaily, G. F., H. M. Hussen and M. C. Thompson (2014). "Validation of thermal equilibrium assumption in free convection flow over a cylinder embedded in a packed bed." International Communications in Heat and Mass Transfer **58**: 184-192.

Allen, K. G. (2014). Rock bed thermal storage for concentrating solar power plants, Stellenbosch: Stellenbosch University.

Allen, K. G., T. W. von Backström and D. G. Kröger (2013). "Packed bed pressure drop dependence on particle shape, size distribution, packing arrangement and roughness." Powder Technology **246**: 590-600.

Allen, K. G., T. W. von Backström and D. G. Kröger (2015). "Rock bed pressure drop and heat transfer: Simple design correlations." Solar Energy **115**: 525-536.

Alshammari, F., A. Pesyridis, A. Karvountzis-Kontakiotis, B. Franchetti and Y. Pesmazoglou (2018). "Experimental study of a small scale organic Rankine cycle waste heat recovery system for a heavy duty diesel engine with focus on the radial inflow turbine expander performance." Applied Energy **215**: 543-555.

Amini, Y., J. Karimi-Sabet and M. N. Esfahany (2016). "Experimental and numerical simulation of dry pressure drop in high-capacity structured packings." Chemical Engineering & Technology **39**(6): 1161-1170.

Amiri, L., S. A. Ghoreishi-Madiseh, F. P. Hassani and A. P. Sasmito (2019). "Estimating pressure loss and Ergun parameters in packed rock bed with large diameter in mining applications." Submitted - Powder Technology Journal.

Amiri, L., S. A. Ghoreishi-Madiseh, A. P. Sasmito and F. P. Hassani (2017). "Evaluation of Heat Transfer Performance between Rock and Air in Seasonal Thermal Energy Storage Unit." Energy Procedia **142**: 576-581.

Amiri, L., S. A. Ghoreishi-Madiseh, A. P. Sasmito and F. P. Hassani (2018). "Effect of buoyancy-driven natural convection in a rock-pit mine air preconditioning system acting as a large-scale thermal energy storage mass." Applied Energy **221**: 268-279.

Anbar, S., K. E. Thompson and M. Tyagi (2018). "The Impact of Compaction and Sand Migration on Permeability and Non-Darcy Coefficient from Pore-Scale Simulations." Transport in Porous Media: 1-21.

Anderson, R., S. Shiri, H. Bindra and J. F. Morris (2014). "Experimental results and modeling of energy storage and recovery in a packed bed of alumina particles." Applied Energy **119**: 521-529.

Andreozzi, A., B. Buonomo, O. Manca, P. Mesolella and S. Tamburrino (2012). Numerical investigation on sensible thermal energy storage with porous media for high temperature solar systems. Journal of Physics: Conference Series, IOP Publishing.

Antohe, B., J. Lage, D. Price and R. Weber (1997). "Experimental determination of permeability and inertia coefficients of mechanically compressed aluminum porous matrices." Journal of fluids engineering **119**(2): 404-412.

Arias, D. A., A. C. McMahan and S. A. Klein (2008). "Sensitivity of long-term performance simulations of solar energy systems to the degree of stratification in the thermal storage unit." International Journal of Energy Research **32**(3): 242-254.
ASHRAE , H. F. S. (1993). "American Society of Heating, Refrigerating and Air Conditioning Engineers." Inc., Atlanta, GA.
Avramenko, A. and A. Kuznetsov (2006). "Renormalization group model of large-scale turbulence in porous media." Transport in porous media **63**(1): 175-193.
Bader, R., A. Pedretti, M. Barbato and A. Steinfeld (2015). "An air-based corrugated cavity-receiver for solar parabolic trough concentrators." Applied energy **138**: 337-345.
Bağcı, Ö., N. Dukhan and M. Özdemir (2014). "Flow regimes in packed beds of spheres from pre-Darcy to turbulent." Transport in porous media **104**(3): 501-520.
Baghapour, B., M. Rouhani, A. Sharafian, S. B. Kalhori and M. Bahrami (2018). "A pressure drop study for packed bed adsorption thermal energy storage." Applied Thermal Engineering **138**: 731-739.
Baidya, D., M. A. R. de Brito, A. P. Sasmito, M. Scoble and S. A. Ghoreishi-Madiseh (2019). "Recovering waste heat from diesel generator exhaust; an opportunity for combined heat and power generation in remote Canadian mines." Journal of Cleaner Production **225**: 785-805.
Balhoff, M. T., K. E. Thompson and M. Hjortsø (2007). "Coupling pore-scale networks to continuum-scale models of porous media." Computers & Geosciences **33**(3): 393-410.
Bari, S. and S. N. Hossain (2013). "Waste heat recovery from a diesel engine using shell and tube heat exchanger." Applied Thermal Engineering **61**(2): 355-363.
Barton, N. (2013). "Simulations of air-blown thermal storage in a rock bed." Applied Thermal Engineering **55**(1-2): 43-50.
Barton, N. G. (2013). "Simulations of air-blown thermal storage in a rock bed." Applied Thermal Engineering **55**(1-2): 43-50.
Barzegar Gerdroodbary, M., O. Jahanian and M. Mokhtari (2015). "Influence of the angle of incident shock wave on mixing of transverse hydrogen micro-jets in supersonic crossflow." International Journal of Hydrogen Energy **40**(30): 9590-9601.
Bayón, R. and E. Rojas (2013). "Simulation of thermocline storage for solar thermal power plants: From dimensionless results to prototypes and real-size tanks." International Journal of Heat and Mass Transfer **60**: 713-721.
Bear, J. (2013). Dynamics of fluids in porous media, Courier Corporation.
Beavers, G. S. and E. M. Sparrow (1969). "Non-Darcy flow through fibrous porous media." Journal of Applied Mechanics **36**(4): 711-714.
Berrada, A., K. Loudiyi and I. Zorkani (2017). "System design and economic performance of gravity energy storage." Journal of Cleaner Production **156**(Supplement C): 317-326.
Bharathan, B., A. P. Sasmito and S. A. Ghoreishi-Madiseh (2017). "Analysis of energy consumption and carbon footprint from underground haulage with different power sources in typical Canadian mines." Journal of Cleaner Production **166**(Supplement C): 21-31.
Blunt, M. J. (2001). "Flow in porous media—pore-network models and multiphase flow." Current opinion in colloid & interface science **6**(3): 197-207.
Bracke, R. and G. Bussmann "Heat-Storage in Deep Hard Coal Mining Infrastructures."
Brauer, H. (1971). Grundlagen der Einphasen-und Mehrphasenströmungen, Sauerländer.
Brooks, M. R. and J. D. Frost (2012). "Providing freight services to remote arctic communities : Are there lessons for practitioners from services to Greenland and Canada's northeast?" Research in Transportation Business & Management **4**: 69-78.
Brown, D. W. (2000). A hot dry rock geothermal energy concept utilizing supercritical CO2 instead of water. Proceedings of the twenty-fifth workshop on geothermal reservoir engineering, Stanford University.
Bruch, A., S. Molina, T. Esence, J. Fourmigué and R. Couturier (2017). "Experimental investigation of cycling behaviour of pilot-scale thermal oil packed-bed thermal storage system." Renewable energy **103**: 277-285.

Bruch, A., S. Molina, T. Esence, J. F. Fourmigué and R. Couturier (2017). "Experimental investigation of cycling behaviour of pilot-scale thermal oil packed-bed thermal storage system." Renewable Energy **103**: 277-285.
Bu, X., W. Ma and H. Li (2012). "Geothermal energy production utilizing abandoned oil and gas wells." Renewable Energy **41**(0): 80-85.
Bufe, A. and G. Brenner (2018). "Systematic Study of the Pressure Drop in Confined Geometries with the Lattice Boltzmann Method." Transport in Porous Media **123**(2): 307-319.
Burdine, N. (1953). "Relative permeability calculations from pore size distribution data." Journal of Petroleum Technology **5**(3): 71-78.
Canada, G. o. (2018). "Historical Climate Data. Environ Nat Resour." from http://climate.weather.gc.ca/historical_data/search_historic_data_e.html (accessed December 10, 2018).
Canada, N. R. (2017). The Atlas of Canada - Remote communities Energy Database.
Carbonell, R. G. and S. Whitaker (1984). Heat and mass transfer in porous media. Fundamentals of transport phenomena in porous media, Springer**:** 121-198.
Cárdenas, B., T. R. Davenne, J. Wang, Y. Ding, Y. Jin, H. Chen, Y. Wu and S. D. Garvey (2019). "Techno-economic optimization of a packed-bed for utility-scale energy storage." Applied Thermal Engineering **153**: 206-220.
Carman, P. C. (1937). "Fluid flow through granular beds." Trans. Inst. Chem. Eng. **15**: 150-166.
Cascetta, M., G. Cau, P. Puddu and F. Serra (2016). "A comparison between CFD simulation and experimental investigation of a packed-bed thermal energy storage system." Applied Thermal Engineering **98**: 1263-1272.
Cengel, Y. (2014). Heat and mass transfer: fundamentals and applications, McGraw-Hill Higher Education.
Chapuis, S. and M. Bernier (2009). "Seasonal storage of solar energy in borehole heat exchangers." Eleventh International IBPSA Conference: 599-606.
Chatterjee, A., L. Zhang and X. Xia (2015). "Optimization of mine ventilation fan speeds according to ventilation on demand and time of use tariff." Applied Energy **146**: 65-73.
Chatterjee, A., L. Zhang and X. Xia (2015). "Optimization of mine ventilation fan speeds according to ventilation on demand and time of use tariff." Applied Energy **146**(Supplement C): 65-73.
Cheng, N.-S. (2011). "Wall effect on pressure drop in packed beds." Powder Technology **210**(3): 261-266.
Cheng, Z. D., Y. L. He and F. Q. Cui (2013). "Numerical investigations on coupled heat transfer and synthetical performance of a pressurized volumetric receiver with MCRT–FVM method." Applied Thermal Engineering **50**(1): 1044-1054.
Chikhi, N., O. Coindreau, L. Li, W. Ma, V. Taivassalo, E. Takasuo, S. Leininger, R. Kulenovic and E. Laurien (2014). "Evaluation of an effective diameter to study quenching and dry-out of complex debris bed." Annals of Nuclear Energy **74**: 24-41.
Choi, Y. S., S. J. Kim and D. Kim (2008). "A Semi-empirical Correlation for Pressure Drop in Packed Beds of Spherical Particles." Transport in Porous Media **75**(2): 133-149.
Cicéron, D., J. Comiti and R. P. Chhabra (2002). "Pressure drops for purely viscous non-newtonian fluid flow through beds packed with mixed-size spheres." Chemical Engineering Communications **189**(10): 1403-1414.
Colclough, S. and T. McGrath (2015). "Net energy analysis of a solar combi system with Seasonal Thermal Energy Store." Applied Energy **147**: 611-616.
Comiti, J. and M. Renaud (1989). "A new model for determining mean structure parameters of fixed beds from pressure drop measurements: application to beds packed with parallelepipedal particles." Chemical Engineering Science **44**(7): 1539-1545.
Coulaud, O., P. Morel and J. Caltagirone (1988). "Numerical modelling of nonlinear effects in laminar flow through a porous medium." Journal of Fluid Mechanics **190**: 393-407.
Da Cunha, J. P. and P. Eames (2016). "Thermal energy storage for low and medium temperature applications using phase change materials–a review." Applied Energy **177**: 227-238.

Dahash, A., F. Ochs, M. B. Janetti and W. Streicher (2019). "Advances in seasonal thermal energy storage for solar district heating applications: A critical review on large-scale hot-water tank and pit thermal energy storage systems." Applied Energy **239**: 296-315.
Das, S., N. G. Deen and J. A. M. Kuipers (2017). "A DNS study of flow and heat transfer through slender fixed-bed reactors randomly packed with spherical particles." Chemical Engineering Science **160**: 1-19.
Das, S., N. G. Deen and J. A. M. Kuipers (2018). "Multiscale modeling of fixed-bed reactors with porous (open-cell foam) non-spherical particles: Hydrodynamics." Chemical Engineering Journal **334**: 741-759.
Davenne, T. R. G., S. D. Garvey, B. Cardenas and J. P. Rouse (2018). "Stability of packed bed thermoclines." Journal of Energy Storage **19**: 192-200.
Davis, A. P. and E. E. Michaelides (2009). "Geothermal power production from abandoned oil wells." Energy **34**(7): 866-872.
DeGroot, C. T. and A. G. Straatman (2011). "Closure of non-equilibrium volume-averaged energy equations in high-conductivity porous media." International Journal of Heat and Mass Transfer **54**(23): 5039-5048.
Di Battista, D., M. Mauriello and R. Cipollone (2015). "Waste heat recovery of an ORC-based power unit in a turbocharged diesel engine propelling a light duty vehicle." Applied Energy **152**: 109-120.
Dincer, I. (2002). "Thermal energy storage systems as a key technology in energy conservation." International journal of energy research **26**(7): 567-588.
Dincer, I. and S. Dost (1996). "A perspective on thermal energy storage systems for solar energy applications." International Journal of Energy Research **20**(6): 547-557.
Dreißigacker, V., S. Zunft and H. Müller-Steinhagen (2013). "A thermo-mechanical model of packed-bed storage and experimental validation." Applied energy **111**: 1120-1125.
du Plessis, G. E., L. Liebenberg and E. H. Mathews (2013). "Case study: The effects of a variable flow energy saving strategy on a deep-mine cooling system." Applied Energy **102**(0): 700-709.
Du Plessis, J. P. (1994). "Analytical quantification of coefficients in the Ergun equation for fluid friction in a packed bed." Transport in porous media **16**(2): 189-207.
du Plessis, J. P. and S. Woudberg (2008). "Pore-scale derivation of the Ergun equation to enhance its adaptability and generalization." Chemical Engineering Science **63**(9): 2576-2586.
Du, S., M.-J. Li, Q. Ren, Q. Liang and Y.-L. He (2017). "Pore-scale numerical simulation of fully coupled heat transfer process in porous volumetric solar receiver." Energy **140**: 1267-1275.
Dudgeon, C. (1966). "An experimental study of the flow of water through coarse granular media." La Houille Blanche(7): 785-801.
Dukhan, N., Ö. Bağcı and M. Özdemir (2014). "Experimental flow in various porous media and reconciliation of Forchheimer and Ergun relations." Experimental Thermal and Fluid Science **57**: 425-433.
Dullien, F. (1975). "Single phase flow through porous media and pore structure." The Chemical Engineering Journal **10**(1): 1-34.
Dumont, E., S. Woudberg and J. Van Jaarsveld (2016). "Assessment of porosity and biofilm thickness in packed beds using porous media models." Powder Technology **303**: 76-89.
Dwivedi, P. N. and S. Upadhyay (1977). "Particle-fluid mass transfer in fixed and fluidized beds." Industrial & Engineering Chemistry Process Design and Development **16**(2): 157-165.
Dybbs, A. and R. V. Edwards (1984). A New Look at Porous Media Fluid Mechanics — Darcy to Turbulent. Fundamentals of Transport Phenomena in Porous Media. J. Bear and M. Y. Corapcioglu. Dordrecht, Springer Netherlands**:** 199-256.
Ednie, H. and F. Hassani (2007). "Extracting geothermal heat from mines." CIM MAGAZINE **2**(2): 18.
England, R. and D. Gunn (1970). "Dispersion, pressure drop, and chemical reaction in packed beds of cylindrical particles." Transactions of the institution of chemical engineers and the chemical engineer **48**(7-10): T265-&.
Envers, P. (1986). "Controlled air through efficient system at inco." Canadian Mining Journal **107**(7): 12-14.

Erdim, E., Ö. Akgiray and İ. Demir (2015). "A revisit of pressure drop-flow rate correlations for packed beds of spheres." Powder Technology **283**: 488-504.
Ergun, S. (1952). "Fluid flow through packed columns." Chem. Eng. Prog. **48**: 89-94.
Ergun, S. and A. A. Orning (1949). "Fluid flow through randomly packed columns and fluidized beds." Industrial & Engineering Chemistry **41**(6): 1179-1184.
Erlund, R. and R. Zevenhoven (2018). Hydration of Magnesium Carbonate in a Thermal Energy Storage Process and Its Heating Application Design. **11**.
Esence, T., A. Bruch, J.-F. Fourmigué and B. Stutz (2019). "A versatile one-dimensional numerical model for packed-bed heat storage systems." Renewable Energy **133**: 190-204.
Esence, T., A. Bruch, S. Molina, B. Stutz and J.-F. Fourmigué (2017). "A review on experience feedback and numerical modeling of packed-bed thermal energy storage systems." Solar Energy **153**: 628-654.
Fan, L. and J. M. Khodadadi (2011). "Thermal conductivity enhancement of phase change materials for thermal energy storage: a review." Renewable and sustainable energy reviews **15**(1): 24-46.
Fand, R., B. Kim, A. Lam and R. Phan (1987). "Resistance to the flow of fluids through simple and complex porous media whose matrices are composed of randomly packed spheres." Journal of fluids engineering **109**(3): 268-273.
Fava, L., Millar, D., Anderson, B., Schafrik, S., O'Connor, D., Allen, C., (2012 ). Modeling of the Natural Heat Exchange Area at Creighton Mine for Operational Decision Support. 14th US/North American Mine Ventilation Symposium.
Feng, J., H. Dong and H. Dong (2015). "Modification of Ergun's correlation in vertical tank for sinter waste heat recovery." Powder Technology **280**: 89-93.
Feng, J., S. Zhang, H. Dong and G. Pei (2019). "Frictional pressure drop characteristics of air flow through sinter bed layer in vertical tank." Powder Technology **344**: 177-182.
Fernández-Yañez, P., O. Armas, A. Capetillo and S. Martínez-Martínez (2018). "Thermal analysis of a thermoelectric generator for light-duty diesel engines." Applied Energy **226**: 690-702.
Feru, E., B. de Jager, F. Willems and M. Steinbuch (2014). "Two-phase plate-fin heat exchanger modeling for waste heat recovery systems in diesel engines." Applied Energy **133**: 183-196.
Fisch, M. N., M. Guigas and J. O. Dalenbäck (1998). "A review of large-scale solar heating systems in Europe." Solar energy **63**(6): 355-366.
Florides, G. and S. Kalogirou (2007). "Ground heat exchangers—A review of systems, models and applications." Renewable Energy **32**(15): 2461-2478.
Forsberg, C. W. (2012). "Gigawat-year geothermal energy storage coupled to nuclear reactors and large concentrated solar thermal systems."
Fried, E. and I. Idelchik (1989). Flow resistance, A Design Guide for Engineering, Hemisphere Publ, Co.
Furnas, C. (1930). "Heat transfer from a gas stream to bed of broken solids." Industrial & Engineering Chemistry **22**(1): 26-31.
Galione, P., C. Pérez-Segarra, I. Rodríguez, S. Torras and J. Rigola (2015). "Numerical evaluation of multi-layered solid-PCM thermocline-like tanks as thermal energy storage systems for CSP applications." Energy Procedia **69**: 832-841.
Gallup, D. L. (2009). "Production engineering in geothermal technology: a review." Geothermics **38**(3): 326-334.
Gan, G. (2015). "Simulation of dynamic interactions of the earth–air heat exchanger with soil and atmosphere for preheating of ventilation air." Applied Energy **158**(Supplement C): 118-132.
Gandomkar, A. and K. E. Gray (2018). "Local thermal non-equilibrium in porous media with heat conduction." International Journal of Heat and Mass Transfer **124**: 1212-1216.
Gavriil, G., E. Vakouftsi and F. A. Coutelieris (2014). "Mathematical Simulation of Mass Transport in Porous Media: An Innovative Method to Match Geometrical and Transport Parameters for Scale Transition." Drying Technology **32**(7): 781-792.
Gelet, R., B. Loret and N. Khalili (2013). "Thermal recovery from a fractured medium in local thermal non-equilibrium." International Journal for Numerical and Analytical Methods in Geomechanics **37**(15): 2471-2501.

Ghomshei, M. and J. Meech (2005). "Usable heat from mine waters: Coproduction of energy and minerals from" mother earth." Intelligence in a Small Materials World: 401.
Ghoreishi-Madiseh, S., F. Hassani, A. Mohammadian and P. Radziszewski (2013). "A transient natural convection heat transfer model for geothermal borehole heat exchangers." Journal of Renewable and Sustainable Energy **5**(4): 043104.
Ghoreishi-Madiseh, S. A., L. Amiri, A. P. Sasmito and F. P. Hassani (2017). "A conjugate natural convection model for large scale seasonal thermal energy storage units: application in mine ventilation." Energy Procedia **105**: 4167-4172.
Ghoreishi-Madiseh, S. A., L. Amiri, A. P. Sasmito and F. P. Hassani (2017). "A Conjugate Natural Convection Model for Large Scale Seasonal Thermal Energy Storage Units: Application in Mine Ventilation." Energy Procedia **105**(Supplement C): 4167-4172.
Ghoreishi-Madiseh, S. A., A. Fahrettin Kuyuk, M. A. Rodrigues de Brito, D. Baidya, Z. Torabigoodarzi and A. Safari (2019). "Application of Borehole Thermal Energy Storage in Waste Heat Recovery from Diesel Generators in Remote Cold Climate Locations." Energies **12**(4): 656.
Ghoreishi-Madiseh, S. A., F. Hassani and F. Abbasy (2015). "Numerical and experimental study of geothermal heat extraction from backfilled mine stopes." Applied Thermal Engineering **90**: 1119-1130.
Ghoreishi-Madiseh, S. A., A. F. Kuyuk, M. A. R. Brito, D. Baidya, Z. Torabigoodarzi and A. Safari (2019). "Application of Borehole Thermal Energy Storage in Waste Heat Recovery from Diesel Generators in Remote Cold Climate Locations." Energies: 13-13.
Ghoreishi-Madiseh, S. A., A. Safari, L. Amiri, D. Baidya, M. Antonio Rodrigues de Brito and A. Fahrettin Kuyuk (2018). "Investigation of viability of seasonal waste heat storage in rock piles for remote communities in cold climates." Energy Procedia.
Ghoreishi-Madiseh, S. A., A. Safari, L. Amiri, D. Baidya, M. A. R. de Brito and A. F. Kuyuk (2019). "Investigation of viability of seasonal waste heat storage in rock piles for remote communities in cold climates." Energy Procedia **159**: 66-71.
Ghoreishi-Madiseh, S. A., A. P. Sasmito, F. P. Hassani and L. Amiri (2015). "Heat Transfer Analysis of Large Scale Seasonal Thermal Energy Storage for Underground Mine Ventilation." Energy Procedia **75**: 2093-2098.
Ghoreishi-Madiseh, S. A., A. P. Sasmito, F. P. Hassani and L. Amiri (2017). "Performance evaluation of large scale rock-pit seasonal thermal energy storage for application in underground mine ventilation." Applied Energy **185**: 1940-1947.
Ghoreishi-Madiseh, S. A., A. P. Sasmito, F. P. Hassani and L. Amiri (2017). "Performance evaluation of large scale rock-pit seasonal thermal energy storage for application in underground mine ventilation." Applied Energy **185, Part 2**: 1940-1947.
Gong, L., Y. Wang, X. Cheng, R. Zhang and H. Zhang (2014). "A novel effective medium theory for modelling the thermal conductivity of porous materials." International Journal of Heat and Mass Transfer **68**: 295-298.
Guardo, A., M. Coussirat, F. Recasens, M. Larrayoz and X. Escaler (2006). "CFD study on particle-to-fluid heat transfer in fixed bed reactors: Convective heat transfer at low and high pressure." Chemical Engineering Science **61**(13): 4341-4353.
Gunn, D. (1987). "Axial and radial dispersion in fixed beds." Chemical Engineering Science **42**(2): 363-373.
Hall, A., J. A. Scott and H. Shang (2011). "Geothermal energy recovery from underground mines." Renewable and Sustainable Energy Reviews **15**(2): 916-924.
Hänchen, M., S. Brückner and A. Steinfeld (2011). "High-temperature thermal storage using a packed bed of rocks–heat transfer analysis and experimental validation." Applied Thermal Engineering **31**(10): 1798-1806.
Happel, J. (1958). "Viscous flow in multiparticle systems: slow motion of fluids relative to beds of spherical particles." AIChE journal **4**(2): 197-201.
Hartman, H. L., J. M. Mutmansky, R. V. Ramani and Y. Wang (2012). Mine ventilation and air conditioning, John Wiley & Sons.

Hasnain, S. (1998). "Review on sustainable thermal energy storage technologies, Part I: heat storage materials and techniques." Energy conversion and management **39**(11): 1127-1138.
He, W., X. Luo, D. Evans, J. Busby, S. Garvey, D. Parkes and J. Wang (2017). "Exergy storage of compressed air in cavern and cavern volume estimation of the large-scale compressed air energy storage system." Applied Energy **208**(Supplement C): 745-757.
Hicks, R. (1970). "Pressure drop in packed beds of spheres." Industrial & engineering chemistry fundamentals **9**(3): 500-502.
Hicks, R. E. (1970). "Pressure Drop in Packed Beds of Spheres." Industrial & Engineering Chemistry Fundamentals **9**(3): 500-502.
Hilson, G. (2003). "Defining “cleaner production” and “pollution prevention” in the mining context." Minerals Engineering **16**(4): 305-321.
Hlushkou, D., K. Hormann, A. Höltzel, S. Khirevich, A. Seidel-Morgenstern and U. Tallarek (2013). "Comparison of first and second generation analytical silica monoliths by pore-scale simulations of eddy dispersion in the bulk region." Journal of Chromatography A **1303**: 28-38.
Hossain, S. N. and S. Bari (2013). "Waste heat recovery from the exhaust of a diesel generator using Rankine Cycle." Energy Conversion and Management **75**: 141-151.
Huang, K., J. Wan, C. Chen, L. He, W. Mei and M. Zhang (2013). "Experimental investigation on water flow in cubic arrays of spheres." Journal of hydrology **492**: 61-68.
Jamialahmadi, M., H. Müller-Steinhagen and M. R. Izadpanah (2005). "Pressure drop, gas hold-up and heat transfer during single and two-phase flow through porous media." International Journal of Heat and Fluid Flow **26**(1): 156-172.
Jemmal, Y., N. Zari and M. Maaroufi (2017). "Experimental characterization of siliceous rocks to be used as filler materials for air-rock packed beds thermal energy storage systems in concentrated solar power plants." Solar Energy Materials and Solar Cells **171**: 33-42.
Jiang, Y., M. Khadilkar, M. Al-Dahhan and M. Dudukovic (2002). "CFD of multiphase flow in packed-bed reactors: I. k-Fluid modeling issues." AIChE Journal **48**(4): 701-715.
Karacan, C. Ö. (2007). "Development and application of reservoir models and artificial neural networks for optimizing ventilation air requirements in development mining of coal seams." International Journal of Coal Geology **72**(3–4): 221-239.
Karacan, C. Ö. (2007). "Development and application of reservoir models and artificial neural networks for optimizing ventilation air requirements in development mining of coal seams." International Journal of Coal Geology **72**(3): 221-239.
Karacan, C. Ö. (2010). "Prediction of Porosity and Permeability of Caved Zone in Longwall Gobs." Transport in Porous Media **82**(2): 413-439.
Karacavus, B. and A. Can (2009). "Thermal and economical analysis of an underground seasonal storage heating system in Thrace." Energy and Buildings **41**(1): 1-10.
Kasaeian, A., R. Daneshazarian, O. Mahian, L. Kolsi, A. J. Chamkha, S. Wongwises and I. Pop (2017). "Nanofluid flow and heat transfer in porous media: a review of the latest developments." International Journal of Heat and Mass Transfer **107**: 778-791.
Kaviany, M. (2012). Principles of heat transfer in porous media, Springer Science & Business Media.
Kececioglu, I. and Y. Jiang (1994). "Flow through porous media of packed spheres saturated with water." Journal of Fluids Engineering **116**(1): 164-170.
Khan, J. A., D. E. Beasley and B. Alatas (1991). "Evaporation from a packed bed of porous particles into superheated vapor." International journal of heat and mass transfer **34**(1): 267-280.
Kim, S. J. and S. P. Jang (2002). "Effects of the Darcy number, the Prandtl number, and the Reynolds number on local thermal non-equilibrium." International Journal of Heat and Mass Transfer **45**(19): 3885-3896.
King, R. and A. Burns (1981). Sensible heat storage in packed beds. Proc. Int. Conf. on Energy Storage, Brighton, UK.
Knowles, J. (2016). Power Shift: Electricity for Canada's Remote Communities, Conference Board of Canada.

Koekemoer, A. and A. Luckos (2015). "Effect of material type and particle size distribution on pressure drop in packed beds of large particles: Extending the Ergun equation." Fuel **158**: 232-238.
Kömürcü, M. İ. and A. Akpınar (2009). "Importance of geothermal energy and its environmental effects in Turkey." Renewable Energy **34**(6): 1611-1615.
Kreith, F., R. M. Manglik and M. S. Bohn (2012). Principles of heat transfer, Cengage learning.
Krishan, O. and S. Suhag (2018). "An updated review of energy storage systems: Classification and applications in distributed generation power systems incorporating renewable energy resources." International Journal of Energy Research.
Kujawa, T., W. Nowak and A. A. Stachel (2006). "Utilization of existing deep geological wells for acquisitions of geothermal energy." Energy **31**(5): 650-664.
Kundu, P., V. Kumar and I. M. Mishra (2016). "Experimental and numerical investigation of fluid flow hydrodynamics in porous media: Characterization of pre-Darcy, Darcy and non-Darcy flow regimes." Powder Technology **303**: 278-291.
Kuravi, S., J. Trahan, Y. Goswami, C. Jotshi, E. Stefanakos and N. Goel (2013). "Investigation of a high-temperature packed-bed sensible heat thermal energy storage system with large-sized elements." Journal of Solar Energy Engineering **135**(4): 041008.
Kurnia, J. C. and A. P. Sasmito (2018). "Numerical investigation of heat transfer performance of a rotating latent heat thermal energy storage." Applied Energy **227**: 542-554.
Kurnia, J. C., A. P. Sasmito and A. S. Mujumdar (2014). "Simulation of a novel intermittent ventilation system for underground mines." Tunnelling and Underground Space Technology **42**: 206-215.
Kurnia, J. C., P. Xu and A. P. Sasmito (2016). "A novel concept of enhanced gas recovery strategy from ventilation air methane in underground coal mines – A computational investigation." Journal of Natural Gas Science and Engineering **35**: 661-672.
Kuwahara, F., M. Shirota and A. Nakayama (2001). "A numerical study of interfacial convective heat transfer coefficient in two-energy equation model for convection in porous media." International journal of heat and mass transfer **44**(6): 1153-1159.
Kyan, C. P., D. T. Wasan and R. C. Kintner (1970). "Flow of single-phase fluids through fibrous beds." Industrial & Engineering Chemistry Fundamentals **9**(4): 596-603.
Lacroix, M., P. Nguyen, D. Schweich, C. Pham Huu, S. Savin-Poncet and D. Edouard (2007). "Pressure drop measurements and modeling on SiC foams." Chemical Engineering Science **62**(12): 3259-3267.
Li, L. and W. Ma (2011). "Experimental characterization of the effective particle diameter of a particulate bed packed with multi-diameter spheres." Nuclear Engineering and Design **241**(5): 1736-1745.
Li, L. and W. Ma (2011). "Experimental Study on the Effective Particle Diameter of a Packed Bed with Non-Spherical Particles." Transport in Porous Media **89**(1): 35-48.
Li, P., J. Van Lew, W. Karaki, C. Chan, J. Stephens and Q. Wang (2011). "Generalized charts of energy storage effectiveness for thermocline heat storage tank design and calibration." Solar Energy **85**(9): 2130-2143.
Li, X., J. Zhao and Q. Zhou (2005). "Inner heat source model with heat and moisture transfer in soil around the underground heat exchanger." Applied Thermal Engineering **25**(10): 1565-1577.
Liu, S., A. Afacan and J. Masliyah (1994). "Steady incompressible laminar flow in porous media." Chemical engineering science **49**(21): 3565-3586.
Love, N. D., J. P. Szybist and C. S. Sluder (2012). "Effect of heat exchanger material and fouling on thermoelectric exhaust heat recovery." Applied Energy **89**(1): 322-328.
Lovekin, D. and D. Heerema (2019). The True Cost of Energy in Remote Communities: Understanding diesel electricity generation terms and economics, PEMBINA Institute**:** 7-7.
Macdonald, I., M. El-Sayed, K. Mow and F. Dullien (1979). "Flow through porous media-the Ergun equation revisited." Industrial & Engineering Chemistry Fundamentals **18**(3): 199-208.
Madiseh, S. G., M. M. Ghomshei, F. Hassani and F. Abbasy (2012). "Sustainable heat extraction from abandoned mine tunnels: A numerical model." Journal of Renewable and Sustainable Energy **4**(3): 033102.

Mahdi, R. A., H. Mohammed, K. Munisamy and N. Saeid (2015). "Review of convection heat transfer and fluid flow in porous media with nanofluid." Renewable and Sustainable Energy Reviews **41**: 715-734.
Manz, B., L. Gladden and P. Warren (1999). "Flow and dispersion in porous media: Lattice-Boltzmann and NMR studies." AIChE journal **45**(9): 1845-1854.
Masnadi, M. S., J. R. Grace, X. T. Bi, C. J. Lim and N. Ellis (2015). "From fossil fuels towards renewables: Inhibitory and catalytic effects on carbon thermochemical conversion during co-gasification of biomass with fossil fuels." Applied Energy **140**(Supplement C): 196-209.
Mathey, F. (2013). "Numerical up-scaling approach for the simulation of heat-transfer in randomly packed beds." International Journal of Heat and Mass Transfer **61**: 451-463.
Mayala, L. P., M. M. Veiga and M. B. Khorzoughi (2016). "Assessment of mine ventilation systems and air pollution impacts on artisanal tanzanite miners at Merelani, Tanzania." Journal of Cleaner Production **116**(Supplement C): 118-124.
Mayerhofer, M., J. Govaerts, N. Parmentier, H. Jeanmart and L. Helsen (2011). "Experimental investigation of pressure drop in packed beds of irregular shaped wood particles." Powder Technology **205**(1): 30-35.
McCartney, J. S., T. Başer, N. Zhan, N. Lu, S. Ge and K. Smits (2017). "Storage of solar thermal energy in borehole thermal energy storage systems."
McDaniel, B. and D. Kosanovic (2016). "Modeling of combined heat and power plant performance with seasonal thermal energy storage." Journal of Energy Storage **7**: 13-23.
McElroy, G. E. (1935). Engineering factors in the ventilation of metal mines, US Government Printing Office.
McPherson, M. J. (2012). Subsurface ventilation and environmental engineering, Springer Science & Business Media.
McQuillan, F. J., J. R. Culham and M. M. Yovanovich (1984). Properties of dry air at one atmosphere (UW/MHTL 8406 G-01). Waterloo, Ontario, Microelectronics Heat Transfer Lab, University of Waterloo.
Mehrabian, R., A. Shiehnejadhesar, R. Scharler and I. Obernberger (2014). "Multi-physics modelling of packed bed biomass combustion." Fuel **122**: 164-178.
Meier, A., C. Winkler and D. Wuillemin (1991). "Experiment for modelling high temperature rock bed storage." Solar energy materials **24**(1-4): 255-264.
Mertens, N., F. Alobaid, L. Frigge and B. Epple (2014). "Dynamic simulation of integrated rock-bed thermocline storage for concentrated solar power." Solar Energy **110**: 830-842.
Modi, A. and C. D. Perez-Segarra (2014). "Thermocline thermal storage systems for concentrated solar power plants: One-dimensional numerical model and comparative analysis." Solar Energy **100**: 84-93.
Mokkapati, V. and C. S. Lin (2014). "Numerical study of an exhaust heat recovery system using corrugated tube heat exchanger with twisted tape inserts." International Communications in Heat and Mass Transfer **57**: 53-64.
Molins, S., D. Trebotich, C. I. Steefel and C. Shen (2012). "An investigation of the effect of pore scale flow on average geochemical reaction rates using direct numerical simulation." Water Resources Research **48**(3).
Montillet, A., E. Akkari and J. Comiti (2007). "About a correlating equation for predicting pressure drops through packed beds of spheres in a large range of Reynolds numbers." Chemical Engineering and Processing: Process Intensification **46**(4): 329-333.
Moutsopoulos, K. N. (2007). "One-dimensional unsteady inertial flow in phreatic aquifers induced by a sudden change of the boundary head." Transport in Porous Media **70**(1): 97-125.
Nagel, T., S. Beckert, C. Lehmann, R. Gläser and O. Kolditz (2016). "Multi-physical continuum models of thermochemical heat storage and transformation in porous media and powder beds—A review." Applied Energy **178**(Supplement C): 323-345.

Nahhas, T., X. Py and R. Olives (2018). "Life Cycle Assessment of Air-Rock Packed Bed Storage System and Its Comparison with Other Available Storage Technologies for Concentrating Solar Power Plants." Waste and Biomass Valorization.
Nahhas, T., X. Py, N. Sadiki and S. Gregoire (2019). "Assessment of four main representative flint facies as alternative storage materials for concentrated solar power plants." Journal of Energy Storage **23**: 79-88.
Nakayama, A. (2014). "A note on the confusion associated with the interfacial heat transfer coefficient for forced convection in porous media." International Journal of Heat and Mass Transfer **79**: 1-2.
Nemec, D. and J. Levec (2005). "Flow through packed bed reactors: 1. Single-phase flow." Chemical Engineering Science **60**(24): 6947-6957.
Nield, D. A. and A. Bejan (2006). Convection in porous media, Springer Science & Business Media.
Nield, D. A. and A. Bejan (2006). Convection in porous media, Springer.
Nimvari, M. E., M. Maerefat and M. K. El-Hossaini (2012). "Numerical simulation of turbulent flow and heat transfer in a channel partially filled with a porous media." International Journal of Thermal Sciences **60**: 131-141.
Nordlund, M., D. J. Lopez Penha, S. Stolz, A. Kuczaj, C. Winkelmann and B. J. Geurts (2013). "A new analytical model for the permeability of anisotropic structured porous media." International Journal of Engineering Science **68**: 38-60.
Novo, A. V., J. R. Bayon, D. Castro-Fresno and J. Rodriguez-Hernandez (2010). "Review of seasonal heat storage in large basins: Water tanks and gravel–water pits." Applied Energy **87**(2): 390-397.
Orr, B., A. Akbarzadeh, M. Mochizuki and R. Singh (2016). "A review of car waste heat recovery systems utilising thermoelectric generators and heat pipes." Applied Thermal Engineering **101**: 490-495.
Ozahi, E., M. Y. Gundogdu and M. Ö. Carpinlioglu (2008). "A modification on Ergun's correlation for use in cylindrical packed beds with non-spherical particles." Advanced Powder Technology **19**(4): 369-381.
Pallares, J. and F. Grau (2010). "A modification of a Nusselt number correlation for forced convection in porous media." International Communications in Heat and Mass Transfer **37**(9): 1187-1190.
Pan, H., X.-Z. Chen, X.-F. Liang, L.-T. Zhu and Z.-H. Luo (2016). "CFD simulations of gas–liquid–solid flow in fluidized bed reactors — A review." Powder Technology **299**: 235-258.
Pandiyarajan, V., M. C. Pandian, E. Malan, R. Velraj, R. V. Seeniraj, M. Chinna Pandian, E. Malan, R. Velraj and R. V. Seeniraj (2011). "Experimental investigation on heat recovery from diesel engine exhaust using finned shell and tube heat exchanger and thermal storage system." Applied Energy **88**(1): 77-87.
Partopour, B. and A. G. Dixon (2017). "An integrated workflow for resolved-particle packed bed models with complex particle shapes." Powder Technology **322**: 258-272.
Persson, J. and M. Westermark (2013). "Low-energy buildings and seasonal thermal energy storages from a behavioral economics perspective." Applied Energy **112**: 975-980.
Ploeg, F. and C. Withagen (2014). "Growth, renewables, and the optimal carbon tax." International Economic Review **55**(1): 283-311.
Pruess, K. (1985). "A practical method for modeling fluid and heat flow in fractured porous media." Society of Petroleum Engineers Journal **25**(01): 14-26.
Quintard, M. and S. Whitaker (2000). Theoretical analysis of transport in porous media, Marcel Dekker Inc., New York.
Raftery, A., P. Shier and T. Obilade (1980). "Domestic space-heating and solar energy in Ireland." International Journal of Energy Research **4**(1): 31-39.
Reichelt, W. (1972). "Zur Berechnung des Druckverlustes einphasig durchströmter Kugel-und Zylinderschüttungen." Chemie Ingenieur Technik **44**(18): 1068-1071.
Ren, T. and J. Edwards (2000). "Three-dimensional computational fluid dynamics modelling of methane flow through permeable strata around a longwall face." Mining technology **109**(1): 41-48.
Rodat, S., A. Bruch, N. Dupassieux and N. El Mourchid (2015). "Unique Fresnel demonstrator including ORC and thermocline direct thermal storage: operating experience." Energy Procedia **69**: 1667-1675.

Rode, S., N. Midoux, M. A. Latifi, A. Storck and E. Saatdjian (1994). "Hydrodynamics of liquid flow in packed beds: an experimental study using electrochemical shear rate sensors." Chemical Engineering Science **49**(6): 889-900.
Rong, L. W., Z. Y. Zhou and A. B. Yu (2015). "Lattice–Boltzmann simulation of fluid flow through packed beds of uniform ellipsoids." Powder Technology **285**: 146-156.
Rose, H. (1945). "On the resistance coefficient–Reynolds number relationship for fluid flow through a bed of granular material." Proceedings of the Institution of Mechanical Engineers **153**(1): 154-168.
Rose, H. and A. Rizk (1949). "Further researches in fluid flow through beds of granular material." Proceedings of the Institution of Mechanical Engineers **160**(1): 493-511.
Royer, J. (2013). Status of remote/off-grid communities in Canada. Ottawa, Natural Resources Canada**:** 44-44.
Rumpf, H. and A. Gupte (1971). "Einflüsse der porosität und korngrößenverteilung im widerstandsgesetz der porenströmung." Chemie Ingenieur Technik **43**(6): 367-375.
Sahimi, M. (2011). Flow and transport in porous media and fractured rock: from classical methods to modern approaches, John Wiley & Sons.
Sanner, B. (1993). Ground Coupled Heat Pumps with Seasonal Cold Storage. Heat Pumps for Energy Efficiency and Environmental Progress, Elsevier Science Publishers B.V.**:** 301-308.
Sarbu, I. and A. Dorca (2019). "Review on heat transfer analysis in thermal energy storage using latent heat storage systems and phase change materials." International Journal of Energy Research **43**(1): 29-64.
Sasmito, A. P., J. C. Kurnia, E. Birgersson and A. S. Mujumdar (2015). "Computational evaluation of thermal management strategies in an underground mine." Applied Thermal Engineering: 1144-1150.
Sbarba, H. D. (2012). Heat Recovery Systems in Underground Mine Ventilation Systems and Novel Mine Cooling Systems, Université Laval.
Schafrik, S. (2015). The use of packed sphere modelling for airflow and heat exchange analysis in broken or fragmented rock, Laurentian University of Sudbury.
Schmidt, T., D. Mangold and H. Müller-Steinhagen (2004). "Central solar heating plants with seasonal storage in Germany." Solar energy **76**(1-3): 165-174.
Seguin, D., A. Montillet and J. Comiti (1998). "Experimental characterisation of flow regimes in various porous media—I: Limit of laminar flow regime." Chemical Engineering Science **53**(21): 3751-3761.
Sharma, A., V. V. Tyagi, C. Chen and D. Buddhi (2009). "Review on thermal energy storage with phase change materials and applications." Renewable and Sustainable energy reviews **13**(2): 318-345.
Sharqawy, M. H., S. Said, E. Mokheimer, M. Habib, H. Badr and N. Al-Shayea (2009). "First in situ determination of the ground thermal conductivity for boreholeheat exchanger applications in Saudi Arabia." Renewable Energy **34**(10): 2218-2223.
Shitzer, A. and M. Levy (1983). "Transient behavior of a rock-bed thermal storage system subjected to variable inlet air temperatures: Analysis and experimentation." Journal of Solar Energy Engineering **105**(2): 200-206.
Singh, H., R. Saini and J. Saini (2010). "A review on packed bed solar energy storage systems." Renewable and Sustainable Energy Reviews **14**(3): 1059-1069.
Singh, H., R. Saini and J. Saini (2013). "Performance of a packed bed solar energy storage system having large sized elements with low void fraction." Solar Energy **87**: 22-34.
Singh, P. L., S. Deshpandey and P. Jena (2015). "Thermal performance of packed bed heat storage system for solar air heaters." Energy for sustainable Development **29**: 112-117.
Singh, P. L., S. D. Deshpandey and P. C. Jena (2015). "Thermal performance of packed bed heat storage system for solar air heaters." Energy for Sustainable Development **29**: 112-117.
Singh, R., R. Saini and J. Saini (2006). "Nusselt number and friction factor correlations for packed bed solar energy storage system having large sized elements of different shapes." Solar Energy **80**(7): 760-771.
Singh, S., K. Sørensen, T. Condra, S. S. Batz and K. Kristensen (2019). "Investigation on transient performance of a large-scale packed-bed thermal energy storage." Applied Energy **239**: 1114-1129.

Singhal, A., S. Cloete, S. Radl, R. Quinta-Ferreira and S. Amini (2017). "Heat transfer to a gas from densely packed beds of cylindrical particles." Chemical Engineering Science **172**: 1-12.
Sommer, W., J. Valstar, I. Leusbrock, T. Grotenhuis and H. Rijnaarts (2015). "Optimization and spatial pattern of large-scale aquifer thermal energy storage." Applied Energy **137**: 322-337.
Sorgulu, F. and I. Dincer (2018). "Design and analysis of a solar tower power plant integrated with thermal energy storage system for cogeneration." International Journal of Energy Research.
Sposito, G., W. A. Jury and V. K. Gupta (1986). "Fundamental problems in the stochastic convection-dispersion model of solute transport in aquifers and field soils." Water Resources Research **22**(1): 77-88.
Stachulak, J. (1991). "Ventilation strategy and unique air conditioning at Inco Limited." CIM(Canadian Mining and Metallurgical) Bulletin **84**(950): 41-45.
Stritih, U., E. Zavrl and H. O. Paksoy (2019). "Energy Analysis and Carbon Saving Potential of a Complex Heating System with Solar Assisted Heat Pump and Phase Change Material (PCM) Thermal Storage in Different Climatic Conditions." European Journal of Sustainable Development Research **3**(1): em0067.
Suekane, T., Y. Yokouchi and S. Hirai (2003). "Inertial flow structures in a simple-packed bed of spheres." AIChE journal **49**(1): 10-17.
Sylvestre, M. J.-G. (1999). Heating and Ventilation Study of Inco's Creighton Mine.
Tallmadge, J. (1970). "Packed bed pressure drop—an extension to higher Reynolds numbers." AIChE Journal **16**(6): 1092-1093.
Templeton, J., S. Ghoreishi-Madiseh, F. Hassani and M. Al-Khawaja (2014). "Abandoned petroleum wells as sustainable sources of geothermal energy." Energy **70**: 366-373.
Templeton, J. D., F. Hassani and S. A. Ghoreishi-Madiseh (2016). "Study of effective solar energy storage using a double pipe geothermal heat exchanger." Renewable Energy **86**: 173-181.
Teruel, F. E. (2009). "A new turbulence model for porous media flows. Part I: Constitutive equations and model closure." International Journal of Heat and Mass Transfer **52**(19): 4264-4272.
Teruel, F. E. and u. Rizwan (2009). "Characterization of a porous medium employing numerical tools: Permeability and pressure-drop from Darcy to turbulence." International Journal of Heat and Mass Transfer **52**(25): 5878-5888.
Thabet, A. and A. G. Straatman (2018). "The development and numerical modelling of a Representative Elemental Volume for packed sand." Chemical Engineering Science **187**: 117-126.
Tian, Y. and C.-Y. Zhao (2013). "A review of solar collectors and thermal energy storage in solar thermal applications." Applied energy **104**: 538-553.
Tian, Y. and C. Y. Zhao (2013). "A review of solar collectors and thermal energy storage in solar thermal applications." Applied Energy **104**: 538-553.
Tiskatine, R., A. Aharoune, L. Bouirden and A. Ihlal (2017). "Identification of suitable storage materials for solar thermal power plant using selection methodology." Applied Thermal Engineering **117**: 591-608.
Tiskatine, R., R. Oaddi, R. Ait El Cadi, A. Bazgaou, L. Bouirden, A. Aharoune and A. Ihlal (2017). "Suitability and characteristics of rocks for sensible heat storage in CSP plants." Solar Energy Materials and Solar Cells **169**: 245-257.
Turrado, S., J. R. Fernández and J. C. Abanades (2018). "Determination of the solid concentration in a binary mixture from pressure drop measurements." Powder Technology **338**: 608-613.
Ucar, A. and M. Inalli (2006). "Exergoeconomic analysis and optimization of a solar-assisted heating system for residential buildings." Building and Environment **41**(11): 1551-1556.
Vafai, K. and C. Tien (1981). "Boundary and inertia effects on flow and heat transfer in porous media." International Journal of Heat and Mass Transfer **24**(2): 195-203.
Vafai, K. and C. Tien (1982). "Boundary and inertia effects on convective mass transfer in porous media." International Journal of Heat and Mass Transfer **25**(8): 1183-1190.
Van Lew, J. T., P. Li, C. L. Chan, W. Karaki and J. Stephens (2011). "Analysis of heat storage and delivery of a thermocline tank having solid filler material." Journal of solar energy engineering **133**(2): 021003.

Vejahati, F., N. Mahinpey, N. Ellis and M. B. Nikoo (2009). "CFD simulation of gas–solid bubbling fluidized bed: a new method for adjusting drag law." The Canadian Journal of Chemical Engineering **87**(1): 19-30.
Velraj, R., R. V. Seeniraj, B. Hafner, C. Faber and K. Schwarzer (1999). "HEAT TRANSFER ENHANCEMENT IN A LATENT HEAT STORAGE SYSTEM1Paper presented at the ISES Solar World Congress, Taejon, South Korea, 24–29 August 1997.1." Solar Energy **65**(3): 171-180.
Venkataraman, P. and P. R. M. Rao (1998). "Darcian, transitional, and turbulent flow through porous media." Journal of hydraulic engineering **124**(8): 840-846.
Villasmil, W., L. J. Fischer and J. Worlitschek (2019). "A review and evaluation of thermal insulation materials and methods for thermal energy storage systems." Renewable and Sustainable Energy Reviews **103**: 71-84.
Vollmari, K., R. Jasevičius and H. Kruggel-Emden (2016). "Experimental and numerical study of fluidization and pressure drop of spherical and non-spherical particles in a model scale fluidized bed." Powder Technology **291**: 506-521.
Vollmari, K., T. Oschmann, S. Wirtz and H. Kruggel-Emden (2015). "Pressure drop investigations in packings of arbitrary shaped particles." Powder Technology **271**: 109-124.
Wakao, N. and S. Kagei (1982). Heat and mass transfer in packed beds, Taylor & Francis.
Wakao, N., S. Kaguei and T. Funazkri (1979). "Effect of fluid dispersion coefficients on particle-to-fluid heat transfer coefficients in packed beds: correlation of Nusselt numbers." Chemical engineering science **34**(3): 325-336.
Walmsley, M. R., T. G. Walmsley, M. J. Atkins, P. J. Kamp and J. R. Neale (2014). "Minimising carbon emissions and energy expended for electricity generation in New Zealand through to 2050." Applied Energy **135**: 656-665.
Wang, J., J. K. Carson, M. F. North and D. J. Cleland (2006). "A new approach to modelling the effective thermal conductivity of heterogeneous materials." International journal of heat and mass transfer **49**(17-18): 3075-3083.
Wang, J., J. Yang, Z. Cheng, Y. Liu, Y. Chen and Q. Wang (2018). "Experimental and numerical study on pressure drop and heat transfer performance of grille-sphere composite structured packed bed." Applied Energy **227**: 719-730.
Wang, T., W. Luan, W. Wang and S. T. Tu (2014). "Waste heat recovery through plate heat exchanger based thermoelectric generator system." Applied Energy **136**: 860-865.
Wang, Y., C. L. Lin and J. D. Miller (2016). "3D image segmentation for analysis of multisize particles in a packed particle bed." Powder Technology **301**: 160-168.
Ward, J. (1964). "Turbulent flow in porous media." Journal of the Hydraulics Division **90**(5): 1-12.
Weise, S., S. Meinicke, T. Wetzel and B. Dietrich (2019). "Modelling the pressure drop of two-phase flow through solid porous media." International Journal of Multiphase Flow **112**: 13-26.
Weller, A., L. Slater, S. Nordsiek and D. Ntarlagiannis (2010). "On the estimation of specific surface per unit pore volume from induced polarization: A robust empirical relation fits multiple data sets." Geophysics **75**(4): WA105-WA112.
Welsch, B., L. Göllner-Völker, D. O. Schulte, K. Bär, I. Sass and L. Schebek (2018). "Environmental and economic assessment of borehole thermal energy storage in district heating systems." Applied Energy **216**: 73-90.
Wentz Jr, C. A. and G. Thodos (1963). "Pressure drops in the flow of gases through packed and distended beds of spherical particles." AIChE Journal **9**(1): 81-84.
Whitaker, S. (1977). "Simultaneous heat, mass, and momentum transfer in porous media: a theory of drying." Advances in heat transfer **13**: 119-203.
Whitaker, S. (1986). "Flow in porous media I: A theoretical derivation of Darcy's law." Transport in Porous Media **1**(1): 3-25.
Wu, J., B. Yu and M. Yun (2008). "A resistance model for flow through porous media." Transport in Porous Media **71**(3): 331-343.

Wu, W., B. Wang, W. Shi and X. Li (2014). "Absorption heating technologies: A review and perspective." Applied Energy **130**(0): 51-71.
Wu, W., B. Wang, W. Shi and X. Li (2014). "Absorption heating technologies: A review and perspective." Applied Energy **130**: 51-71.
Wu, Z., C. Caliot, G. Flamant and Z. Wang (2011). "Numerical simulation of convective heat transfer between air flow and ceramic foams to optimise volumetric solar air receiver performances." International Journal of Heat and Mass Transfer **54**(7): 1527-1537.
Xu, B., D. Rathod, S. Kulkarni, A. Yebi, Z. Filipi, S. Onori and M. Hoffman (2017). "Transient dynamic modeling and validation of an organic Rankine cycle waste heat recovery system for heavy duty diesel engine applications." Applied Energy **205**: 260-279.
Xu, C., Z. Song and Y. Zhen (2011). "Numerical investigation on porous media heat transfer in a solar tower receiver." Renewable Energy **36**(3): 1138-1144.
Yan, B., J. Wieberdink, F. Shirazi, P. Y. Li, T. W. Simon and J. D. Van de Ven (2015). "Experimental study of heat transfer enhancement in a liquid piston compressor/expander using porous media inserts." Applied Energy **154**(Supplement C): 40-50.
Yang, Z. and S. V. Garimella (2013). "Cyclic operation of molten-salt thermal energy storage in thermoclines for solar power plants." Applied energy **103**: 256-265.
Yu, S., S. Gao and H. sun (2016). "A dynamic programming model for environmental investment decision-making in coal mining." Applied Energy **166**(Supplement C): 273-281.
Zafari, M., M. Panjepour, M. Davazdah Emami and M. Meratian (2015). "Microtomography-based numerical simulation of fluid flow and heat transfer in open cell metal foams." Applied Thermal Engineering **80**: 347-354.
Zalba, B., J. M. Marın, L. F. Cabeza and H. Mehling (2003). "Review on thermal energy storage with phase change: materials, heat transfer analysis and applications." Applied thermal engineering **23**(3): 251-283.
Zanganeh, G., M. Commerford, A. Haselbacher, A. Pedretti and A. Steinfeld (2014). "Stabilization of the out fl ow temperature of a packed-bed thermal energy storage by combining rocks with phase change materials." Applied Thermal Engineering **70**(1): 316-320.
Zanganeh, G., A. Pedretti, A. Haselbacher and A. Steinfeld (2015). "Design of packed bed thermal energy storage systems for high-temperature industrial process heat." Applied Energy **137**: 812-822.
Zanganeh, G., A. Pedretti, S. Zavattoni, M. Barbato and A. Steinfeld (2012). "Packed-bed thermal storage for concentrated solar power–Pilot-scale demonstration and industrial-scale design." Solar Energy **86**(10): 3084-3098.
Zeng, Z. and R. Grigg (2006). "A Criterion for Non-Darcy Flow in Porous Media." Transport in Porous Media **63**(1): 57-69.
Zhang, H., H. Wang, X. Zhu, Y.-J. Qiu, K. Li, R. Chen and Q. Liao (2013). "A review of waste heat recovery technologies towards molten slag in steel industry." Applied Energy **112**: 956-966.
Zhang, H. G., E. H. Wang and B. Y. Fan (2013). "Heat transfer analysis of a finned-tube evaporator for engine exhaust heat recovery." Energy Conversion and Management **65**: 438-447.
Zhang, P., X. Xiao, Z. N. Meng and M. Li (2015). "Heat transfer characteristics of a molten-salt thermal energy storage unit with and without heat transfer enhancement." Applied Energy **137**: 758-772.
Zhou, J.-Q., S.-H. Hu, Y.-F. Chen, M. Wang and C.-B. Zhou (2016). "The friction factor in the forchheimer equation for rock fractures." Rock Mechanics and Rock Engineering **49**(8): 3055-3068.
Zhu, Y., P. J. Fox and J. P. Morris (1999). "A pore-scale numerical model for flow through porous media." International journal for numerical and analytical methods in geomechanics **23**(9): 881-904.